Spectroscopic Studies of Palladium Catalysed Reactions between Carbon Monoxide and Ethene

THE UNIVERSITY *of* LIVERPOOL

Thesis submitted in accordance with the requirements of the University of Liverpool for the degree of Doctor in Philosophy by Stefano Zacchini

Department of Chemistry

December 2000

Declaration

I declare that, except otherwise stated, the work contained within this thesis is my own research, carried out from February 1998 until December 2000 at the Department of Chemistry, University of Liverpool.

Signed

Stefano Zacchini

Non chiederci la parola che squadri da ogni lato

l'animo nostro informe, e a lettere di fuoco

lo dichiari e risplenda come un croco

perduto in mezzo a un polveroso prato.

Ah l'uomo che se ne va sicuro,

agli altri ed a se stesso amico,

e l'ombra sua non cura che la canicola

stampa sopra uno scalcinato muro!

Non domandarci la formula che mondi possa aprirti,

sì qualche storta sillaba e secca come un ramo.

Codesto solo oggi possiamo dirti,

ciò che non siamo, ciò che non vogliamo.

(E. Montale)

Acknowledgements

I would really like to express all my thanks to my supervisors in Liverpool, Prof. B. T. Heaton, Dr. J. A. Iggo and Dr. R. Whyman, and at Ineos Acrylics, Dr. G. R. Eastham and Dr. R. P. Tooze, for all I have learned in these three years, for the support and the help. I have to particularly thank Dr. C. Jacob for all the help in the lab and with the NMR machines, and for his very useful suggestions. Many thanks also to Anne Flaherty for helping me with all the bureaucratic stuff, making my life easier.

I would like to thank also all the technical staff of the Chemistry Department for their help and support, and in particular Jamie Bickley for the X-ray determinations and Dr. P. Leonard for the help with the NMR spectrometers.

Many thanks to all the people who have worked in these last three years in the Lab 227 (and around), for the support, the friendship and the nice moments spent together: Andy, Nieves, Clare, Dan, Darren, Charles, Emma.

In particular, I owe a special thanks to Lucia for having helped me a lot (and probably more) when I first arrived in L'pool and also after and still now. For being present when I needed and making me laugh, thanks.

A special thanks also to Joanna, for the support and the friendship over the last year and a half; and also for making me not feel alone.

Thousands of thanks to Kerry, for being always so sweet and kind to me.

And, the words are not enough to express all my gratefulness and love to Lidia and John, people are sometimes so extraordinary.

A big thanks also to Maurizio, per le risate assieme ma anche le tante chiacchierate serie (o quasi); e dopo 3 anni mi parli ancora!!!!!

And then, there is the Italian community of L'pool (past and present), un po' di casa anche qua: Eva (si sogna meglio con i piedi ben saldi per terra), Claudia (grazie a te sono ancora qui che rido.....e sorrido), Martina (forse non ci si vede spesso, ma e' sempre un piacere), and Lavinia (member ad honorem).

I would like also to thank Marc and Noelia, for all the fun we had together.

And thanks to Mariana, my South American link, because in the life there is always another point of view. *Uruguay es la ropa tendida en el oro de un día de viento/ es el pan en la mesa de América, la pureza del pan en la mesa.* (P. Neruda)

In these years, a part from L'pool, I have also received a big support from Cardiff (Luisa, Paola) and Bologna (Capo, Carmela, Cri, Francesco, Francy, Raffa, Samanza, Tonno, Passerotto, Silvia, Betta, Beppe). Thanks to all of you for everything.

And , in the end, the begin: I would like to thank my family for all you gave to me.

During these years, it happened that a lot of people appeared and disappeared in my life. Someone for minutes, someone for more. From each of them I have received something. So, I would like to extend my thanks to all of these people.

.....è stato meglio lasciarci, che non esserci mai incontrati. (F. de Andre')

Abstract

This Thesis is concerned with the study of the mechanistic aspects involved in the methoxycarbonylation of ethene promoted by a catalytic system based on Pd(d^{t}bpx)(dba) and $MeSO_3H$

Chapter 1 surveys the literature of the reactions between carbon monoxide and ethene, with particular regard to the mechanistic studies. Moreover, the new catalyst for the synthesis of MeP recently developed by Ineos Acrylics is described.

Chapter 2 describes the reactivity of Pd(d^{t}bpx)(dba) with TfOH. $[Pd(d^tbpx)(dbaH)]^+$ is, first, formed and, then, it further reacts with O_2 resulting in the formation of $[Pd(d^tbpx)H(solv)]^+$. This hydride complex has been fully characterised in solution *via* multinuclear NMR spectroscopy in the temperature range 193-353 K. Its reactivity with oxidants and different ligands (*e.g.* Py, PPh_3, H_2O, Cl^-, Br^-, I^-) is also described. Moreover, the mechanism of formation of $[Pd(d^tbpx)H(solv)]^+$ from Pd(d^{t}bpx)(dba) is discussed.

Chapter 3 describes the reactivity of Pd(d^{t}bpx)(dba) with $MeSO_3H$. Addition of the acid and BQ (or O_2) to Pd(d^{t}bpx)(dba) results in the formation of $[Pd(d^tbpx)(\eta^2\text{-}MeSO_3)]^+$, which has been characterised in the solid state *via* X-ray diffraction. Its structure is compared to analogous complexes $[Pd(d^tbpx)(\eta^2\text{-}TfO)]^+$ and $[Pd(d^tbpx)(\eta^2\text{-}TsO)]^+$, obtained in similar conditions. The behaviour in solution of $[Pd(d^tbpx)(\eta^2\text{-}MeSO_3)]^+$ is also described; it can exist as two different conformers which mutually inter-convert in solution. Moreover, the conditions for the conversion of $[Pd(d^tbpx)(\eta^2\text{-}MeSO_3)]^+$ into $[Pd(d^tbpx)H(solv)]^+$ are described.

Chapter 4 describes the reactivity of some catalyst precursors and catalytic intermediates with olefins. Reaction of $[Pd(d^tbpx)H(solv)]^+$ with ethene results in the formation of $[Pd(d^tbpx)(CH_2CH_3)]^+$, containing an agostic-interaction. This complex has been fully characterised in solution *via* multinuclear variable temperature NMR spectroscopy and ^{13}C-labelling; different exchange processes have been detected and fully characterised. In the second part of the Chapter, the reactivity of $[Pd(d^tbpx)H(solv)]^+$ with other α-olefins is described, and the last part of the Chapter deals with the reactivity of $[Pd(d^tbpx)(\eta^2\text{-}MeSO_3)]^+$ with ethene.

Chapter 5 describes the reactivity of some catalyst precursors and catalytic intermediates with CO. $[Pd(d^tbpx)(CH_2CH_3)]^+$ reacts with CO in non-alcoholic solvents resulting in the formation of $[Pd(d^tbpx)(COEt)(solv)]^+$, which has been characterised in solution *via* multinuclear variable temperature NMR spectroscopy and ^{13}C-labelling. The reactivity of $[Pd(d^tbpx)(COEt)(solv)]^+$ with MeOH is found to result in the formation of $[Pd(d^tbpx)H(solv)]^+$ and MeP, whereas rapid decomposition is observed after addition of CO. Moreover, the reaction between $[Pd(d^tbpx)H(solv)]^+$ and CO results in the formation of $[Pd(d^tbpx)H(CO)]^+$; this complex is stable only at low temperature. Finally, the synthesis and characterisation of $Pd(d^tbpx)(CO)_x$ (x = 1,2) is reported.

Chapter 6 describes the effect of the diphosphine ligand on some of the reactions reported in the previous Chapters. The product of the reaction between Pd(P-P)(dba), BQ and TfOH in MeOH strongly depends on the nature of the ligand. Thus, the hydride $[Pd(P\text{-}P)H(MeOH)]^+$ is formed only when P-P = d^tbpx, d^tppx, $^tb^tppx$, d^tbpp, dapp and dapx; whereas no hydride has been observed when P-P = dcpx, dppp, dppx and d^ippx. The case of ^tbcpx is not very clear. The reactivity of these complexes with ethene is also described.

Chapter 7 contains general conclusions about the mechanistic aspects of the catalytic process. The catalytic cycle and the catalyst activation are described in detail. Moreover, some considerations on the catalyst deactivation are reported. Finally, the reasons of the particular selectivity of this process are discussed.

Chapter 8 describes all the experimental details of the work reported in Chapters 2, 3, 4, 5 and 6.

Contents

1. The reactions between carbon monoxide and ethene

2. Reactivity of Pd(d^{t}bpx)(dba) with acids: the TfOH system

3. Reactivity of Pd(d^{t}bpx)(dba) with acids: the $MeSO_3H$ system

4. Reactivity of some catalyst precursors and catalytic intermediates with olefins

5. Reactivity of some catalyst precursors and catalytic intermediates with carbon monoxide

6. The effect of the P-P ligand

7. General conclusions

8. Experimental Section

Abbreviations

IR	infra-red
NMR	Nuclear Magnetic Resonance
PM-RAIRS	polarisation modulation reflection absorption infrared spectrosopy
δ	chemical shift
J(A-B)	coupling constant between nuclei A and B
^{n}J	n-bond coupling constant
ppm	parts per million
Hz	Hertz
m	multiplet
d	doublet
br	broad
t	triplet
VT	variable tempertaure
Me	methyl
Et	ethyl
Ph	phenyl
THF	tetrahydrofuran
MeP	methyl propanoate
TsOH	para-toluenesulfonic acid
TfOH	CF_3SO_3H
TFA	trifluoroacetic acid
COD	cycloocta-1,5-diene
BQ	benzoquinone

Py	pyridine
TMEDA	tetra-methyl-ehylenediamine
dba	*trans,trans*-dibenzylideneacetone
dppp	1,3-bis(diphenylphosphino)propane
dmpe	1,2-bis(dimethylphospino)ethane
dppe	1,2-bis(diphenylphosphino)ethane
dcpe	1,2-bis(cyclohexylphosphino)ethane
d^{t}bpp	1,3-bis(di-tertbutylphosphino)propane
d^{t}bpx	1,2-bis(di-tertbutylphosphinomethyl)benzene
dcpp	1,3-bis(dicyclohexylphosphino)propane
d^{t}bpe	1,2-bis(di-tertbutylphopshino)ethane
dppb	1,4-bis(diphenylphosphino)butane
d^{i}ppx	1,2-bis(di-isopropylphospinomethyl)benzene
dcpx	1,2-bis(dicyclohexylphosphinomethyl)benzene
^{t}bcpx	1,2-bis(tertbutylcyclohexylphosphinomethyl)benzene
d^{t}ppx	1,2-bis(di-tertpentylphosphinomethyl)benzene
^{t}b^{t}ppx	1,2-bis(tertbutyltertpentylphosphinomethyl)benzene
dppx	1,2-bis(diphenylphosphinomethyl)benzene
dapp	1,3-bis(diadamantylphosphino)propane
dapx	1,2-bis(diadamantylphosphinomethyl)benzene
d^{i}ppe	1,2-bis(di-isopropylphosphino)ethane
d^{i}ppp	1,3-bis(di-isopropylphosphino)propane
d^{i}ppb	1,4-bis(di-isopropylphophino)butane
(S,S)-BDPP	(2S,4S)-2,4-bis(diphenylphosphino)pentane
(R,R)-Duphos	1,2-bis[(2R,5R)-2,5-dimethylphospholanyl]benzene

Chapter One

The reactions between carbon monoxide and ethene

1.1 Historical background

The reactions between carbon monoxide and ethene have attracted considerable interest from both academia and industry over the last few decades.[1-5] First, the two monomers, *i.e.* ethene and carbon monoxide, are quite cheap and readily available. Second, this reaction can give rise to a broad spectrum of products, which can range from high melting thermoplastic polymers – the so called "polyketones" – to low boiling liquids such as methyl propanoate. The former materials are very interesting from different points of view. In fact it is reported that a perfect alternating CO/C_2H_4 copolymer, because of its crystallinity, has high mechanical strength, making these copolymers very interesting as new thermoplastic materials.[6] Moreover, because of the relative reactivity of the carbonyl group (especially in photochemical reactions) present in the polymer backbone, these polyketones are expected to constitute a new class of photodegradable and, perhaps, biodegradable polymers.[7,8] Finally, because of the ease with which the carbonyl group can be chemically modified, the polyketones serve as excellent starting materials for other classes of functionalised polymers.[9-12] As a result of all this interest, Shell has recently started the production of these polyketones on an industrial scale.[13] The first commercial polymer is an ethene/propene/CO terpolymer which is marketed by Shell under the trade name of Carilon. Recently, methyl

propanoate has also attracted interest as a possible intermediate for the production of methyl methacrylate (see section 1.5).

The first example of non-alternating CO/C_2H_4 copolymerisation was reported in the late 1940s.[14] At that time, a free radical process was used under very extreme conditions (500-1500 bar). The product obtained was a polymer with a low molecular weight containing branched molecular structures and irregular carbon monoxide incorporation.

In 1951 Reppe and Mangin reported the first example of a metal-catalysed process.[15] They used the complex $K_2[Ni(CN)_4]$ in water; as products they obtained low melting oligomers, in addition to diethyl ketone and propionic acid. In the early 1970s, Shryne and Holler succeeded in improving the catalyst by the addition of strong acids such as TfOH and TsOH in solvents such as hexafluoroisopropanol.[16] With that system, they obtained a polymer with a relatively high molecular weight, but the yield of polymer per gram of catalyst was still low. Recently Klabunde[17] has reported a new nickel catalyst, based on a bidentate P-O anionic ligand. With all these nickel catalysts, the copolymerisation has to be started with pure ethene.

At the same time, rhodium catalysts were also investigated,[18] but gave low molecular weight copolymer and also the rates of formation of the products were low.

The most successful route to polyketones as well as methyl propanoate has been that using palladium catalysts. These were first disclosed by Gouch at ICI in 1967.[19] He used bis(tertiaryphosphine)palladiumdichloro complexes as catalysts. The disadvantage was that severe conditions were required (250°C, 2000 bar) and that yields in gram of polymer/gram of palladium were low. During the following 15 years only small advances were made in increasing catalyst efficiency.[20] In

particular, Sen[21] reported that cationic bis(triphenylphosphine)-palladium tetrafluoroborate complexes in aprotic solvents such as dichloromethane, produced C_2H_4/CO copolymers under very mild conditions. The reaction rates were, however, very low as were the molecular weights.

In addition to the synthetic problems mentioned above, insurmountable processing problems were encountered for the resulting polymers. Extensive crosslinking under melt processing conditions led to a lack of significant thermoplastic properties of the resulting materials, and this also presented a major development hurdle. At the end of the 1970s, it was therefore concluded (1) that the polymer backbone of polyketone was inherently unstable and (2) that polyketones could not be efficiently produced. Both conclusions proved to be invalid.

In the early 1980s, workers at Shell could demonstrate melt processability of polyketone produced by palladium cyanide catalysts, after extensive extraction of catalyst residues from the polymers and blending these with other polymers. From these studies, it was suggested that thermoplastic properties were possible in principle, and that the polyketone backbone was not inherently unstable in the melt as previously concluded. However, catalyst extraction did not offer a viable production option from a technical and economical viewpoint.

At the same time, another big development occurred, as a consequence of research at Shell in Amsterdam. Cationic palladium complexes containing tertiary phosphine ligands and weakly co-ordinating anions (*e.g.* sulfonates) were studied in MeOH as catalysts for the synthesis of methyl propanoate from CO and ethene. Experiments in which bidentate tertiary phosphine ligands were used, surprisingly gave no methyl propanoate; instead high molecular weight polyketone was formed at very high rates. These catalysts[22] are very active, and high yields have been achieved

under economically attractive conditions (90°C, 45 bar). Also, the catalysts are easy to prepare either separately or *in-situ*.

1.2 Production of polyketone; the Shell process

The discovery made by Shell of a very efficient catalyst for the synthesis of polyketone has persuaded a lot of scientific research groups all around the world to focus their attention to the study of this new catalytic process. A lot of work has been done in order to understand the mechanism of the reaction;[3,4,23,24] moreover, new catalytic systems have been developed (see Section 1.3). In all cases, the Shell process remains the central point in order to understand this new technology. Hence, it will be described in detail in the rest of this section.

1.2.1 General features

Usually, the catalyst is formed *in-situ* by mixing in MeOH a Pd(II) salt (*e.g.* $Pd(OAc)_2$) with a diphosphine, *e.g.* $Ph_2P(CH_2)_nPPh_2$ (n = 1-6, Pd/phosphine = 1:1), in order to obtain polyketone, or an excess of PPh_3 if methyl propanoate is the desired product. Then, an acid (usually TsOH) is added. Polyketone is formed according to eq. 1.1.

$$nC_2H_2 + nCO + MeOH \longrightarrow H(CH_2CH_2CO)_nOCH_3 \qquad (1.1)$$

The formation of methyl propanoate can be considered to be a particular case of the polymerisation process, which involves only the initiation and termination steps, without the propagation processes. A typical reaction rate would be ~10^4 mol of converted ethene (mol of Pd)$^{-1}$ h^{-1} to give a polymer with an average molecular weight (M_n) of ~20000 (dppp/TsOH/MeOH, 65°C).[3,25] Under suitable conditions, the catalysts are highly stable and total conversions of more than 10^6 mole of ethene per mole of Pd can be obtained.

Different factors can control both the reaction rate and the molecular weight of the product, *i.e.* the amount and the nature of the acid, the ligand, the solvent, the temperature, the pressure and composition of the gas, the use of particular promoters. As described above, ligand variation can lead to large changes in the product formed. The most noteworthy effect is the change of selectivity from polyketone to methyl propanoate by passing from a bidentate to a monodentate phosphine. Furthermore, varying the nature of the bidentate ligand also results in significant changes in the activity and selectivity of the process. This topic will be further discussed in Section 1.5, where some new diphosphine ligands, which contradict the previous statement, will be described.

For the moment, only the production of polyketone will be analysed. Table 1.1[4] shows the effect of changing the chain length, m, of the diphosphine, $Ph_2P(CH_2)_mPPh_2$, on the rate and molecular weight. The best results are obtained when m=3, whereas both the rate and molecular weight rapidly decrease by either increasing or decreasing the chain length. It has been suggested[4] that the control exerted by the phosphine is due to its ability to stabilise both square-planar and trigonal-bipyramidal geometries, the maximum activity being observed for phosphines in which the bite angle (P-Pd-P) allows complexation in both geometries.

Table 1.1

Synthesis of polyketone: the effect of variation of the chain length between bidentate phosphine groups [a]

$Ph_2P(CH_2)_mPPh_2$ (m)	Product [b] $H(CH_2CH_2CO)_nOCH_3$ (ñ)	Reaction rate [c] (g/g Pd.h)
1	2	1
2	100	1000
3	180	6000
4	45	2300
5	6	1800
6	2	5

[a] Reaction carried out in 150 ml MeOH with $Pd(MeCN)_2(TsO)_2$ (0.1 mmol), and $Ph_2P(CH_2)_mPPh_2$ (0.1 mmol); $C_2H_4/CO=1$; the temperature was maintained at 357 K; the pressure was maintained at 4.5 MPa. See ref.4. [b] The averaged degree of polymerisation determined by end-group analysis from ^{13}C NMR spectra, except for the low molecular weight products, where a combination of GC and NMR was used. [c] Reaction time was between 1 and 5 h; the rate was the highest measured during the reaction period.

Further studies have subsequently shown that the activity of the catalyst correlates better with the parallel pocket angle ($\theta_\parallel$) rather than with the bite angle (see Table 1.2).[26] In fact, if the bite angle was the most important factor, then (dmpe)Pd[C(O)^{t}Bu]Cl, (dppe)Pd[C(O)^{t}Bu]Cl and (dcpe)Pd[C(O)^{t}Bu]Cl should exhibit similar catalytic behaviours, which they do not. It appears from this work that there is an optimum size for the active site, which corresponds to a value of $\theta_\parallel$ of 106-108°. If $\theta_\parallel$ is too small, then ethene is precluded from complexation (see

Scheme 1.1). If $\theta_{\parallel}$ is too big, two different explanations have been proposed for the low catalytic activity. (1) The lack of steric hindrance about palladium could provide a facile pathway for the decomposition of the active catalyst. (2) Large $\theta_{\parallel}$ can favour the formation of stable metallacycles, which oppose the insertion of the next monomer unit. Which explanation is true depends on the ligand used. Palladium metal is in fact observed during reactions using dmpe, but not using dppe.

Table 1.2

Catalytic activity and pocket angles for a series of palladium phosphine complexes

Phosphine	Bridge Length	Initial Rate dP/dt(psi.min^{-1})	Total Polymer Yield (g)	Parallel Pocket Angle	Perpendicular Pocket Angle
dppe	2	0.19	0.22	132	129
dppp	3	0.75	1.42	108	146
dppb	4	0.12	0.03	93	102
dmpe	2	not reported	none	141	174
dcpe	2	0.83	1.25	106	115

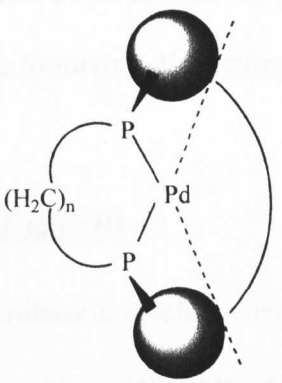

Parallel Pocket Angle

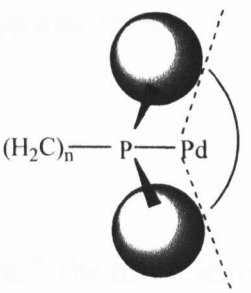

Perpendicular Pocket Angle

Scheme 1.1

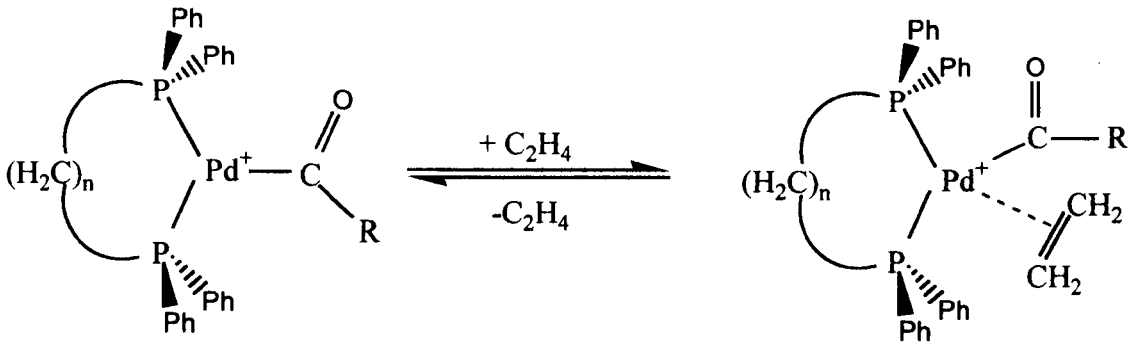

1.2.2 Mechanism of polymerisation

Most of the mechanistic considerations about the formation of polyketone have been proposed on the basis of the analysis of the end-groups of the products. Some more detailed studies appeared in the literature and will be discussed in Section 1.4. It is important to note that the ligand used affects not only the activity and selectivity of the catalyst, but sometimes also some changes in the mechanism have been proposed. Therefore, it is difficult to draw general conclusions on the mechanism by comparing results obtained with different systems. Despite that, it is possible to outline some basic characteristics, which are common to most of the systems studied. Most of these results have been reviewed by Drent,[3,4,25] which is the source for the following discussion unless otherwise stated.

1.2.2.1 Initiation

Two initiation mechanisms are possible.[4] The first initiation pathway involves the formation of a palladium carbomethoxy species,[27] by CO insertion into a

palladium methoxide (eqs. 1.2 and 1.3) or by direct attack of MeOH on co-ordinated CO (eqs. 1.4 and 1.5).

$$L_2Pd^{2+} + MeOH \longrightarrow L_2Pd(OMe)^+ + H^+ \quad (1.2)$$

$$L_2Pd(OMe)^+ + CO \longrightarrow L_2Pd(COOMe)^+ \quad (1.3)$$

$$L_2Pd^{2+} + CO \longrightarrow L_2Pd(CO)^{2+} \quad (1.4)$$

$$L_2Pd(CO)^{2+} + MeOH \longrightarrow L_2Pd(COOMe)^+ \quad (1.5)$$

The next step is the insertion of ethene in the Pd-COOMe bond (eq. 1.6)

$$L_2Pd(COOMe)^{2+} + C_2H_4 \longrightarrow L_2Pd(CH_2CH_2COOMe)^+ \quad (1.6)$$

The second initiation pathway involves the insertion of ethene into a palladium hydride (eq. 1.7), followed by CO insertion into the Pd-C bond of the resulting Pd-ethyl complex (eq. 1.8).

$$L_2PdH^+ + C_2H_4 \rightleftharpoons L_2Pd(CH_2CH_3)^+ \quad (1.7)$$

$$L_2Pd(CH_2CH_3)^+ + CO \rightleftharpoons L_2Pd(COCH_2CH_3)^+ \quad (1.8)$$

These two steps are believed to be both rapid and reversible, whereas the second ethene insertion (eq. 1.9) is irreversible and traps the acyl to start the chain propagation.

$$L_2Pd(COCH_2CH_3)^+ + C_2H_4 \longrightarrow L_2Pd(CH_2CH_2COCH_2CH_3)^+ \quad (1.9)$$

Many different hypotheses have been advanced to account for hydride formation:

i) by β-hydrogen elimination from a palladium methoxide (eq. 1.10)

$$L_2Pd^{2+} + MeOH \longrightarrow L_2PdH^+ + CH_2O + H^+ \quad (1.10)$$

ii) *via* the water-gas shift reaction (eq. 1.11)

$$L_2Pd^{2+} + CO + H_2O \longrightarrow L_2PdH^+ + CO_2 + H^+ \quad (1.11)$$

iii) by a Wacker-type oxidation of ethene (eq. 1.12)

$$L_2Pd^{2+} + MeOH + C_2H_4 \longrightarrow L_2PdH^+ + CH_2{=}CHOMe + H^+ \quad (1.12)$$

iv) by hydrogen activation (when H_2 is added, eq. 1.13)

$$L_2Pd^{2+} + H_2 \longrightarrow L_2PdH^+ + H^+ \quad (1.13)$$

During the catalysis, hydrides can also be produced by two termination steps:

v) by alcoholysis (eq. 1.14)

$$L_2PdCOP^+ + MeOH \longrightarrow L_2PdH^+ + PCOOMe \qquad (1.14)$$

vi) by β-hydrogen elimination (eq. 1.15)

$$L_2PdCH_2CH_2COP^+ \longrightarrow L_2PdH^+ + CH_2{=}CHCOP \qquad (1.15)$$

In MeOH, vinyl ketone end-groups have never been observed, but their presence is considerable in strongly polar but aprotic solvents.

1.2.2.2 Propagation

The catalytically active species in polyketone formation is thought to be a d^8 square-planar cationic complex L_2PdP^+, where L_2 represents the bidentate ligand and **P** is the growing polymer chain. The fourth co-ordination site at palladium may be filled by an anion, a solvent molecule, a carbonyl group of the chain or a monomer molecule. The competition among all these species is very important for the catalysis, and explains the sensitivity of the system to the choice of solvent and anion. The two alternating propagation steps are migratory insertion of CO into a palladium-alkyl bond [28] (eq. 1.16) and migratory insertion of ethene into the resulting palladium-acyl bond (eq. 1.17).

$$L_2PdCH_2CH_2P^+ + CO \longrightarrow L_2PdCOCH_2CH_2P^+ \qquad (1.16)$$

$$L_2PdCOP^+ + C_2H_4 \longrightarrow L_2PdCH_2CH_2COP^+ \quad (1.17)$$

Ethene insertion is the slowest (rate-determining) and irreversible step.[25] The reason for the perfect alternation is probably the stronger co-ordination of CO to Pd(II) compared with ethene. Once a Pd-alkyl is formed, the stronger CO co-ordination ensures that the next monomer to insert will usually be a CO molecule.[29] Of course, CO also co-ordinates more strongly to a Pd-acyl but since CO insertion is thermodynamically unfavourable,[30] the system will now wait for an ethene molecule to displace CO, to co-ordinate and insert. This competition between ethene and CO also explains the necessity of using a high C_2H_4/CO ratio, in order to have high rates of product formation.

1.2.2.3 Termination

The two most relevant termination pathways in MeOH are:

a) protolysis of the Pd-alkyl bond (eq. 1.18).

$$L_2PdCH_2CH_2COP^+ + MeOH \longrightarrow L_2PdOMe^+ + EtCOP \quad (1.18)$$

b) alcoholysis of the Pd-acyl bond (eq. 1.14).

Hence, two catalytic cycles are possible: a methoxy cycle, starting with a Pd-OMe species and terminating by a protolysis process, and a hydride cycle, starting with a Pd-H complex and terminating by alcoholysis. Each cycle produces a polymer which contains a keto and an ester-group (keto-ester).

CH_3-CH_2-(-$COCH_2CH_2$-)$_n$-$COOCH_3$ $n \geq 0$

keto-ester **1**

CH_3-O-(-$COCH_2CH_2$-)$_n$-$COOCH_3$ $n \geq 1$

diester **2**

CH_3-CH_2-(-$COCH_2CH_2$-)$_n$-$COCH_2CH_3$ $n \geq 0$

diketone **3**

End group analysis of the CO/ethene copolymer by ^{13}C NMR has demonstrated the presence of 50% ester and 50% ketone groups.[3] It is not *a priori* clear which group is the head and which is the tail of the polymer. Moreover, GC and MS analyses of oligomer fractions show, in addition to the expected keto-ester product, the presence of diester and diketone compounds. At low temperature (≤85°C), the majority of the products are keto-esters, with only small, but balanced, quantities of diesters and diketones. At higher temperatures (≥85°C), the same products are produced in a ratio (**1/2/3**) close to 2:1:1. This product distribution has been explained assuming that at high temperature both the catalytic cycles are operating and that they are connected by cross termination steps (see Scheme 1.2). However, at low temperature only one cycle seems to operate, and between the two proposed the hydride one is the more probable.[4]

Scheme 1.2

Proposed mechanism of ethene/CO co-polymerisation

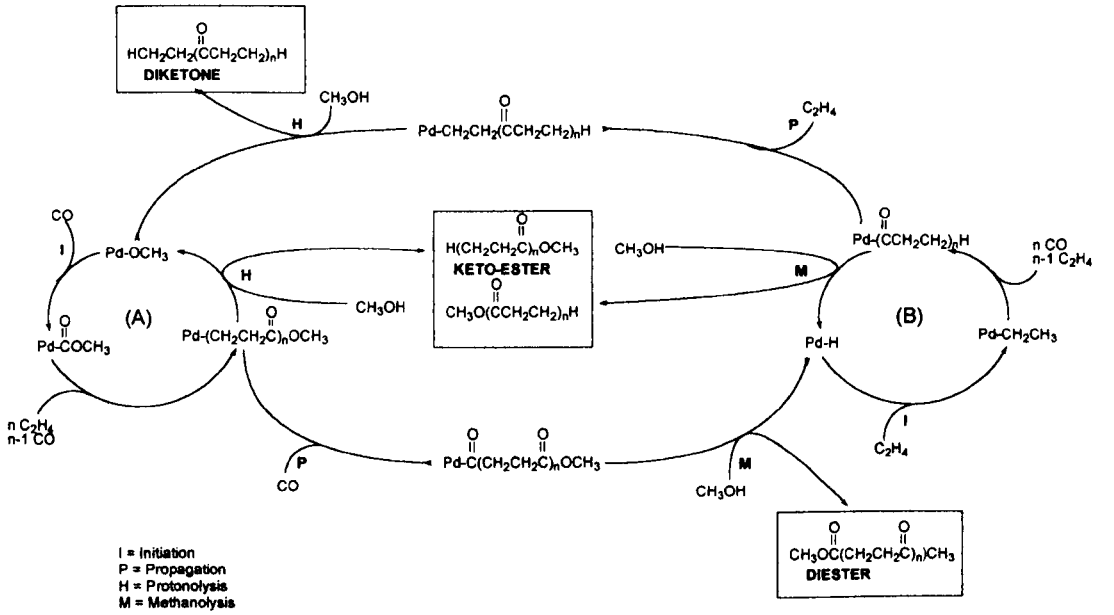

1.2.3 The role of the acid

In these catalysts the main role of the acids HX is to introduce the anion, according to eq. 1.19.

$$L_2Pd(OAc)_2 + 2HX \longrightarrow L_2PdX_2 + 2AcOH \qquad (1.19)$$

In fact, in some cases, a metal salt of the anion can be used instead of the free acid. The effect of the anion is shown in Table 1.3. It is evident that the reaction rate increases greatly on going from a strongly co-ordinating anion, like chloride, to a weakly or completely non co-ordinating one, like p-toluenesulfonate or tetrafluoroborate. This observation can be explained by a competition between the anion and the monomers for the co-ordination sites of the metal.

Table 1.3

Synthesis of polyketone: the effect of the anion [a]

Acid Added Type	Acid Added Amount (mmol)	Product $H(CH_2CH_2CO)_nOCH_3$ (n̄)	Reaction Rate (g/g Pd.h)
HCl [b]	2.0	50	30
TsOH [b]	2.0	50	5000
TfOH	0.20	150	6900
TsOH	0.20	150	6200
HBF_4	0.20	115	5000
AcOH	10.0	-	-
CCl_3COOH	0.20	>100	300
TFA	0.20	200	6000

[a] Reaction carried out in 50 ml MeOH with $Pd(OAc)_2$ (0.1 mmol) and dppp (0.1 mmol, except [b]) at 90°C and 4.0 MPa CO/ethene (1:1). Ref.4. [b] 0.15 mmol dppp, 115°C and 4.5 MPa.

A weakly co-ordinating anion favours co-ordination of the monomer and, hence, speeds up the reaction rate.

The amount of added acid also plays an important role.[31] In general, the best results are obtained with a significant excess of acid with respect to that required by eq. 1.19 (see Figure 1.1). The beneficial effect of the excess acid may have several origins. The acid may increase the concentration of $[Pd\text{-}H]^+$ species reactivating the complexes of Pd(0) which inevitably form in the reducing reaction medium.

Figure 1.1

Influence of the amount of the added acid

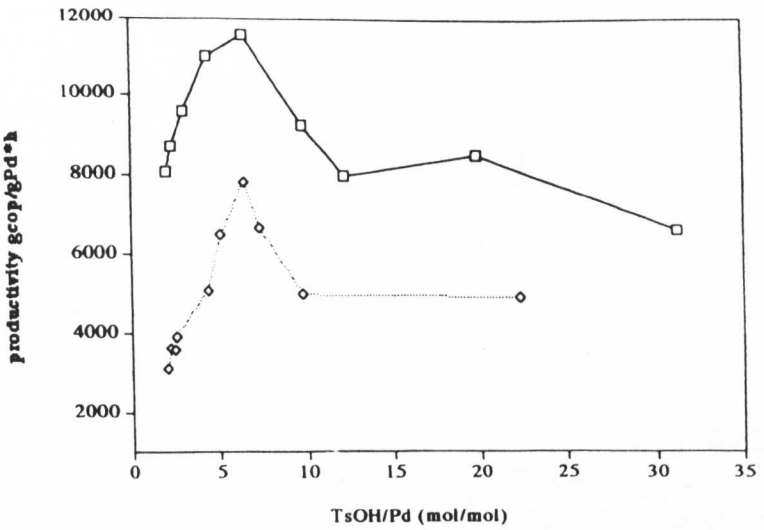

Influence of the dppp/Pd ratio on the productivity. Run conditions: pressure: dotted line 45 atm, solid line 60 atm; temperature: 90°C; MeOH: dotted line 50 ml; solid line 80 ml; [Pd]: dotted line 5.6×10^{-5} mol $\cdot l^{-1}$, solid line 4.5×10^{-5} mol $\cdot l^{-1}$; Pd/dppp = 1/1 (mol/mol); [H_2O] dotted line 100 ppm; solid line 800 ppm, (w/w); reaction time: 2 h.

Moreover, the acid can shift equilibria of the type 1.20 towards more active monomeric species.[32]

$$2[L_2Pd(H_2O)_2]^{2+} \rightleftharpoons [L_2Pd(\mu\text{-}OH)_2PdL_2]^{2+} + 2H^+ \qquad (1.20)$$

The fact that the productivity decreases with increasing concentration of palladium (see Figure 1.2) gives further support to the previous hypothesis that in solution there are monomeric catalytic species in equilibrium with dimeric ones, and that the latter are less active.

However, at high acid concentrations, the acid becomes a poison, because the anion can compete with the monomers for the co-ordination sites of the metal.

Figure 1.2

Influence of the concentration of the catalyst precursor

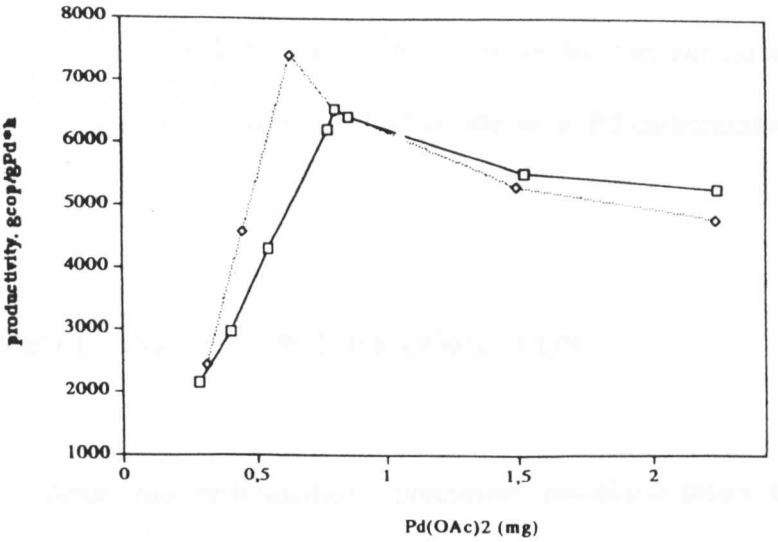

Influence of the concentration of the catalyst precursor on the productivity. Run conditions: pressure: dotted line 45 atm, solid line 60 atm; temperature: 90°C; MeOH: dotted line 50 ml; solid line 80 ml; Pd/dppp/TsOH: 1/1/2 (mol/mol); [H_2O]: dotted line 450 ppm; solid line 400 ppm. (w/w); reaction time: 2 h.

1.2.4 The role of oxidant promoters

The copolymerisation catalysts generally show a higher activity in the presence of added oxidants like quinones. Rate enhancements vary from 2-15 for catalysts based on diphosphines [33] to more than 200 for bipyridine-type ligands.[34] These rate enhancements are not due to faster propagation, since chain lengths are not affected by the addition of oxidants. Therefore, added quinones must cause the participation of a larger number of active centres. As discussed before, a chain can be started either from a palladium hydride or from a carbomethoxy species. Both initiation reactions are rapid, at least for alkyl olefins. Initiation by a hydride gives alkyl end groups, while initiation by a carbomethoxy gives an ester end group. Termination can produce either a hydride (by β-elimination or methanolysis) or a

methoxide (by protonolysis) which is rapidly converted to a carbomethoxy species. Addition of low concentrations of oxidants does not affect the chain length (and therefore the propagation or termination steps) but results in a greater proportion of ester end groups. This means that it causes more chains to start *via* carbomethoxy species. Quinones can in fact oxidise a Pd-hydride to a Pd-carbomethoxide (eq. 1.21).

$$L_2PdH^+ + Q + MeOH + CO \longrightarrow L_2PdCOOMe^+ + QH_2 \qquad (1.21)$$

If both hydride and carbomethoxy precursors remained intact until they started a new chain, and (as suggested above) both initiation steps were rapid relative to propagation, oxidants could affect the end groups (*via* eq. 1.21) but should not affect the rate. The fact that they do indicates that the palladium hydride can drop out the catalytic cycle. The most obvious way for it to do so is by decomposition to Pd(0).

$$L_2PdH^+ \rightleftharpoons L_2Pd + H^+ \qquad (1.22)$$

For complexes bearing nitrogen ligands, the Pd(0)-complex may immediately lose its ligand and precipitate as metallic palladium. For diphosphine systems, the Pd(0) complexes might have a reasonable stability. In the case of aryldiphosphines, they could combine with a Pd(II) species to form a palladium dimer, thus removing two Pd atoms from the catalysis.

$$L_2Pd + L_2Pd^{2+} \rightleftharpoons [L_2Pd]_2^{2+} \qquad (1.23)$$

Such palladium dimers have been detected by Dekker,[35] and one example has been structurally characterised.[36] Each of these three reactions (formation of Pd(0), precipitation of Pd metal, formation of Pd_2^{2+} dimers) reduces the rate at which palladium hydrides can reenter the catalytic cycle. Presumably, oxidants function by oxidising some or all these dead ends to Pd^{2+}, which can then immediately reenter the cycle.

$$[L_2Pd]_2^{2+} + 2H^+ + Q \longrightarrow 2\,L_2Pd^{2+} + QH_2 \qquad (1.24)$$

1.2.5 Selectivity. Polyketone vs. methyl propanoate

Under conditions of polyketone synthesis, cationic Pd(II) catalysts modified with excess monodentate phosphines and Bronsted acids of weakly co-ordinating anions, selectively give methyl propanoate with high rates. Methyl propanoate formation can be considered as the result of the polyketone initiation and termination steps, without the intervening propagation steps. As in polyketone catalysis two catalytic cycles are possible (see Scheme 1.3).[4] The absence of cycle-transfer products diethylketone and dimethyl succinate suggests that only one cycle is operative, but it is also possible that both cycles operate in isolation. The main difference between monodentate and bidentate phosphines is the fact that in the case of bidentate ligands the two phosphorus atoms are always in *cis*-position, hence the growing polymer chain and the empty fourth co-ordination site are always *cis* to each other, which is the most favourable position for insertion.

Scheme 1.3

Proposed Mechanisms for the formation of MeP

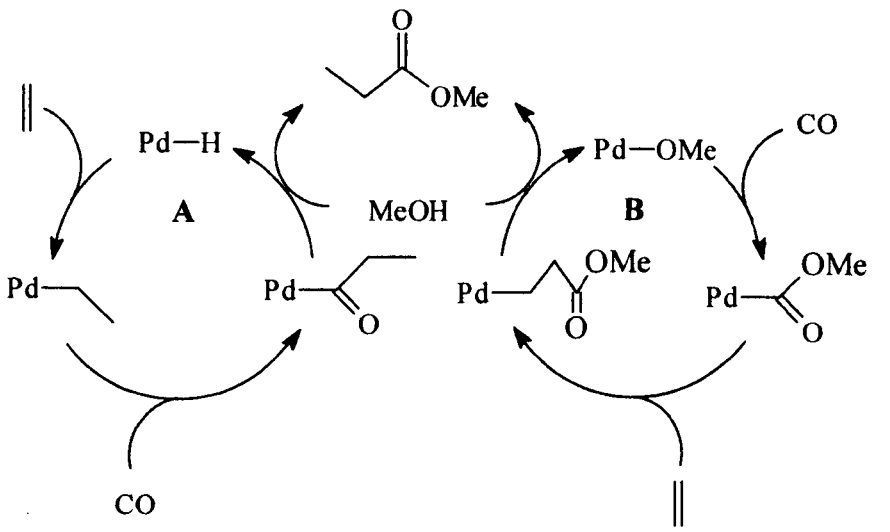

Hydride Cycle Methoxy Cycle

However, in the case of monodentate ligands a *trans* orientation is favoured, for steric reasons and probably also because it avoids the unfavourable situation of a Pd-P bond *trans* to a Pd-C bond. Moreover, because of the presence of excess ligand, *cis/trans* isomerisation is expected to be rapid.[37] It is reasonable to assume that both the insertion of ethene into a Pd-H bond and the insertion of CO into a Pd-alkyl can only occur when the reacting ligands are *cis*, requiring *cis* phosphines. Immediately after insertion, a *cis/trans* isomerisation is likely to occur, which places the chain and the fourth site *trans*, preventing further monomer insertion. These considerations about the change in selectivity are summarised in Scheme 1.4, where a hydride cycle has been assumed. If *cis/trans* isomerisation is suppressed (by the absence of excess ligand and/or at low temperature) one could expect a higher tendency to form oligomers. Indeed, it has been shown [21] that at low temperature in MeOH,

$[Pd(PPh_3)_2(CH_3CN)_2]^{2+}$ converts CO and ethene into methyl propanoate and a significant amount of keto ester oligomers.

Scheme 1.4

Effect of the nature of the phosphine on the selectivity

a) Monophosphine

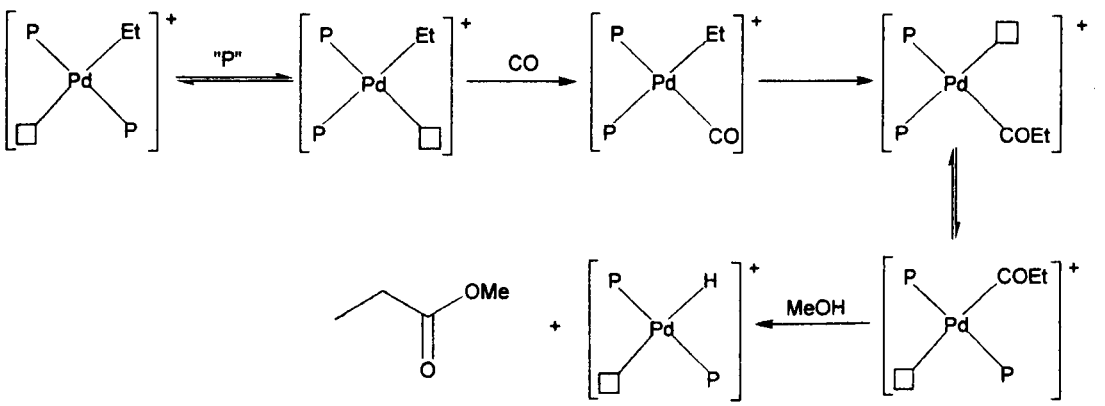

b) Diphosphine

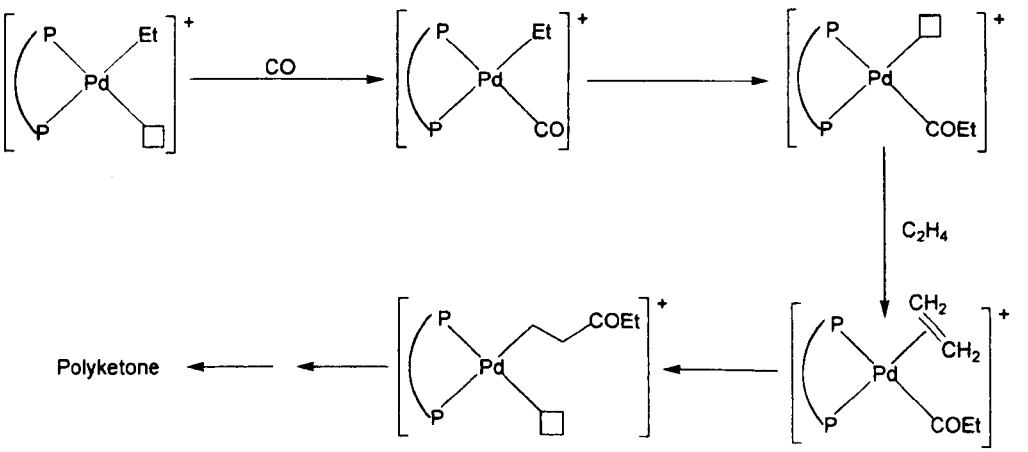

1.3 Other catalytic systems

The success of the Shell process has promoted much attention to this kind of chemistry. As a result, a lot of new catalytic systems have been investigated. Different metals have been studied in the past (*e.g.* cobalt,[38] rhodium,[18,39] nickel [16,17]), but giving results very far away from the ones obtained using palladium complexes. Hence, palladium remains, at the moment, the best choice for the copolymerisation of carbon monoxide and alkenes, and for the alkoxycarbonylation of olefins in general. A lot of different parameters (*i.e.* the ligand, the solvent, the olefin, the promoters) can be changed, resulting in a never ending list of possible new catalysts. Therefore, we will focus our attention on just some of them.

Diphosphines of general formula $Ph_2P(CH_2)_nPPh_2$ and monophosphines PR_3 are the widest used ligands in this kind of chemistry. With these ligands the catalyst is usually formed *in-situ*. Preformed complexes of the type L_2PdX_2 [27] and $L_2Pd(R)X$ [40] where L_2 represents the phosphine ligand, X a weakly co-ordinating anion, and R a hydrocarbyl group (*e.g.* methyl) have also been tested as catalysts. The results are, generally, very similar to those obtained with the catalysts prepared *in-situ*.

A lot of other diphosphine ligands, which differ from the standard dppp ligand because of different substituents on the phosphorus or/and because of a different backbone, have been studied. Some examples are reported in Scheme 1.5; other examples will be discussed in Section 1.5. A lot of different reasons have aimed the investigations of all these new ligands. The most obvious reason is, of course, the desire to find more active and selective catalysts. Moreover, the fact that it is possible to gradually change the electronic and steric properties of the phosphines allows, in theory, a better understanding of the relationships between

these factors and the catalyst performance. At present, however, this work has not been completely successful.

Scheme 1.5

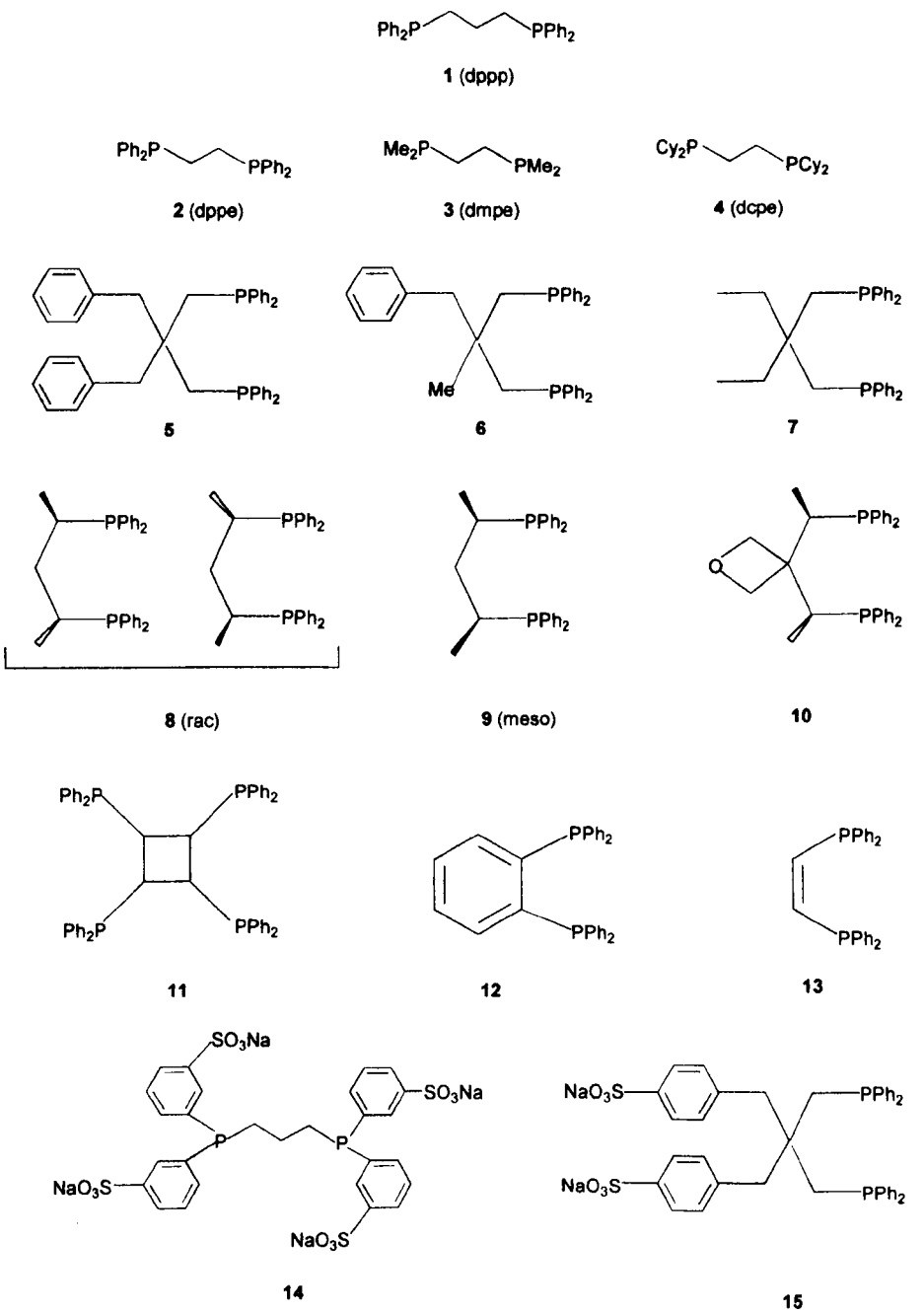

It has been shown in Section 1.2.1 that for diphosphines with an aliphatic $(CH_2)_n$ backbone, it is possible to correlate the activity with the parallel pocket angle.[26] Recent work by Bianchini [41] shows that for diphosphines with a C_2 backbone the activity for CO/ethene copolymerisation increases by decreasing the flexibility of the backbone (see Table 1.4).

Table 1.4

Effect of the backbone flexibility on the co-polymer productivity [a]

P-P Ligand [b]	Copolymer Productivity (Kg of polymer/g Pd)
2	1.1
11	9.8
12	6.4
13	5.5

[a] Conditions: catalyst (0.01 mmol $Pd(P\text{-}P)(OAc)_2$), MeOH (100 ml), BQ (0.8 mmol), TsOH (0.2 mmol), initial $p(C_2H_4)$ (300 psi), initial p(CO) (300 psi), temperature (85°C), time (3 h). Ref.42. [b] See Scheme 1.5 for the numeration of the P-P ligands.

Different dppp-analogue ligands have been also studied (entries **5-10** in Scheme 1.5), but the introduction of alkyl substituents in the 2-position of the carbon backbone of dppp does not significantly improve the catalytic performance of the dppp-based Pd(II) precursors.[42] Eventually, a decrease may be observed. In contrast, the productivity increases remarkably when methyl groups are introduced into the backbone at both 1-positions. These are, in all cases, only experimental trends observed for particular classes of diphosphine ligands. At present, the activity and

selectivity of the copolymerisation catalysts seem to be governed by a very complex web of electronic and steric effects and, therefore, it is not possible to draw general conclusions. Things are even more complicated. For instance, it has been shown that for CO/cyclopentene copolymerisation different ligands require different anions in order to obtain the best performances.[43]

Looking to Scheme 1.5, there are a few entries containing $-SO_3Na$ groups, This is in order to confer solubility in water to the catalyst and, hence, to carry out the copolymerisation process in water or in a biphasic system.[44]

Finally, palladium catalysis offers the possibility of reacting CO with a lot of different olefins, *i.e.* propene and higher homologues;[45] functionalised olefins in which the functionality is separated by at least one methylene group from the olefinic bond;[46] styrene and its functionalised analogues;[47] internal olefins.[43,48] This introduces new problems, like regioselectivity and stereoselectivity. Hence, the need to find an adequate ligand for every substrate.

For the same reasons, bidentate ligands with other donor atoms have also been studied. These include: P-O ligands (*e.g.* $Ph_2P(CH_2)_nCOOR$,[49] R = H, Me, Et, n =1-3), N-N ligands (*e.g.* phenanthrolines,[23,50] bis(arylamino)acenaphthene,[51] bipyridines [40,50]), N-O [52] and P-N [53] ligands and, even, carbene complexes. [54]

1.4 Mechanistic studies

As described above (Section 1.2), two different catalytic cycles (*i.e.* a hydride and a methoxy cycle) have been proposed for the copolymerisation of CO and ethene. It has been also shown that under certain conditions, they are believed to

operate at the same time. A third catalytic mechanism involving palladium carbene species has been proposed by Consiglio.[55] Subsequent work by Drent [3] and Sen [2] have ruled out this possibility; hence, there is now complete agreement for the assumption that copolymerisation takes place *via* a hydride or a methoxy route, or both at the same time. However, a detailed study to distinguish between these two mechanisms is very difficult. Most of the reasons in support of them and also in order to discriminate between them are usually inferred by end-group analysis of the polymer. The real polyketone catalytic systems are highly active, and intermediates are usually too reactive to isolate or even detect. Therefore, several groups have studied model systems using other ligands (mainly dinitrogen systems) and olefins (styrene, norbornene, norbornadiene) for which intermediates can be detected or sometimes isolated. While such model studies provide valuable background information, it is often difficult to translate the results to the real catalytic systems. Despite that, some *in-situ* studies have recently appeared in literature.[56-59] The main results obtained will be now briefly summarised.

1.4.1 Propagation

The mechanism for copolymer chain growth involves two sequential propagation steps: migratory CO insertion into the Pd-alkyl bond of the growing polymer chain followed by migratory ethene insertion into the resulting Pd-acyl bond. There is consensus that double CO insertion does not occur for thermodynamic reasons, while double ethene insertion is kinetically hampered due to the higher affinity of Pd(II) centres for CO over ethene.[58] Both these insertion processes have been widely studied on model compounds from a qualitative and quantitative point

of view. Some thermodynamic and kinetic data are available;[23,60] the major problem is that they depend a lot on the system considered and, therefore, generalisations are very difficult. In all cases, all these data suggest that olefin insertion is the rate-determining step in polyketone formation.[3] Moreover, all the studies on the effect of the anion, agree with the fact that the rates for the insertion processes increase by decreasing the co-ordinating ability of the anion.[61,62] This confirms that the anion can compete with the monomer during the propagation.

Another very interesting feature of the propagation process is that, after ethene insertion into a Pd-acyl complex, the carbonyl group is actually in the right position to occupy the fourth co-ordination site of the complex and form a five-membered palladacycle (see Scheme 1.6).

Scheme 1.6

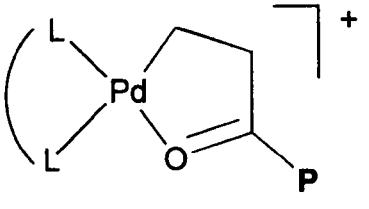

5-membered palladacycle

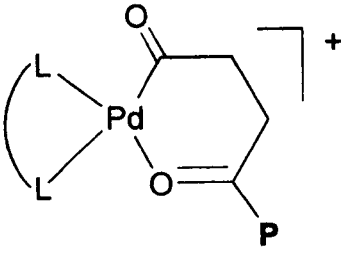

6-membered palladacycle

In the same way, further CO insertion can results in the formation of a six-membered palladacycle. The formation of both this class of compound has been confirmed spectroscopically [23,40,51-53,63] and, in some cases, it has been possible to isolate and characterise them in the solid state.[60] The formation of these palladacycles is very important. If they are too stable, they can slow down the

process, or even stop it. It should also be noted that a five-membered palladacycle is more stable than a six-membered one, and it is believed that one of the reasons for the perfect alternation of the polymer is the fact that ethene can open a six-membered palladacycle but not a more stable five-membered complex. Hence, only CO can react with the last one,[23] making it very difficult for the insertion of a second ethene unit.

As highlighted recently by Drent,[58] all the mechanistic studies published focus on copolymerisation on solution, while under actual process conditions (slurry or gas-phase), the initial single-site palladium catalyst is heterogenised and resides on the surface or in the bulk of the copolymer. So far, only one brief communication has appeared on this topic, which outlines the identification by PM-RAIRS of different intermediates involved in the CO/ethene copolymerisation at a single site Pd catalyst, [Pd(dppp)(CH_3)(OTf)].[58] On the basis of this study, a quite detailed mechanism for the propagation process has been proposed (see Scheme 1.7). Apart from the involvement of five and six-membered palladacycles, two other features are noteworthy. First, the fact that five co-ordinate palladium complexes are supposed to be formed during the process; other authors support this hypothesis.[62] Moreover, substitution reactions in square-planar complexes are usually believed to occur *via* penta-co-ordinate intermediates.[64,65] Second, it is established that during polymer growth ethene insertion into the Pd-acyl bond of the six-membered palladacycle is CO-assisted. This has never been observed during studies in solution, nor evaluated theoretically.[66]

Scheme 1.7

Proposed catalytic propagation cycle

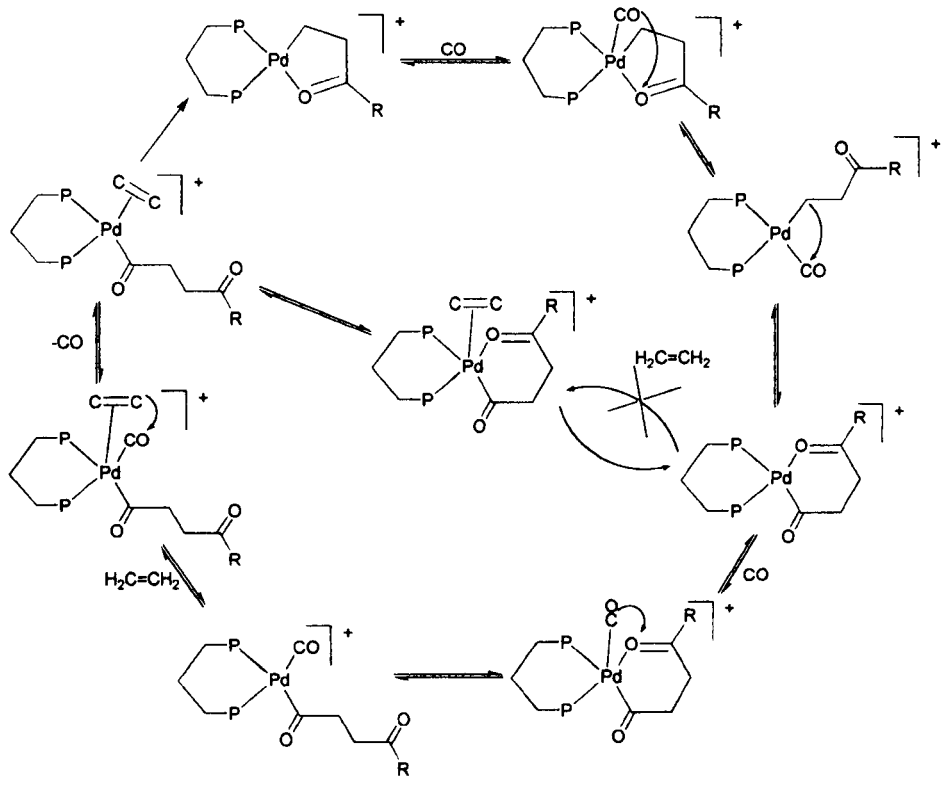

1.4.2 Initiation and termination

Chain initiation and termination mechanisms have been mostly discussed only on the basis of the end-group analysis of the polymer, and on how they are affected by changes in the copolymerisation conditions. Very few spectroscopic studies are available,[56,57] and they do not produce very clear results. In all cases, all these studies agree with the fact that the process proceeds *via* a hydride or a methoxy cycle. As mentioned before, the end-group analysis of low molecular weight oligomers obtained by copolymerisation of CO and ethene at high temperature in alcoholic media, results in a mixture of keto-ester, diketone and diester products,

indicating that in these conditions both the cycles are operative and they are also linked by cross-termination reactions. By contrast, at lower temperatures, keto-esters are mainly obtained, suggesting that only one mechanism is operating. Similar considerations apply to methyl propanoate production, though no temperature effect has been observed, *i.e.*. only one mechanism is always operating. It is very difficult to be sure which mechanism is correct, although most of the researchers in this area believe that under normal conditions the hydride mechanism is the preferred one. First, a change in the rate and product distribution is observed in MeOH when oxidants are added (see Section 1.2). As already discussed, these results can be easily interpreted by assuming that copolymerisation mainly proceeds *via* the hydride cycle in the absence of oxidants, whereas the methoxy cycle is the predominant when oxidants are added. Moreover, it has been noticed that addition of water or hydrogen results in copolymers with mainly ketone end-groups.[3] This effect can be explained assuming that, according to eqs. 1.11 and 1.13, water and hydrogen help the formation of hydride complexes. For higher olefins, the hydride cycle seems the preferred one also by considering the regiochemistry of the process.[24,67] As far as we know, an *in-situ* characterisation of some of the intermediates involved in the hydride cycle has been reported in only one case. [56] The system investigated in this case was the methoxycarbonylation of styrene in MeOH promoted by $Pd(OAc)_2/PPh_3/TsOH$; the hydride, the alkyl and the acyl complexes have been spectroscopically detected, and the hydride and the acyl also isolated in the solid state (but no X-ray structures). A quite detailed catalytic cycle for this process has, then, been proposed (see Scheme 1.8).

Scheme 1.8

Proposed catalytic cycle for the methoxycarbonylation of styrene

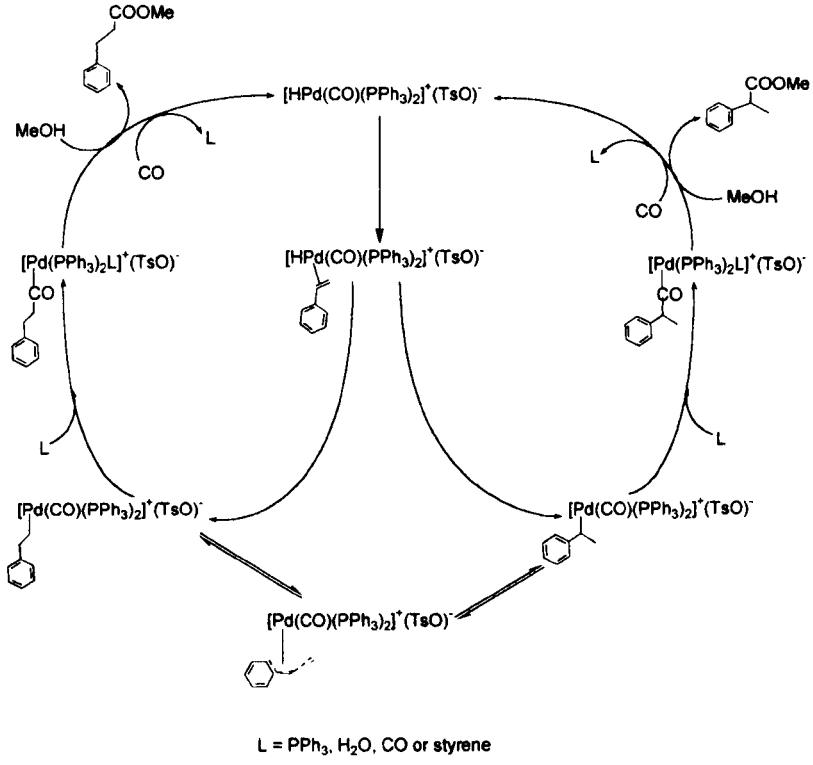

To the best of our knowledge, only one paper [57] disagrees with the fact that the hydride cycle is the preferred one in the absence of oxidants. Luo *et al.* have in fact recently reported an *in-situ* NMR, IR and EXAFS study on the CO/ethene copolymerisation promoted by a $Pd(OAc)_2$/dppp/CF_3COOH catalyst in MeOH. They do not have any evidence for the formation of the hydride intermediate. Moreover, from the IR data they conclude that a carbomethoxy species is formed. The problem is that they do not have any NMR evidence for this complex, and also the IR data are quite confused. Hence, the hydride hypothesis still remains the best one.

1.5 Recent developments. The Ineos process

Recent patents by Shell [68] and Ineos Acrylics (formerly ICI Acrylics) [69] partially contradict the hypothesis made in Section 1.2.5 about the relationship between the nature of the phosphine and the observed products. In particular, they have reported some examples of tertiary butyl substituted bidentate phosphines which give methyl propanoate in high yield and selectivity. In the Shell patent, the ligand 1,3-bis(di-*tert*-butylphosphino)propane (d^{t}bpp) is used, whereas the Ineos process is based on 1,2-bis(di-*tert*-butylphosphinomethyl)benzene (d^{t}bpx).

In the case of the Ineos process, the catalyst is formed *in-situ via* the reaction of Pd(d^{t}bpx)(dba) [dba = *trans,trans*-(PhCH=CH)$_2$CO] with *e.g.* $MeSO_3H$ in MeOH. The resulting catalytic system gives methyl propanoate (MeP) with a selectivity of 99.98% at a production rate of 50000 mol product (mol Pd)$^{-1}$ h^{-1} under very mild conditions (353 K and 10 atm of CO-ethene).[70] These features make this process very attractive from a commercial point of view since MeP is an attractive precursor for the synthesis of methyl methacrylate.[71] It is noteworthy the fact that the catalyst based on $Pd(OAc)_2/PPh_3$ (excess)/TsOH gives MeP with a selectivity of 95% at a production rate of only 500 mol product (mol Pd)$^{-1}$ h^{-1}.[72]

Other bidentate ligands have been studied for the same process,[72] and the most relevant results are reported in Table 1.5. It is clear from these data that the best overall performance is obtained using d^{t}bpx as ligand. This catalytic system gives the best initial rate, turn over number and also selectivity. For example, the selectivity reported for the Shell catalyst based on d^{t}bpp is only 98%. From the data in Table 1.5, it is also evident that the activity and selectivity of the catalyst are greatly influenced by changing the substituents on the phosphorus atom and/or the

phosphine backbone. Both electronic and steric factors could influence the catalyst behaviour. The analysis of structural data of some Pd(P-P)(dba) complexes suggests a relationship between the selectivity of the catalyst and the parallel pocket angle (see Table 1.6). In particular, it seems that a small parallel pocket angle is needed in order to achieve high selectivity on MeP.

Table 1.5

Influence of the P-P ligand in the methoxycarbonylation of ethene [a]

Ligand	Initial rate [b]	TON [c]	Selectivity	Lag Time [d]
d^{t}bpx	35000	24000	MeP	0
d^{i}ppx	5800	6000	MeP/co-poly	18
dcpx	0	0	trace co-poly	n/a
^{t}bcpx (1) [e]	1300	3500	MeP	37
^{t}bcpx (2) [e]	2300	5000	MeP	33
d^{t}ppx	1000	2400	MeP	45
^{t}b^{t}ppx	5800	6400	MeP	9
dppx	0	0	n/a	n/a
d^{t}bpp	9000	6000	MeP	not reported

[a] Catalyst formed *in-situ* from Pd(P-P)(dba) and $MeSO_3H$ in MeOH. [b] Maximum initial rate in moles product/mole catalyst/h. [c] Turn-over number in moles product/mole catalyst. [d] Time (in minutes) taken before maximum initial rate is attained. [e] The catalyst derived from d^{t}bcpx has been evaluated as two separate fractions, because it exists as different stereo-isomers.

In all cases, the behaviour of this tertiary butyl substituted bidentate phosphines is quite astonishing. Moreover, even the co-ordination chemistry seems to be quite different from that observed for complexes containing the ligands which are normally used for the synthesis of polyketone.

Table 1.6

Relationship between selectivity and parallel pocket angle for different Pd(P-P)(dba) catalysts

P-P	Parallel Pocket Angle	Perpendicular Pocket Angle	Bite Angle	Selectivity
d^{t}bpx	127.8	196.2	103.9	MeP
d^{i}ppx	157.92	277.2	104.3	MeP/co-poly
dcpx	150.5	220.3	103.9	MeP/co-poly
dppx	145.44	196.2	104.6	MeP/co-poly
dppp	156.2	205.2	94.9	co-poly

For example, dppp reacts with Pd(II) species as $Pd(OAc)_2$ and $Pd(PhCN)_2Cl_2$ resulting in the formation of $Pd(dppp)(OAc)_2$ and $Pd(dppp)Cl_2$, respectively, whereas d^{t}bpx reacts with $Pd(OAc)_2$ to give a tetrameric species containing metallated phosphines (see Scheme 1.9); the same reaction using d^{t}bpp results in the formation of $[Pd(d^tbpp)(OAc)_2]_4$ (see Figure 1.3).

The particular behaviour of this class of phosphines has been studied also by Spencer.[73] Protonation of M(P-P)(alkene) [M = Ni, Pd, Pt; P-P = dcpe, dcpp, d^{t}bpe, d^{t}bpp, d^{t}bpx; alkene = styrene, norbornene, ethene] results in the formation of quite unusual complexes. In the case of styrene, cationic η^3-methylbenzyl complexes are formed, whereas the formation of cationic alkyl complexes containing a β-agostic interaction is observed in the case of ethene and norbornene.

Scheme 1.9

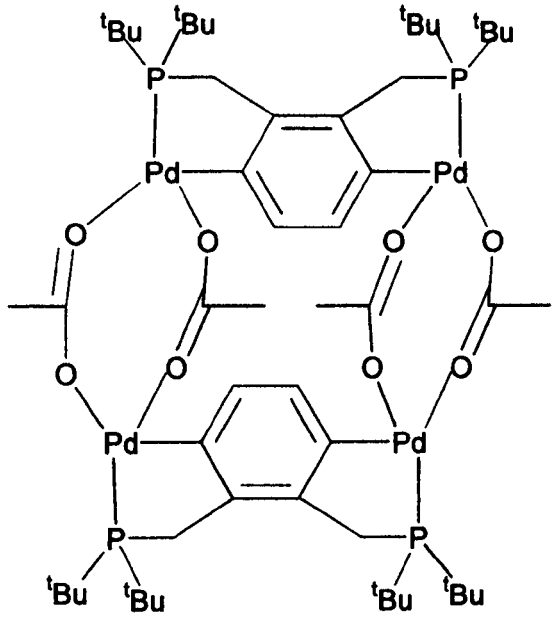

Figure 1.3

Structure of [Pd(d^{t}bpp)(OAc)$_2$]$_4$

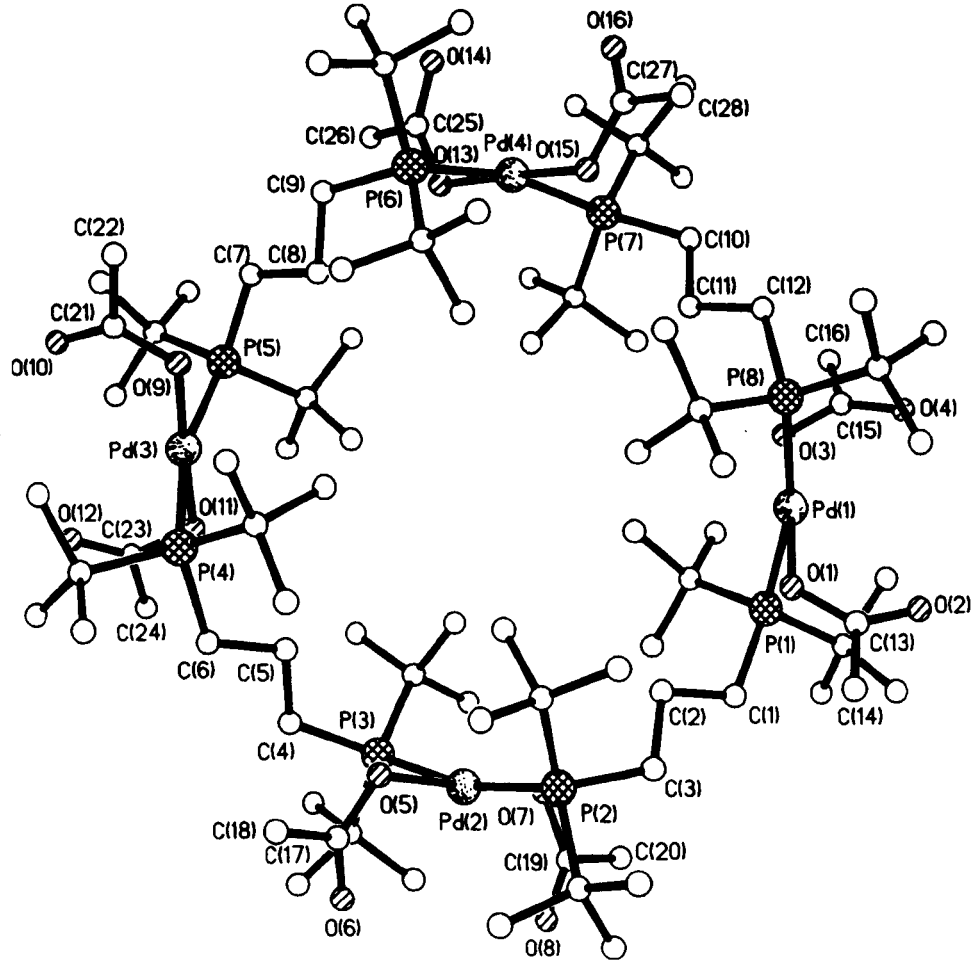

Moreover, in the case of ethene, it has been shown that there is an equilibrium between the ethyl agostic complex and a classic ethene-hydride complex, and the position of this equilibrium depends on the steric properties of the ligand (see Scheme 1.10). In the case of the more bulky d^{t}bpx and d^{t}bpp ligands, the non-classic ethyl-agostic complex is preferred.

Scheme 1.10

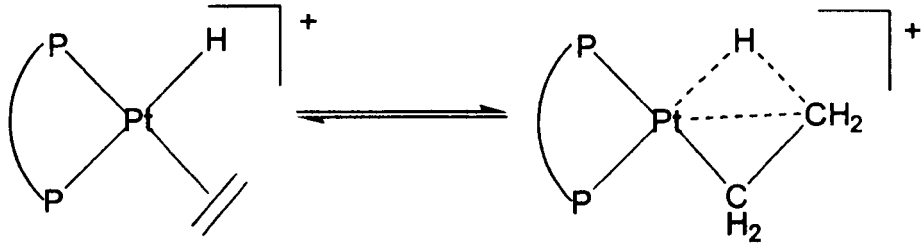

1.6 Aim and scope of this thesis

The results described in the last Section are quite surprising. Questions arise with regard to the reasons for this complete change in selectivity. Moreover, a fundamental question concerning the mechanism for the methoxycarbonylation of ethene remains unresolved. Ineos is making a big effort to develop this system into a commercial process. Therefore, a full understanding of the intermediates involved in the catalytic process becomes very important.

This thesis describes spectroscopic and preparative studies aimed at elucidating the mechanism involved in the methoxycarbonylation of ethene promoted by the palladium catalyst containing d^{t}bpx. This requires a full understanding of the

chemistry of this ligand together with a detailed step-wise investigation of the single components involved in the catalytic cycle. *In-situ* spectroscopic studies have also been found to be very important. Second, the reasons for the selectivity of the catalyst has been investigated by carrying out similar studies on other related ligands.

References for Chapter One

1. A. Sen, *Adv. Polym. Sci.*, **1986**, *73/74*, 125
2. A. Sen, *Acc. Chem. Res.*, **1993**, *26*, 303
3. E. Drent and P. H. M. Budzelaar, *Chem. Rev.*, **1996**, *96*, 663
4. E. Drent, J. A. M. van Broekhoven and M. Y. Doyle, *J. Organomet. Chem.*, **1991**, *417*, 235
5. A. Sen, *Chemtech.*, **1986**, 48
6. Numerous Patents by Shell. Representative examples: U.S. Patent 4,904,744 (1990); Eur. Pat. Appl. 400,719 (1990); Eur. Pat. Appl. 373,725 (1990); Eur. Pat. Appl. 360,358 (1990); Eur. Pat. Appl. 345,854 (1989)
7. M. Heskins and J. E. Guillet, *Macromolecules*, **1970**, *3*, 224
8. G. H. Hartley and J. E. Guillet, *Macromolecules*, **1986**, *1*, 413
9. M. M. Brubaker, D. D. Coffman and H. H. Hoehn, *J. Am. Chem. Soc.*, **1952**, *74*, 1509
10. Y. Moroshima, T. Takizawa and S. Murahashi, *Eur. Polym. J.*, **1973**, *9*, 669
11. A. Sen, Z. Jiang and J. T. Chen, *Macromolecules*, **1989**, *22*, 2012
12. Z. Jiang and A. Sen, *Macromolecules*, **1992**, *25*, 880
13. C. E. Ash, *J. Mater. Educ.*, **1994**, *16*, 1; D. Madema and A. Noordam, *Chemish Magazine*, **1995**
14. DuPont (M. M. Brubacher) U.S. Patent 2,459,286 (1950)
15. W. Reppe and A. Mangin, U.S. Paten 2,577,208 (1951); *Chem. Abstr.*, **1952**, *46*, 6143
16. T. M. Shryne and H. V. Holler, U.S. Patent 3,984,388 (1976); *Chem. Abstr.*, **1976**, *85*, 178219

17. U. Klabunde, T. H. Tulip, D. C. Roe and S. D. Ittel, *J. Organomet. Chem.*, **1987**, *334*, 141; U. Klabunde and S. D. Ittel, *J. Mol. Catal.*, **1987**, *41*, 123; U. Klabunde, U.S. Patent 4,698,403 (1987)

18. Y. Iwashita and M. Sakaruba, *Tetrahedron Lett.*, **1971**, *26*, 2409; A. Sen and J. S. Brumbaugh, *J. Organomet. Chem.*, **1985**, *279*, C5

19. A Gouch, British Pat. 1,081,304 (1967); *Chem. Abstr.*, **1967**, *67*, 100569

20. D. M. Fenton, U.S. Patent 4,076,911 (1978); K. Nozaki, U.S. Patent 3,835,123 (1974)

21. A. Sen and T. W. Lai, *J. Am. Chem. Soc.*, **1982**, *104*, 3520; A. Sen and T. W. Lai, *Organometallics*, **1984**, *3*, 866

22. E. Drent, Eur. Pat. Appl. 121,965,A2 (1984); *Chem. Abstr.*, **1985**, *102*, 46423

23. F. C. Rix, M. Brookhart and P. S. Wite, *J. Am. Chem. Soc.*, **1996**, *118*, 4746

24. M. Sperrle and G. Consiglio, *Chem. Ber.*, **1997**, *130*, 1557

25. E. Drent, J. A. M. van Broekhoven and P. H. M. Budzelaar, *Applied Homogeneous Catalysis with Organometallics Compounds*, ed. B. Cornils and W. A. Herrmann, VCH, 1996, p. 333

26. Y. Koide, S. G. Bott and A. R. Borrow, *Organometallics*, **1996**, *15*, 2213

27. Z. Jiang, G. M. Dahlen, K. Houseknecht and A. Sen, *Macromolecules*, **1992**, *25*, 2999

28. P. W. N. M. van Leeuwen, C. F. Roobeeck and H. J. Van der Heijden, *J. Am. Chem. Soc.*, **1994**, *116*, 12117

29. F. C. Rix and M. Brookhart, *J. Am. Chem. Soc.*, **1995**, *117*, 1137

30. J. T. Chen and A. Sen, *J. Am. Chem. Soc.*, **1987**, *109*, 148

31. A. Vavasori and L. Toniolo, *J. Mol. Cat. A*, **1996**, *110*, 13

32. C. Pisano, G. Consiglio, A. Sironi and M. Moret, *J. Chem. Soc. Chem. Commun.*, **1991**, 421

33. J. A. M. van Broekhoven and E. Drent, Eur. Pat. Appl. 235,865 (1987); *Chem. Abstr.* , **1988**, *108*, 76068

34. E. Drent, Eur. Pat. Appl. 229,408 (1986); *Chem. Abstr.*, **1988**, *108*, 6617

35. G. P. C. M. Dekker, C. J. Elsevier, K. Vrieze, P. W. N. M. van Leeuwen and C. F. Roobeek, *J. Organomet. Chem.*, **1992**, *430*, 357; R. van Asselt, E. C. G. Gielens, E. R. Rulke, K. Vrieze and C. J. Elsevier, *J. Am. Chem. Soc.*, **1994**, *116*, 977

36. P. H. M. Budzelaar, P. W. N. M. van Leeuwen, C. F. Roobeek and A. G. Orpen, *Organometallics*, **1992**, *11*, 23

37. D. G. Cooper and J. Powell, *Can J. Chem.*, **1973**, *51*, 1634; D. A. Redfield and J. H. Nelson, *Inorg. Chem.*, **1973**, *12*, 15

38. W. F. Gresham and R. E. Brooks, U.S. Patent 2,542,767 (1951)

39. G. Consiglio, B. Studer, F. Oldani and P. Pino, *J. Mol. Catal.*, **1990**, *58*, L9

40. M. Brookhart, F. C. Rix, J. M. DeSimone and J. C. Barborak, *J. Am. Chem. Soc.*, **1992**, *114*, 5894

41. C. Bianchini, H. M. Lee, A. Meli, W. Oberhauser, F. Vizza, P. Bruggeller, R. Haid and C. Langes, *Chem. Commun.*, **2000**, 777

42. C. Bianchini, H. M. Lee, A. Meli, S. Monetti, F. Vizza, M. Fontani and P. Zanello, *Macromolecules*, **1999**, *32*, 4183

43. E. Amevor, R. Burli and G. Consiglio, *J. Organomet. Chem.*, **1995**, *497*, 81

44. G. Verspui, G. Papadogianakis and R. A. Sheldon, *Chem. Commun.*, **1998**, 401; C. Bianchini, H. M. Lee, A. Meli, S. Monetti, V. Patinec, G. Petrucci and

F. Vizza, *Macromolecules*,**1999**, *32*, 3859; G. Vespui, I. I. Moiseev and R. A. Sheldon, *J. Organomet. Chem.*, **1999**, *586*, 196

45. E. Drent and R. L. Wife, Eur. Pat. Appl. 181,014 (1985); A. Battistini, G. Consiglio and U. W. Suter, *Angew. Chem.*, **1992**, *104*, 306; M. Barsacchi, A. Battistini, G. Consiglio and U. W. Suter, *Macromolecules*, **1992**, *25*, 3604

46. E. Drent, Eur. Pat. Appl. 272,727 (1988); *Chem. Abstr.*, **1988**, *109*, 191089; Eur. Pat. Appl. 463,689 (1992); *Chem. Abstr.*, **1992**, *116*, 129879

47. M. Barsacchi, G. Consiglio, L. Medici, G. Petrucci and U. W. Suter, *Angew. Chem.*, **1991**, *103*, 992

48. Z. Jiang and A. Sen, *J. Am. Chem. Soc.*, **1995**, *117*, 4455

49. G. J. P. Britovsek, W. Keim, S. Mecking, D. Sainz and T. Wagner, *Chem. Commun.*, **1993**, 632

50. B. Milani, L. Vicentini, A. Sommazzi, F. Garbassi, E. Chiarparin, E. Zangrando and G. Mestroni, *J. Chem. Soc. Dalton Trans.*, **1996**, 3139

51. R. van Asselt, E. E. C. G. Gielsen, R. E. Rulke, K. Vrieze and C. J. Elsevier, *J. Am. Chem. Soc.*, **1994**, *116*, 977

52. M. J. Green, G. J. P. Britovsek, K, J. Cavell, F. Gerhards, B. F. Yates, K. Frankcombe, B. W. Skelton and A. H. White, *J. Chem. Soc. Dalton Trans.*, **1998**, 1137

53. A. Aeby and G. Consiglio, *J. Chem. Soc. Dalton Trans.*, **1999**, 655

54. M. G. Gardiner, W. A. Herrmann, C. P. Reisinger, J. Schwarz and M. Spiegler, *J. Organomet. Chem.*, **1999**, *572*, 239

55. A. Battistini and G. Consiglio, *Organometallics*, **1992**, *11*, 1766

56. A. Seayad, S. Jayasree, K. Damondaran, L. Toniolo and R. V. Chaudhari, *J. Organomet. Chem.*, **2000**, *601*, 100

57. H. K. Luo, Y. Kou, X. W. Wang and D. G. Li, *J. Mol. Cat. A*, **2000**, *151*, 91

58. W. P. Mul, H. Oosterbeek, G. A. Beitel, G. J. Kramer and E. Drent, *Angew. Chem.*, **2000**, *39*, 1848

59. K. Nozaki, T. Hiyama, S. Kacker and I. T. Horvath, *Organomet.*, **2000**, *19*, 2031

60. J. S. Brumbaugh, R. R. Whittle, M. Parvez and A. Sen, *Organometallics*, **1990**, *9*, 1735

61. A. Macchioni, G. Bellachioma, G. Cardaci, M. Travaglia and C. Zuccaccia, *Organometallics*, **1999**, *18*, 3061

62. G. P. C. M. Dekker, C. J. Elsevier, K. Vrieze and P. W. N. M. van Leeuwen, *Organometallics*, **1992**, *11*, 1598

63. S. Kacker and A. Sen, *J. Am. Chem. Soc.*, **1995**, *117*, 10591

64. P. M. Maitlis, *The Organic Chemistry of Palladium*, Academic Press, New York, 1971, vol. 1, p. 36

65. S. F. A. Kettle, *Physical Inorganic Chemistry*, Oxford University Press, 1998, p. 328

66. P. Margl and T. Ziegler, *J. Am. Chem. Soc.*, **1996**, *118*, 7337; M. Svensson, T. Matsubara and K. Morakuma, *Organometallics*, **1996**, *15*, 5568

67. H. S. Yun, K. H. Lee and J. S. Lee, *J. Mol. Cat. A*, **1995**, *95*, 11

68. E. Drent and E. Kragtwijk (Shell), EP 0 495 548, priority date 19/11/91; J. C. L. J. Suykerbuyk, E. Drent and P. G. Pringle (Shell), WO 98/427/17, priority date 26/03/97

69. G. R. Eastham, R. P. Tooze, X. L. Wang and K. Whiston (ICI/INEOS), WO 96/19434, priority date 22/12/94

70. W. Clegg, G. R. Eastham, M. R. J. Elsegood, R. P. Tooze, X. L. Wang and K. Whiston, *J, Chem. Soc. Chem. Commun.*, **1999**, 1877

71. K. Othmer, *Encyclopedia of Chemical Technology*, Wiley, New York, 4th edn, 1995, vol. 16, p. 487; *Chem. Week*, 1999, Nov. 10th, 14

72. G. R. Eastham, Ph.D. thesis, University of Durham, 1998

73. N. Carr, B. J. Dunne, L. Mole, A. G. Orpen and J. L. Spencer, *J. Chem. Soc. Dalton Trans.*, **1991**, 863; L. E. Crascall and J. L. Spencer, *J. Chem. Soc. Dalton Trans.*, **1992**, 3445; L. Mole, J. L. Spencer, N. Carr and A. G. Orpen, *Organometallics*, **1991**, *10*, 49; F. M. Conroy-Lewis, L. Mole, A. D. Redhouse, S. A. Lister and J. L. Spencer, *J. Chem. Soc. Chem. Commun.*, **1991**, 1601; N. Carr, L. Mole, A. G. Orpen and J. L. Spencer, *J. Chem. Soc. Dalton Trans.*, **1992**, 2653

Chapter Two

Numbering scheme for Chapter 2

$Pd(d^tbpx)(dba)$	**1**
$[Pd(d^tbpx)(dbaH)]^+$	**2**
$[Pd(d^tbpx)H(MeOH)]^+$	**3**
$[Pd(d^tbpx)H(THF)]^+$	**3a**
$[Pd(d^tbpx)H(H_2O)]^+$	**3b**
$[Pd(d^tbpx)H(CH_3CN)]^+$	**3c**
$[Pd(d^tbpx)H(EtCN)]^+$	**3d**
$[Pd(d^tbpx)H(MeP)]^+$	**3e**
$Pd(d^tbpx)HCl$	**3f**
$Pd(d^tbpx)HBr$	**3g**
$Pd(d^tbpx)HI$	**3h**
$[Pd(d^tbpx)H(Py)]^+$	**3i**
$[Pd(d^tbpx)H(PPh_3)]^+$	**3j**
$[Pd(d^tbpx)H(PPh_2H)]^+$	**3k**
$[Pd(d^tbpx)H(CO)]^+$	**3l**
$[Pd(d^tbpx)H(^{13}CO)]^+$	**3m**
$Pd(d^tbpx)(\eta^1\text{-}TfO)_2$	**4**
$[Pd(d^tbpx)(\eta^2\text{-}TfO)]^+$	**5**
$[Pd(d^tbpx)(solv)_2]^{2+}$	**6**
$[Pd(d^tbpx)(CH_3CN)_2]^{2+}$	**6a**
$[Pd(d^tbpx)(EtCN)_2]^{2+}$	**6b**
$[Pd(d^tbpx)(H_2O)_2]^{2+}$	**6c**
$[Pd(d^tbpx)(Py)_2]^{2+}$	**6d**
$Pd(d^tbpx)H(TfO)$	**7**
$[Pd(d^tbpx)D(CD_3OD)]^+$	**8**
$Pd(d^tbpx)Cl_2$	**9**
$[Pd\{\eta^2\text{-}P(^tBu)_2CH_2C_6H_3CH_2PH^tBu_2\}(\eta^2\text{-}TfO)]^+$	**10**
$[Pd\{\eta^2\text{-}P(^tBu)_2CH_2C_6H_2(OCH_3)CH_2PH^tBu_2\}(\eta^2\text{-}TfO)]^+$	**11**
$Pd(d^tbpx)Br_2$	**12**
$Pd(d^tbpx)I_2$	**13**

Reactivity of Pd(d^{t}bpx)(dba) with acids: the TfOH system

2.1 Introduction

The Ineos catalyst for the synthesis of MeP is formed *in-situ* by mixing Pd(d^{t}bpx)(dba), **1**, in MeOH with a sulfonic acid (*e.g.* $MeSO_3H$) followed by heating to 80-100°C under 10 atm of CO/C_2H_4. The resulting catalytic system is very active and, then, it is very difficult to look at it under these operative conditions. Therefore, the approach adopted in this work has been, first, to dissect the catalytic system into single components and to study their chemistry under different conditions. Then, these components have been, gradually, put together again, in order to re-obtain the initial catalytic system.

Thus, the reactivity of Pd(d^{t}bpx)(dba) with different acids under nitrogen has been studied first. In the actual catalytic process, the best catalytic results are obtained using $MeSO_3H$ and the reactivity of **1** with this acid will be discussed in the next chapter. However, we find that analogous but cleaner reactions occur with TfOH which are described in this chapter; this allows the introduction of many very important concepts which will be useful in the subsequent discussion.

2.2 Synthesis and characterisation of [Pd(d^{t}bpx)H(solv)]$^+$

2.2.1 Protonation of Pd(d^{t}bpx)(dba), 1

The complex Pd(d^{t}bpx)(dba) is only slightly soluble in MeOH, and the resulting solution is pale-yellow. Addition of one equivalent of HX (X = $MeSO_3$, TsO, TfO, BF_4) results in the complete dissolution of the solid and the solution becomes deep-red; further addition of acid does not cause any noticeable change. The $^{31}P\{^1H\}$ NMR spectrum at 193 K (see Figure 2.1) consists of two sets of doublets which indicates the presence of two different species, containing two *cis* inequivalent phosphorus atoms. Moreover, the spectrum changes with temperature and this indicates the existence of an exchange process involving these two compounds. The reaction seems to be completely independent of the nature of the acid. In fact, in all four cases examined, the phosphorus spectrum at 193 K shows four doublets with nearly the same chemical shift, coupling constant and intensities. In particular, in the case of HBF_4 no P-F coupling has been observed. This clearly means that the resulting product does not contain a direct interaction between the metal and the anion. Moreover, the NMR spectra of the protonation products are not significantly affected by the solvent, even in very different solvents (*i.e.* MeOH, THF, CH_2Cl_2). Thus, no direct interactions between the solvent and the metal seem to be involved. The simplest explanation to account for all these data is to assume that the addition of acid to **1** results in the protonation of the co-ordinated dba ligand and, therefore, the formation of [Pd(d^{t}bpx)(dbaH)]$^+$, **2**.

Figure 2.1

$^{31}P\{^1H\}$ NMR spectra of [Pd(d^{t}bpx)(dbaH)]$^+$, 2, in MeOH

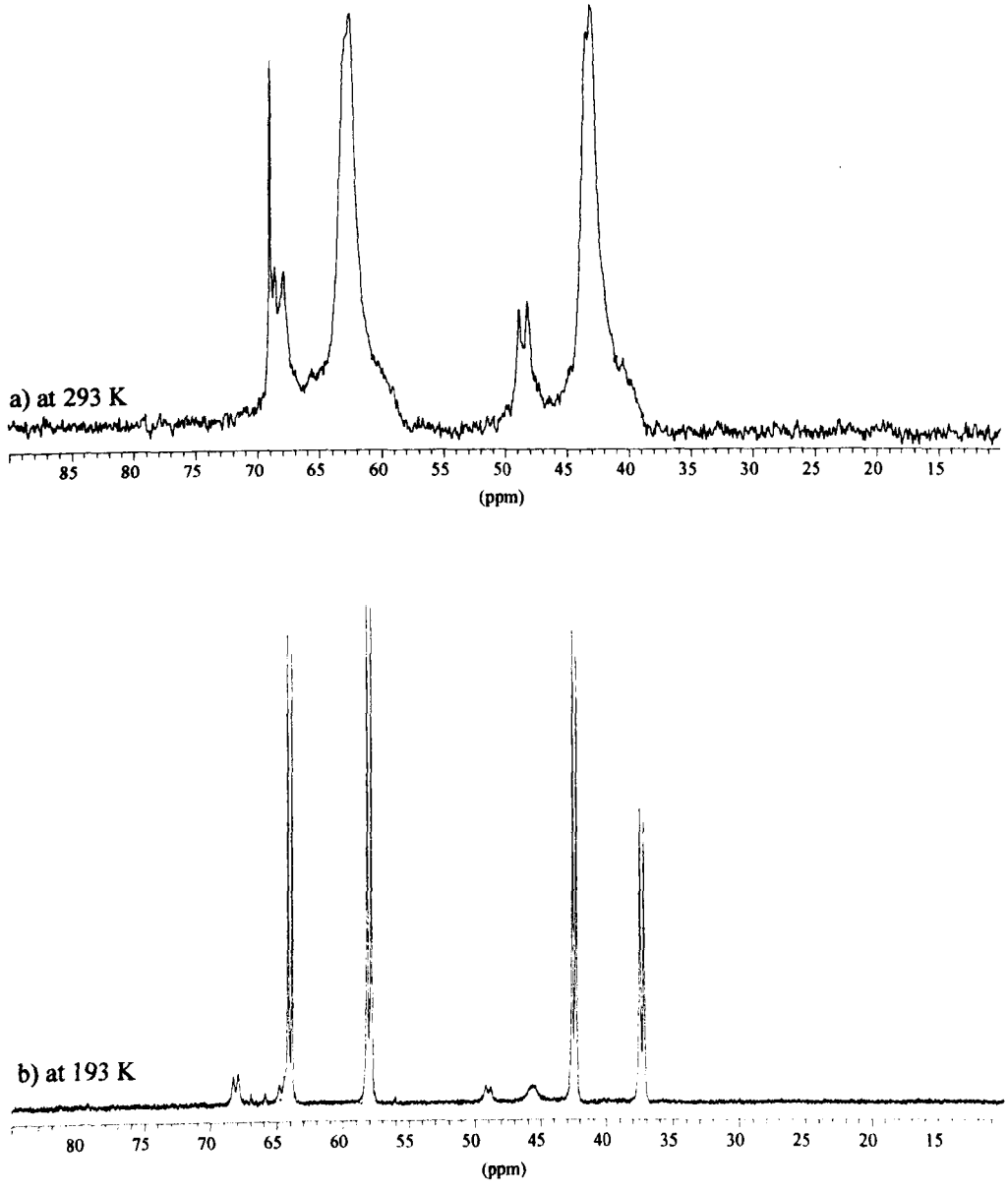

The protonation can occur on a C=C bond or on the C=O bond. Spencer [1] has reported examples in which protonation of Pd(d^{t}bpx)(olefin) containing non substituted olefins (*e.g.* ethene, styrene, nonrborn-2-ene) gives [Pd(d^{t}bpx)(alkyl)]$^+$ which contains a β-agostic Pd-H interaction as a result of the protonation of the C=C bond. This should be contrasted with protonation of the benzoquinone ligand in

Pd(COD)(BQ) [2] which results in protonation of the oxygen atom. Hence, it seems that when the olefin ligand is an α,β-unsaturated ketone, protonation of the oxygen atom is preferred (see Scheme 2.1). In agreement with this conclusion, the complex $[Pd(dcpx)(dbaH)]^+$ has been isolated during the protonation of Pd(dcpx)(dba), and characterised by X-ray diffraction (see Chapter 6), which clearly indicates that protonation occurs on the oxygen atom. Finally, a conformational equilibrium in solution can easily account for the presence of two different species in the $^{31}P\{^1H\}$ NMR of **2**.

Scheme 2.1

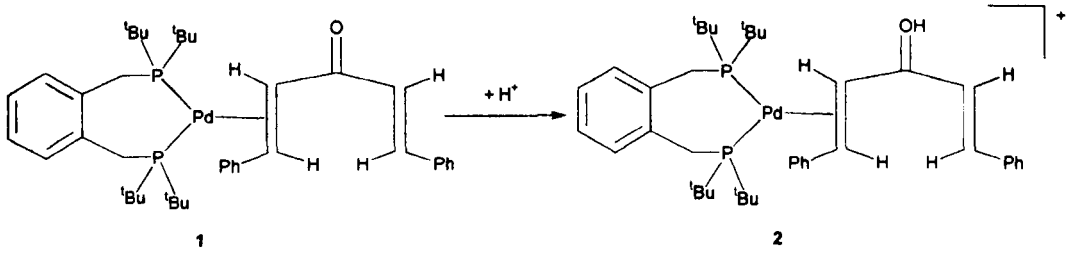

2.2.2 Oxidation of [Pd(d^{t}bpx)(dbaH)]$^+$, 2

The deep-red solution of **2** slowly turns pale-yellow with time, with a concomitant change in the NMR spectrum. This process can be accelerated by bubbling oxygen through the solution or by addition of benzoquinone (BQ). In this case, the product of the reaction depends on the acid previously used. In the case of $MeSO_3H$ and TsOH, the complex $[Pd(d^tbpx)(\eta^2\text{-}MeSO_3)]^+$ and $[Pd(d^tbpx)(\eta^2\text{-}TsO)]^+$ are formed, respectively (see Chapter 3). Whereas, $[Pd(L\text{-}L)H(MeOH)]^+$, **3**, is formed when TfOH or HBF_4 are used. Complex **3** can also be obtained by dissolution of $Pd(d^tbpx)(\eta^1\text{-}TfO)_2$, **4**, in MeOH. This second method of synthesis is

very useful since it avoids the presence of free acid. Using other primary and secondary alcohols (*e.g.* EtOH, n-PrOH, i-PrOH, n-BuOH; class A), both the synthetic routes described above result in the formation of similar Pd-hydride complexes. However, in CF_3CH_2OH, tertiary alcohols or non-alcoholic media (^{t}BuOH, THF, CH_2Cl_2, CH_3CN, EtCN, MeP, acetone; class B) a palladium-hydride is not formed. In these cases, the hydride has first to be synthesised in MeOH; then, the solvent can be removed *in vacuum* and the residue dissolved in the new solvent. The stability of the hydride in non-alcoholic solvents decreases in the presence of free acid and, hence, for these solvents it is better to use the synthesis from **4**. The oxidation of **2** in solvents of class B, as well as dissolution of **4**, results in the formation of $[Pd(d^tbpx)(\eta^2\text{-TfO})]^+$, **5**, or $[Pd(d^tbpx)(solv)_2]^{2+}$, **6**, depending on the solvent used (see Scheme 2.2 for a summary of the synthesis of all these complexes).

Scheme 2.2

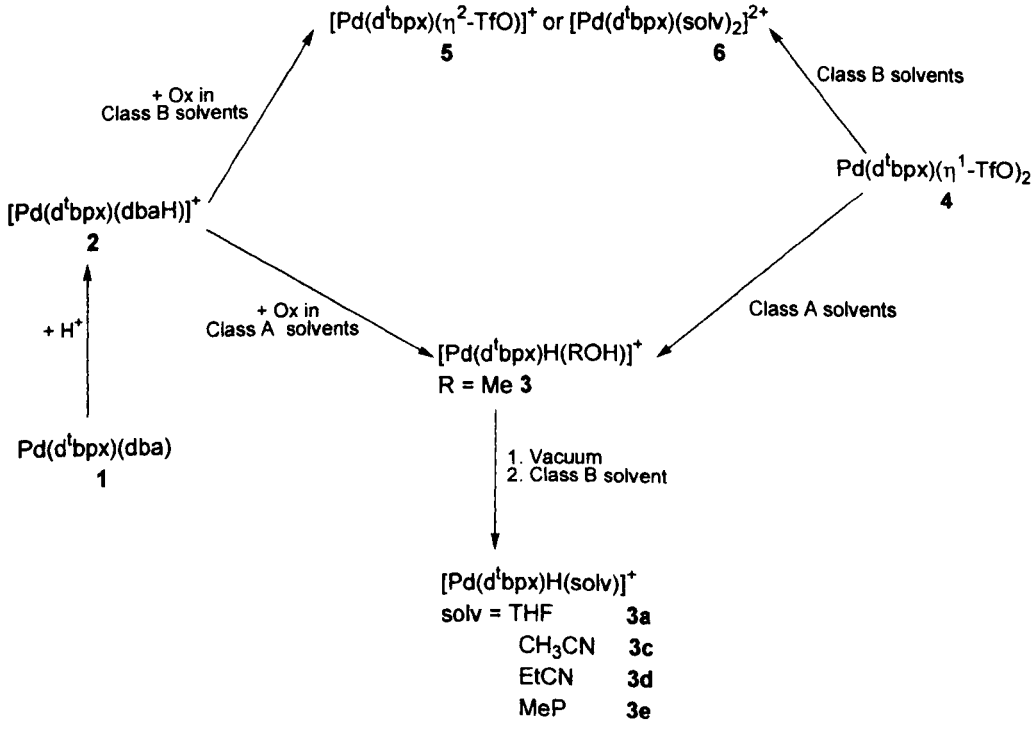

2.2.3 Characterisation of [Pd(d^{t}bpx)H(MeOH)]$^+$, 3

Complex **3** has been fully characterised by multinuclear NMR spectroscopy (see Figure 2.2). The $^{31}P\{^1H\}$ NMR spectrum at 293 K shows two doublets at 25.8 and 77.5 ppm, with $^2J(P\text{-}P) = 17$ Hz, indicating the presence of two inequivalent *cis*-P atoms. Moreover, in the ^{31}P spectrum, the resonance at higher field is split into a doublet with $^2J(P\text{-}H) = 179.4$ Hz, showing that this phosphorus is *trans* to the hydride. Finally, a doublet of doublets at –10 ppm is present in the ^1H spectrum, and this is the typical region for terminal Pd-hydride complexes.[3,4] In agreement with this conclusion, a strong band at 1963 cm^{-1} is present in the IR spectrum recorded in MeOH; ν(Pd-H) usually occurs in the range 2060-1890 cm^{-1}. In this way, the ligands present in three of the four co-ordination sites of the complex have been determined, *i.e.* d^{t}bpx (two *cis*-sites) and a hydride ligand. Basically, the fourth co-ordination site could be occupied by a TfO$^-$ anion or by a MeOH molecule and, hence, the hydride complex could be formulated as [Pd(d^{t}bpx)H(MeOH)]$^+$, **3**, or Pd(d^{t}bpx)H(TfO), **7**. This problem has been solved by studying the effect of the acid and the solvent. In particular, on using HBF_4 instead of TfOH, the same hydride complex has been obtained, without any significant change in the NMR spectra. Moreover, no P-F or H-F coupling constant is present, even at low temperature. Therefore, the product formed is the solvato-hydride complex **3**. According to this formulation, the NMR spectra of the hydride are strongly solvent-dependent (see Table 2.1). In particular, the resonance due to the P-atom *trans* to the co-ordinated solvent molecule shows a noticeable shift in different solvents, consistent with a change of the *trans* group.

Figure 2.2

NMR spectra of [Pd(d^{t}bpx)H(MeOH)]$^+$, 3, in MeOH at 293 K

a) $^{31}P\{^1H\}$

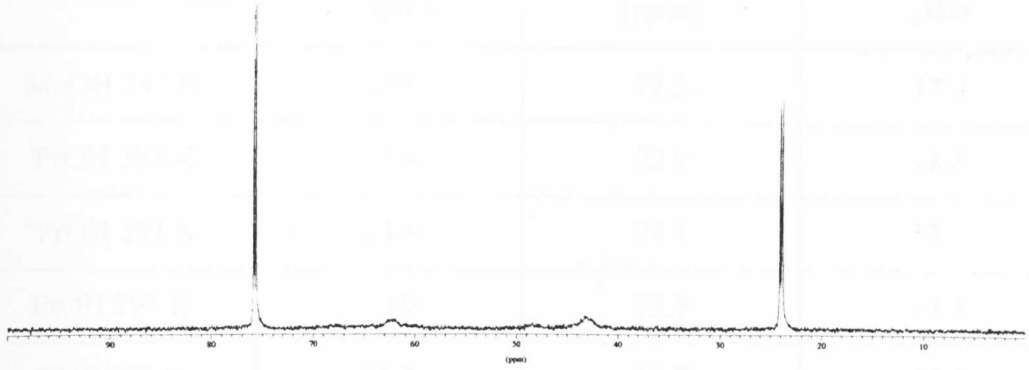

b) ^{31}P

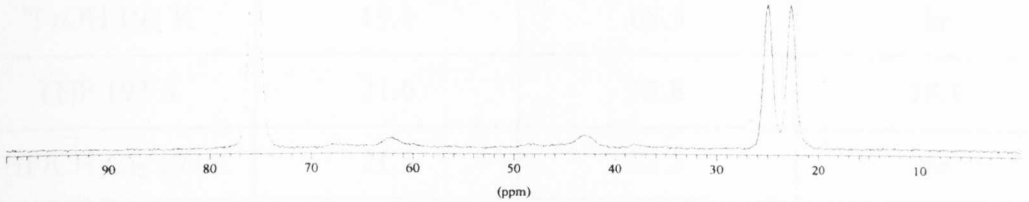

c) ^1H

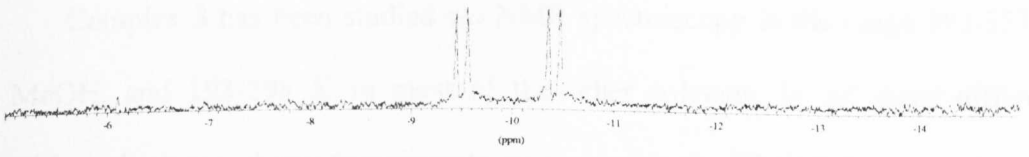

Table 2.1

$^{31}P\{^1H\}$ NMR data for $[Pd(d^tbpx)H(solv)]^+$ in different solvents

Solvent and Temperature (K)	δP_A (ppm)	δP_B (ppm)	$^2J(P_A\text{-}P_B)$ (Hz)
MeOH 293 K	25.8	77.5	17.0
^{i}PrOH 293 K	24.4	72.9	18.8
^{n}PrOH 293 K	24.4	74.1	17.0
EtOH 293 K	23.9	73.9	17.3
THF 293 K	21.3	69.7	18.3
THF/CH_2Cl_2 293 K	23.3	72.4	br
CH_3CN 293 K	23.9	68.8	19.8
EtCN 293 K	23.0	69.4	19.6
MeP 293 K	24.3	72.7	18.6
MeOH 193 K	21.8	75.5	16.1
^{n}PrOH 193 K	19.4	68.5	br
THF 193 K	21.6	72.8	18.1
THF/CH_2Cl_2 193 K	21.5	73.3	br
EtCN 193 K	21.1	67.1	19.8

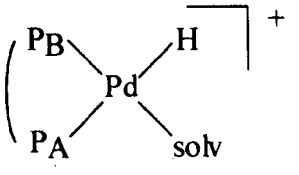

Complex **3** has been studied *via* NMR spectroscopy in the range 193-353 K in MeOH, and 193-298 K in most of the other solvents. In all these different conditions, it always shows two separate resonances in the $^{31}P\{^1H\}$ spectrum. Hence,

the two P-atoms remain always inequivalent. This is surprising, because analogous square-planar Rh(I)-compounds undergo rapid solvent inter-exchange on the NMR time-scale [5] and there is also exchange at room temperature between the hydride and CO ligand in the bridged Pd(I)-hydride complex [6] $[Pd_2(\mu\text{-}CO)(\mu\text{-}H)\{(S,S)\text{-}BDPP\}_2]^{2+}$. Not a lot of examples of mononuclear Pd(II) hydride complexes containing a diphosphines are reported in literature [7-9] and, as far as we know, in only one case NMR data at variable temperature have been reported.[10] Thus, the NMR spectra of the complexes *cis*-$(R'_2PC_2H_4PR'_2)PdH(SnR_3)$ (R' = ^{i}Pr, ^{t}Bu; R = Me, ^{n}Bu) are reported to be almost temperature independent. But, in this case, the presence of the very particular ligand , $-SnR_3$, could be the explanation for the lack of exchange.

2.2.4 Synthesis of [Pd(d^{t}bpx)D(CD$_3$OD)]$^+$, 8

Dissolution of Pd(d^{t}bpx)$(TfO)_2$ in CD_3OD results in the formation of the new deuteride [Pd(d^{t}bpx)D$(CD_3OD)]^+$, **8**. Its $^{31}P\{^1H\}$ spectrum at 293 K shows two multiplets at 75.4 and 23.4 ppm, each composed of six resonances with the same intensities, because of the mutual coupling of the two *cis*-P atoms and their couplings with the deuteride ligand [*cis*-^2J(P-P) = 17.1 Hz, *cis*-^2J(P-D) = 3 Hz, *trans*-^2J(P-D) = 27.4 Hz]. The measured values for *cis* and *trans*-^2J(P-D) are fully consistent with the values calculated from the relative ^2J(P-H), γ_H and γ_D. Addition of TfOH results only in a partial conversion of **8** into **3**. The rate of H/D-exchange is thus very slow; at 293 K, the NMR spectrum consists of the sum of the spectra of **3** and **8** and it is interesting to note that, once more, **3** shows a very static behaviour.

2.3 On the formation of [Pd(d^{t}bpx)H(MeOH)]$^+$, 3

Palladium(II) hydrides are usually obtained by (i) treatment of Pd(II) complexes with hydric reagents and (ii) oxidative addition to Pd(0) complexes.[3,4] Other methods include β-elimination reactions,[9,11] ligand exchange,[12-14] addition of H_2 to Pd(II) complexes.[15]

The formation of [Pd(d^{t}bpx)H(MeOH)]$^+$ is clearly not a case of oxidative addition. In fact, addition of TfOH to Pd(d^{t}bpx)(dba) results in the formation of [Pd(d^{t}bpx)(dbaH)]$^+$ and not **3**. The fact that protonation and not oxidative addition is observed is due to steric and electronic factors. Oxidative addition of acids to Pd(0) compounds is usually reported to occur more easily in the case of co-ordinatively unsaturated complexes.[3] **1** is co-ordinatively unsaturated, but both d^{t}bpx and dba are very bulky ligands. It should be noted that **1** contains two basic sites, *i.e.* the Pd(0) centre and the oxygen atom; since H^+ is a hard acid, it shows more affinity towards the hard basic centre (*i.e.* the oxygen atom) rather than the softer metal centre.

The hydride **3** can be also obtained from the Pd(II) complex **4** in the absence of acid. These data suggest that the role of the acid and the oxidant in the synthesis of **3** from **1** is just to oxidise the starting Pd(0) complex and to form a Pd(II) compound. In this case, the hydric reagent is the solvent, as suggested by the formation of **8** when CD_3OD is used as solvent. In agreement with this, formation of acetone is observed *via* IR when the hydride is synthesised by dissolution of **4** in *iso*-propanol (eq. 2.1)

$$Pd(d^tbpx)(\eta^1\text{-}TfO)_2 + 2CH_3CH(OH)CH_3 \longrightarrow [Pd(d^tbpx)H(^iPrOH)]^+ + CH_3COCH_3 + TfOH + TfO^- \quad (2.1)$$

Being the solvent also a key reagent in the formation of the hydride explains why the solvent is so important (see Table 2.2).

Table 2.2

Effect of the solvent on the formation of the hydride by direct dissolution of 4 or oxidation of 2

Hydride Formed (Class A)	**Hydride Not Formed (Class B)**
MeOH, EtOH, ^{n}PrOH, ^{i}PrOH, ^{n}BuOH, THF/H_2O	^{t}BuOH, CF_3CH_2OH, THF, CH_2Cl_2, CH_3CN, EtCN, MeP, acetone

The hydride is probably formed *via* β-hydride elimination from a molecule of alcohol co-ordinated to the metal (see Scheme 2.3). As consequence of this process, the alcohol is oxidised to form an aldehyde or a ketone. No hydride is formed in CF_3CH_2OH, probably because the presence of a very strong electron withdrawing group (*i.e.* CF_3-) makes the alcoholic site electron poor and, hence, more difficult to oxidise than in a normal aliphatic alcohol.

Scheme 2.3

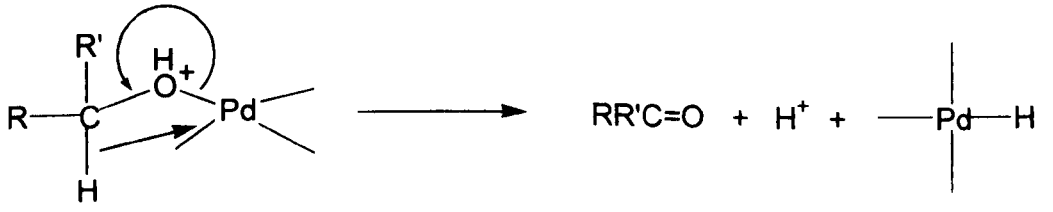

Examination of Table 2.2 shows that the only non-alcoholic medium in which it is possible to obtain the hydride is in a mixture of THF/H_2O (the amount of water to be added depends on the amount of acid present, as described in Section 2.3.2). In this case, the hydride is formed by oxidation of water (eq. 2.2); gas evolution (probably O_2) is observed during the process.

$$\underset{\mathbf{4}}{Pd(d^tbpx)(\eta^1\text{-}TfO)_2} + 2H_2O \longrightarrow \underset{\mathbf{3b}}{[Pd(d^tbpx)H(H_2O)]^+} + 0.5O_2 + TfOH + TfO^- \quad (2.2)$$

Formation of Pd-hydrides from the reaction of Pd(II) complexes and MeOH has been widely claimed as one of the possible routes to hydride species during the catalytic alchoxycarbonylation of ethene (see Section 1.2.2.1). Therefore, the full characterisation of such a process during the study of the Ineos catalytic process represents a very important goal in the understanding of the real catalytic mechanism. Oxidation of alcohols by Pd(II) salts is a well known process,[16] and it is believed that it takes place *via* co-ordination of the alcohol, transfer of an α-hydrogen from the alcohol to the metal with formation of a Pd(II)-hydride, which usually decomposes very fast to form Pd-metal. This process is also believed to be the main reason for the instability of Pd(II) salts in alcoholic solvents towards metal formation. To the best of our knowledge, the formation of **3** is the first case in which this kind of process has been successfully used for the synthesis of a stable and fully characterised Pd(II)-hydride complex. A similar reaction has been observed in the case of platinum,[17] and in fact, the complex $Pt(PR_3)_2Cl_2$ is converted into $Pt(PR_3)_2HCl$ in EtOH or ^{i}PrOH.

$$cis\text{-}Pt(PR_3)_2Cl_2 + KOH + RR'CHOH \longrightarrow trans\text{-}Pt(PR_3)_2HCl + RR'CO + H_2O$$

$$(R = R' = Me;\ R = Me,\ R' = H) \qquad (2.3)$$

A mechanism involving transfer of hydride from the α-carbon on the alcohol to the metal in a metal alkoxide intermediate has been proposed (see Scheme 2.4).

Scheme 2.4

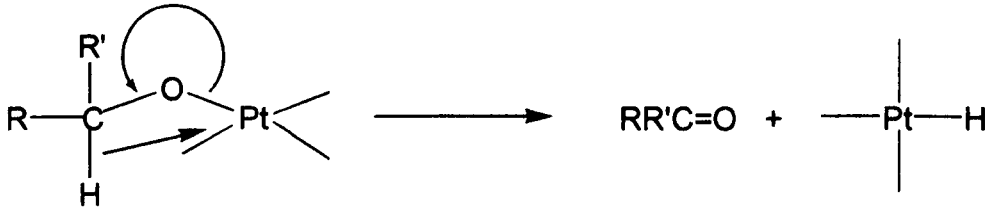

It is important to note that this reaction is carried out in basic conditions, whereas the formation of **3** occurs in neutral or even acidic conditions. Bases are usually used in order to make the reduction of the alcohol easier. Therefore, the formation of **3** under acidic conditions suggests that in the presence of d^{t}bpx, palladium can easily activate the solvent. It is also interesting to note that it has already been shown that methanol reduction is involved in the formation of Pd(I)-hydride dimers.[4,18] It is believed that the formation of these dimers involves the formation of an intermediate Pd(II)-hydride and a Pd(0)-complex which, then, condense to form the final Pd(I) dimer. Also in this case, the reactions are usually performed in the presence of bases (*e.g.* amines). In the case of the bulky d^{t}bpx ligand, steric effects probably make it very difficult to form binuclear species and, hence, the Pd(II)-hydride is the final, stable product.

2.3.1 The crystal structure of [Pd(d^{t}bpx)(η^2-TfO)]$^+$, 5

Pd(d^{t}bpx)(dba) reacts with TfOH and BQ (or O_2) in class B solvents (see Table 2.2) to give a new species which shows a singlet at *ca.* 80 ppm in the $^{31}P\{^1H\}$ spectrum, whereas in CH_3CN and EtCN, the resonance occurs at 58 ppm. Considering the strong co-ordinating ability of these last solvents, it is possible to conclude that the species present in CH_3CN and EtCN is $[Pd(d^tbpx)(RCN)_2]^{2+}$(R = Me, **6a**; Et, **6b**). Other experiments support this hypothesis. Pd(d^{t}bpx)Cl_2, **9**, reacts in CH_2Cl_2 with two equivalents of $AgBF_4$ to give the same species at 58 ppm; the same result is obtained by reacting **1** with HBF_4 in the same solvent and an oxidant (see Scheme 2.5). It is interesting to note that the complex obtained in the case of tetrafluoroborate, is not very stable, and its stability increases using CH_2Cl_2 with traces of water. Thus, the compound obtained in the last two cases can be formulated as $[Pd(d^tbpx)(H_2O)_2]^{2+}$, **6c**; in agreement with this conclusion, no P-F coupling has been observed. Other bis-solvento species will be described in Section 2.4 and Chapter 3, and they always show a singlet in the phosphorus spectrum at 52-60 ppm (see Table 2.3).

Reaction of **9** with two equivalents of AgOTf in CH_2Cl_2 results, again, in a species which resonates at 79 ppm in the phosphorus spectrum. Therefore, it is possible to conclude that all the species resonating at *ca.* 80 ppm contain a direct interaction between the metal and the TfO^- anion. One of these compounds has been crystallised from THF/hexane showing that the species formed is $[Pd(d^tbpx)(\eta^2\text{-}TfO)]^+$, **5**.

Scheme 2.5

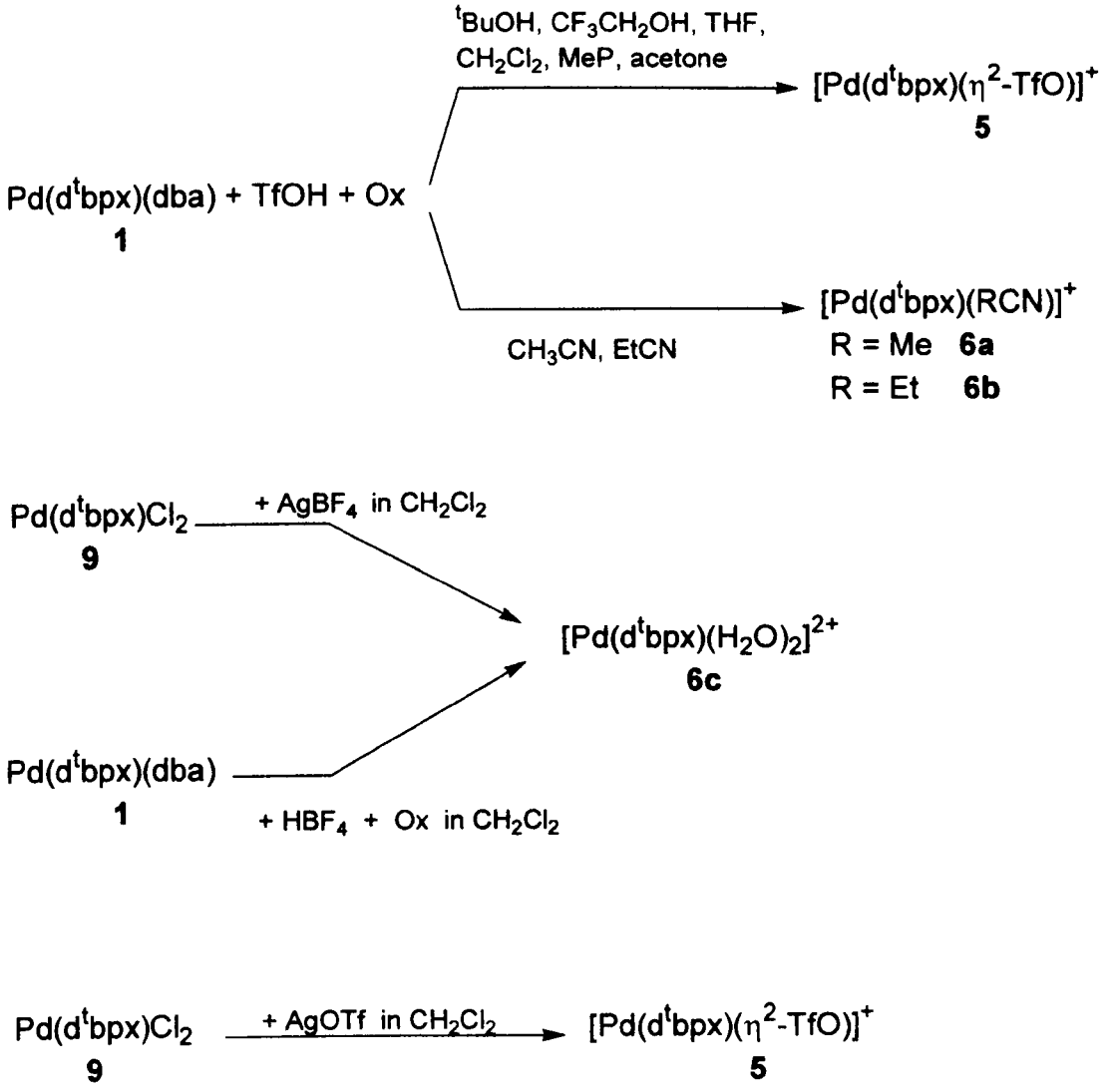

Table 2.3

$^{31}P\{^1H\}$ NMR data at 293 K for [Pd(d^{t}bpx)(solv)$_2$]$^{2+}$ in different solvents

solvent	δP (ppm)	solvent	δP (ppm)
CH_3CN	57.3	MeP/MeOH (3:1)	59.8
MeP [a]	51.9	MeP/MeOH (3:1) [a]	58.5
MeP/MeOH (4:1)	60.0	THF/H_2O	53.9
MeP/MeOH (2:1)	60.6	DCM/H_2O	53.6

[a] at 193 K

In the solid state, **5** is present as the triflate salt [Pd(d^{t}bpx)(η^2-TfO)][TfO] (see Figure 2.3 and Table 2.4).

Figure 2.3

*Crystal structure of [Pd(d^{t}bpx)(η^2-TfO)]$^+$, **5**. Different views*

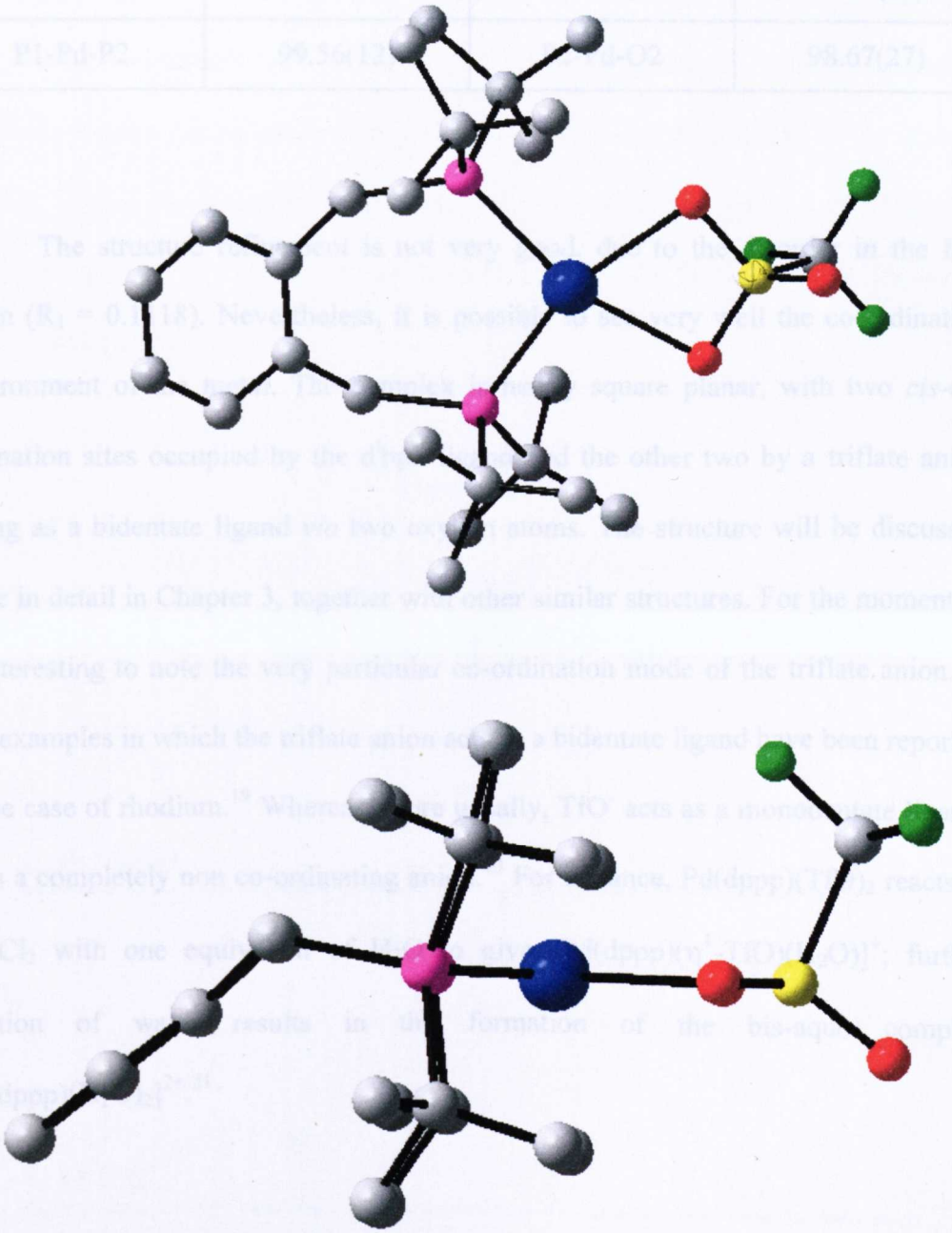

Table 2.4

Main bond distances and angles for [Pd(d^{t}bpx)(η^2-TfO)]$^+$, 5

Pd-P1	2.267(3)	P2-Pd-O1	161.75(27)
Pd-P2	2.267(3)	O1-Pd-O2	63.08(35)
Pd-O1	2.261(10)	O2-Pd-P1	161.75(27)
Pd-O2	2.261(10)	P1-Pd-O1	98.67(27)
P1-Pd-P2	99.56(12)	P2-Pd-O2	98.67(27)

The structure refinement is not very good, due to the disorder in the free anion (R_1 = 0.1118). Nevertheless, it is possible to see very well the co-ordination environment of the metal. The complex is nearly square planar, with two *cis*-co-ordination sites occupied by the d^{t}bpx ligand and the other two by a triflate anion acting as a bidentate ligand *via* two oxygen atoms. The structure will be discussed more in detail in Chapter 3, together with other similar structures. For the moment, it is interesting to note the very particular co-ordination mode of the triflate anion. A few examples in which the triflate anion acts as a bidentate ligand have been reported in the case of rhodium.[19] Whereas, more usually, TfO^- acts as a monodentate ligand, or as a completely non co-ordinating anion.[20] For instance, Pd(dppp)$(TfO)_2$ reacts in CH_2Cl_2 with one equivalent of H_2O to give [Pd(dppp)(η^1-TfO)(H_2O)]$^+$; further addition of water results in the formation of the bis-aquo complex [Pd(dppp)$(H_2O)_2$]$^{2+}$.[21]

2.3.2 The free acid system based on Pd(d^{t}bpx)(η^1-TfO)$_2$, 4

As seen before, **4** dissolves in CH_2Cl_2 to give **5**, which reacts with H_2O resulting in the formation of **6c**. The reaction can be partially reversed by addition of TfOH. The process is not completely reversible because (1) the presence of water also promotes partial decomposition to form Pd-metal and the protonated ligand and (2) all these complexes are not very soluble in the presence of water. In the same way, **4** dissolves partially in dry THF to give the same species **5**. As described above, a hydride species can be obtained in THF, by synthesising **3** in MeOH in the absence of acid, drying the solution *in vacuum* and dissolving the residue in THF. The compound present in THF is the new hydride [Pd(d^{t}bpx)H(THF)]$^+$, **3a**, as shown by NMR (see Figure 2.4).

Figure 2.4

$^{31}P\{^1H\}$ NMR at 293 K of [Pd(d^{t}bpx)H(solv)]$^+$

(solv = MeOH, 3; THF, 3a)

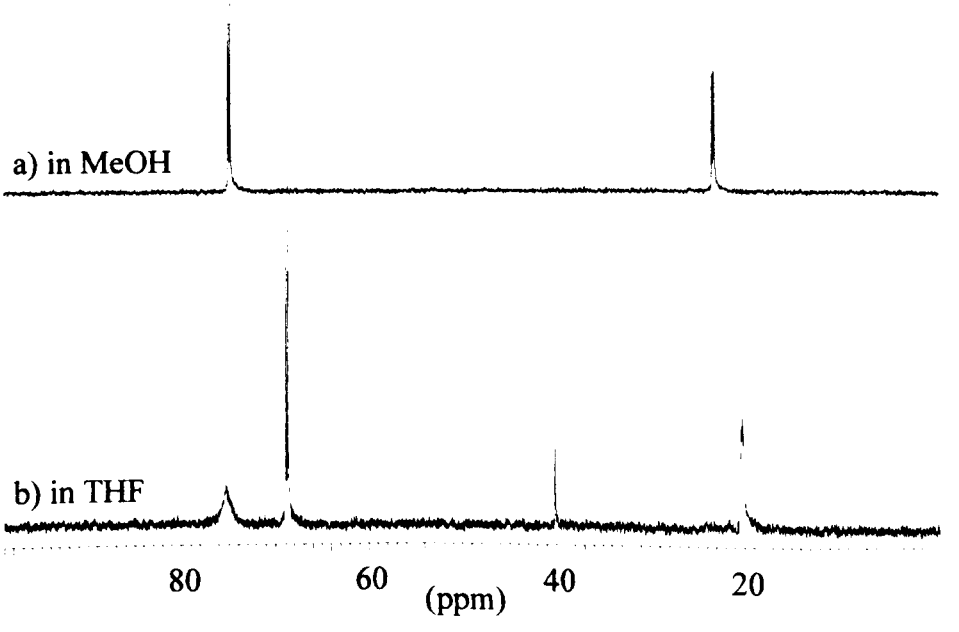

It is also possible to obtain a hydride in THF by adding very carefully water to a THF solution of **5**. The complex so formed is $[Pd(d^tbpx)H(H_2O)]^+$, **3b** (for its spectroscopic characterisation see Section 2.4); once formed, **3b** further reacts with water to give **6c** (see Scheme 2.6).

Scheme 2.6

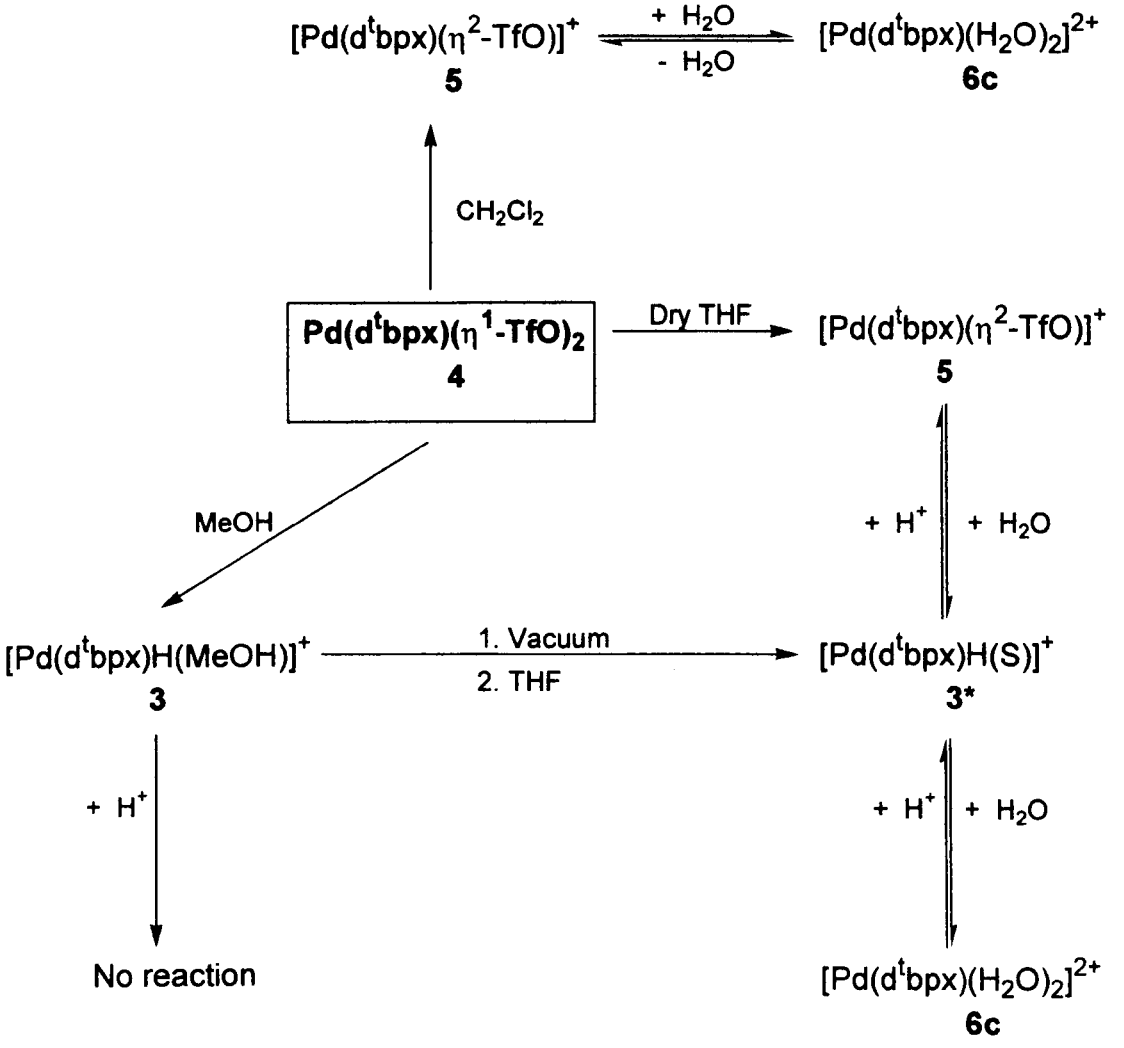

* S = THF, **3a**; H_2O, **3b**

All these reactions can be partially reversed by addition of TfOH. It is enough to add 6-7 equivalents of acid to a THF solution of the hydride in order to convert it

nearly completely into **5**; gas evolution (probably H_2) is observed during this reaction. This last process can be reversed by addition of water. Hence, there is a three-components two-equilibria system in THF, involving **5**, $[Pd(d^tbpx)H(solv)]^+$ (solv = THF or H_2O) and **6c**. The main product present in solution depends on the acid to water ratio used. The only limit to the complete reversibility of the system is the low solubility of these complexes when excess water is used.

Further information on the hydride formation can be obtained using mixtures of MeP/MeOH as solvent. This system is also very interesting, because engineering considerations on the process suggest that it is better to carry out the reaction on the industrial scale in such mixtures rather than in pure MeOH. MeP seems to behave quite similar to THF. The reaction of **1** with TfOH and BQ (or O_2) in MeP results in the formation of **5**, which reacts with MeOH to give **6** (MeP/MeOH = 4:1). Further addition of MeOH results in the formation of the hydride. This result is quite important, because it shows that **6** is a precursor in the hydride formation. Probably, MeOH has first to co-ordinate to the metal in order to be activated and, then, the redox process described in Section 2.3 can take place.

Dissolution of **4** in pure MeP results in the formation of **5** (δ_P = 81 ppm); on cooling the solution down to 193 K, **6** (δ_P = 52 ppm) is formed. Hence, an equilibrium between these two species exists in solution (eq. 2.4) and its position depends on the temperature and the acid present.

$$[Pd(d^tbpx)(\eta^2\text{-}TfO)]^+ + 2solv \rightleftharpoons [Pd(d^tbpx)(solv)_2]^{2+} + TfO^- \qquad (2.4)$$

5 **6**

Using the same procedure described above in the case of THF, it is possible to obtain the hydride also in MeP. Similarly, the stability of the hydride in MeP

decreases after addition of acid. In all cases, also in the absence of acid, **5** is slowly formed, suggesting that the presence of the hydride in pure MeP is more likely due to kinetic than thermodynamic factors. Interestingly, dissolution of **4** in MeP/MeOH results in a mixture of **6** and **3**, and the relative amounts depend on the ratio of MeP/MeOH. **5** is the only product present (at room temperature) in pure MeP. By adding MeOH, **6** is first formed and, then, the hydride starts to appear. In a MeOH rich solution, the hydride is the main species (see Scheme 2.7).

Scheme 2.7

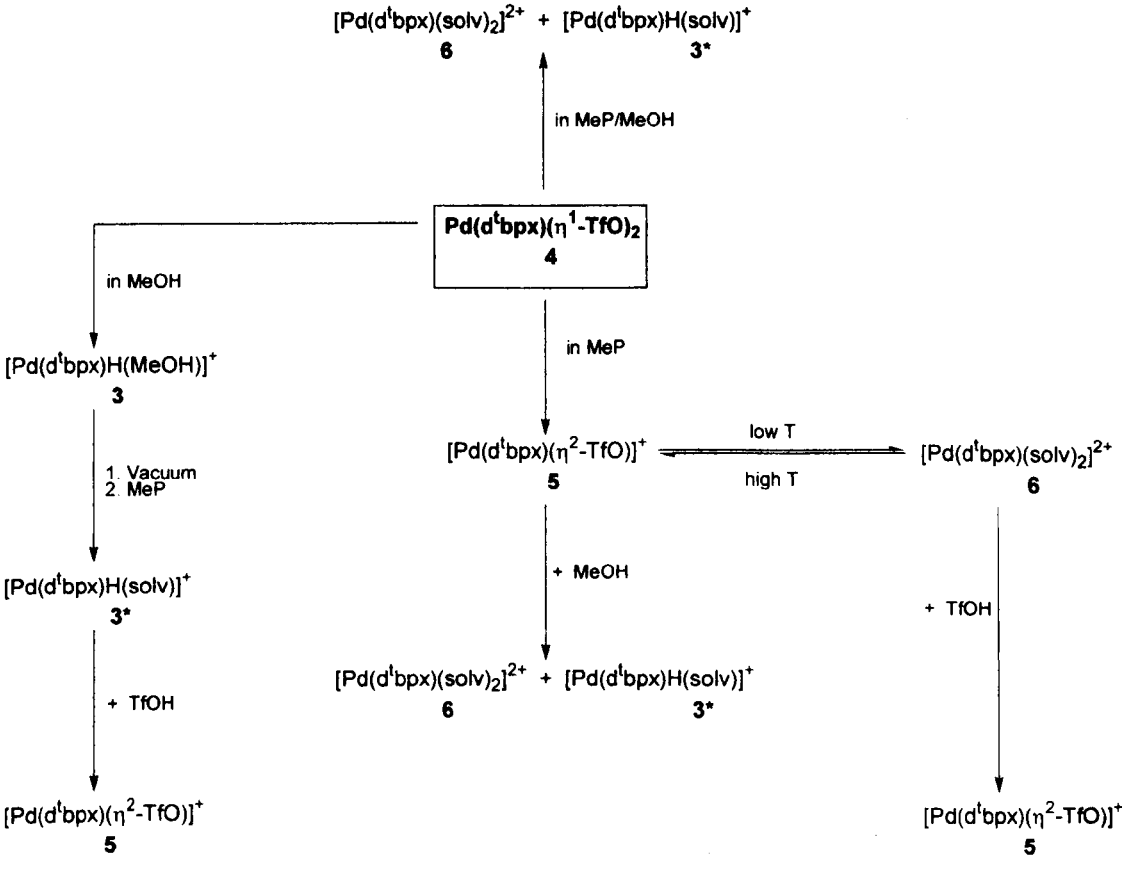

* solv = MeOH, **3**; MeP, **3e**

These results once more confirm the conclusion that **6** is a precursor in the hydride formation. They also show that the stability of the hydride **3**, once formed, strongly depends on the solvent used. A lot of different factors contribute to the stabilisation of **3**, *i.e.* the stability of the Pd-solvent bond, the ability of the medium to solvate ionic species and in particular H^+ (if H^+ is not well solvated, it becomes very reactive towards the hydride and, in fact, H_2 is formed in non-alcoholic solvents), the nucleophilicity of the solvent (a very strong basic ligand can in fact displace H^- from **3** and form **6**, see Section 2.4.2).

2.4 Reactivity of [Pd(d^{t}bpx)H(MeOH)]$^+$, 3

The hydride complex **3** has been studied in MeOH in the temperature range 193-353 K. Apart from the lack of any dynamic process over this temperature range which has already been discussed, this study has shown that the thermal decomposition of **3** always results in the formation of Pd-metal and the protonated ligand. None of the intermediates involved in this process has been observed, maybe because the decomposition, once started, is very fast. Nevertheless, it is very interesting to note that it is possible to detect the hydride even at 353 K, which is very similar to the conditions used for the catalysis. As expected, the thermal decomposition of **3** becomes faster and faster by increasing the temperature. Hence, the half life of **3** in solution at 293 K is 2-3 days, whereas at 353 K it is *ca.* 10 minutes. Its stability, of course, depends also on other factors, *e.g.* the amount of acid present. It is not very clear how the presence of acid contributes to the stabilisation of **3** in MeOH. As discussed before, addition of TfOH to a solution of the hydride in a

non-alcoholic solvent results in the formation of **5** and H_2. Whereas, addition of up to 60 equivalents of TfOH to a solution of **3** in MeOH does not cause any change in the species present. As reported in Section 1.2.3, it has been suggested that acids stabilise Pd-catalysts by stopping their decomposition pathways,[22] but also hydrogen bonds between the hydride **3** and the counter-ion could be important. In fact, it has been shown that such a hydrogen bonds are very important for the stabilisation in solution of other Pd-hydrides, *e.g.* $[Pd(PCy_3)_2H(H_2O)]^+$.[23]

2.4.1 Reactivity of [Pd(d^{t}bpx)H(MeOH)]$^+$, 3, with oxidants

Palladium hydrides are usually reported to be very air sensitive.[4] However, **3** was first obtained by bubbling O_2 for *ca.* 20 minutes through a solution of **2** in MeOH at room temperature. This reaction is very clean, giving only **3**, and there is no other compound present in solution even after bubbling O_2 for a further hour.

The reaction of **3** with BQ is more interesting. As reported in Section 2.2.2, it is possible to obtain **3** by reacting a solution of **2** in MeOH with BQ. The reaction goes to completion in a few minutes, and the best results have been obtained using 1-7 moles of BQ per mole of palladium. Using these conditions, **3** is the only product formed. On using more BQ, a second species starts to appear, which shows in the $^{31}P\{^1H\}$ NMR spectrum two singlets at 42.4 and 105.6 ppm (see Figure 2.5). The resonance at higher field is split into a doublet [^1J(P-H) = 460 Hz] in the ^{31}P spectrum. This species can be formulated as $[Pd\{\eta^2\text{-}P(^tBu)_2CH_2C_6H_3CH_2PH^tBu_2\}(\eta^2\text{-}TfO)]^+$, **10** (see Scheme 2.8), by analogy with the NMR data of a similar compound, *i.e.* $[Pd\{\eta^2\text{-}P(^tBu)_2CH_2C_6H_2(OCH_3)CH_2P^tBu_2\}(\mu\text{-}Br)]_2$, **11**, which has been recently synthesised and characterised by NMR (105 ppm,

s) and X-ray diffraction (see Scheme 2.9).[24] The complete conversion of **3** into **10** requires *ca.* 50 moles of BQ per mole of palladium.

Figure 2.5

*NMR spectra of [Pd{η^2-P(^{t}Bu)$_2$CH$_2$C$_6$H$_3$CH$_2$P^{t}Bu$_2$}(η^2-TfO)]$^+$, **10**, in MeOH at 293 K*

a) $^{31}P\{^1H\}$

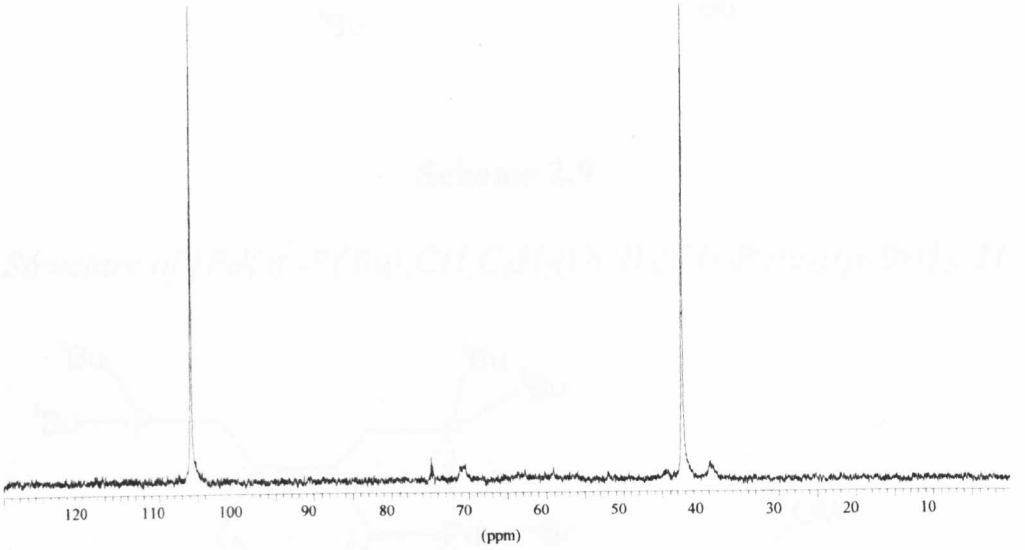

b) ^{31}P

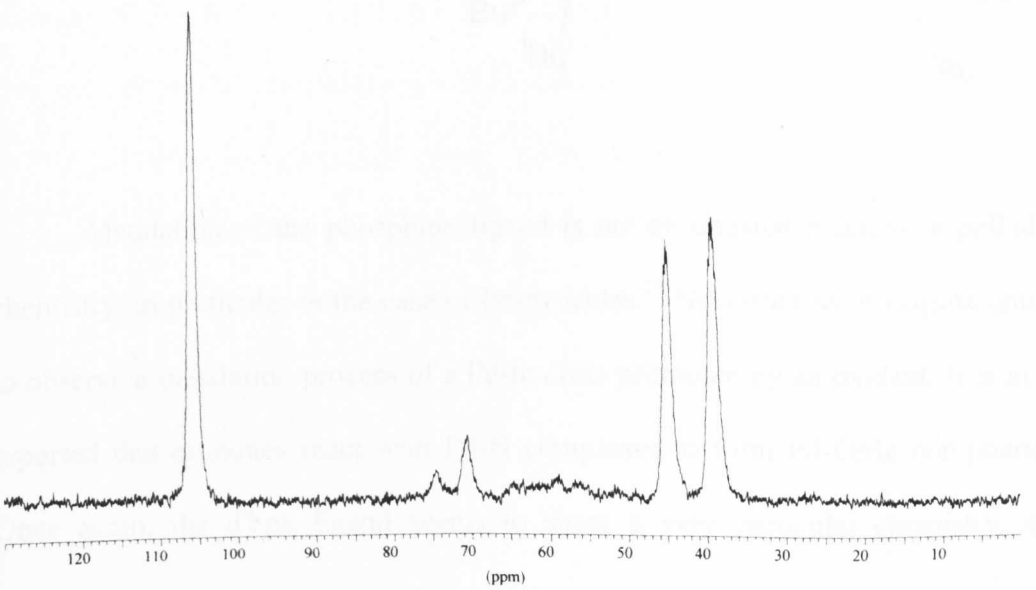

Scheme 2.8

Proposed structure for ***10***

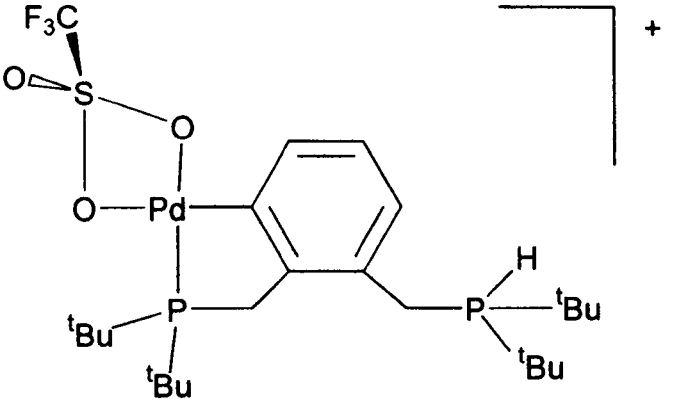

Scheme 2.9

Structure of $[Pd\{\eta^2\text{-}P(^tBu)_2CH_2C_6H_2(OCH_3)CH_2P^tBu_2\}(\mu\text{-}Br)]_2$, ***11***

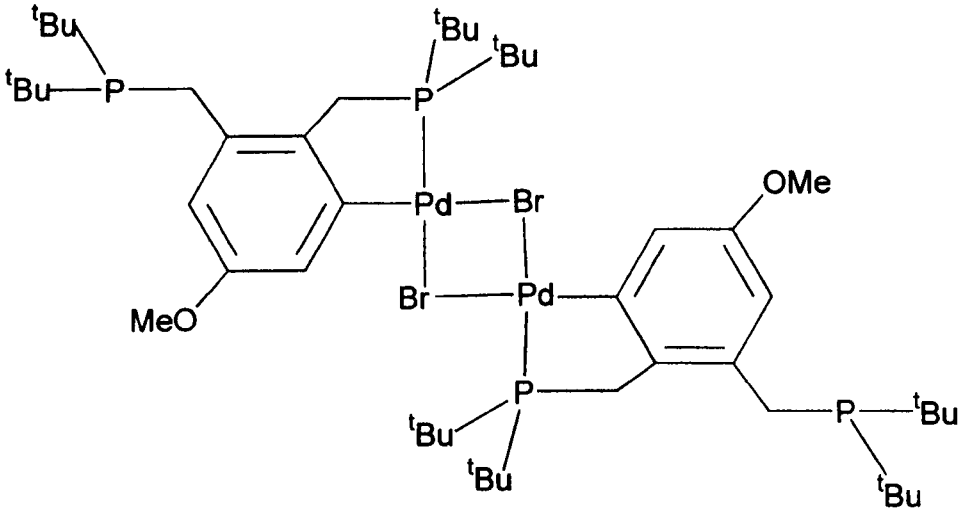

Metalation of the phosphine ligand is not an unusual reaction in palladium chemistry, in particular in the case of Pd-hydrides.[25] Nevertheless, it is quite unusual to observe a metalation process of a Pd-hydride promoted by an oxidant. It is in fact reported that quinones react with Pd-H complexes to form Pd-OMe compounds.[26] Once again, the d^{t}bpx ligand seems to show a very particular chemistry, quite

different from the one usually shown by the phopshines used for the synthesis of polyketones. Moreover, the fact that no Pd-OMe complexes have ever been observed even in the presence of a large excess of BQ seems to rule out the possibility of a methoxy cycle for the Ineos catalyst.

2.4.2 Substitution reactions

Complex **3** is a very useful starting material for the preparation of other Pd-hydride complexes *via* the substitution of the co-ordinated MeOH molecule with other ligands. Some examples of this reaction have already been discussed, when it has been shown that the synthesis of **3** in MeOH followed by evaporation of the solvent and dissolution of the residue in a new solvent results in the formation of the complexes $[Pd(d^tbpx)H(solv)]^+$ (solv = THF, **3a**; CH_3CN, **3c**; EtCN, **3d**; MeP, **3e**). The aquo-hydrido complex **3b** can be obtained in MeOH by addition of an excess of water, or in THF using traces of water. Moreover, **3** reacts in MeOH with $[Me_4N]X$ (X = Cl, Br, I) to give $Pd(d^tbpx)HX$ (X = Cl, **3f**; Br, **3g**; I, **3h**). In the same way, $[Pd(d^tbpx)H(Py)]^+$, **3i**, $[Pd(d^tbpx)H(PPh_3)]^+$, **3j**, and $[Pd(d^tbpx)H(PPh_2H)]^+$, **3k**, can be obtained by addition of Py, PPh_3 or PPh_2H to a solution of **3** in MeOH. Finally, addition of CO to **3** at 198 K results in the formation of $[Pd(d^tbpx)H(CO)]^+$, **3l** (this last reaction will be discussed more in detail in Chapter 6).

All these compounds have been characterised spectroscopically by multinuclear NMR measurements. None of them show any exchange process in the range 173-293 K. All the relevant NMR data are summarised in Table 2.5. As found for **3**, the compounds **3a-i** show in the $^{31}P\{^1H\}$ spectrum two doublets and the resonance at higher field is further split into a doublet in the ^{31}P spectrum; a doublet of doublets is always present in the ^1H spectrum.

Table 2.5

NMR data for Pd-hydride complexes containing d^{t}bpx

at 293 K in MeOH [a]

	P_A	P_B	H	$^2J(P_AP_B)$	$^2J(P_AH)$	$^2J(P_BH)$
MeOH 3	75.7	23.9	-10.0	16.0	22.0	181
THF 3a	69.7	21.3	-12.4	18.3	28.3	184
H_2O 3b	72.9	22.4	- [b]	br	- [b]	190
H_2O 3b [c]	71.7	23.1	- [b]	18.3	- [b]	186
CH_3CN 3c	68.8	23.9	-9.1	19.8	21.6	185
EtCN 3d	69.4	23.0	- [b]	19.6	- [b]	189
MeP 3e	72.7	24.3	- [b]	18.6	- [b]	183
Cl^- 3f	67.2	20.0	-10.4	21.6	28.4	180.7
Br^- 3g	67.6	21.6	-9.7 [d]	21.4 [e]	26.2 [d]	203
I^- 3h	63.5	21.0	-9.3 [e]	21.2	38.0 [e]	182
Py 3i	66.6	23.3	-9.4	18.4	17.1	182
PPh_3 3j [f]	60.0	35.0	-8.1	27.1	23 or 11 [g]	160
PPh_2H 3k [h]	59.2	32.9	-6.4	26.4	Not resolved	168.0
CO 3l [e]	60.3	30.7	-5.3	21.6	15.8	167.4

[a] δ in ppm, J in Hz. [b] ^1H not recorded. [c] in THF at 293 K. [d] in THF at 193 K. [e] in MeOH at 193 K.

[f] Supplementary NMR data: $\delta(\underline{P}Ph_3)$=11 ppm, $^2J(PPh_3\text{-}P_A)$=330 Hz, $^2J(PPh_3\text{-}P_B)$=26.3 Hz, $^2J(PPh_3\text{-}H)$= 23 or 11 Hz. [g] Impossible to distinguish between the two *cis*-^2J(P-H). [h] Supplementary NMR data: $\delta(\underline{P}Ph_2H)$=5.4 ppm, $\delta(PPh_2\underline{H})$=6.6 ppm, $^2J(PPh_2H\text{-}P_A)$=327.0 Hz, $^2J(PPh_2H\text{-}P_B)$=33.1 Hz, $^1J(\underline{P}Ph_2H\text{-}H)$=315.0 Hz.

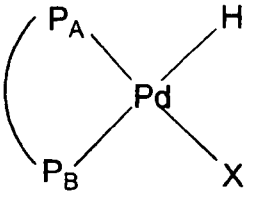

The $^{31}P\{^1H\}$ spectra of **3j** and **3k** show an AMX pattern due to the presence of three inequivalent P-atoms, and a doublet of doublets of doublets is present in the ^1H spectrum. **3l** has been fully characterised by repeating the reaction using ^{13}CO. In this way, $[Pd(d^tbpx)H(^{13}CO)]^+$, **3m**, is clearly formed [NMR data at 193 K: δ_H = -5.3 ppm, δ_P = 60.3 and 30.7 ppm, δ_C = 183.3 ppm, ^2J(P-P) = 21.6 Hz, ^2J(P-C) = 12.6 and 108 ppm, ^2J(P-H) = 15.8 and 167.4 Hz].

The stoichiometries of all these reactions are quite different. The formation of **3a** and **3c-e** requires the use of the ligand as solvent and the absence of acid. In the presence of acid, **5** (in THF and MeP) and **6** (CH_3CN and EtCN) are respectively formed. The formation of **3b** in THF requires the addition of a few equivalents of water, and the exact amount depends on the amount of free acid present. Further addition of water results in the formation of **6c**. Whereas, the same reaction in MeOH requires the addition of a large excess of water, and no further reaction has been observed. Complexes **3f-h** have been always obtained in mixture with $Pd(d^tbpx)X_2$ (X = Cl, **9**; Br, **12**; I, **13**). The formation of **3j-k** requires the addition of exactly one equivalent of the phosphine, whereas 5-10 equivalents of Py have been used for the synthesis of **3i**. Further addition of Py results in the formation of $[Pd(d^tbpx)(Py)_2]^{2+}$, **6d**. The NMR data for all these dicationic and neutral Pd-complexes are reported in Table 2.6. The formation of such complexes, formally, involves the displacement of a H^- ligand with a neutral or anionic ligand (*i.e.* H_2O, Py, Cl^-, Br^-, I^-). The hydride ion H^- can not exist in this form in solution, but it transforms into H_2 by combination with a proton (from the acid or the solvent). A similar reaction has been reported for other Pd-hydride complexes. For instance, $Pd(PEt_3)_2H(Cl)$ [27] reacts with KCN in MeOH to give $Pd(PEt_3)_2H(CN)$ (one equivalent of KCN) and then $Pd(PEt_3)_2(CN)_2$ after addition of a second equivalent of KCN. Formation of H_2 has been observed,

and it has been supposed that the proton comes from the methanol, according to eq. 2.5.

$$Pd(PEt_3)_2H(Cl) + 2KCN + MeOH \longrightarrow Pd(PEt_3)_2(CN)_2 + H_2 + KCl + KOMe \quad (2.5)$$

Table 2.6

^{31}P NMR data for $Pd(d^tbpx)X_2$ and $[Pd(d^tbpx)X_2]^{2+}$ at 293 K in MeOH

X	δP in ppm
H_2O **6c**	53.8 [a]
Py **6d**	48.7
Cl^- **9**	39.3
Br^- **12**	42.9 [b]
I^- **13**	40.0 [a]

[a] in THF. [b] in MeOH at 193 K

2.5 Conclusions

It has been shown in this Chapter that it is possible to easily form the hydride **3** from **1**, even using conditions which are similar to those used for the catalytic process. In particular, it has been possible to observe the presence of the hydride in solution at temperatures similar to those used in the catalytic process carried out in an autoclave (*i.e.* 80°C). Moreover, **3** is surprisingly stable toward addition of oxidants. No reaction has been observed with O_2, and only a large excess of BQ is able to convert **3** into **10**. This reaction is quite unusual and contradicts what has

previously been reported about oxidation of Pd-hydrides in MeOH to give methoxy complexes. Also the mechanism for the formation of **3** has been elucidated in detail. **1** is first protonated to give **2**, which is then easily oxidised to form **3**. The last process takes place in at least three steps. First, **2** is oxidised by O_2 or BQ to form **5**. TfO^- can then be displaced from the metal in **5** by the solvent in a polar medium to give **6**. Finally, the bis-solvento complex **6**, in the presence of an alcohol with an α-hydrogen, activates the alcohol, which is oxidised to form a carbonyl-containing species and a proton is reduced to give the hydride.

The formation of the hydride **3**, its extraordinary stability and its unusual reactivity with BQ further support the idea introduced in Chapter 1 that the d^{t}bpx ligand induces a quite particular chemistry, significantly different from the one observed with more classic diphosphine ligands, and this could be correlated with the selectivity of the catalytic system based on **1** for the formation of MeP.

References for Chapter Two

1. F. M. Conroy-Lewis, L. Mole, A. D. Redhouse, S. A. Lister and J. L. Spencer, *J. Chem. Soc. Chem. Commun.*, **1991**, 1601; N. Carr, B. J. Donne, L. Mole, A. G. Orpen and J. L. Spencer, *J. Chem. Soc. Dalton Trans.*, **1991**, 863; L. Crascall and J. L. Spencer, *J. Chem. Soc. Dalton Trans.*, **1992**, *24*, 3445
2. H. Grennberg, A. Gogoll and J. E. Backvall, *Organometallics*, **1993**, *12*, 1790
3. P. M. Maitlis, P. Espinet and M. J. H. Russell, *Comprehensive Organometallic Chemistry*, ed. G. Wilkinson, Pergamon Press, 1982, vol.6, p.340
4. V. V. Grushin, *Chem. Rev.*, **1996**, *96*, 2011
5. B. T. Heaton, C. Jacob and J. T. Sampanthar, *J. Chem. Soc. Dalton Trans.*, **1998**, 1403
6. I. Toth and C. J. Elsevier, *Organometallics*, **1994**, *13*, 2118
7. M. L. H. Green and H. Munokata, *J. Chem. Soc. Chem. Commun.*, **1971**, 549
8. F. Schager, K. Seevogel, K. R. Porschke, M. Kessler and C. Kruger, *J. Am. Chem. Soc.*, **1996**, *118*, 13075
9. D. J. Mabbott and P. M. Maitlis, *J. Organomet. Chem.*, **1975**, *102*, C34; D. J. Mabbott and P. M. Maitlis, *J. Chem. Soc. Dalton Trans.*, **1976**, 2156
10. R. Trebbe, F. Schager, R. Goddard and K. R. Porschke, *Organometallics*, **2000**, *19*, 521
11. A. B. Goel and S. Goel, *Inorg. Chim. Acta*, **1980**, *45*, L85
12. H. Imoto, H. Moriyama, T. Saito and Y. Sasaki, *J. Organomet. Chem.*, **1976**, *120*, 453
13. L. Abis, R. Santi and J. Halpern, *J. Organomet. Chem.*, **1981**, *215*, 263
14. H. C. Clark and C. R. Milne, *J. Organomet. Chem.*, **1978**, *161*, 51

15. B. T. Heaton, S. P. A. Herbert, J. A. Iggo, F. Metz and R. Whyman, *J. Chem. Soc. Dalton Trans.*, **1993**, 3081

16. P. M. Maitlis, *The Organic Chemistry of Palladium*, Academic Press, New York, 1971

17. J. Chatt and B. L. Shaw, *J. Chem. Soc.*, **1962**, 5075

18. M. Portnoy, F. Frolow and D. Milstein, *Organometallics*, **1991**, *10*, 3960

19. H. Werner, M. Bosh, M. E. Schneider, C. Hahn, F. Kukla, M. Manger, B. Windmuller, B. Wederndorfer and M. Laubender, *J. Chem. Soc. Dalton Trans.*, **1998**, 3549

20. G. A. Lawrance, *Chem. Rev.*, **1986**, *86*, 17

21. P. J. Stang, D. H. Cao, G. T. Poulter and A. M. Arif, *Organometallics*, **1995**, *14*, 1110

22. A. Vavasori and L. Toniolo, *J. Mol. Cat. A*, **1996**, *110*, 13

23. P. Leoni, M. Sommovigo, M. Pasquali, S. Midollini, D. Braga and P. Sabatino, *Organometallics*, **1991**, *10*, 1038

24. G. R. Eastham, Ph.D. Thesis, University of Durham, 1998

25. H. C. Clark, A. B. Goel and S. Goel, *Inorg. Chem.*, **1979**, *18*, 2803; H. C. Clark, A. B. Goel and S. Goel, *J. Organomet. Chem.*, **1979**, *166*, C29; D. F. Hill, B. E. Mann and B. L. Shaw, *J. Chem. Soc. Dalton Trans.*, **1973**, 270; R. F. Heck, *Org. React.*, **1982**, *27*, 345; A. D. Ryabov, *Chem. Rev.*, **1990**, *90*, 403

26. E. Drent and P. H. M. Budzelaar, *Chem. Rev.*, **1996**, *96*, 663; E. Drent, J. A. M. van Broekhoven and M. Y. Doyle, *J. Organomet. Chem.*, **1991**, *417*, 235; E. Drent, J. A. M. van Broekhoven and P. H. M. Budzelaar, *Applied Homogeneous Catalysis with Organometallics Compounds*, ed. B. Cornils and W. A. Herrmann, VCH, 1996, p. 333

27. E. H. Brooks and F. Glockling, *J. Chem. Soc. (A)*, **1967**, 1030

Chapter Three

Numbering scheme for Chapter 3

Pd(d^{t}bpx)(dba)	**1**
[Pd(d^{t}bpx)(dbaH)]$^+$	**2**
[Pd(d^{t}bpx)H(solv)]$^+$	**3**
[Pd(d^{t}bpx)H(Py)]$^+$	**3a**
[Pd(d^{t}bpx)(η^2-TfO)]$^+$	**4**
[Pd(d^{t}bpx)(solv)$_2$]$^{2+}$	**5**
[Pd(d^{t}bpx)(H_2O)$_2$]$^{2+}$	**5a**
[Pd(d^{t}bpx)(CH_3CN)$_2$]$^{2+}$	**5b**
[Pd(d^{t}bpx)(η^2-$MeSO_3$)]$^+$	**6**
[Pd(d^{t}bpx)(η^2-TsO)]$^+$	**7**
Pd(d^{i}ppx)($MeSO_3$)$_2$	**8**
[Pd(dppp)(H_2O)(TsO)][TsO]	**9**
[Pd(dppp)(H_2O)(TfO)][TfO]	**10**

Reactivity of Pd(d^{t}bpx)(dba) with acids: the $MeSO_3H$ system

3.1 Synthesis and characterisation of [Pd(d^{t}bpx)(η^2-$MeSO_3$)]$^+$, 6

It has been shown in Chapter 2 that the complex Pd(d^{t}bpx)(dba), **1**, is protonated by TfOH, TsOH, $MeSO_3H$ or HBF_4 resulting in the formation of [Pd(d^{t}bpx)(dbaH)]$^+$, **2**. In the case of TfOH and HBF_4, **2** is readily oxidised by O_2 or BQ in primary and secondary alcohols to give [Pd(d^{t}bpx)H(solv)]$^+$, **3**. In other solvents, [Pd(d^{t}bpx)(η^2-TfO)]$^+$, **4**, is normally obtained, apart from in CH_3CN and EtCN, where [Pd(d^{t}bpx)(solv)$_2$]$^{2+}$, **5**, is formed. In all cases, the initial solution deep-red of **2**, becomes pale-yellow at the end of the reaction. The same colour change of the solution is observed on addition of O_2 or BQ to a solution of **2** in the presence of $MeSO_3H$; in this case, the reaction is completely independent of the solvent. In fact, in all the solvents studied (MeOH, EtOH, CF_3CH_2OH, CH_3CN, MeP, THF, CH_2Cl_2, acetone), the $^{31}P\{^1H\}$ NMR spectrum at 293 K always shows a singlet at *ca.* 70 ppm. Moreover, no P-H coupling is present in the ^{31}P spectrum. It has been possible to crystallise this compound from THF/hexane, and X-ray analysis showed that it is [Pd(d^{t}bpx)(η^2-$MeSO_3$)]$^+$, **6**, the analogue of **4**. Using the same conditions with TsOH, a similar compound [Pd(d^{t}bpx)(η^2-TsO)]$^+$, **7**, is obtained and characterised *via* X-ray diffraction.

3.1.1 The crystal structures of $[Pd(d^tbpx)(\eta^2\text{-}RSO_3)]^+$ (R = Me, 6; CF_3, 4; p-$CH_3C_6H_4$, 7)

The three compounds referred to above have all been obtained as single crystals from THF/hexane using a similar procedure. Complex **6** is present in the solid state as the salt $[Pd(d^tbpx)(\eta^2\text{-}MeSO_3)][MeSO_3][MeSO_3H]$, where the anion is actually a dimer in which a methylsulfonate anion interacts through a hydrogen bond with a molecule of methylsulfonic acid. This is probably due to the fact that **6** has been crystallised in the presence of an excess of acid. Nevertheless, the refinement of the structure is quite good ($R_1 = 0.0397$).

7 crystallises in an even more complicated form; the elemental cell contains two independent cations, which show the same connectivity but slightly different bond angles and distances, two TsO^- anions, four molecules of free TsOH acid and six molecules of water. Moreover, there are disordered groups in some of the molecules of the free acid and free anion, and there are also residual electronic densities that could not be attributed during the refinement. This is probably due to the poor quality of the crystals used for the analysis. The resulting R_1 factor is very high (0.1447); the overall connectivity is not in doubt, whereas, the quality of the refinement does not allow a detailed discussion of the structural parameters.

4 crystallises as $[Pd(d^tbpx)(\eta^2\text{-}TfO)][TfO]$, but the refinement is not very good due to disorder in the fluorine atoms of the free anion (R_1= 0.1118). The structures of the cations **6** and **7** are reported in Figure 3.1 and 3.2, and the structure of **4** has been already reported in the last Chapter. The main bond distances and angles for the all three cations are reported in Table 3.1.

Figure 3.1

*Crystal structure of [Pd(d^{t}bpx)(η^2-$MeSO_3$)]$^+$, **6**. Different views.*

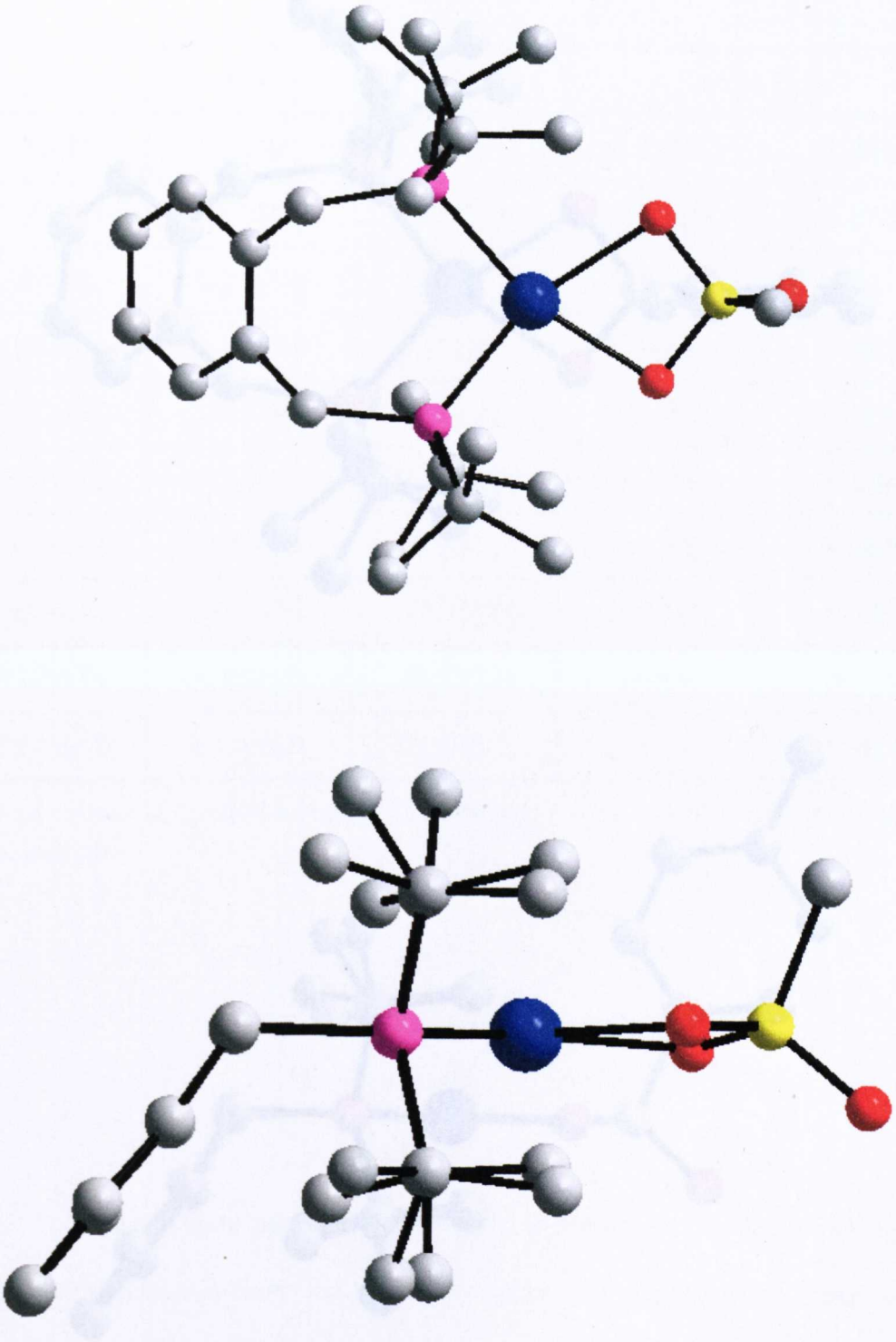

Figure 3.2

Crystal structure of [Pd(d^{t}bpx)(η^2-TsO)]$^+$, 7. Different views.

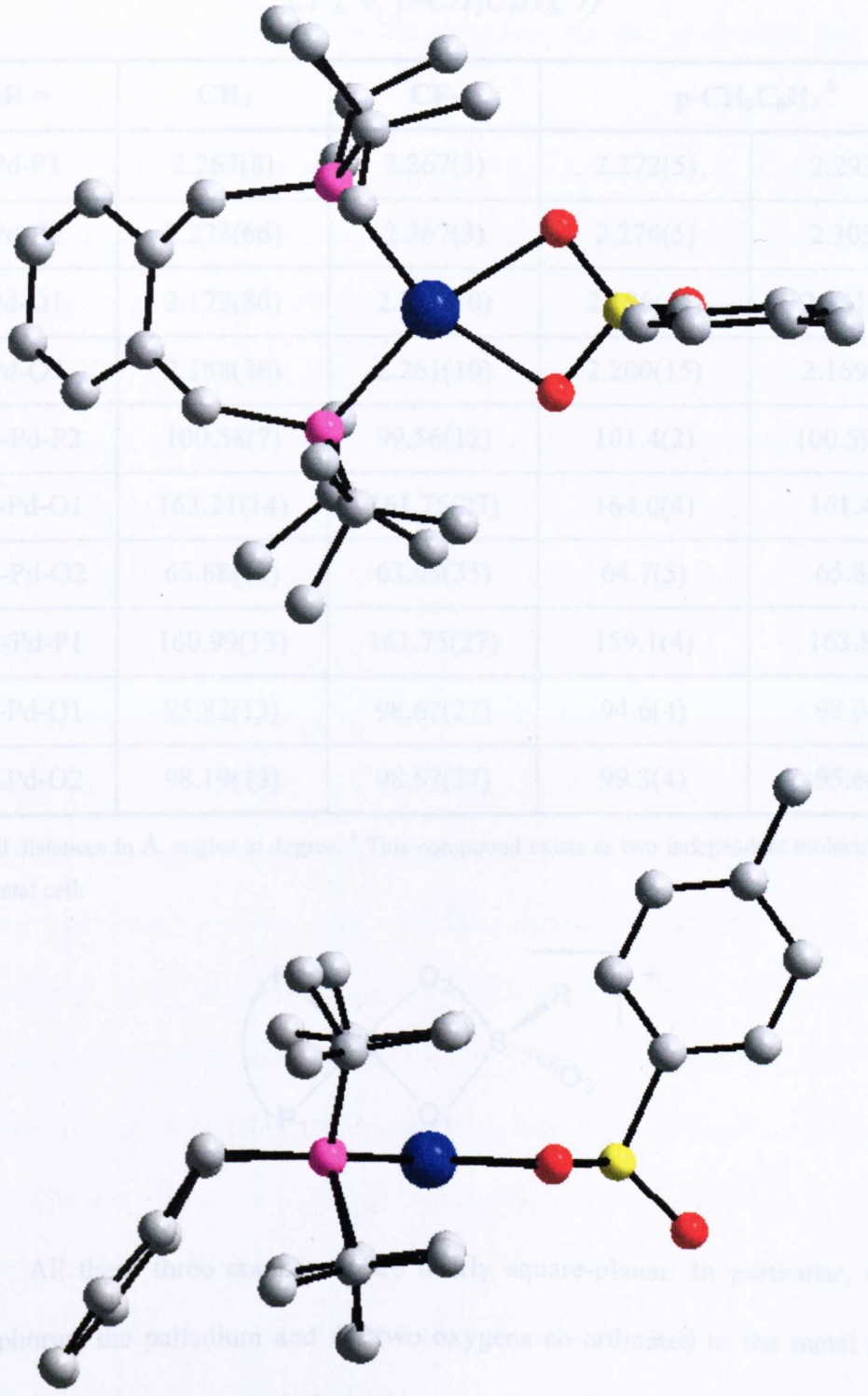

Table 3.1

*Main bond distances and angles for [Pd(d^{t}bpx)(η^2-RSO_3)]$^+$ (R = CH_3, **6**; CF_3, **4**; p-$CH_3C_6H_4$, **7**)* [a]

R =	CH_3	CF_3	p-$CH_3C_6H_4$ [b]	
Pd-P1	2.267(8)	2.267(3)	2.272(5)	2.293(5)
Pd-P2	2.273(66)	2.267(3)	2.276(5)	2.305(5)
Pd-O1	2.172(80)	2.261(10)	2.186(15)	2.161(16)
Pd-O2	2.188(38)	2.261(10)	2.200(15)	2.169(14)
P1-Pd-P2	100.58(7)	99.56(12)	101.4(2)	100.59(19)
P2-Pd-O1	163.21(14)	161.75(27)	164.0(4)	161.4(4)
O1-Pd-O2	65.68(17)	63.08(35)	64.7(5)	65.8(6)
O2-Pd-P1	160.99(13)	161.75(27)	159.1(4)	163.8(4)
P1-Pd-O1	95.82(13)	98.67(27)	94.6(4)	98.0(4)
P2-Pd-O2	98.19(13)	98.67(27)	99.3(4)	95.6(4)

[a] Bond distances in Å, angles in degree. [b] This compound exists as two independent molecules in the elemental cell.

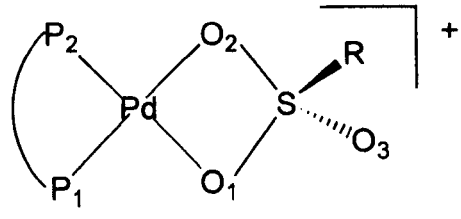

All these three complexes are nearly square-planar. In particular, the two phosphorus, the palladium and the two oxygens co-ordinated to the metal and the sulphur atoms are approximately in the same plane. The bond angles systematically deviate from the perfect geometry: the P1-Pd-P2 angle is *ca.* 100° in all the

complexes, whereas O1-Pd-O2 is in the range 63-66°. The resulting local symmetry around the metal centre is nearly C_{2v}. In all the three cases, the benzene ring of d^{t}bpx and the alkyl or aryl substituent of RSO_3^- adopt a pseudo-*trans* configuration with respect to the plane determined by the palladium, the two phosphorus and the two oxygen atoms.

The R_1 factors for **4** and **7** are very high and, hence, it is not possible to discuss in detail their structural parameters. Whereas, the R_1 value for **6** is quite good and, therefore, its structure will be further discussed. The structure of the bis-aquo complex $[Pd(d^tbpx)(H_2O)_2]^{2+}$, **5a**, has been reported previously.[1] Also in this case, the bite angle of the diphosphine is *ca.* 100°, whereas the average value of the Pd-P bonds (2.296 Å) is greater than in **6**. At the same time, the average value for Pd-O in **5a** (2.137 Å) is shorter than in **6**. This is due to the fact that water is a stronger ligand than RSO_3^-.

The co-ordination mode of RSO_3^- in the three cationic complexes is very particular and rare, especially for palladium. To the best of our knowledge, the structure of a palladium complex containing a chelating sulfonate anion has not been reported previously, and examples with other metals are also very rare.[2,3] The co-ordination of RSO_3^- as a monodentate ligand is more common. As examples, it is worthwhile to report $Pd(d^ippx)(MeSO_3)_2$,[1] **8**, $[Pd(dppp)(H_2O)(TsO)][TsO]$,[4] **9**, and $[Pd(dppp)(H_2O)(TfO)][TfO]$,[5] **10**. In all these cases, the Pd-O bond for the sulfonate anion is shorter than in **6** [2.117(2) and 2.131(2) Å for **8**; 2.152(3) Å for **9** and 2.159(3) Å for **10**]. This is obviously due to the fact that the sulfonate anion is a stronger base when it acts as a mono-dentate ligand rather than when it co-ordinates as a chelating ligand.

3.1.2 The behaviour in solution of [Pd(d^{t}bpx)(η^2-$MeSO_3$)]$^+$, 6

The complex **6** shows a very interesting behaviour in solution. The case of CH_3CN will be discussed apart in Section 3.1.3, since in this solvent the co-ordinated $MeSO_3^-$ anion partially dissociates to form $[Pd(d^tbpx)(CH_3CN)_2]^{2+}$, **5b**. Whereas, in the solvents used in this Section (*i.e.* MeOH, acetone, THF, MeP and CH_2Cl_2) the dissociation of the anion has not been observed under any conditions. In all these solvents, only one singlet at *ca.* 70 ppm is present at room temperature. On cooling the solution down to 193 K, two separate singlets appear in all solvents except for CH_2Cl_2 (see Table 3.2).

Table 3.2

$^{31}P\{^1H\}$ NMR data at 193 K for [Pd(d^{t}bpx)(η^2-$MeSO_3$)]$^+$, 6

in different solvents

Solvent	δ_P (1st singlet) ppm	δ_P (2nd singlet) ppm	$\Delta\delta$ ppm
Acetone	66.9	65.6	1.3
MeOH	66.7	65.5	1.2
MeOH (213 K)	67.0	66.0	1.0
THF	66.1	65.4	0.7
THF (173 K)	66.3	62.1	1.2
MeP	66.6	66.0	0.6
CH_2Cl_2	66.2	none	0

These two singlets never integrate 1:1, and the relative intensities depend on the experimental conditions (*i.e.* solvent and temperature). It is interesting to note that the difference in chemical shift (Δδ) between the two singlets is greater in more polar solvents, *e.g.* MeOH and acetone, than in the less polar solvent THF. Moreover, in THF Δδ increases from 0.7 ppm to 1.2 ppm by cooling the solution from 193 K to 173 K, whereas, in MeOH, Δδ increases from 1.0 to 1.2 ppm on cooling the solution from 213 K to 193 K. Further information about this system comes from the use of mixtures of different solvents. In Table 3.3, the NMR data obtained at 193 K in mixtures of CH_2Cl_2/MeOH at different compositions are reported. It is evident that Δδ increases as the amount of MeOH (and so, the polarity of the medium) increases.

Table 3.3

*$^{31}P\{^1H\}$ NMR data at 193 K for $[Pd(d^tbpx)(\eta^2\text{-}MeSO_3)]^+$, **6**, in mixtures CH_2Cl_2/MeOH*

Composition (% CH_2Cl_2)	δ_P (1st singlet) ppm	δ_P (2nd singlet) ppm	Δδ ppm
100	66.19	none	0
75	66.63	66.52	0.11
63	66.76	66.56	0.19
50	66.82	66.55	0.28
25	66.95	66.33	0.62
10	66.96	66.09	0.87
0	67.06	65.99	1.07

Moreover, in Table 3.4 the NMR data obtained at different temperatures in a mixture 1:1 THF/CH_2Cl_2 are reported. In this case, $\Delta\delta$ increases as the temperature decreases. Therefore, two well resolved singlets are present at 154 K. As the temperature increases, they start to broaden, until at 223 K only one singlet is present.

Table 3.4

*NMR data at VT for [Pd(d^{t}bpx)(η^2-$MeSO_3$)]$^+$, **6**, in mixtures CH_2Cl_2/THF 1:1*

Temperature K	δ_P (1st singlet) ppm	δ_P (2nd singlet) ppm	$\Delta\delta$ ppm
154	65.6	64.8	0.8
193	66.3	65.9	0.4
223	66.4	none	0
290	67.4	none	0

All these data can be explained by assuming that **6** exists in solution as two conformers, A and B, which differ only in the orientation of the benzene ring of the d^{t}bpx ligand with respect to the Me-group of the chelating $MeSO_3^-$ anion relative to the plane determined by Pd, the two P and the two co-ordinated oxygen atoms (see Scheme 3.1). These two conformers can exchange and, hence, at higher temperatures only one resonance is present. The coalescence temperature depends on the solvent, and increases with the polarity of the medium. At 193 K, MeOH, acetone, MeP and THF are all below the coalescence temperature and, hence, two resonances are

present, whereas CH_2Cl_2 is above the coalescence temperature and, so, only one singlet is present in the spectrum. Moreover, at 193 K the exchange rate in THF is greater than in MeOH. In fact, in THF the two singlets are broad and quite close together (small $\Delta\delta$): only at 173 K do they become well resolved. In a similar way, all the other observations can be explained easily using this hypothesis (no dissociation, two conformers with an exchange rate which decreases as the polarity of the medium increases).

Scheme 3.1

Orthogonal representations of the proposed conformers of

$[Pd(d^tbpx)(\eta^2\text{-}MeSO_3)]^+$, 6

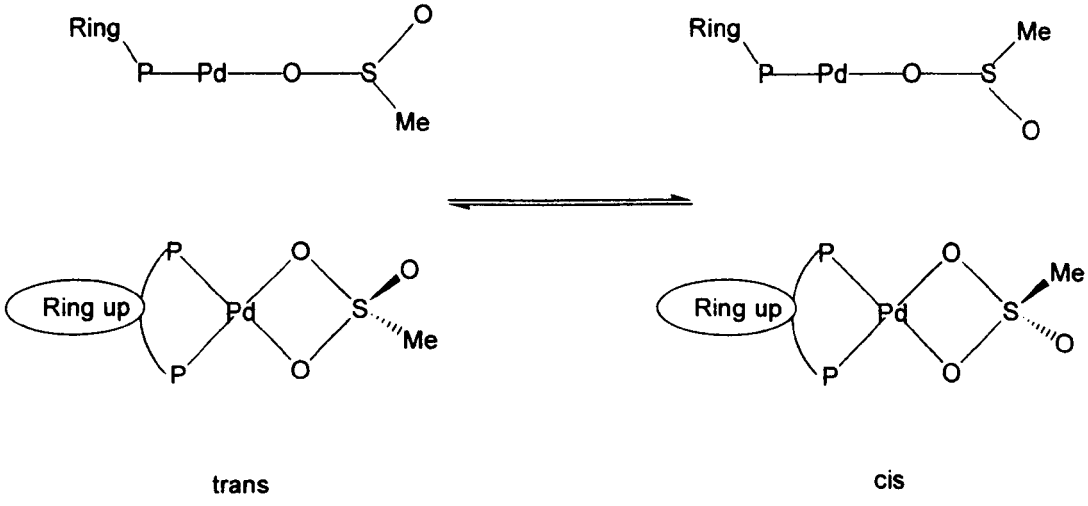

The outstanding problem is to understand the mechanism of the exchange. The inverse relationship between rate and polarity excludes the involvement of a direct interaction between the metal and the solvent. In fact, supposing a mechanism (see Scheme 3.2) in which a) the solvent co-ordinates to the metal, b) the co-ordination mode of $MeSO_3^-$ changes from η^2 to η^1, c) η^1-$MeSO_3^-$ rotates, d) $MeSO_3^-$

becomes again η^2 by displacing the solvent, a direct relationship between rate and polarity would be expected (a more polar solvent interacts more strongly with the metal).

Scheme 3.2

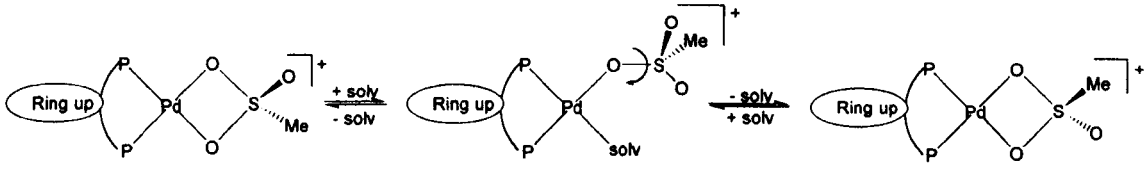

Hence, a different mechanism has to be used to explain the exchange between the *cis* and *trans* conformers of **6**. Two hypotheses are possible:

1) Intra-molecular mechanism. The exchange between the conformers could involve just the rotation of some bonds inside the molecule, without any bond dissociation. As a particular case of this mechanism, an isomerisation through a tetrahedral intermediate can be assumed. The solvent-dependence can be explained considering the interactions between the cation and the solvent. In particular, the "free" oxygen of the co-ordinated $MeSO_3^-$ is a centre with a partial negative charge, which can interact *via* dipolar interactions and/or hydrogen bond with the solvent. These interactions are stronger in polar solvents and create a network of forces that slows down the exchange.
2) Inter-molecular (anion assisted) mechanism. In this case, it is supposed that the exchange between the conformers takes place *via* exchange of the co-ordinated $MeSO_3^-$ with the free anion. In a polar solvent, the two ions are quite far away and, hence, the exchange is slow. Reducing the polarity of the medium, the cation and anion come close together and, therefore, the exchange becomes faster.

The actual mechanism involved in the exchange process can be distinguished by studying the effect of the concentration of the free anion on the exchange rate. In fact, if the anion-assisted mechanism is correct, and the free anion is directly involved in the inter-molecular mechanism, the rate of the exchange should increase by increasing the concentration of the anion. For the intra-molecular mechanism the anion is not involved, and the rate of the process should not change on varying the anion concentration. As shown before, the easiest way to measure the exchange rate in different conditions is to report the difference in chemical shift ($\Delta\delta$) between the two singlets due to the two conformers of **6** *vs.* the concentration of the anion (see Table 3.5).

Table 3.5

*$^{31}P\{^1H\}$ NMR data at 193 K for $[Pd(d^tbpx)(\eta^2\text{-}MeSO_3)]^+$, **6**, in MeOH*

Number of equivalents of $MeSO_3^-$ per mole of palladium	$\Delta\delta$ **(ppm)**
2	0.90
5	0.88
10	0.87
15	0.81
20	0.91
30	0.92
45	0.91
60	0.99
80	1.00

It is clear from the NMR data reported, that there is not a significant dependence of the exchange rate on the concentration of the anion and, therefore, the actual mechanism for the exchange process is the intra-molecular one, probably *via* a tetrahedral intermediate (see Scheme 3.3). The involvement of a tetrahedral intermediate has been widely claimed in order to explain other exchange processes on a square-planar centre, like *cis-trans* isomerisation.[6] Moreover, other kinds of intra-molecular rearrangements in **6** are very difficult. Thus, inversion of the sulphur centre without any bond dissociation is very unlikely, whereas theoretical calculations [1] rule out the possibility of an internal rotation of the d^{t}bpx ligand.

Scheme 3.3

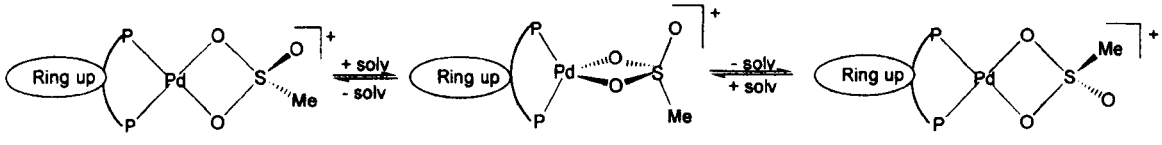

3.1.3 The behaviour of [Pd(d^{t}bpx)(η^2-$MeSO_3$)]$^+$, 6, in CH_3CN

Dissolution of **6** in CH_3CN results in a system different from those described in the previous section. The spectrum at 298 K (see Figure 3.3) is very broad, whereas a sharp singlet at 55 ppm is present at 237 K. By increasing the temperature, this resonance starts to broad and its intensity decreases, whereas a new resonance at *ca.* 68 ppm begins to appear; finally, at 327 K, only the resonance at 68 ppm is present.* By analogy with the NMR data of other species studied in this thesis, the

* The apparent change in chemical shift is due to the fact that the spectra at low and room temperature have been recorded using CD_2Cl_2 as external lock, whereas the spectra at 315 K and 327 K have been recorded using D_2O as external lock.

species at 68 ppm can be formulated as **6**, whereas the one at 55 ppm is **5b**. Thus, an equilibrium between these two species exists in CH_3CN.

Figure 3.3

*$^{31}P\{^1H\}$ NMR at VT of $[Pd(d^tbpx)(\eta^2\text{-}MeSO_3)]^+$, **6**, in CH_3CN*

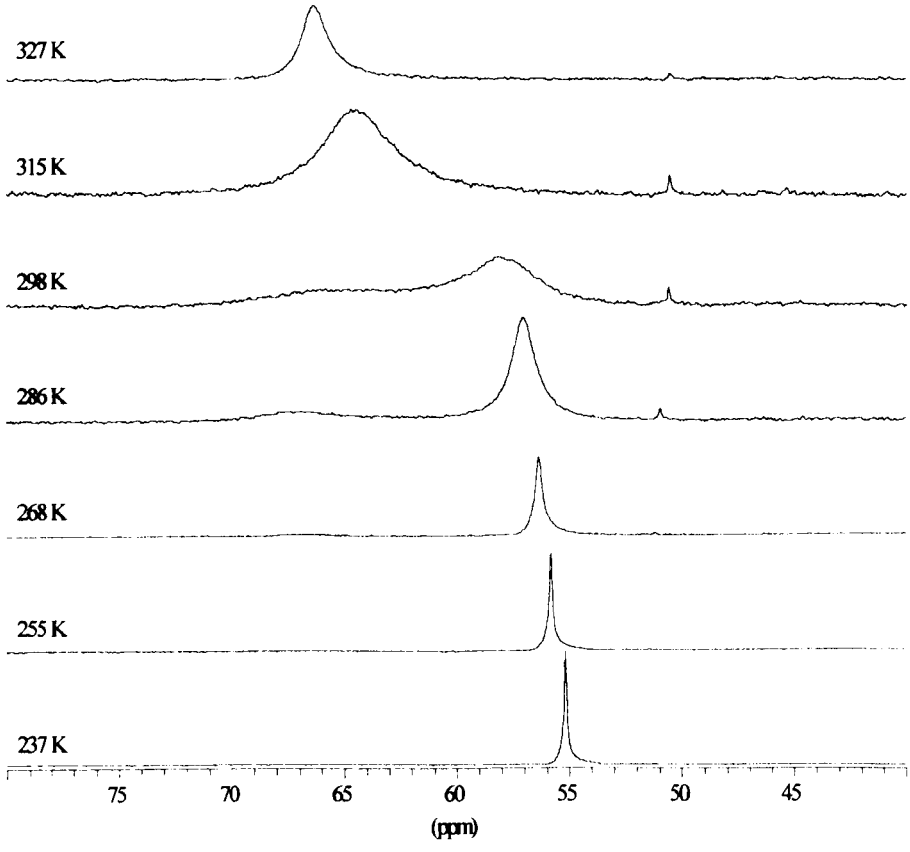

$$[Pd(d^tbpx)(\eta^2\text{-}MeSO_3)]^+ + 2CH_3CN \rightleftharpoons [Pd(d^tbpx)(CH_3CN)_2]^{2+} + MeSO_3^- \quad (3.1)$$

6 **5b**

Due to the fact that the spectrum is very broad, it is very difficult to do a quantitative analysis of the equilibrium. In all cases, it is very surprising that even a strongly co-ordinating solvent such as CH_3CN is not able to fully displace the "weakly" co-ordinating methanesulfonate anion. Once again, the bulky d^{t}bpx ligand seems to be able to stabilise species which are supposed to be very reactive.

3.2 Reactivity of [Pd(d^{t}bpx)(η^2-$MeSO_3$)]$^+$, 6

It is noteworthy that **6** is very stable in MeOH at room temperature, whereas in the same conditions **4** reacts very fast with the solvent to give the hydride **3**. This is probably due to the fact that $MeSO_3^-$ co-ordinates more strongly to the metal than TfO^-. Thus, in a polar medium the triflate anion readily dissociates to form the bis-solvento complex **5**. In an inert solvent as CH_3CN, the bis-solvento complex is stable, whereas in an alcoholic medium the dicationic species **5** activates the solvent and a redox process takes place (see Chapter 2) resulting in the formation of the hydride. The fact that $MeSO_3^-$ is more strongly bound to the metal explains the stability of **6** in MeOH and, at the same time, suggests that probably more forcing conditions are needed in order to form the hydride with this anion. This can be achieved in different ways.

The fact that dissociation of the anion is required in order to form the hydride, suggests that addition of an appropriate ligand should be able to induce the elimination of $MeSO_3^-$. Indeed, this has been confirmed by addition of pyridine (Py). Thus, reaction of **6** in MeOH with 6-10 equivalents of pyridine results in the nearly complete formation of the hydride complex [Pd(d^{t}bpx)H(Py)]$^+$, **3a** (see Chapter 2 for its characterisation). The following mechanism can be proposed to be responsible for hydride formation on addition of pyridine to **6**. Pyridine is quite a strong ligand and, thus, it can co-ordinate to the metal, forcing the methylsulfonate anion to pass from a η^2 to a η^1 co-ordination. The loss of the extra-stabilisation due to the chelating effect labilises the $MeSO_3^-$ which is readily displaced by one molecule of MeOH. Finally, co-ordination to the metal activates MeOH and the hydride is formed (see Scheme

3.4). Water can be used instead of pyridine, but in this case a large excess is needed, probably because of the fact that water is a weaker ligand than pyridine.

Scheme 3.4

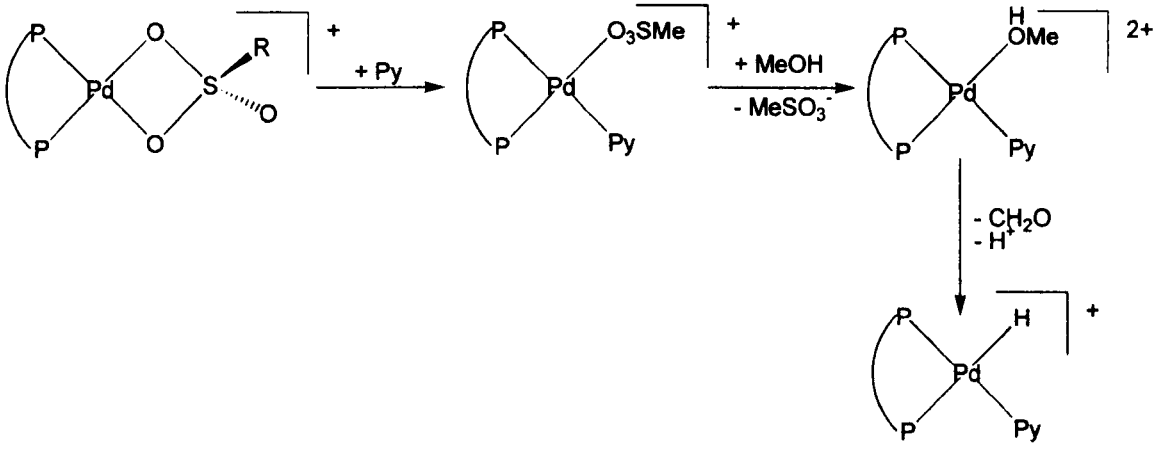

Finally, the hydride can also be partially formed by thermal activation of **6**. In fact, refluxing **6** in MeOH under nitrogen for *ca.* 1 hr results in the partial formation of the hydride as indicated by NMR (see Figure 3.4). This result is very important, since it shows that the hydride can be formed in the presence of $MeSO_3H$ using the operative conditions of the industrial process.

3.3 Reactivity of Pd(d^{t}bpx)(dba), 1, with TsOH

The reaction between **1** and TsOH is very similar to the analogous reaction with $MeSO_3H$. Addition of TsOH to **1** results in the formation of **2**, which is, then, readily oxidised by oxygen or BQ affording **7**. No hydride has been observed in all the solvents considered at room temperature, as in the case of $MeSO_3H$, whereas, it is possible to form the hydride by addition of water to a solution of **7** in MeOH.

Figure 3.4

$^{31}P\{^1H\}$ NMR spectrum at 293 K of Pd(d^{t}bpx)(dba)/$MeSO_3H$ after refluxing for 1 hour under nitrogen

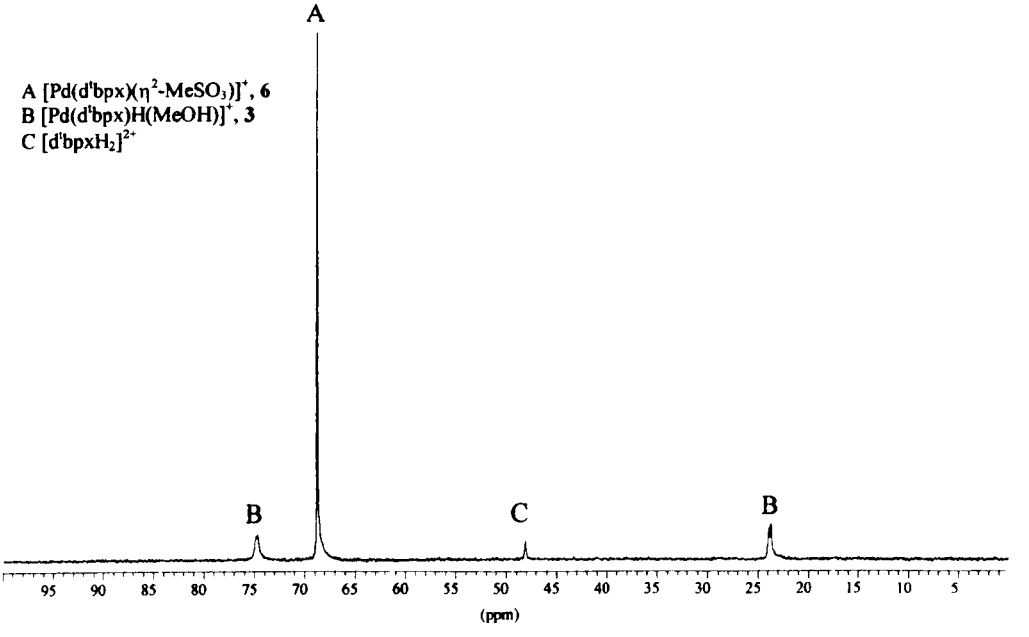

The $^{31}P\{^1H\}$ NMR spectrum of **7** at 293 K always shows a singlet at *ca.* 70 ppm, in all the solvents considered (except CH_3CN), whereas at 193 K it is possible to have one of two singlets, dependent on the solvent (see Table 3.6). As in the case of **6**, it is possible to explain this observation for the tosylate complex by assuming that **7** exists in solution as two conformers, which can mutually inter-convert. The presence of only one singlet means that the conversion is fast on the NMR time-scale, whereas the rate is slow when two singlets are present. Hence, it is also possible to correlate the rate of exchange with the polarity of the solvent. Surprisingly, **7** shows a direct relationship between the rate and the polarity, whereas an inverse relationship has been observed for **6**. Therefore, it is possible to conclude

that the exchange for **7** occurs *via* a solvent-assisted mechanism (see Scheme 3.5 and Section 3.1.2 for a detailed discussion of the different mechanisms).

Table 3.6

$^{31}P\{^1H\}$ NMR data at 193 K for $[Pd(d^tbpx)(\eta^2\text{-}TsO)]^+$, 7, in different solvents

Solvent	Δδ (ppm)
MeOH	0
Acetone	0
THF	0.24
MeP	0.36
CH_2Cl_2	0.55

Scheme 3.5

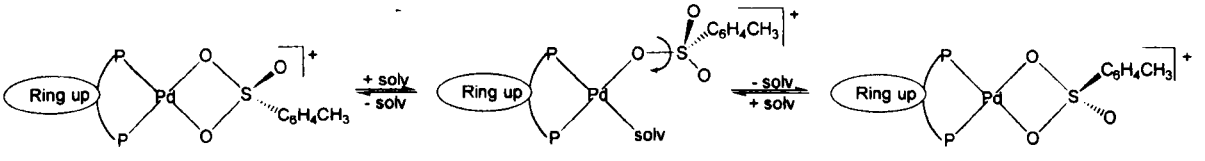

It is very surprising that replacing a methyl group on the anion with a tolyl group affects the mechanism of the exchange process so much. At the same time, this also suggests that the chemistry of these palladium complexes is regulated by a very delicate balance between the steric and electronic properties of all the ligands involved, and it could explain also the change in catalytic activity induced by

$MeSO_3H$ *versus* TsOH (*i.e.* the catalyst based on **1** and $MeSO_3H$ has higher performances than the one based on **1** and TsOH).

Also in the case of **7**, partial dissociation of the sulfonate anion is observed in CH_3CN at low temperature. In fact, one main species which resonates at 55 ppm (see Figure 3.5) is present at 238 K, whereas, on raising the temperature a second species at 68-70 ppm starts to appear, until at 284 K this become the main species in solution.

Figure 3.5

$^{31}P\{^1H\}$ NMR at VT of $[Pd(d^tbpx)(\eta^2\text{-}TsO)]^+$, 7, in CH_3CN

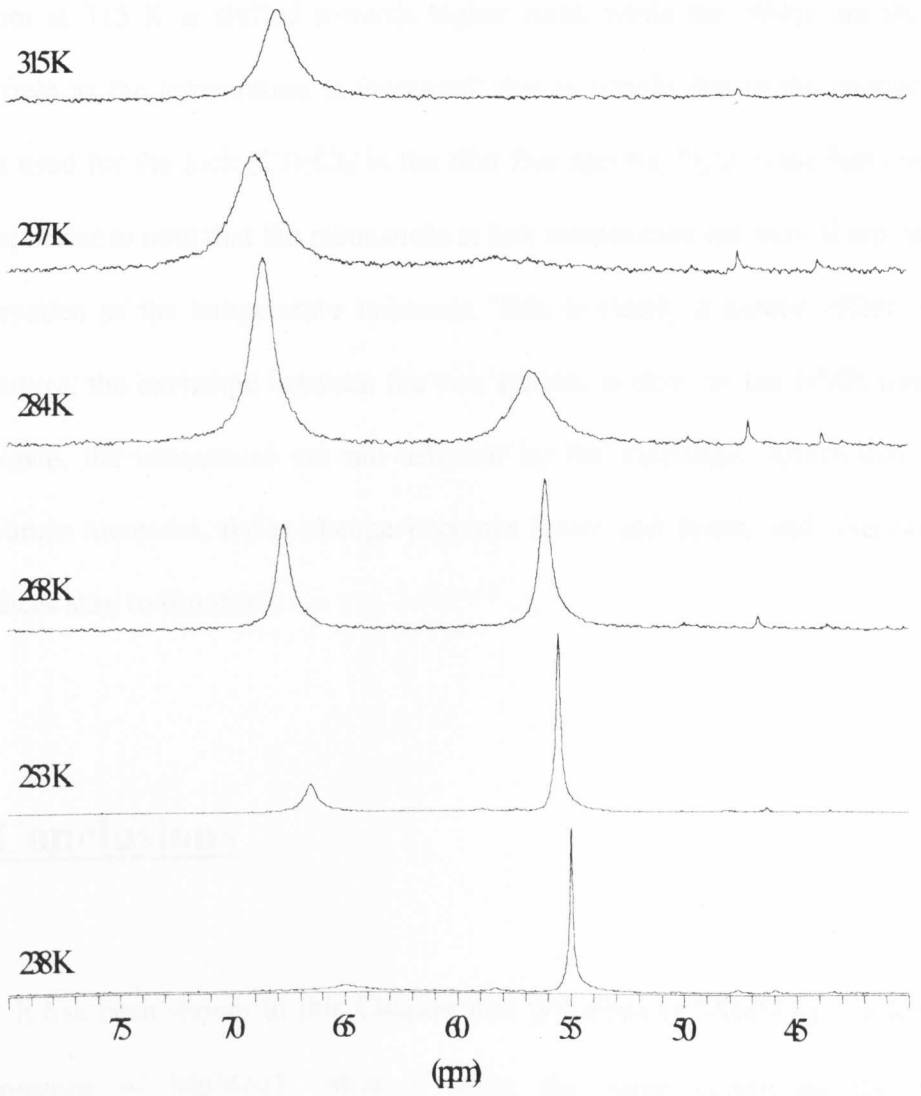

On the basis of all the results discussed previously, the resonance at 65 ppm can be assigned to **7** and the one at 55 ppm to **5b**. Hence, the following equilibrium is present in solution:

$$[Pd(d^tbpx)(\eta^2\text{-}TsO)]^+ + 2CH_3CN \rightleftharpoons [Pd(d^tbpx)(CH_3CN)_2]^{2+} + TsO^- \qquad (3.2)$$

7 **5b**

In this case, the NMR spectra are less broad than found for **6** and, and this allows calculation of the thermodynamic parameters for the equilibrium 3.2, giving $\Delta H° = -5.3 \pm 0.4$ kcal mol^{-1} and $\Delta S° = -21.8 \pm 1.5$ cal mol^{-1} K^{-1}. Hence, **7** is the entropic product, whereas **5b** is favoured enthalpically. It is important to note that the spectrum at 315 K is shifted towards higher field, while the others are shifted to lower field as the temperature is increased; this is simply due to the change in the solvent used for the lock (CD_2Cl_2 in the first five spectra, D_2O in the last one). It is also important to note that the resonances at low temperature are very sharp, whereas they broaden as the temperature increases. This is clearly a kinetic effect. At low temperature, the exchange between the two species is slow on the NMR time-scale and, hence, the resonances are not affected by the exchange. Afterwards, as the temperature increases, the exchange becomes faster and faster, and, therefore, the resonances start to broaden.

3.4 Conclusions

It has been shown in this Chapter that $[Pd(d^tbpx)(\eta^2\text{-}MeSO_3)]^+$ is formed in the presence of $MeSO_3H$, whereas using the same conditions the hydride

$[Pd(d^tbpx)H(solv)]^+$ is formed in the presence of TfOH. This change in the product formed is due to the different co-ordination ability of the two anions TfO^- and $MeSO_3^-$. It is very interesting to note the very high sensitivity of the complexes containing d^{t}bpx towards also little changes in the electronic and/or steric properties of the other ligands present. Moreover, complexes containing a chelating sulfonate anion are quite rare and, in all cases, the anion is usually easily displaced by polar solvents, whereas, $MeSO_3^-$ in $[Pd(d^tbpx)(\eta^2\text{-}MeSO_3)]^+$ is very strongly bound and is only partially displaced in CH_3CN. Thus, d^{t}bpx seems to stabilise this particular co-ordination mode of the anion, probably because in this way the steric repulsions between the diphosphine and the other ligands are reduced.

$[Pd(d^tbpx)(\eta^2\text{-}MeSO_3)]^+$ can be converted into the hydride in different ways. The reaction involving pyridine clearly shows that the anion has to be dissociated and MeOH co-ordinated to the metal before the hydride is formed. Moreover, the fact that the hydride can also be obtained by thermal activation of $[Pd(d^tbpx)(\eta^2\text{-}MeSO_3)]^+$ indicates that a hydride might be present in the operative conditions of the industrial process based on Pd(d^{t}bpx)/$MeSO_3H$ and, therefore, it could be involved in the catalytic process. At the same time, $[Pd(d^tbpx)(\eta^2\text{-}MeSO_3)]^+$ is more stable than the hydride and this could explain why the Pd(d^{t}bpx)/$MeSO_3H$ system results in higher catalytic performances than the Pd(d^{t}bpx)/TfOH system.

References for Chapter Three

1. G. R. Eastham, Ph.D. Thesis, University of Durham, 1998
2. H. Werner, M. Bosh, M. E. Schneider, C. Hahn, F. Kukla, M. Manger, B. Windmuller, B. Weberndorfer and M. Laubender, *J. Chem. Soc. Dalton Trans.*, **1998**, 3549
3. G. A. Lawrance, *Chem. Rev.*, **1986**, *86*, 17
4. F. Benetollo, R. Bertani, G. Bombieri and L. Toniolo, *Inorg. Chimica Acta*, **1995**, *233*, 5
5. P. J. Stang, D. H. Cao, G. T. Poulter and A. M. Arif, *Organometallics*, **1995**, *14*, 1110
6. B. E. Mann, *Comprehensive Organometallic Chemistry*, ed. G. Wilkinson, Pergamon Press, 1982, vol.3, p.89

Chapter Four

Numbering scheme for Chapter 4

Pd(d^{t}bpx)(dba)	**1**
[Pd(d^{t}bpx)H(MeOH)]$^+$	**2**
[Pd(d^{t}bpx)H(EtCN)]$^+$	**2a**
[Pd(d^{t}bpx)H(solv)]$^+$	**2b**
[Pd(d^{t}bpx)(η^2-TfO)]$^+$	**3**
[Pd(d^{t}bpx)(CH_2CH_3)]$^+$	**4**
[Pd(d^{t}bpx)($CH_2{}^{13}CH_3$)]$^+$	**4a**
[Pd(d^{t}bpx)($^{13}CH_2CH_3$)]$^+$	**4b**
Pd(d^{t}bpx)(C_2H_4)	**5**
[Pt(d^{t}bpx)(CH_2CH_3)]$^+$	**6**
[Pd(d^{t}bpx)(solv)$_2$]$^{2+}$	**7**
Pd(d^{t}bpx)HCl	**8a**
Pd(d^{t}bpx)HBr	**8b**
Pd(d^{t}bpx)HI	**8c**
[Pd(d^{t}bpx)($CH_2CH_2CH_3$)]$^+$	**9**
[Pd(d^{t}bpx)($CH_2CH_2(CH_2)_3CH_3$)]$^+$	**10**
[Pd(d^{t}bpx)($CH_2CH_2(CH_2)_{13}CH_3$)]$^+$	**10a**
[Pd(d^{t}bpx)(η^2-$MeSO_3$)]$^+$	**11**

Reactivity of some catalyst precursors and catalytic intermediates with olefins

4.1 Introduction

It has been shown in the last two Chapters that it is possible to convert under certain conditions the complex Pd(d^{t}bpx)(dba), **1**, into the hydride [Pd(d^{t}bpx)H(MeOH)]$^+$, **2**. Of particular interest is the fact that **2** can be partially obtained in the presence of $MeSO_3H$ under conditions very similar to the ones used for the catalytic process. All the reactions presented in the previous Chapters have been carried out under N_2. Hence, in this Chapter the reactivity of the same complexes under ethene will be considered.

The reaction between metal-hydrides and olefins is one of the classic routes for the synthesis of metal-alkyl complexes.[1] One of the problems associated with the compounds obtained in this way is that they contain a β-hydrogen and, as a result, the reaction can be, sometimes, reversed *via* β-H-elimination. In all cases, β-H-elimination is one of the main reasons for the decomposition of metal-alkyl complexes,[1] and this is widely exemplified in palladium chemistry.[2,3] Different strategies have been adopted in order to avoid this problem. The most obvious solution is to use alkyl groups without a β-hydrogen; this strategy has been very successful in a very large number of cases. Thus, it is interesting to note that, whereas the complex Pd(TMEDA)IMe is quite stable, the analogous ethyl complex

Pd(TMEDA)IEt decomposes over one day in $CHCl_3$ to form palladium metal.[4] β-H-elimination in an ethyl-palladium square planar complex is favoured by the presence of a labile ligand in the *cis* position. Thus, ethyl complexes can be stabilised using strongly bound ligands *cis* to the ethyl group. Phosphines have been largely used for this purpose. It is interesting to note that most of the known palladium-ethyl complexes containing monophosphine ligands adopt a *trans* geometry.[5-7] In all cases, the stability of these complexes is increased if the ligand *trans* to the ethyl group is also not labile (*e.g.* a halide anion or a thiolate group); otherwise, *cis-trans* isomerisation becomes quite facile and, hence, β-H-elimination can occur. In the case of diphosphine ligands, the *trans* arrangement is not possible and, therefore, ethyl complexes are quite rare. Also in this case, the introduction of a good *cis* ligand is fundamental; *e.g.* the complex Pd[(R,R)-Duphos]Et(C_6F_5) has been recently characterised.[8]

A completely different strategy has been adopted by Spencer, who has synthesised new nickel, palladium and platinum ethyl complexes, stabilised by bulky diphosphine ligands and an agostic interaction between the metal and one of the β-hydrogens of the ethyl ligand.[9,10] These compounds are very interesting, because they represent a stable form of one of the possible intermediates in the β-H-elimination process. Moreover, Spencer has shown clearly that these complexes are in equilibrium with the ethene-hydride form, which can then lose ethene resulting (in the case of platinum) in a binuclear di-hydride species (see Scheme 4.1); what is the ground state of the complex (*i.e.* the β-agostic ethyl compound or the ethene-hydride one) and the possibility of the formation of the dimer, is completely controlled by the phosphine used. Bulky and basic diphosphines (*e.g.* d^{t}bpx and d^{t}bpp) favour the β-agostic ethyl compound, whereas, decreasing the size of the ligand, the ethene-

hydride form and, then, the dimer become the main product present in solution. Spencer's work represents a very important analogy for the work described in this Chapter.

Scheme 4.1

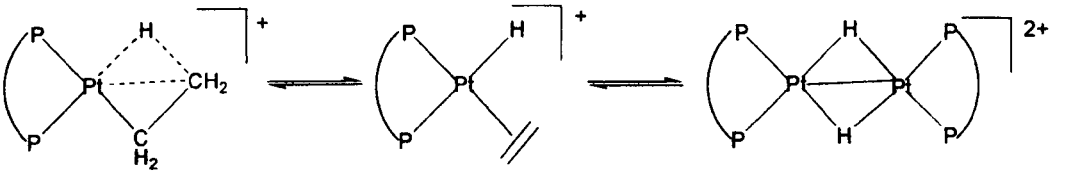

4.2 Reactivity of [Pd(d^{t}bpx)H(solv)]$^+$, 2, with ethene: synthesis, characterisation and dynamic behaviour of [Pd(d^{t}bpx)(CH$_2$CH$_3$)]$^+$, 4

The hydride complex [Pd(d^{t}bpx)H(MeOH)]$^+$, **2** (obtained using TfOH, see Chapter 2), reacts in MeOH with one equivalent of ethene to give in a new species which shows in the $^{31}P\{^1H\}$ NMR spectrum at 193 K two doublets at 36.3 and 67.7 ppm with $^2J(P\text{-}P) = 31.0$ Hz (see Figure 4.1). Further addition of ethene (up to 10 bar) does not result in any change in the product formed. The same reaction can be carried out in a wide range of solvents, using the procedures described in Chapter 2 for the synthesis of the corresponding hydride precursor. The NMR spectrum of the product obtained is not very sensitive to the solvent used (see Table 4.1); moreover, the spectra at room temperature are slightly broader than at low temperature, but the two resonances always remain well separated and, usually, the fine structure of the spectrum is well resolved.

Figure 4.1

*$^{31}P\{^{1}H\}$ NMR spectrum of $[Pd(d^{t}bpx)(CH_2CH_3)]^+$, **4**, in MeOH at 193 K*

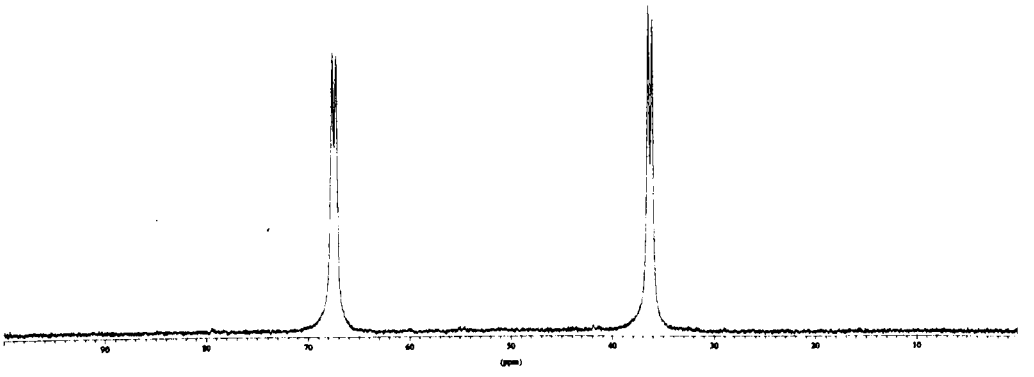

Table 4.1

*$^{31}P\{^{1}H\}$ NMR data for $[Pd(d^{t}bpx)(CH_2CH_3)]^+$, **4**, in different solvents*

Solvent	T (K)	δP_A	δP_B	$^2J(P_A\text{-}P_B)$
MeOH	293	38.0	70.0	25.4
MeOH	193	36.3	67.7	31.0
^{n}PrOH	293	37.8	69.8	br
THF	293	38.7	70.3	br
THF	193	37.1	67.9	31.5
THF/CH_2Cl_2	193	36.5	67.9	30.0
CH_3CN	293	39.0	70.3	27.0
EtCN	293	38.1	69.7	br
EtCN	193	36.4	67.1	31.5

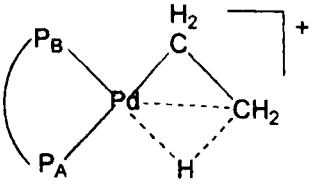

The stability of this new compound depends on the solvent used, as found for the hydride. In particular, it is very stable in primary and secondary alcohols, whereas it slowly transforms into $[Pd(d^tbpx)(\eta^2\text{-}TfO)]^+$, **3**, in non-alcoholic solvents; this reaction is faster in the presence of TfOH.

In order to better understand the nature of the product formed, the reaction has been repeated using $^{13}CH_2{=}CH_2$ instead of $CH_2{=}CH_2$. The experiment has been carried out by adding $^{13}CH_2{=}CH_2$ (1 equivalent) to a solution of **2** in MeOH. The $^{31}P\{^1H\}$ NMR spectrum at 193 K (see Figure 4.2) clearly shows that the resonance at 67.7 ppm is still a doublet [^2J(P-P) = 31.0 Hz], whereas the resonance at 36.3 ppm is now a more complicated multiplet.

Figure 4.2

*$^{31}P\{^1H\}$ NMR spectrum of a mixture of **4a** and **4b** in MeOH at 193 K*

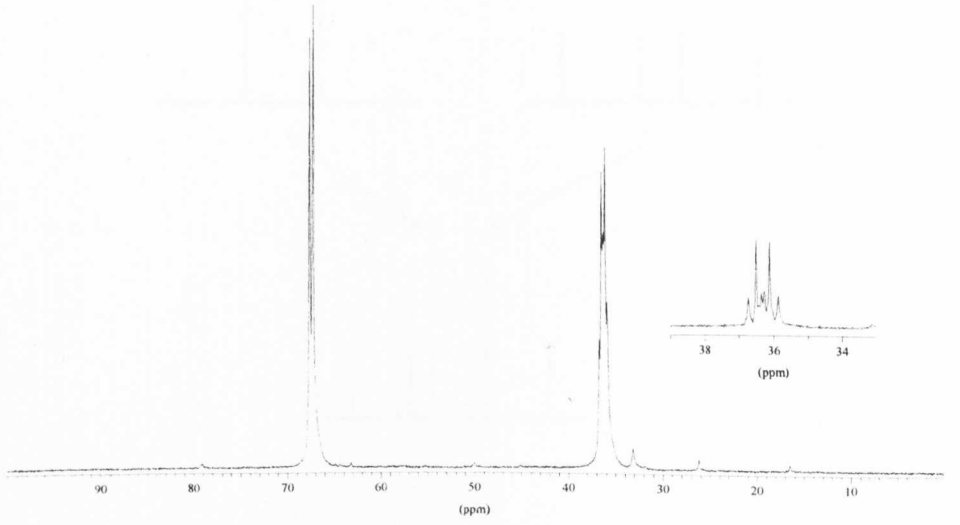

Assuming that ethene inserts into the Pd-H bond of **2** to give a Pd-ethyl complex $[Pd(d^tbpx)(CH_2CH_3)]^+$, **4** (for the formulation of **4** as a β-agostic ethyl complex see the remaining part of this section), this spectrum can be fully explained.

On using $^{13}CH_2{=}CH_2$, two different isotopomers can be formed, *i.e.* $[Pd(d^tbpx)(CH_2{}^{13}CH_3)]^+$, **4a**, and $[Pd(d^tbpx)(^{13}CH_2CH_3)]^+$, **4b** (see Scheme 4.2). In the isotopomer **4a**, P_A couples only with P_B (the coupling with C_B is too small to be resolved), and, hence, the expected signal is a doublet with $^2J(P_A\text{-}P_B) = 31$ Hz. For the isotopomer **4b**, P_A couples with both P_B [$^2J(P_A\text{-}P_B) = 31$ Hz] and the *trans* ^{13}C atom [$^2J(P_A\text{-}C_A) = 38$ Hz], resulting in a doublet of doublets.

Scheme 4.2

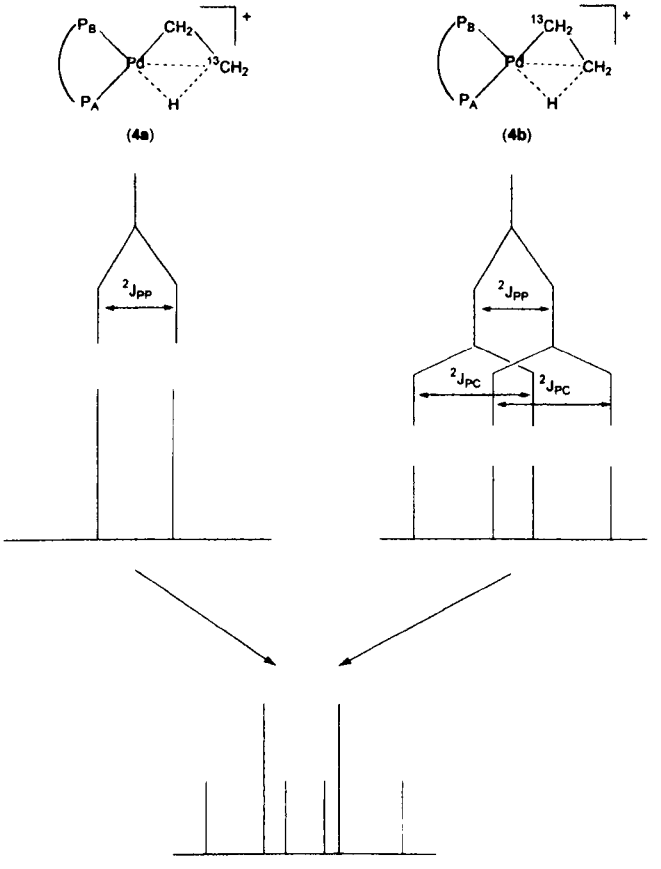

Of course, in solution an equal amount of the two isotopomers is present but, because **4b** gives four resonances and **4a** only two, the intensity of each of the resonance due to **4b** has to be one half of the intensity of each of the resonances due to **4a**. Hence, the resulting signal for P_A is a multiplet consisting of six lines, with

relative intensities 1:2:1:1:2:1, as observed in the experimental spectrum. Similar considerations can be applied to P_B; the problem is that, usually, *cis*-^{2}J(P-C) coupling constants are very small (less than 10 Hz) and so, the fact that P_B appears as a simple doublet is probably due to the fact that the P-C coupling is not resolved in the spectrum.

In the $^{13}C\{^1H\}$ spectrum at 193 K (see Figure 4.3), two main signals are clearly present at high field: a singlet at 8 ppm and a doublet at 31 ppm [^{2}J(P-C) = 38 Hz]. It is reasonable to assign the singlet to the -CH_3 group of the ethyl ligand, and the doublet to the –CH_2- group, which couples strongly with the *trans*-P atom. On using a gaussian enhancement of this spectrum, it is possible to resolve also the *cis* coupling constant, as ^{2}J(P-C) = 5 Hz.

Figure 4.3

*$^{13}C\{^1H\}$ NMR spectrum of a mixture of **4a** and **4b** in MeOH at 193 K*

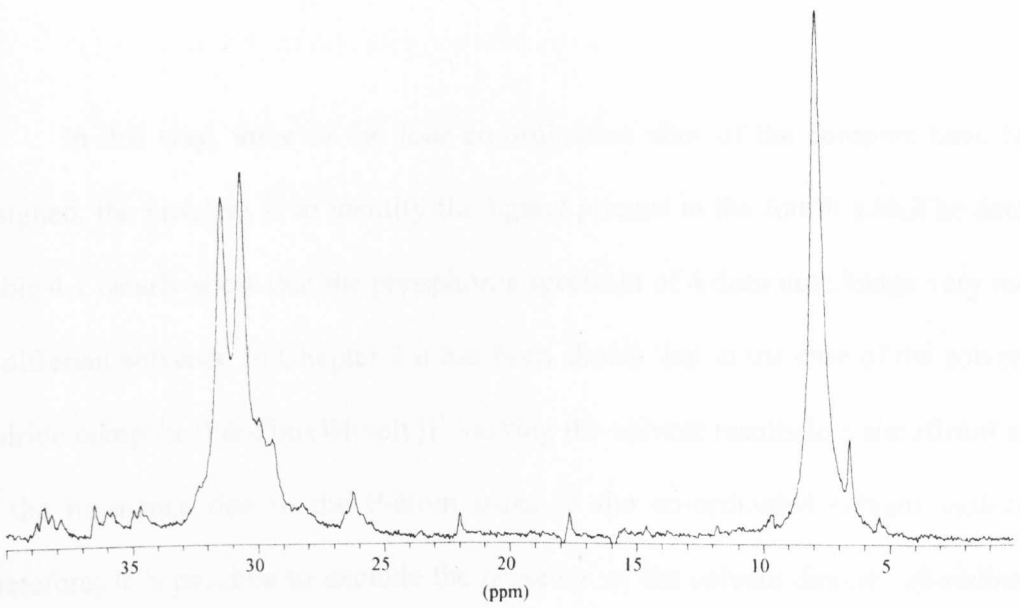

Finally, the ^{13}C spectrum at 193 K has also been recorded (see Figure 4.4). In this spectrum, the signal at 8 ppm is a quartet [^{1}J(C-H) = 124 Hz], and that at 31 ppm is a triplet of doublets [^{1}J(C-H) = 158 Hz, ^{2}J(C-P) = 38 Hz], in perfect agreement with the formulation of **4** as an ethyl complex.

Figure 4.4

*^{13}C NMR spectrum of a mixture of **4a** and **4b** in MeOH at 193 K*

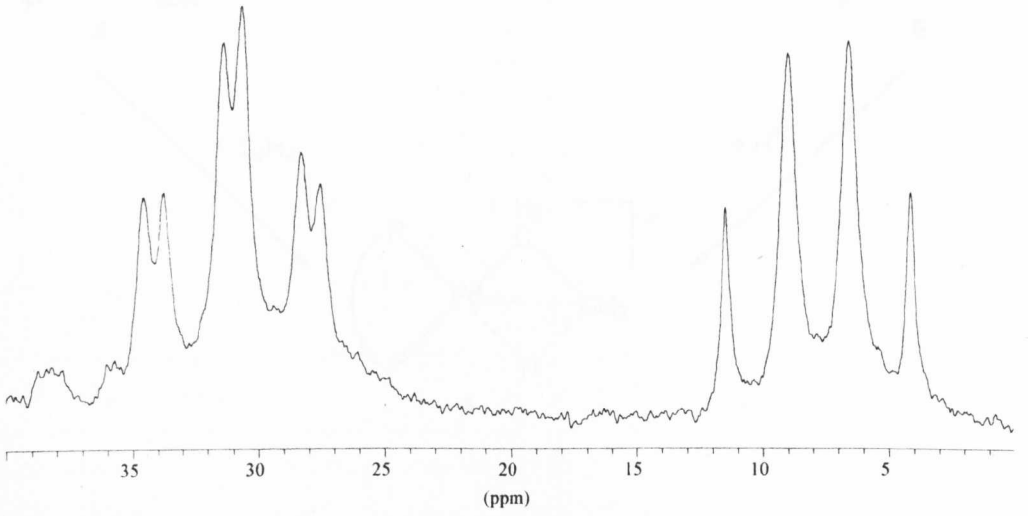

In this way, three of the four co-ordination sites of the complex have been assigned; the problem is to identify the ligand present in the fourth site. The data in Table 4.1 clearly show that the phosphorus spectrum of **4** does not change very much in different solvents. In Chapter 2 it has been shown that in the case of the solvento-hydride complex [Pd(d^{t}bpx)H(solv)]$^{+}$ varying the solvent results in a significant shift of the resonance due to the P-atom *trans* to the co-ordinated solvent molecule. Therefore, it is possible to exclude the presence of the solvent directly co-ordinated to the metal in **4**. Spencer has reported that protonation of Pd(d^{t}bpx)(C_2H_4), **5**, results

in an ethyl complex containing a β-agostic interaction, which would be identical to **4**.[10] Unfortunately, no NMR data for this species has been reported. Hence, the reaction of **5** with TfOH in MeOH has been studied, resulting in the formation of the same product **4** (see Scheme 4.3).

Scheme 4.3

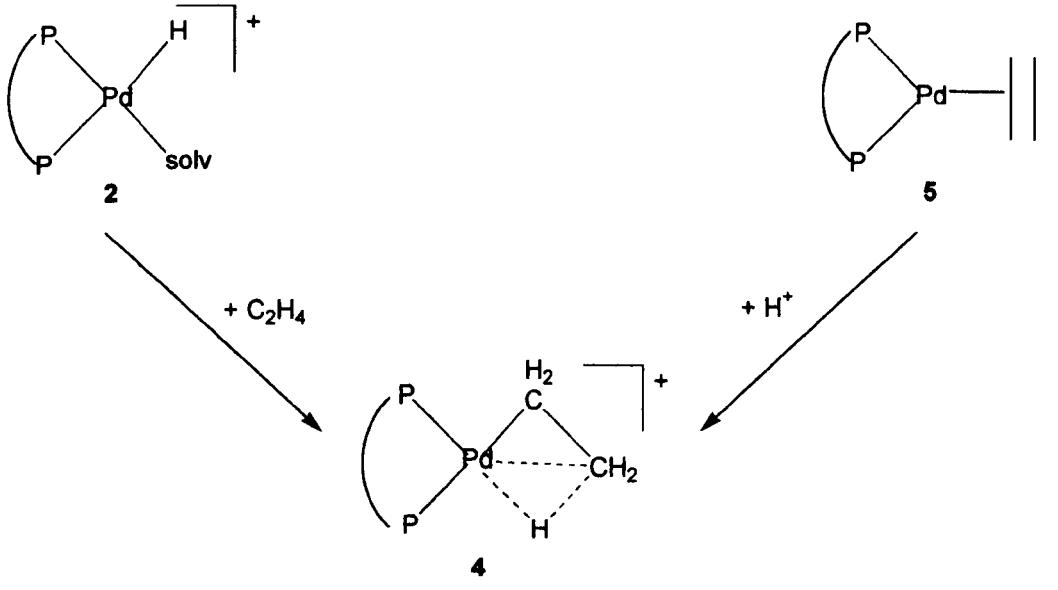

The easiest way to detect an agostic interaction in an ethyl complex is to run the ^{13}C NMR spectrum at a temperature low enough to freeze the rotation of the methyl group.[11] Spencer has reported that this process is frozen, for $[Pt(d^tbpx)(CH_2CH_3)]^+$, **6**, at *ca.* 150 K.[9] Hence, the ^{13}C NMR spectrum of the palladium-ethyl complex has been run in THF/CH_2Cl_2 at 155 K, but even at this temperature the exchange process is still too fast on the NMR time-scale and, hence, the resonance of the methyl group is still a quartet. Therefore, other data must be considered. A literature search on "classical" Pd-ethyl complexes [6-8] (where there is no agostic interaction) shows that, in all the compounds reported, $^1J(C\text{-}H)$ for both the CH_2 and the CH_3 groups is in the range 125-135 Hz, which is normal for an sp^3

carbon; moreover the CH_2 group always resonates at higher field than the CH_3 group (see Table 4.2). No NMR data exists for Pd-ethyl complexes with an agostic interaction. Therefore, analogous Pt-complexes must be considered.

Table 4.2

NMR data for palladium and platinum ethyl complexes

Complex	CH_2 [a]	CH_3 [a]
trans-$Pd(PMe_3)_2(Et)(SPh)$ [b]	9.4 (131)	16.1 (124)
trans-$Pd(PMe_3)_2(Et)(Cl)$ [b]	8.6 (134)	16.5 (125)
trans-$Pd(PMe_3)_2(Et)(I)$ [b]	15.5 (133)	16.5 (125)
Pd[(R,R')-Duphos](Et)(C_6F_5) [c]	10.0	15.9
Pt(d^tbpp)$(Et)_2$ [d]	11.1	17.2
[Pt(d^tbpp)(CH_2CH_3)]$^+$ [e]	22.0 (158)	8.2 (60 + 153)
[Pt(d^tbpx)(CH_2CH_3)]$^+$ [e]	22.0 (155)	9.0 (75 + 155)

[a] Chemical shift in ppm and ^1J(C-H) in Hz (when reported). [b] at 233 K in CD_2Cl_2, see ref. 7. [c] at 293 K in CD_2Cl_2, see ref. 8. [d] at 298 K in C_6D_6, see ref. 9. [e] at 145 K in CD_2Cl_2/THF, see ref. 9

In all these complexes, the CH_2 group resonates at lower field than the CH_3 group. Moreover, ^1J(C-H) for the CH_2 group assumes a higher value (150-160 Hz) than in classical ethyl complexes, nearer to a sp^2 than a sp^3 carbon. The value observed for the coupling constant in the methyl group depends on the temperature. When the rotation of the methyl group is frozen, two different values are observed, *i.e.* 150-160 Hz for the two non-agostic proton and 60-80 Hz for the agostic proton. Whereas, when the rotation is fast, an averaged constant is observed, which assumes a value similar to the classical one, *i.e.* 120-130 Hz. [Pd(d^tbpx)(CH_2CH_3)]$^+$, **4**, clearly shows the inversion of the chemical shifts of the CH_2 and CH_3 groups, typical of an

agostic ethyl ligand. Moreover, also the values of ^1J(C-H) (158 and 133 Hz for CH_2 and CH_3, respectively) agree with the presence of an agostic interaction. Hence, it is possible to conclude that the product formed by reaction of **2** with ethene is $[Pd(d^tbpx)(CH_2CH_3)]^+$, **4**, which contains an agostic interaction.

The NMR data reported in Table 4.1 also suggest that the agostic interaction is maintained in all the solvents examined, even in strongly co-ordinating solvents such as CH_3CN and EtCN. In order to confirm this, the reaction between $[Pd(d^tbpx)H(EtCN)]^+$, **2a**, and $^{13}CH_2{=}CH_2$ in EtCN has been studied. The NMR data for the resulting ^{13}C-enriched ethyl complex are reported in Table 4.3 and compared with the analogous data in MeOH.

Table 4.3

*NMR data at 193 K for $[Pd(d^tbpx)(CH_2CH_3)]^+$, **4**, in MeOH and EtCN*

	MeOH	**EtCN**
δP_A	36.3	36.4
δP_B	67.7	67.1
δC_A	31.0	31.8
δC_B	7.9	9.3
$^2J(P_A\text{-}P_B)$	31.1	31.5
$^2J(P_A\text{-}C_A)$	38.0	39.8
$^2J(P_B\text{-}C_A)$	5	5.5
$^1J(C_A\text{-H})$	158	157
$^1J(C_B\text{-H})$	124	*

* Hidden by the solvent

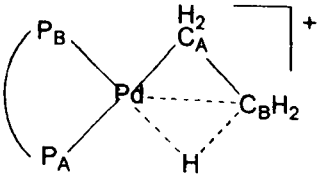

These data clearly show that even in EtCN the agostic interaction is also maintained intact. This conclusion is quite surprising, since it is usually reported that agostic interactions are relatively weak.

4.2.1 The dynamic behaviour of $[Pd(d^t bpx)(CH_2CH_3)]^+$, 4: low temperature processes

It has been shown in the last Section that the protons of the methyl group of the ethyl substituent in **4** are equivalent in the NMR time-scale, even at 155 K. This can be explained assuming a very low energy barrier for the rotation of the methyl group. A similar behaviour has been observed by Spencer in analogous platinum complexes.[9] The rotation can occur with or without full dissociation of the agostic interaction, as described by Green and Wong.[12] Usually, such a kind of dynamic process in agostic-ethyl complexes is explained on the base of a dissociative mechanism (see Scheme 4.4). First the agostic interaction is broken, then the free methyl group can rotate and, finally, the agostic interaction is re-formed.

Scheme 4.4

Dissociative mechanism for the methyl-rotation in 4

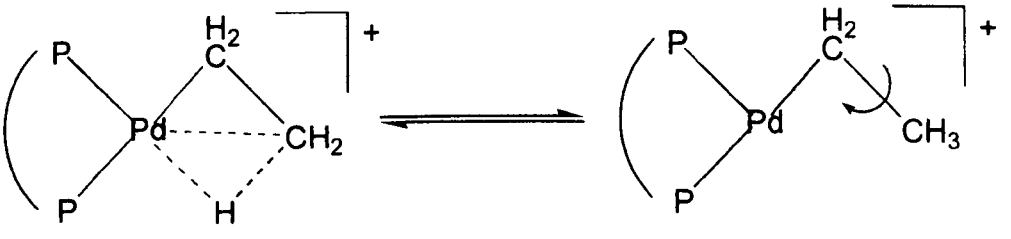

Green and Wong have, instead, demonstrated that scrambling of the β-hydrogens of the agostic ethyl group in some molybdenum and cobalt complexes

occurs *via* a mechanism analogous to that described in Scheme 4.5. They also claim that this mechanism may be quite general for such β-agostic interactions. This mechanism requires, of course, a gradual weakening of H_a-Pd and strengthening of H_b-Pd agostic interactions and, therefore, the dissociative mechanism can be considered to be the limiting case. It is thus very difficult to quantify the degree of weakening of the agostic interaction during the rotation of the methyl group in **4**. In all cases, the fact that this interaction has been shown to be very strong even in very polar solvents and, moreover, the fact that the process is very fast even at low temperature, seems to suggest that the mechanism shown in Figure 4.5 is preferable to the dissociative one shown in Figure 4.4.

Scheme 4.5

In-place rotation mechanism

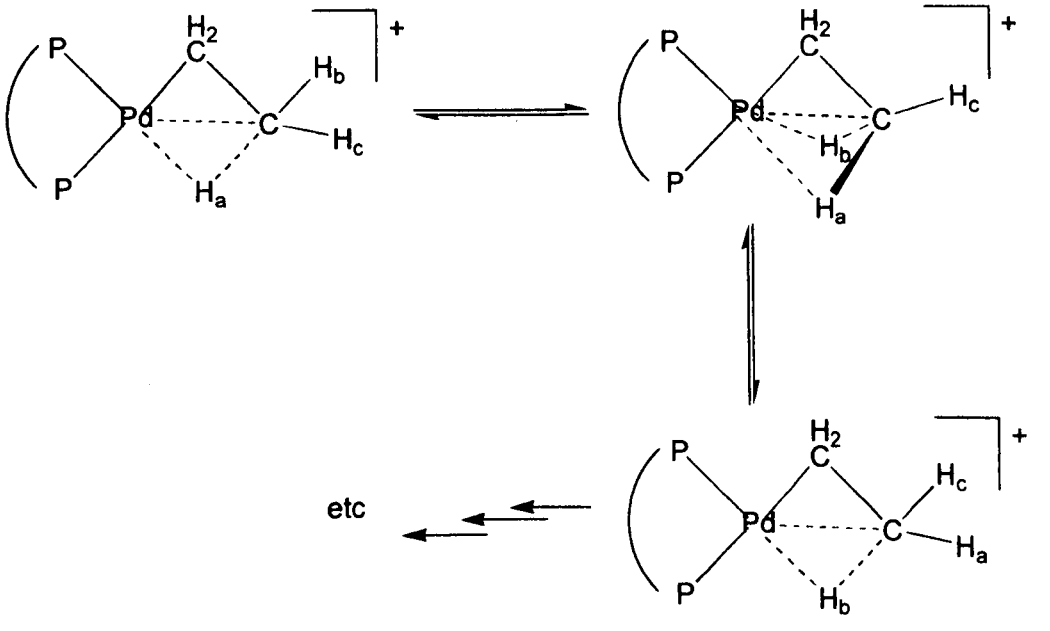

There is another exchange process which occurs below room temperature. In Figure 4.5, the $^{31}P\{^1H\}$ NMR spectra of a 1:1 mixtures of **4a** and **4b** in MeOH from

183 K to 293 K are reported. These spectra clearly change with temperature, and it is interesting to note that the two resonances of the complex change in a different way.

Figure 4.5 A

*VT $^{31}P\{^{1}H\}$ NMR spectra of a mixture of **4a** and **4b** in MeOH*

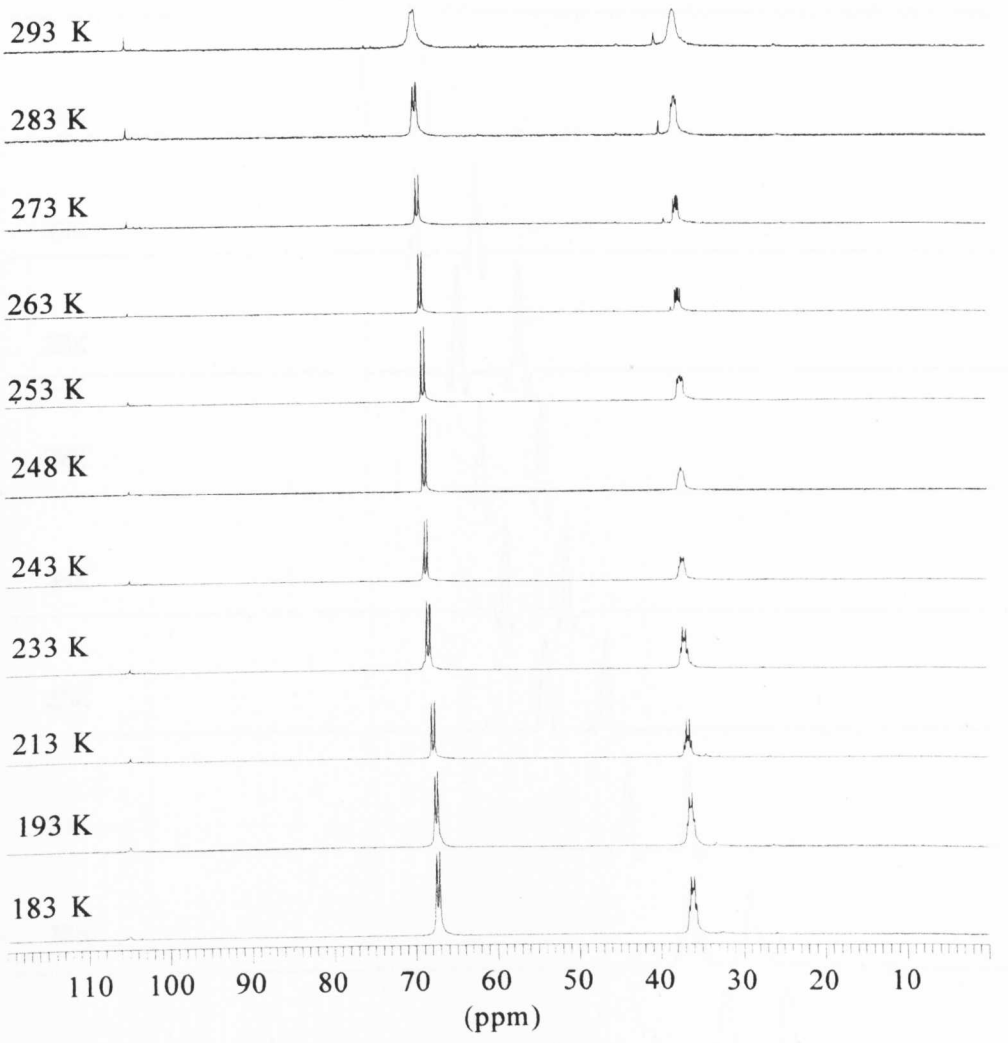

Figure 4.5 B

*VT $^{31}P\{^{1}H\}$ NMR spectra of a mixture of **4a** and **4b** in MeOH (P_B-resonance)*

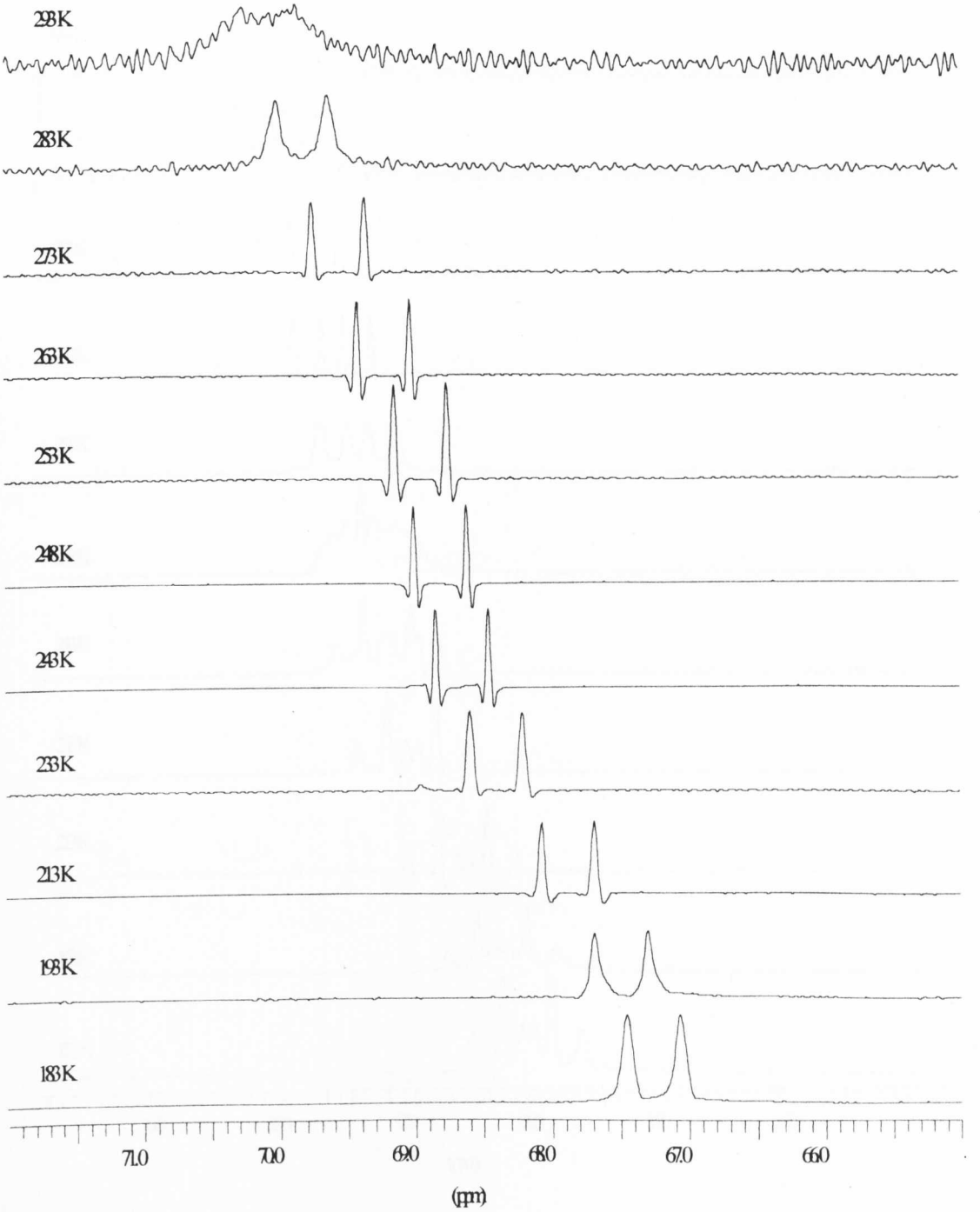

Figure 4.5 C

*VT $^{31}P\{^{1}H\}$ NMR spectra of a mixture of **4a** and **4b** in MeOH (P_A-resonance)*

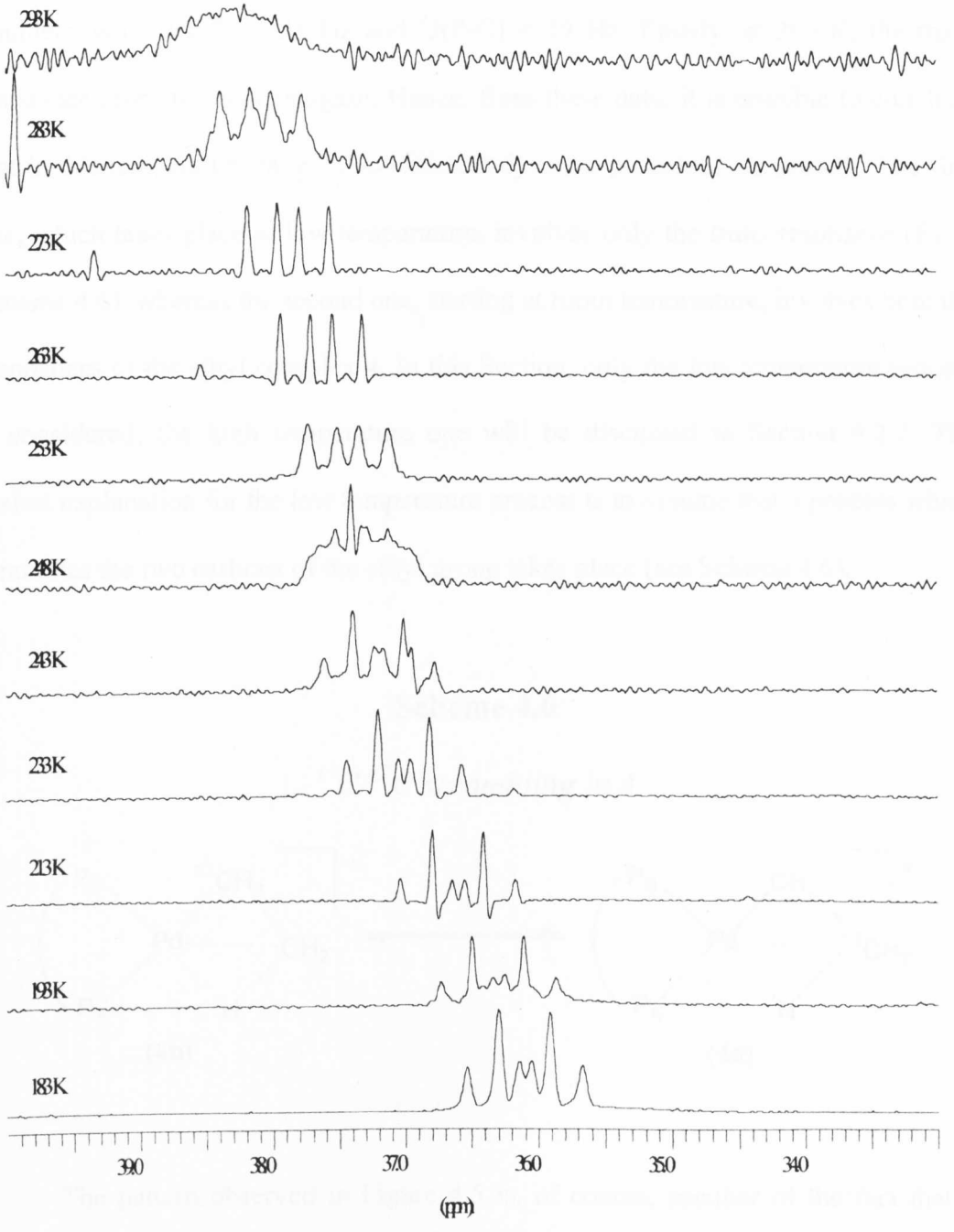

The *cis* resonance is always a well resolved doublet from 183 K to 283 K, and only at 293 K starts to broaden. Whereas, the *trans* resonance from 183 K to 233 K appears as a 1:2:1:1:2:1 multiplet, which starts to broaden at 243 K. At 248 K there is complete coalescence, and from 253 K to 283 K, it becomes a doublet of doublets, with $^{2}J(P\text{-}P) = 31$ Hz and $^{2}J(P\text{-}C) = 19$ Hz. Finally, at 293 K, the *trans* resonance starts to broaden again. Hence, from these data, it is possible to conclude that in this temperature range, two different dynamic processes are present. The first one, which takes place at low temperature, involves only the *trans* resonance (P_A in Scheme 4.6), whereas the second one, starting at room temperature, involves both the resonances of the ethyl complex **4**. In this Section, only the low temperature process is considered; the high temperature one will be discussed in Section 4.2.2. The easiest explanation for the low temperature process is to assume that a process which scrambles the two carbons of the ethyl group takes place (see Scheme 4.6).

Scheme 4.6

$^{13}C/^{12}C$ scrambling in 4

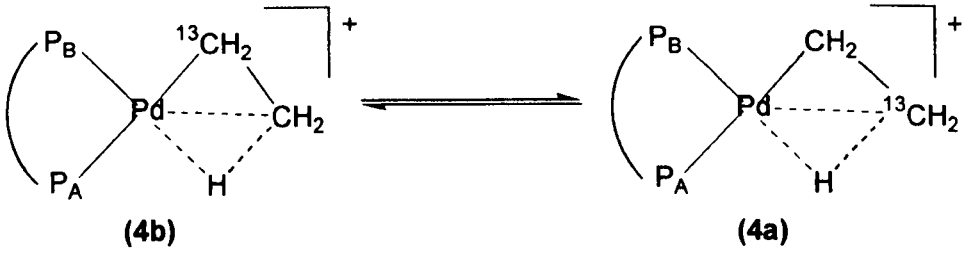

The pattern observed in Figure 4.5 is, of course, peculiar of the fact that a mono-labelled sample has been used. On repeating the experiment using non labelled ethene, the low temperature process is, in fact, not observed (see Figure 4.6). Whereas, using $^{13}CH_2{=}CH_2$, after the coalescence point, P_A for half of the time sees a

trans a ^{12}C with, of course, no coupling, and for half of the time sees a ^{13}C with $^{2}J(P\text{-}C) = 38$ Hz. Hence, the average value for the coupling constant, when the scrambling process is fast on the NMR time-scale, is $^{2}J(P\text{-}C)_{av} = (38+0)/2 = 19$ Hz, as observed in the experimental spectra.

Figure 4.6

*$^{31}P\{^{1}H\}$ NMR spectra at VT of $[Pd(d^{t}bpx)(CH_2CH_3]^{+}$, **4**, in MeOH ($P_A$-resonance)*

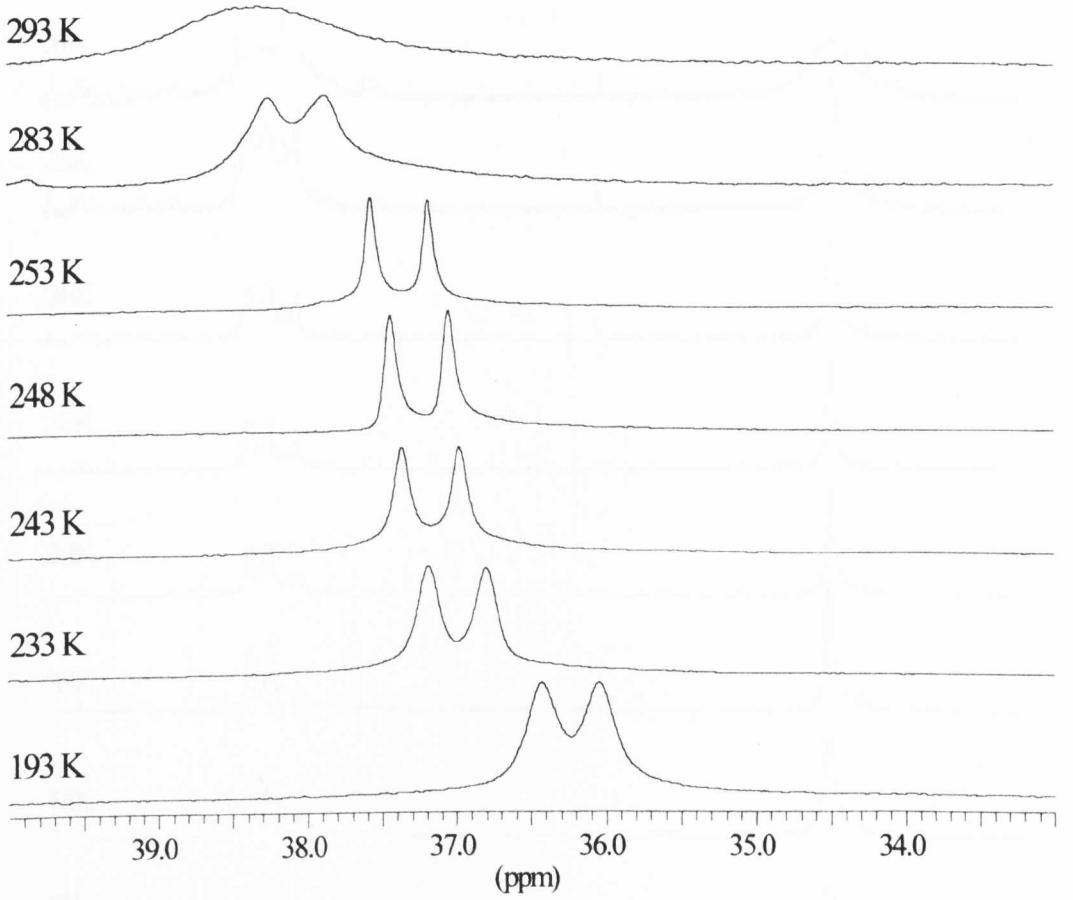

As expected for such a process, the $^{13}C\{^{1}H\}$ resonances due to the methyl and methylene groups both broaden with increasing temperature. When the scrambling is fast enough to make them equivalent, a broad resonance at *ca.* 18 ppm appears (see

Figure 4.7; the nature of the resonance at 30 ppm which appears on increasing the temperature is not at present understood).

Figure 4.7

*VT $^{13}C\{^{1}H\}$ NMR spectra of a mixture of **4a** and **4b** in MeOH*

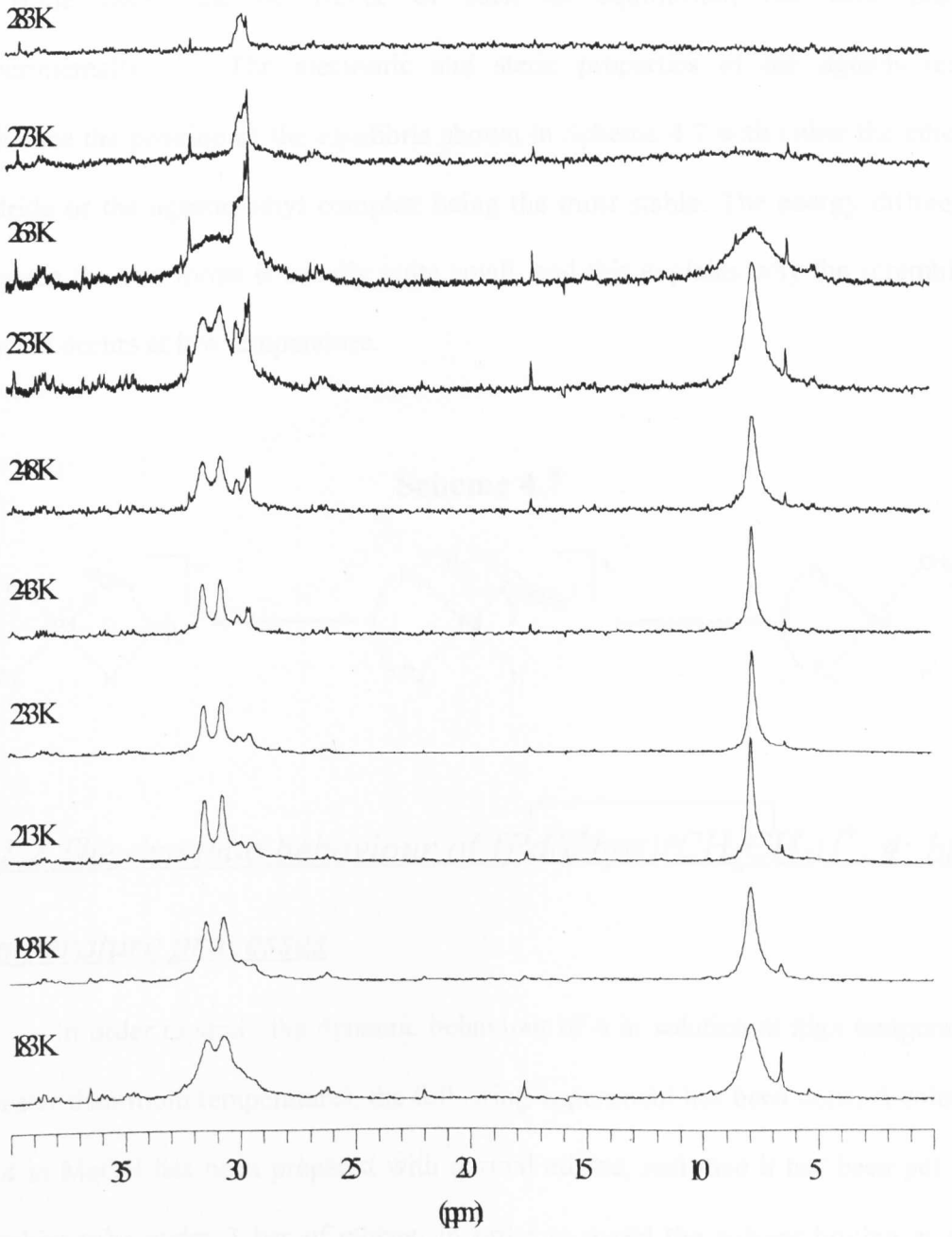

Spencer has shown that in the case of similar platinum complexes,[9] the carbon atoms of the ethyl group, which are inequivalent at low temperature, also become equivalent on increasing the temperature. It is usually accepted that the scrambling process occurs *via* an equilibrium between the ethyl-agostic complex and a hydride-ethene complex which readily undergoes ethene-rotation (see Scheme 4.7). In some cases, the occurrence of such an equilibrium has been proved experimentally.[9,11,13] The electronic and steric properties of the ligands really influence the position of the equilibria shown in Scheme 4.7 with either the ethene-hydride or the agostic-ethyl complex being the most stable. The energy difference between the two forms is usually quite small, and this explains why the scrambling process occurs at low temperature.

Scheme 4.7

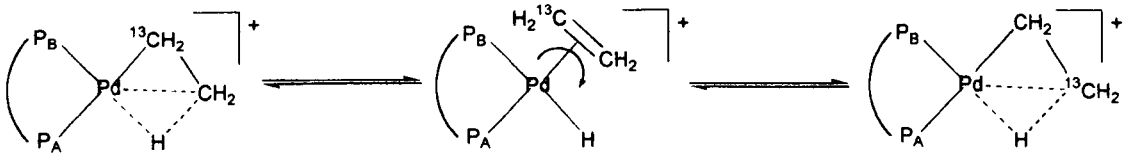

4.2.2 The dynamic behaviour of [Pd(d^t bpx)(CH2CH3)]+, 4: high temperature processes

In order to study the dynamic behaviour of **4** in solution at high temperature (greater than room temperature), the following experiment has been done. A solution of **4** in MeOH has been prepared with normal ethene, and then it has been put in a sapphire tube under 3 bar of ethene, in order to avoid the solvent boiling at high temperature. Hence, the $^{31}P\{^{1}H\}$ spectra have been recorded from 293 K to 353 K

(see Figure 4.8). At 293 K the two peaks of the ethyl complex are clearly present; some impurities are also present (mainly the metallated phosphine). On increasing the temperature, the resonances of the ethyl complex start to broaden, until they collapse at 353 K to form only one broad resonance at 54 ppm.

Figure 4.8

*VT $^{31}P\{^1H\}$ NMR spectra of $[Pd(d^tbpx)(CH_2CH_3)]^+$, **4**, in MeOH; high temperature experiment*

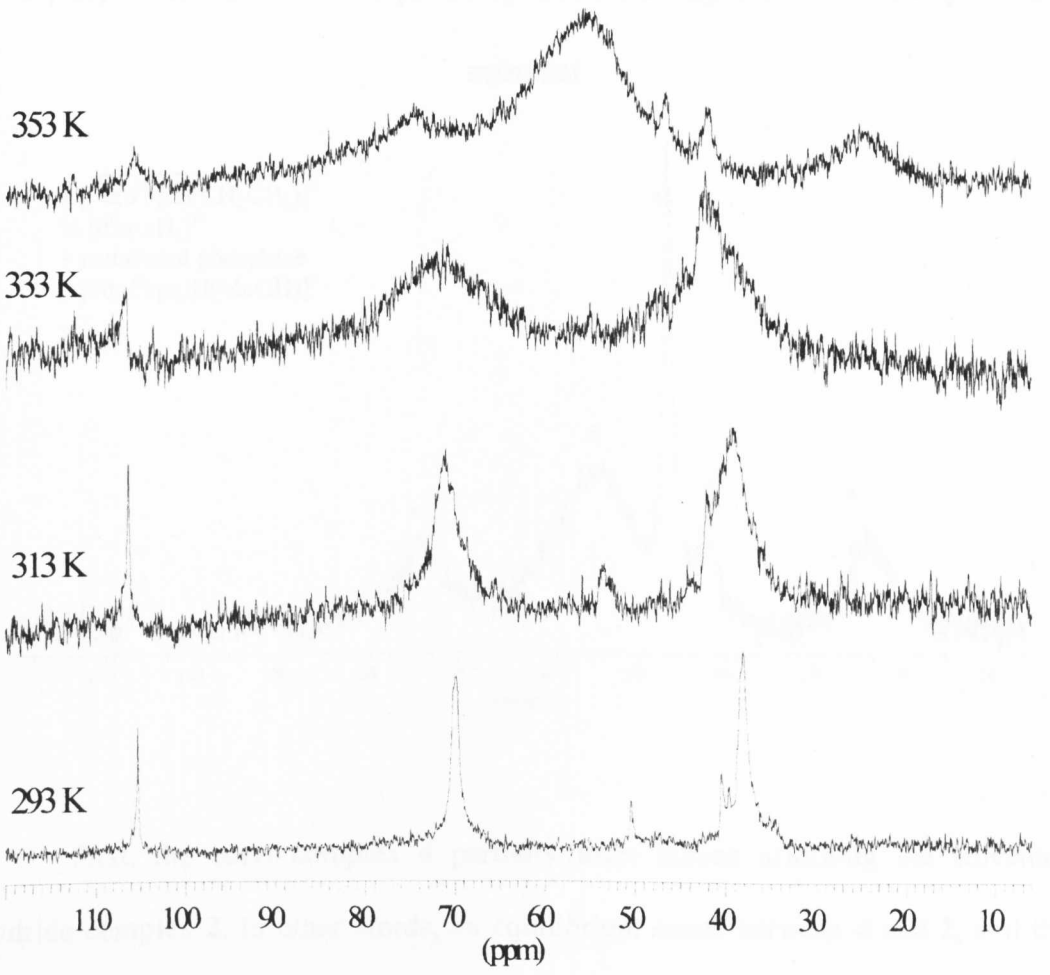

Three other species are clearly present at this point: the metallated phosphine, the protonated phosphine and **2**. The metallated phosphine is an impurity which was present from the beginning of the experiment, whereas the protonated phosphine is a decomposition product. In fact, at this temperature, decomposition starts to be quite fast, even under ethene. After 45 minutes at 353 K, the amount of $[d^tbpxH_2]^{2+}$ greatly increases (see Figure 4.9) and Pd-metal is also present in the tube. Apart from this, two other processes occur at these high temperatures.

Figure 4.9

*$^{31}P\{^1H\}$ NMR spectrum of $[Pd(d^tbpx)(CH_2CH_3)]^+$, **4**, at 353 K after 45 minutes*

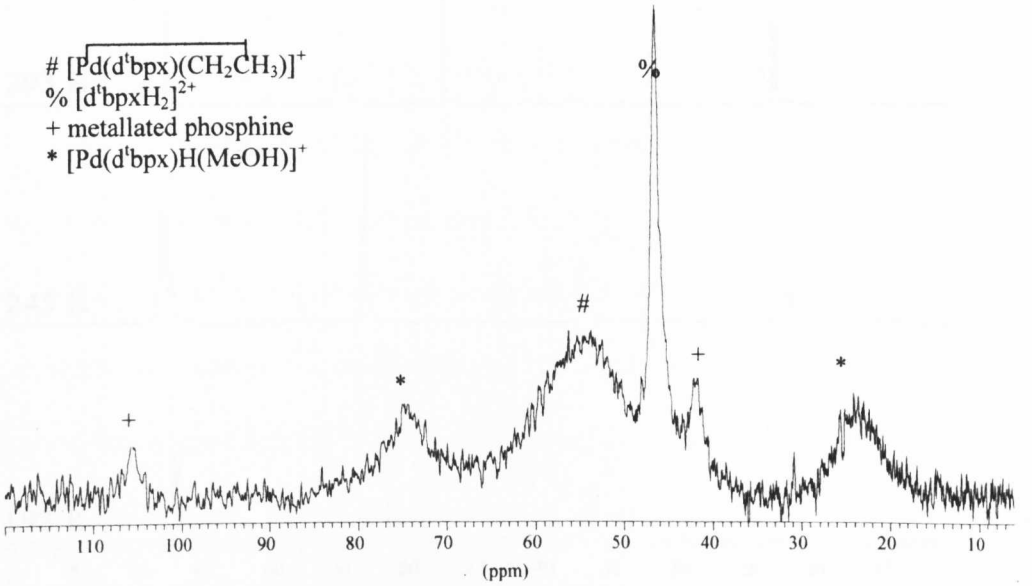

First, the ethyl complex **4** partially loses ethene affording the solvento-hydride complex **2**. In other words, an equilibrium exists between **4** and **2**, and the position of this equilibrium depends on the temperature, the pressure of ethene and the solvent.

$$[Pd(d^tbpx)(CH_2CH_3)]^+ + solv \rightleftharpoons [Pd(d^tbpx)H(solv)]^+ + C_2H_4 \qquad (4.1)$$

4 **2**

In MeOH, there is an appreciable amount of **2** only at 353 K, whereas, in EtCN, it is possible to detect the presence of a small amount of the hydride $[Pd(d^tbpx)H(EtCN)]^+$, **2a**, at 193 K (see Figure 4.10); in this solvent, the hydride is the main species present in solution at room temperature.

Figure 4.10

*VT $^{31}P\{^1H\}$ NMR spectra of a mixture of **4a** and **4b** in EtCN*

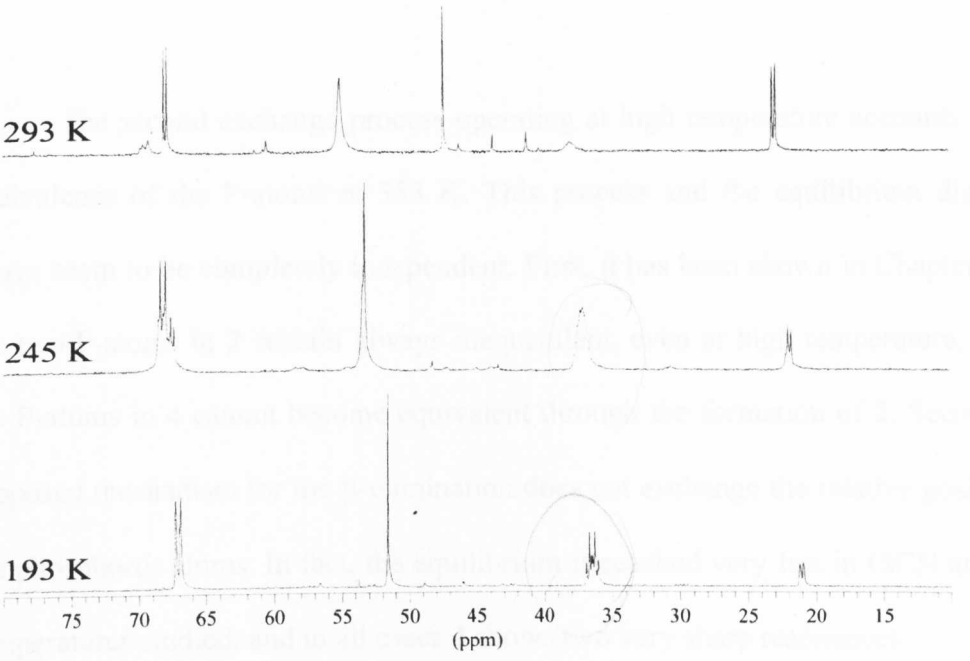

This enormous dependence of the equilibrium 4.1 on the solvent can be explained on the basis of the different co-ordinating ability of MeOH and EtCN, and it suggests the involvement of an associative mechanism (*via* a penta co-ordinated species) for the elimination of ethene from **4** (see Scheme 4.8). It has been shown in

many cases that substitution in square-planar complexes often occurs by such a mechanism.[14]

Scheme 4.8

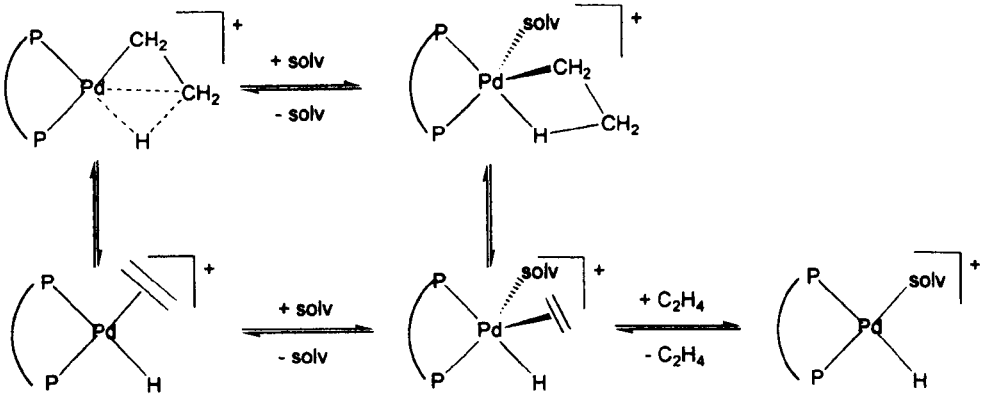

The second exchange process operating at high temperature accounts for the equivalence of the P-atoms at 353 K. This process and the equilibrium discussed above seem to be completely independent. First, it has been shown in Chapter 2 that the two P-atoms in **2** remain always inequivalent, even at high temperature; hence, the P-atoms in **4** cannot become equivalent through the formation of **2**. Second, the proposed mechanism for the β-elimination does not exchange the relative position of the phosphorus atoms. In fact, the equilibrium is reached very fast in EtCN at all the temperatures studied, and in all cases **4** shows two very sharp resonances.

Two different mechanisms can be proposed in order to explain the equivalence of the P-atoms of **4** at high temperature (see Scheme 4.9). The first mechanism involves an intra-molecular rearrangement of **4** *via* a tetrahedral intermediate. Such a kind of mechanism has been proposed in order to explain other internal rearrangement occurring in four co-ordinated square-planar complexes, such

as *cis-trans* isomerisation.[15] Tetrahedral geometry is widely exemplified in nickel chemistry,[16] whereas not a lot of stable tetrahedral palladium compounds are known. For instance, Hor *et al.*[17] recently reported the synthesis, solid state structure (X-ray) and spectroscopic characterisation in solution of the tetrahedral complex $PdCl_2(dppfO_2\text{-}O,O')$; interestingly, it does not exhibit an unusual value for δ_P as a result of the expected paramagnetic shift.

Scheme 4.9

A) Mechanism without dissociation of the agostic interaction

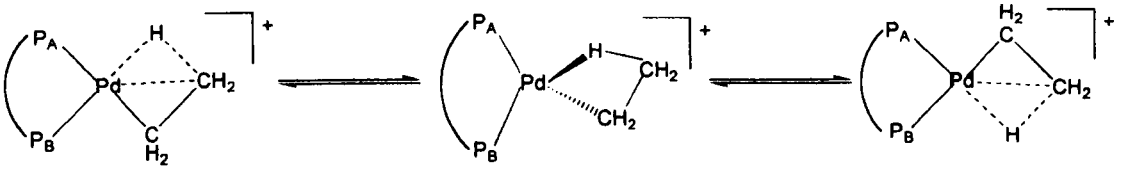

B) Mechanism with dissociation of the agostic interaction

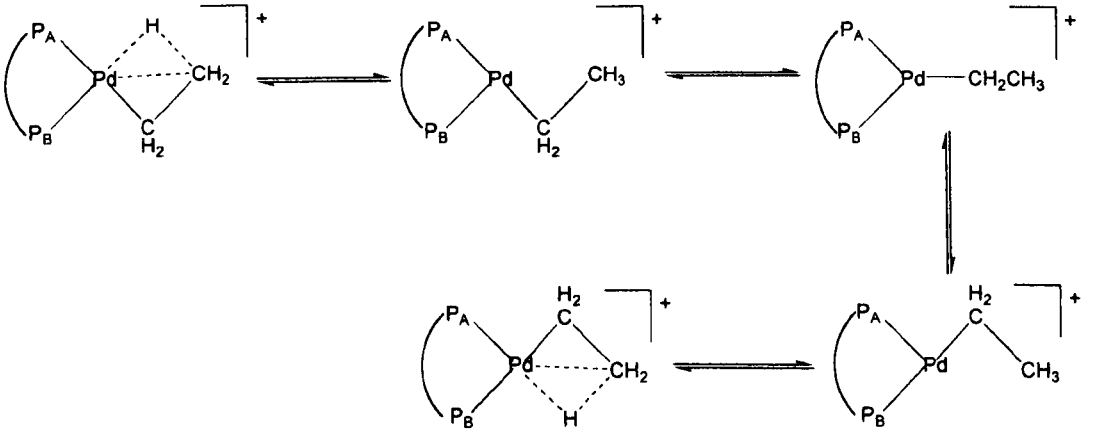

The second mechanism involves dissociation of the agostic interaction with formation of a 14 electron T-shaped intermediate which can, then, become Y-shaped allowing the change of the relative positions of the ethyl group and the P-atoms.

Spencer [9] has proposed this second mechanism in order to explain the same process in similar platinum complexes. Romeo *et al.*[5] have claimed the formation of T-shaped intermediates and their rearrangement *via* a Y-shaped form for explaining the *cis-trans* isomerisation process in $Pt(PR_3)_2(Me)_2$ (R = alkyl or aryl substituents). The theoretical possibility of this mechanism has been proved by Thorn and Hoffmann [18] who made quantomechanical calculations on model platinum compounds. They calculated a very low activation energy for the T-Y interconversion, whereas all the experimental data (including those presented in this thesis) suggest a higher value. This is probably due to the very simplistic model adopted in the calculation (*i.e.* the complex $[PtH(PH_3)]^+$). Also the work by Yamamoto suggests a high activation energy for this process.[19] Hence, even though the experimental data do not allow a clear distinction between the two mechanisms proposed for the equivalence of the P-atoms at high temperature, the analysis of the literature suggests that the second mechanism (dissociation of the agostic interaction and rearrangement of the resulting T-shaped intermediate) is probably preferable.

4.2.3 The reactivity of $[Pd(d^tbpx)(CH_2CH_3)]^+$, 4

It is interesting to note that the ethyl complex **4** is more stable in MeOH than the hydride **2**. The half-life of **2** at room temperature in MeOH is in fact 2-3 days, whereas **4** is still the main species in solution even after one week. Also, at high temperature **4** is more stable than **2**. For instance, **2** completely decomposes at 353 K after 20 minutes, whereas it is still possible to observe the presence of **4** even after 1 hour at this temperature. As found for **2**, **4** also decomposes to give $[d^tbpxH_2]^{2+}$ and Pd-metal as main products, and its stability in MeOH (and other alcoholic media) depends on the amount of acid present; addition of TfOH, usually, stabilises all these

complexes in MeOH. The behaviour in non-alcoholic media is different. As in the case of **2**, **4** converts with time into **3** or $[Pd(d^tbpx)(solv)_2]^{2+}$, **7**, depending on the solvent; **3** is formed in most of the non-alcoholic solvents studied (*e.g.* THF, MeP, THF/CH_2Cl_2, acetone) whereas **7** is formed in EtCN and CH_3CN. These reactions are accelerated by addition of TfOH. Apart from the formation of these complexes, the usual decomposition pathway to form $[d^tbpxH_2]^{2+}$ and Pd-metal is also observed in non-alcoholic solvents; decomposition can start from either **4** or **3** and **7** (see Scheme 4.10).

Scheme 4.10

*Decomposition of **4** in non-alcoholic solvents*

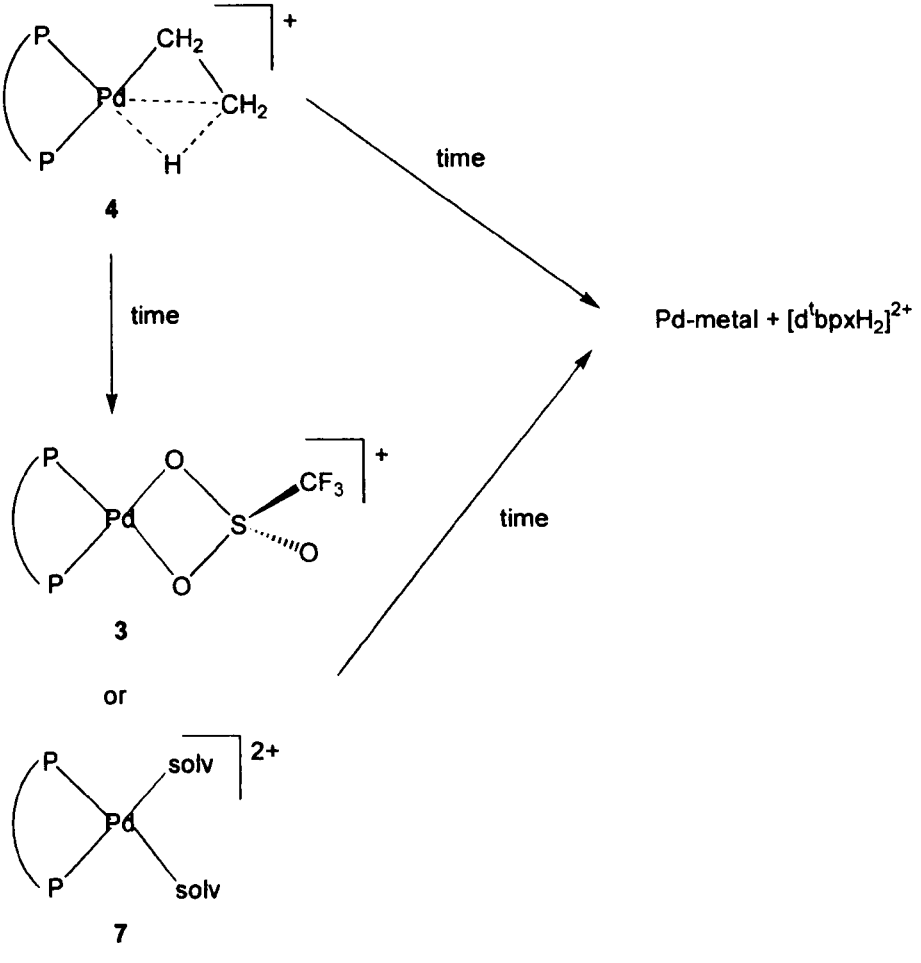

It has been shown in Section 2.4.2 that the solvent in $[Pd(d^tbpx)H(solv)]^+$, **2b**, can be displaced by a variety of neutral (*i.e.* PPh_3, PPh_2H, Py, THF, H_2O, CH_3CN, EtCN) and anionic ligands (Cl^-, Br^-, I^-) to give quantitatively new cationic and neutral Pd-hydrides, respectively. The behaviour of **4** seems quite different. In fact, its reaction with different halide salts results in the quantitative formation of $Pd(d^tbpx)HX$ (X = Cl, **8a**; Br, **8b**; I, **8c**) and not $Pd(d^tbpx)EtX$. Gas evolution has been observed during this reaction.

$$\underset{\mathbf{4}}{[Pd(d^tbpx)(CH_2CH_3)]^+} + X^- \longrightarrow \underset{\mathbf{8}}{Pd(d^tbpx)HX} + C_2H_4 \qquad (4.2)$$

Moreover, **4** reacts with PPh_3 to give a mixture containing many different compounds, among which it is possible to identify $[Pd(d^tbpx)H(PPh_3)]^+$, $OPPh_3$, $[d^tbpxH_2]^{2+}$, **4** and the metallated ligand. However, there is no evidence for the formation of $[Pd(d^tbpx)Et(PPh_3)]^+$. The reaction of **4** with pyridine also results in the formation of a complicated mixture of products. However, there is no trace of resonances attributable to $[Pd(d^tbpx)Et(Py)]^+$. It should be noted that **4** does not seem to react with water in MeOH. In fact, starting with a MeOH solution (2 ml) of the ethyl complex and adding of water (up to 4 ml), the chemical shifts of the two resonances change by only few tenths of a ppm, whereas in the case of **2** a shift of *ca.* 3 ppm had been observed (see Section 2.4.2). Further addition of water results in the complete precipitation of the complex. It has already been shown that dissolution of **4** in EtCN results in a mixture of **4** and **2a**; in all cases, there is no evidence for the formation of $[Pd(d^tbpx)Et(EtCN)]^+$. Such complexes are probably unstable because of steric problems.

4.3 Reactivity of [Pd(d^{t}bpx)H(MeOH)]$^+$, 2, with other olefins

The catalyst based on Pd(d^{t}bpx)(dba), **1**, has been mainly studied for the methoxycarbonylation of ethene. However, some preliminary studies aimed to test the possibility of using the same catalyst for the methoxycarbonylation of other olefins have been undertaken.[20] Apart from commercial reasons, these studies are of interest in order to better understand the chemical behaviour of this catalytic system. The autoclave experiments have shown that, using the same conditions in which the methoxycarbonylation of ethene is usually carried out, the catalyst is able to convert higher α-olefins into the respective esters, but not internal alkenes. Moreover, the activity of the catalyst rapidly decreases by increasing the chain length of the α-olefin used, and the catalyst is also very selective. In fact, only the linear ester is formed. Thus, in order to have a better understanding of all these reactions, the reactivity of **2** with a few α-olefins will be examined in this Section.

The variable temperature $^{31}P\{^1H\}$ NMR spectra obtained by adding 3 equivalents of propene to a MeOH solution of **2** are reported in Figure 4.11. In the spectra at low temperatures, two doublets at *ca.* 40 and 70 ppm are present. The chemical shifts of both these resonances are very close to those observed for the two resonances of **4**. Moreover, no P-H coupling is present in the ^{31}P spectrum. Hence, it seems that in this case the olefin also inserts into the Pd-H bond to form a Pd-alkyl complex. In theory, propene can insert in two different ways, to give either the linear or the branched Pd-propyl complex; whereas, only one species is present in solution and, for steric reasons, it is possible to reasonably conclude that the isomer formed is

the linear one, *i.e.* $[Pd(d^tbpx)(CH_2CH_2CH_3)]^+$, **9**. The fact that propene inserts forming only **9** explains why $CH_3CH_2CH_2COOCH_3$ is the only product of the reaction between propene, CO and MeOH promoted by **1**.

Figure 4.11

*VT $^{31}P\{^1H\}$ NMR spectra of $[Pd(d^tbpx)(CH_2CH_2CH_3)]^+$, **9**, in MeOH*

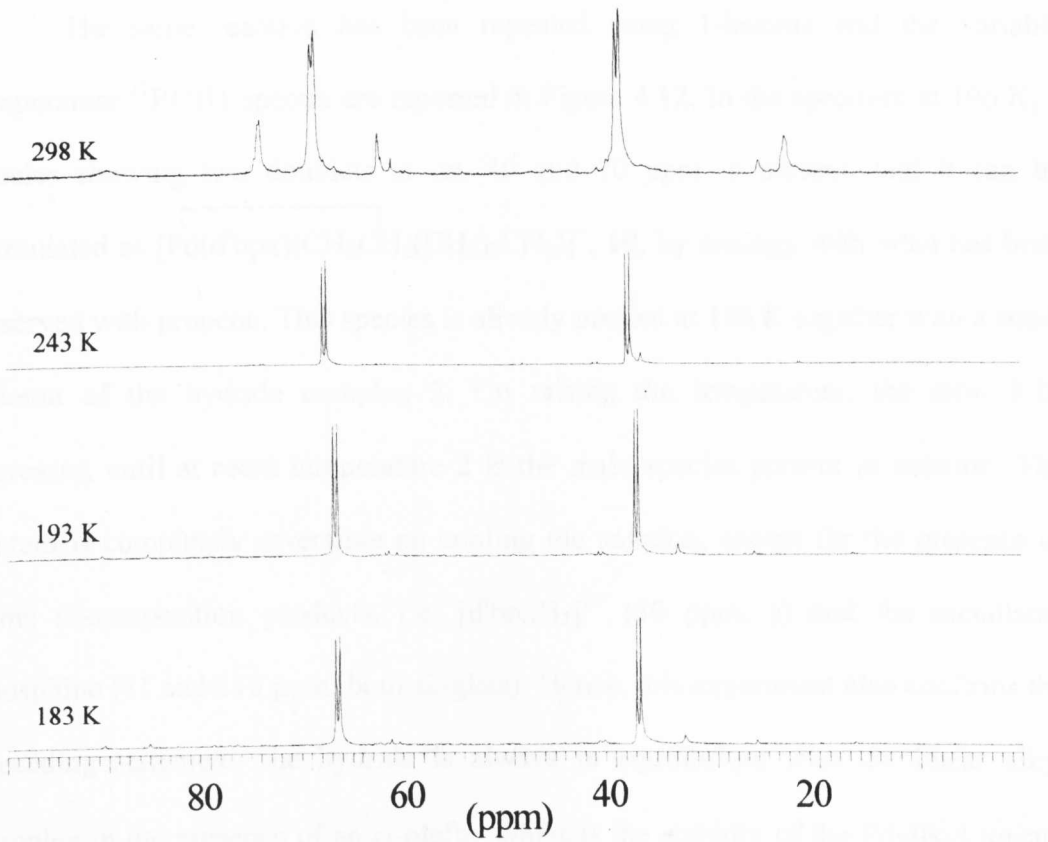

It is interesting to note that in the above spectrum at room temperature there is also an appreciable amount of the hydride **2**. Hence, on raising the temperature, the propyl complex loses propene. The process is reversible; in fact, on cooling the

solution down to 193 K, **2** disappears and **9** is the only species detected by NMR. Thus, it is possible to conclude that **2**, in presence of propene, is in equilibrium with **9**. The same behaviour has been observed in Section 4.2.2 for the ethyl complex **4**. The only difference is the temperature at which an appreciable amount of **2** starts to appear in the NMR spectrum. For the propene system, this happens at room temperature, whereas on using ethene the hydride is only observed at 353 K. Hence, it seems that it is sufficient to add one carbon atom to the olefin chain in order to destabilise the Pd-alkyl complex and favour β-elimination.

The same reaction has been repeated using 1-hexene and the variable temperature $^{31}P\{^{1}H\}$ spectra are reported in Figure 4.12. In the spectrum at 196 K, a species showing two doublets at *ca.* 40 and 70 ppm is present, and it can be formulated as $[Pd(d^tbpx)(CH_2CH_2(CH_2)_3CH_3)]^+$, **10**, by analogy with what has been observed with propene. This species is already present at 196 K together with a small amount of the hydride complex **2**. On raising the temperature, the ratio **2**:**10** increases, until at room temperature **2** is the main species present in solution. The system is completely reversible on cooling the solution, except for the presence of some decomposition products, *i.e.* $[d^tbpxH_2]^{2+}$ (50 ppm, s) and the metallated phosphine (41 and 110 ppm, both singlets). Hence, this experiment also confirms the preceding statement: the hydride is always in equilibrium with the linear alkyl complex in the presence of an α-olefin, whereas the stability of the Pd-alkyl toward β-elimination and formation of **2** depends on the length of the olefin aliphatic chain.

Figure 4.12

*VT $^{31}P\{^{1}H\}$ NMR spectra of $[Pd(d^{t}bpx)(CH_2CH_2(CH_2)_3CH_3)]^+$, **10**, in MeOH*

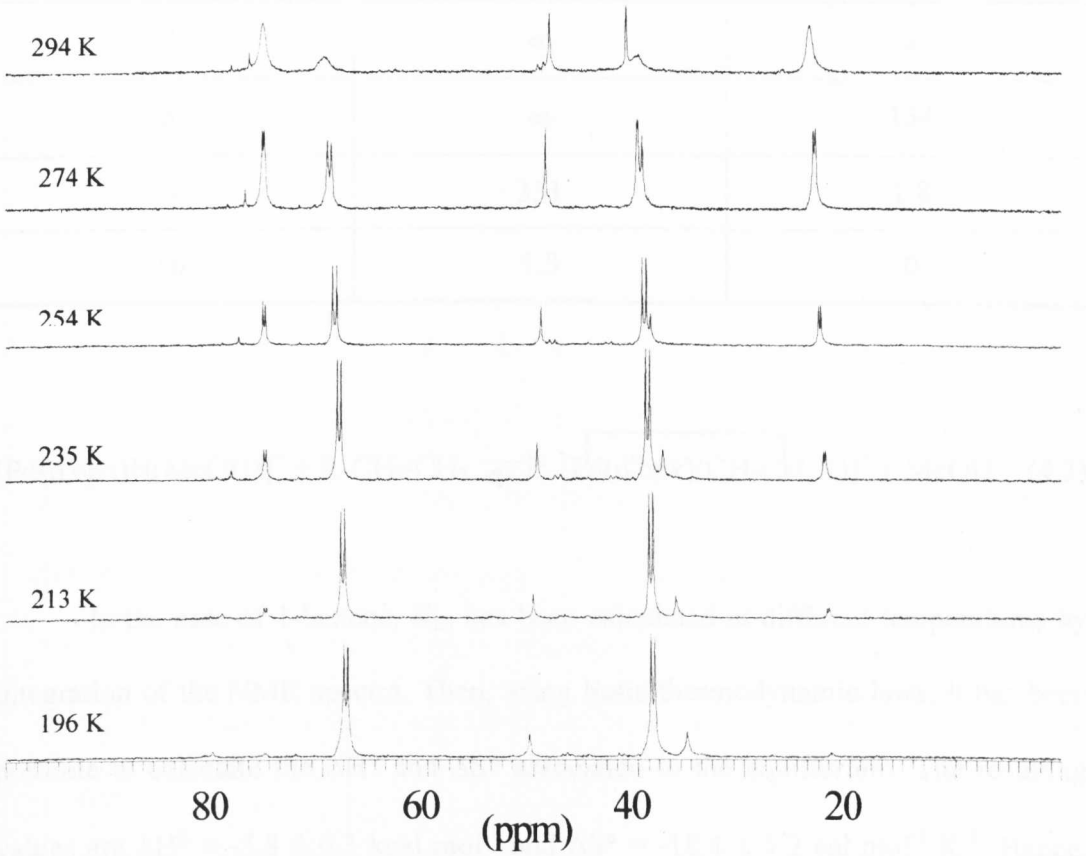

Further confirmation of this hypothesis has been obtained by studying the reaction of **2** with 1-hexadecene. In this case, traces of the insertion product $[Pd(d^{t}bpx)(CH_2CH_2(CH_2)_{13}CH_3)]^+$, **10a**, have been observed at 193 K, whereas at 293 K only **2** is present. The values of K_{eq} for the equilibrium described in eq. 4.3 at different temperatures and with different olefins are reported in Table 4.4

Table 4.4

Equilibrium constant (K_{eq}) for different linear α-olefins (C_nH_{2n}) (see eq.4.3)

n	K_{eq} at 193 K	K_{eq} at 293 K
2	∞	∞
3	∞	134
6	351	1.8
16	1.3	0

$$[Pd(d^tbpx)H(MeOH)]^+ + R\text{-}CH{=}CH_2 \rightleftharpoons [Pd(d^tbpx)(CH_2CH_2R)]^+ + MeOH \quad (4.3)$$

In the case of 1-hexene, K_{eq} has been calculated at different temperatures by integration of the NMR spectra. Then, using basic thermodynamic laws, it has been possible to calculate the $\Delta H°$ and $\Delta S°$ associated to the equilibrium. The resulting values are $\Delta H° = -5.8 \pm 0.3$ kcal mol^{-1} and $\Delta S° = -18.4 \pm 1.2$ cal mol^{-1} K^{-1}. Hence, the olefin insertion is an exothermic process with a decrease of entropy. Then, the Pd-alkyl is enthalpically favoured, whereas the Pd-hydride is entropically favoured.

The fact that the position of the equilibrium 4.3 strongly depends on the alkyl group R is probably connected with the fact that d^tbpx is a very bulky ligand, and this fact is probably very closely related with the very high selectivity of this catalysts toward the formation of methylpropanoate. In the same context, it is noteworthy that **4** does not react with excess ethene to give a higher alkyl complex. Moreover, it is usually reported that the catalysts used for the formation of

polyketones result in the oligomerisation of ethene, if the process is carried out in the absence of CO,[21] whereas, the catalytic system based on **1** is completely inactive under the same conditions.[22]

4.4 Reactivity of $[Pd(d^tbpx)(\eta^2\text{-}MeSO_3)]^+$, 11, with ethene

Three different classes of experiments have been considered in order to understand the reactivity of $[Pd(d^tbpx)(\eta^2\text{-}MeSO_3)]^+$, **11**, under ethene.

1) Ethene has been bubbled through a solution of **11** in MeOH at room temperature and atmospheric pressure. In this way, **11** is completely converted into **4** after *ca.* 30 minutes. Leaving this solution under nitrogen for a few days results in the partial reformation of **11**. The reaction can be reversed again by further bubbling ethene.
2) A solution of **11** in MeOH has been pressurised with 2-10 bar of ethene. Under 2 bar of ethene at room temperature, **4** became the main species present in solution after 24 hours. The sample was, then, degassed and stored under nitrogen; after 4 days, **4** was still the main species present in solution. Operating at 353 K under 10 bar of ethene, a considerable amount of **4** is formed after *ca.* 1 hr. **11** was always present in these experiments. In all these reactions, the inadequate mixing of gas with solution has been always a great problem, causing a low reproducibility of the results.

3) A solution of **11** in MeOH has been refluxed under atmospheric pressure of ethene at 353 K. The solution was, then, cooled under ethene to room temperature and analysed by NMR. **4** was the main species in solution after 1 hour and the other species present were **11** and $[d^tbpxH_2]^{2+}$

These data can be explained by assuming the presence of the three components in the two equilibria system described in Scheme 4.11 The equilibrium between **4** and **2** has been discussed previously in this Chapter, where it has been shown that an appreciable amount of **2** is present only at 353 K, when the β-H-elimination process is favoured for entropic reasons; whereas, at lower temperatures, the equilibrium is nearly quantitatively shifted towards **4**.

Scheme 4.11

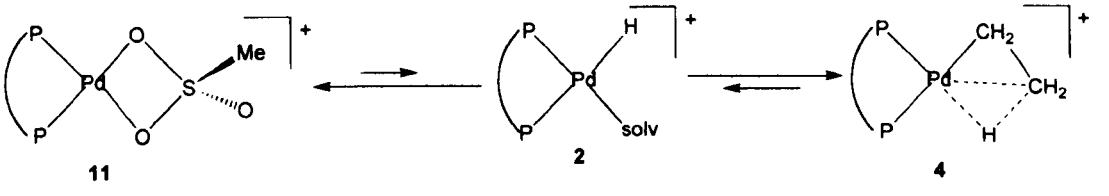

The inter-conversion of **11** into **2** has been discussed in Chapter 3. It is very difficult in this case to distinguish between thermodynamic and kinetic parameters. Considering a MeOH solution of **11** at room temperature, there is no evidence for the formation of **2** even after a few days. However, it is possible to observe small traces of **2** after refluxing the same solution at 353 K for 1 hour. Addition of $MeSO_3H$ to a solution of **2** in MeOH results in the formation of **11**, but it is possible to have complete conversion only after a few hours in the presence of an excess of acid. Thus, however the position of the equilibrium between **11** and **2** is, the rate of the

direct and inverse reaction is very low at room temperature. Moreover, the present data suggest that the equilibrium is always shifted towards the formation of **11**.

When ethene is added, thermodynamic effects favour the formation of **4**. It is known that the conversion of **2** into **4** is very fast. Hence, the rate determining step is the conversion of **11** into **2**. The experiments described above suggest that addition of ethene has not only a thermodynamic effect, but also a kinetic effect. In fact, it is possible to suppose that ethene co-ordination to the metal can favour the dissociation of the methanesulfonate anion and the co-ordination of MeOH, which becomes activated for β-hydride elimination. The hydride and, then, the ethyl complex are formed in this way.

4.5 Conclusions

It has been shown in this Chapter that it is possible to convert the hydride **2** into the ethyl complex **4**. This reaction is very fast and goes to completion after the addition of one equivalent of ethene. The same reaction, starting from **11**, requires much more forcing conditions. Despite this, it has been possible to demonstrate that **4** forms also in the presence of $MeSO_3H$ and in conditions similar to the ones used for the catalytic process (10 bar of ethene, 353 K).

The complex **4** exists in solution as an ethyl-agostic complex; this agostic interaction is surprisingly very strong and this is probably due to the presence of the very bulky and basic d^{t}bpx ligand. The ethyl complex **4** undergoes four different exchange processes in solution. The first process is the scrambling of the β-hydrogens of the ethyl group, which occurs *via* in-place rotation mechanism without

apparent dissociation of the agostic interaction. The energy barrier for this process is very low and, thus, the β-hydrogens are equivalent even at 155 K. The second exchange process scrambles the two carbon atoms of the ethyl substituent, and occurs *via* an ethene-hydride intermediate. This process is frozen below 248 K, but is fast at higher temperatures. The other two processes can only be clearly detected at 353 K; one makes the two P-atoms in **4** equivalent *via* a Y-shaped intermediate, whereas the other process involves the elimination of ethene and formation of the hydride **2**.

Other α-olefins can insert in the Pd-H bond of **2**. The reaction is completely regioselective; in fact only the linear Pd-alkyl complex is formed. The formation of the alkyl complex is disfavoured on increasing the length of the olefin, probably for steric reasons. This accounts for the decrease of catalytic activity passing from ethene to other terminal olefins. Moreover, it suggests that the bulkiness of the d^{t}bpx ligand controls most of the chemistry of these complexes. In particular, it can be correlated to the very high selectivity of the catalytic system based on **1**. Polyketones are not formed mainly because there is not enough room for the growing polymer chain. The problem of the selectivity will be examined again in Chapter 6.

References for Chapter Four

1. C. Elschenbroich and A. Salzer, *Organometallics- A Concise Introduction*, second edition, VCH, Weinheim, 1992, p.195
2. P. M. Maitlis, *The Organic Chemistry of Palladium*, Academic Press, New York, 1971
3. A. J. Canty, *Comprehensive Organometallic Chemistry II*, eds. E. W. Abel, F. G. A. Stone and G. Wilkinson, Pergamon Press, New York, 1995, vol.9, p.225
4. W. de Graaf, J. Boersman and G. van Koten, *Organometallics*, **1990**, *9*, 1479
5. R. Romeo and G. Alibrandi, *Inorg. Chem.*, **1997**, *36*, 4822
6. K. Osakada, Y. Ozawa and A. Yamamoto, *Bull. Chem. Soc. Jpn.*, **1991**, *64*, 2002
7. K. Osakada, Y. Ozawa and A. Yamamoto, *J. Chem. Soc. Dalton Trans.*, **1991**, 759
8. D. Drago and P. S. Pregosin, *J. Chem. Soc. Dalton Trans.*, **2000**, 3191
9. L. Mole, J. L. Spencer, N. Carr and A. G. Orpen, *Organometallics*, **1991**, *10*, 49; N. Carr, L. Mole, A. G. Orpen and J. L. Spencer, *J. Chem. Soc. Dalton Trans.*, **1992**, 2653
10. F. M. Conroy-Lewis, L. Mole, A. D. Redhouse, S. A. Lister and J. L. Spencer, *J. Chem. Soc. Chem. Commun.*, **1991**, 1601
11. R. H. Crabtree, *Angew. Chem. Int. Ed. Engl.*, **1993**, *32*, 789; M. Brookhart and M. L. H. Green, *J. Organomet. Chem.*, **1983**, *250*, 395
12. M. L. H. Green and L. L. Wong, *J. Chem. Soc. Chem. Commun.*, **1988**, 677
13. H. Werner and R. Feser, *Angew. Chem. Int. Ed. Engl.*, **1979**, *18*, 157

14. S. F. A. Kettle, *Physical Inorganic Chemistry*, Oxford University Press, 1998, p.328

15. B. E. Mann, *Comprehensive Organometallic Chemistry*, ed. G. Wilkinson, Pergamon Press, 1982, vol.3, p.89

16. N. N. Greenwood and A. Earnshaw, *Chemistry of the Elements*, Pergamon Press, New York, 1984

17. J. S. L. Leo, J. J. Vittal and T. S. A. Hor, *J. Chem. Soc., Chem. Commun.*, **1999**, 1477

18. D. L. Thorn and R. Hoffman, *J. Am. Chem. Soc.*, **1978**, *100*, 2079

19. A. Yamamoto, *J. Chem. Soc., Dalton Trans.*, **1999**, 1027

20. G. R. Eastham Ph.D. Thesis, University of Durham, 1998

21. E. Drent, J. A. M. van Broekhoven and M. J. Doyle, *J. Organomet. Chem.*, **1991**, *417*, 235; E. Drent and P. H. M. Budzelaar, *Chem. Rev.*, **1996**, *96*, 663

22. G. R. Eastham, personal communication

Chapter Five

Numbering scheme for Chapter 5

Pd(d^{t}bpx)(dba)	**1**
[Pd(d^{t}bpx)H(MeOH)]$^+$	**2**
[Pd(d^{t}bpx)(CH_2CH_3)]$^+$	**3**
[Pd(d^{t}bpx)($^{13}CH_2CH_3$)]$^+$	**3a**
[Pd(d^{t}bpx)($CH_2{}^{13}CH_3$)]$^+$	**3b**
[Pd(d^{t}bpx)(COEt)(MeOH)]$^+$	**4**
[Pd(d^{t}bpx)(COEt)(THF)]$^+$	**5**
[Pd(d^{t}bpx)(^{13}COEt)(THF)]$^+$	**5a**
[Pd(d^{t}bpx)($^{13}CO^{13}CH_2CH_3$)(THF)]$^+$	**5b**
[Pd(d^{t}bpx)($^{13}COCH_2{}^{13}CH_3$)(THF)]$^+$	**5c**
Pd(d^{t}bpx)(COEt)(Cl)	**6**
Pd(d^{t}bpx)Cl_2	**7**
Pd(d^{t}bpx)$(CF_3COO)_2$	**8**
[Pd(d^{t}bpx)$(CH_3CN)_2$]$^{2+}$	**9**
[Pd(d^{t}bpx)(COEt)(EtCN)]$^+$	**10**
[Pd(d^{t}bpx)(^{13}COEt)(EtCN)]$^+$	**10a**
[Pd(d^{t}bpx)(η^2-TfO)]$^+$	**11**
Pd(d^{t}bpx)(COMe)Cl	**12**
[Pd(d^{t}bpx)(COEt)(CO)]$^+$	**13**
[Pd(d^{t}bpx)H(CO)]$^+$	**14**
[Pd(d^{t}bpx)(η^2-$MeSO_3$)]$^+$	**15**
Pd(d^{t}bpx)(CO)	**16**
Pd(d^{t}bpx)$(CO)_2$	**17**

Reactivity of some catalyst precursors and catalytic intermediates with carbon monoxide

5.1 Introduction

Two of the three main intermediates involved in the hydride cycle for the methoxycarbonylation of ethene promoted by the catalytic system based on Pd(d^{t}bpx)(dba), **1**, have been characterised in the previous Chapters, *i.e.* [Pd(d^{t}bpx)H(MeOH)]$^+$, **2**, and [Pd(d^{t}bpx)(CH_2CH_3)]$^+$, **3**. The last step in order to close the catalytic cycle is to add CO.

CO insertion into a M-alkyl bond is a classic reaction for the synthesis of metal-acyl complexes;[1] Pd-acyl compounds are usually not very stable.[2] However, spectroscopic data [3,4] and, in a few cases, X-ray structures are now available.[5,6] The mechanism of the carbonylation of metal-alkyl or metal-aryl bonds has been extensively studied for many systems both experimentally [7-10] and theoretically.[11,12] The generally accepted mechanism contains four main features (see Scheme 5.1): (i) co-ordination of a CO molecule to the metal centre, (ii) isomerisation of the metal-carbonyl complex *via* pseudorotations to achieve a configuration suitable for alkyl migration, (iii) migration of the alkyl or aryl group to CO co-ordinated in a *cis* position, and (iv) stabilisation of the unsaturated complex *via* association with an additional ligand or η^2-acyl co-ordination. Relatively little work has been carried out on the carbonylation of organopalladium compounds.

Scheme 5.1

Generally accepted simplified mechanism of CO insertion in M-R bonds in square-planar complexes [15]

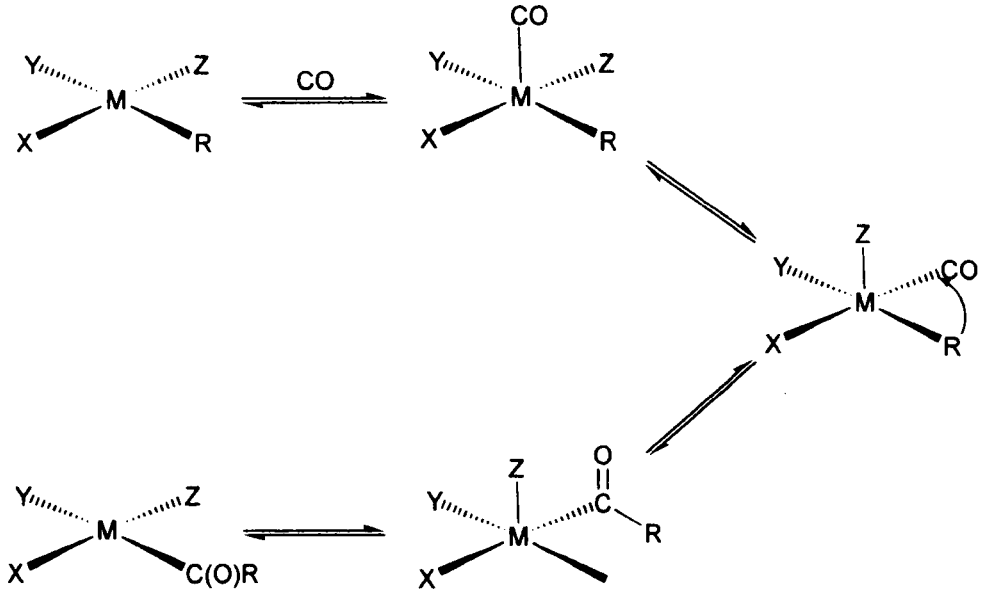

Heck *et al.*[13] have studied the carbonylation of *trans*-$M(PR_3)_2(R')X$ (M = Ni, Pd, Pt; R' = alkyl or aryl; X = Cl, Br, I), showing that the first step of the reaction is the co-ordination of CO to the metal to give a penta co-ordinated species, $M(PR_3)_2(R')X(CO)$, which can exist as different isomers. The reaction can, then, follow two different pathway (or both to different extents), depending on the conditions (see Scheme 5.2). The first mechanism involves direct migration of R' onto CO in $M(PR_3)_2(R')X(CO)$, whereas the second mechanism involves dissociation of one phosphine ligand and, then, migration to the resulting square-planar complex.

Scheme 5.2

Proposed mechanism for the carbonylation of trans-$M(PR_3)_2(R')X$

(M = Ni, Pd, Pt) [13]

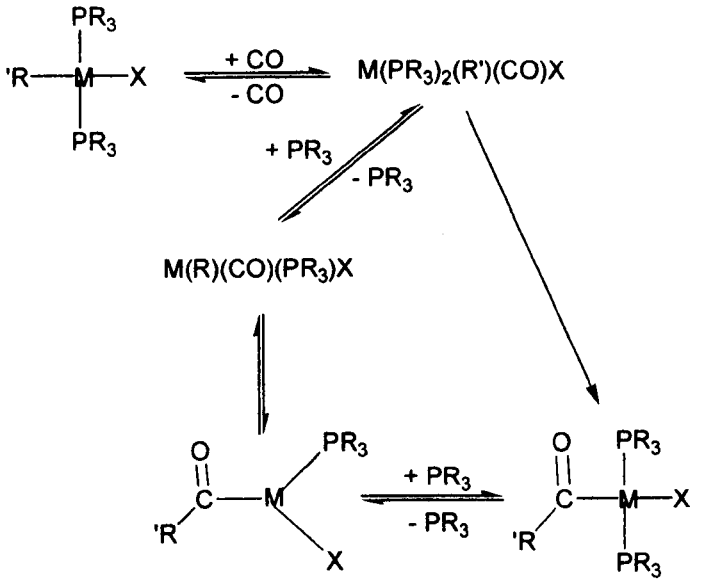

In the case of palladium complexes containing diphosphine ligands, the dissociation of the diphosphine is unfavourable and, hence, the mechanism must be reviewed. Also in this case, the first step is CO co-ordination resulting in a 5 co-ordinate complex (see Scheme 5.3). Then, the alkyl or aryl group can directly migrate onto the co-ordinated CO, probably after pseudo-rotation of the ligands in order to achieve an appropriate geometry for the migration (associative mechanism); alternatively, the complex can lose the ancillary ligand X (dissociative mechanism) to give a square planar complex, *cis*-$[Pd(P\text{-}P)(CO)R]^+$; the *cis* geometry favours migration and, finally, the solvent or another ligand can enter in the fourth co-ordination site of the complex. The dissociative mechanism has been proved experimentally in some cases. In particular, Toth and Elsevier [14] have shown that

$[Pd\{(S,S')\text{-}BDPP\}(CH_3)(CO)]^+$ is one of the intermediates in the carbonylation of $[Pd\{(S,S')\text{-}BDPP\}(CH_3)(solv)]^+$. Moreover, this mechanism is in some cases clearly indicated by the fact that the rate of the carbonylation process increases by replacing strongly co-ordinating ligands (*e.g.* halides) with labile ligands.[15]

Scheme 5.3

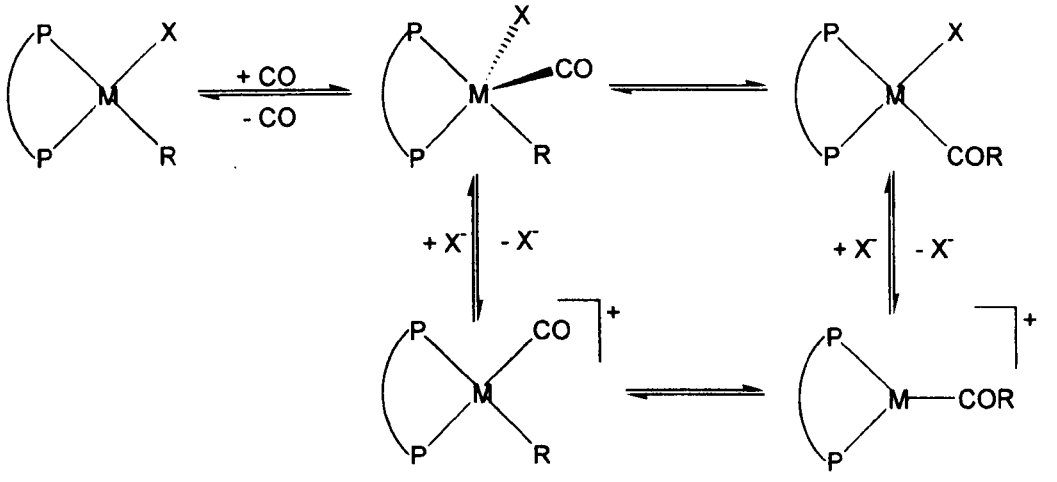

5.2 Reactivity of $[Pd(d^tbpx)(CH_2CH_3)]^+$, 3, with CO

$[Pd(d^tbpx)(CH_2CH_3)]^+$, **3**, reacts in MeOH under N_2 with one equivalent of CO to give $[Pd(d^tbpx)H(MeOH)]^+$, **2**, and MeP (this last product is detected by ^{13}C NMR when labelled compounds are used). On using more CO, decomposition becomes a serious problem, but it is always possible to detect the formation of MeP. This data can be explained assuming that CO inserts in **3** to give $[Pd(d^tbpx)(COEt)(MeOH)]^+$, **4**, followed by rapid methanolysis and formation of the final products (see Scheme 5.4). On using excess of CO, the formation of MeP suggests that the same process takes place (at least partially) followed by CO-

induced decomposition of **2** (see Section 5.3 for more detail). In this way, the last step of the catalytic cycle has been achieved.

Scheme 5.4

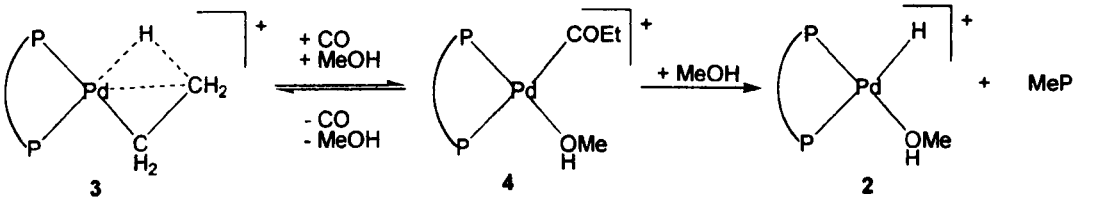

In order to characterise the last intermediate, this reaction has been repeated in non-alcoholic solvents. Thus, **3** reacts in THF at low temperature with one equivalent of CO resulting in the formation of a new species which shows two doublets at 36.3 and 83.4 ppm [^{2}J(P-P) = 40 Hz] in the ^{31}P{^{1}H} NMR spectrum at 193 K. These NMR data indicate that the new species contains two *cis* inequivalent P-atoms, in agreement with the formulation [Pd(d^{t}bpx)(COEt)(THF)]$^+$, **5**. The complex Pd(d^{t}bpx)(COEt)(Cl), **6**, is well known,[16] and shows two doublets at 15.1 and 44.2 ppm [^{2}J(P-P) = 52.6 Hz]. The shift to lower field observed for **5** agrees perfectly with the substitution of an anionic ligand, Cl$^-$, with a neutral and less basic molecule of THF. The same behaviour has been observed during this work for other Pd(II) species containing d^{t}bpx, *e.g.* Pd(d^{t}bpx)Cl$_2$, **7** (36 ppm), Pd(d^{t}bpx)(CF$_3$COO)$_2$, **8** (42 ppm), and [Pd(d^{t}bpx)(CH$_3$CN)$_2$]$^{2+}$, **9** (55 ppm).

In order to confirm the nature of the product formed, the reaction has been repeated using one equivalent of ^{13}CO instead of ^{12}CO. In these conditions, the two resonances at 36.4 and 83.4 ppm appear as two doublets of doublets (see Figure 5.1), instead of the two doublets present in the previous experiment, due to the formation of [Pd(d^{t}bpx)(^{13}COEt)(THF)]$^+$, **5a**. The *cis* P-P coupling constant is still 40 Hz,

whereas the resonance at 36.4 ppm (P_A in Scheme 5.5) clearly also shows a P-C coupling constant of 84.0 Hz due to the *trans* acyl group, and the resonance at 83.4 ppm (P_B in Scheme 5.5) has a P-C coupling constant of 17.0 Hz (*cis*-coupling).

Figure 5.1

*$^{31}P\{^1H\}$ NMR spectrum of [Pd(d^{t}bpx)(^{13}COEt)(THF)]$^+$, **5a**, in THF at 193 K*

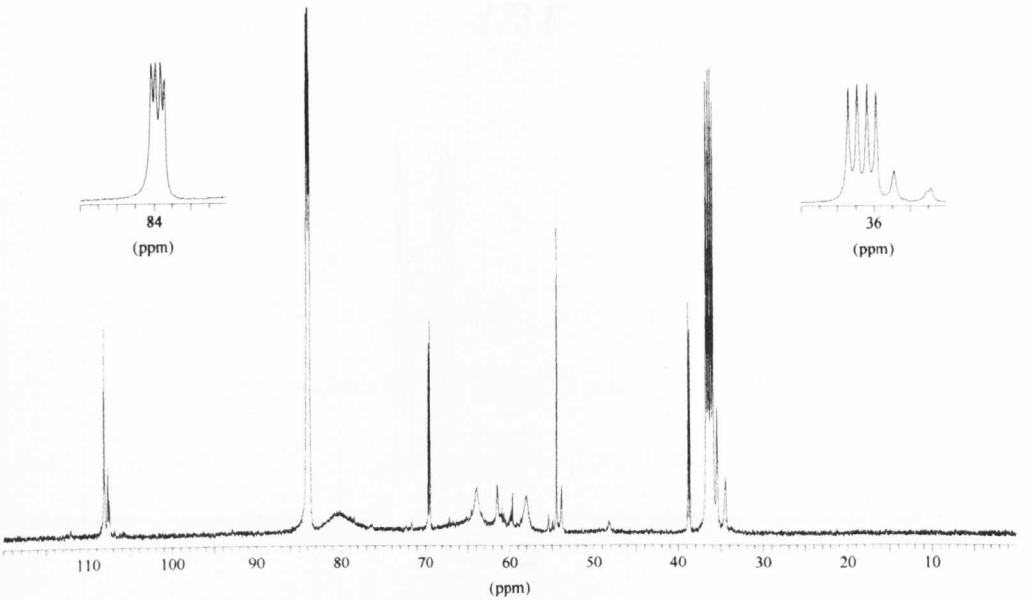

Scheme 5.5

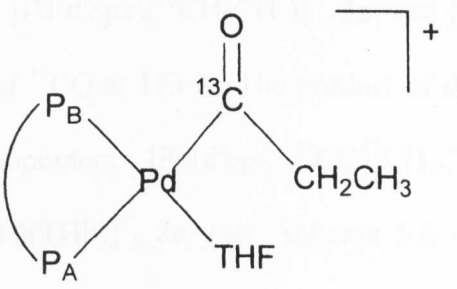

5a

Finally, the $^{13}C\{^{1}H\}$ NMR spectrum shows an acyl resonance [3,4,14,15] at *ca.* 232 ppm. The carbon spectrum is strongly temperature dependent, because of the presence of a dynamic process (see Section 5.2.1). The system is completely static at 173 K (see Figure 5.2), and, hence, in these conditions the acyl resonance is a doublet of doublets, with *trans*-$^{2}J(P\text{-}C)$ = 84.0 Hz and *cis*-$^{2}J(P\text{-}C)$ = 17.0 Hz.

Figure 5.2

*$^{13}C\{^{1}H\}$ NMR spectrum of $[Pd(d^{t}bpx)(^{13}COEt)(THF)]^{+}$, **5a**, in THF at 173 K*

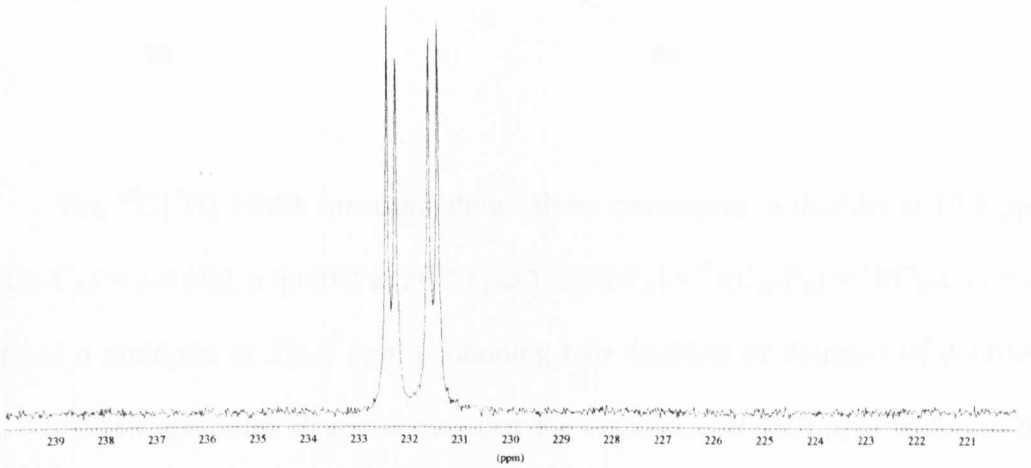

A doubly ^{13}C-enriched acyl can be obtained in THF or THF/CH_2Cl_2 by reacting a 1:1 mixture of $[Pd(d^{t}bpx)(^{13}CH_2CH_3)]^{+}$, **3a**, and $[Pd(d^{t}bpx)(CH_2{}^{13}CH_3)]^{+}$, **3b**, with one equivalent of ^{13}CO at 193 K. The product of this reaction is a mixture 1:1 of the two isotopomers $[Pd(d^{t}bpx)(^{13}CO^{13}CH_2CH_3)(THF)]^{+}$, **5b**, and $[Pd(d^{t}bpx)(^{13}COCH_2{}^{13}CH_3)(THF)]^{+}$, **5c**, (see Scheme 5.6 for the labelling of the atoms). The exchange process is completely frozen below 173 K and, hence, the NMR spectra are just the sum of the separate spectra of **5b** and **5c**. Two resonances

are present in the $^{31}P\{^{1}H\}$ NMR spectrum at 173 K in THF/CH_2Cl_2, at 33.5 and 82.0 ppm, both consist of a doublet of doublets due to **5c** [$^{2}J(P_A\text{-}P_B)$ = 39 Hz; $^{2}J(P_A\text{-}C_A)$ = 83 Hz; $^{2}J(P_B\text{-}C_A)$ = 18 Hz] and a doublet of doublets of doublets due to the extra coupling with C_B in **5b** [$^{3}J(P_A\text{-}C_B)$ = 23 Hz; $^{3}J(P_B\text{-}C_B)$ = 23 Hz], with relative intensity 2:1.

Scheme 5.6

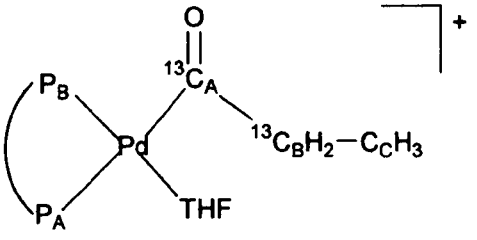

5b

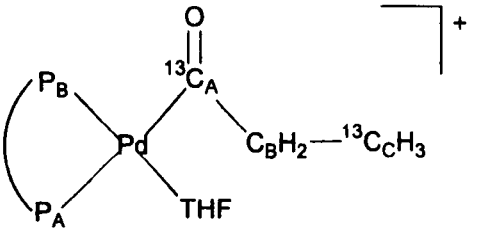

5c

The $^{13}C\{^{1}H\}$ NMR spectrum shows three resonances: a doublet at 10.9 ppm [$^{2}J(C_C\text{-}C_A)$ = 3-4 Hz], a quartet at 38.2 ppm [$^{3}J(C_B\text{-}P_A) = {}^{3}J(C_B\text{-}P_B) = {}^{1}J(C_B\text{-}C_A)$ = 23 Hz] and a multiplet at 231.9 ppm containing two doublets of doublets of doublets. The ^{13}C NMR spectrum clearly shows that the resonance at 10.9 ppm is due to the CH_3 group [quartet, $^{1}J(C_C\text{-}H)$ = 130 Hz] and the one at 38.2 ppm to the CH_2 group [triplet, $^{1}J(C_B\text{-}H)$ = 133 Hz]. All the NMR data are summarised in Table 5.1. The fact that $^{3}J(P_A\text{-}C_B)$ and $^{3}J(P_B\text{-}C_B)$ are very similar suggests that C_B lies very close to the bisector of the $P_A\text{-}Pd\text{-}P_B$ angle. A similar behaviour has been found previously for $[Pd(d^{i}ppe)(CO^{13}CH_3)(CO)]^{+}$.[17]

The values for $^{1}J(C\text{-}H)$ are as expected for normal sp^3 carbons; therefore, in this case there is no evidence for any agostic interaction which is in keeping with the suggestion at the beginning of this Section that the fourth co-ordination site is occupied by a solvent molecule.

Table 5.1

NMR data for [Pd(d^{t}bpx)(COEt)(THF)]$^+$ in THF/CH_2Cl_2 at 173 K

a) NMR chemical shifts

	P_A	P_B	C_A	C_B	C_C
δ (ppm)	33.5	82.0	231.9	38.2	10.9

b) Coupling constants (Hz)

	P_A	P_B	C_A	C_B	C_C
P_A	-	39	83	23	-
P_B	39	-	18	23	-
C_A	83	18	-	23	3-4
C_B	23	23	23	-	-
C_C	-	-	3-4	-	-

$^1J(C_B\text{-}H) = 133$ Hz

$^1J(C_C\text{-}H) = 130$ Hz

In order to confirm this hypothesis, the syntheses of the unenriched and mono-enriched acyl have been repeated in EtCN, following the same procedures as before, *i.e.* addition at low temperature of one equivalent of CO or ^{13}CO to a EtCN solution of **3**. In the ^{13}C spectrum (see Table 5.2 for all the NMR data) a resonance at 233 ppm clearly indicates that an acyl complex has been formed, *i.e.* [Pd(d^{t}bpx)(COEt)(EtCN)]$^+$, **10**, or [Pd(d^{t}bpx)(^{13}COEt)(EtCN)]$^+$, **10a**. The two *cis*-inequivalent P-atoms resonate in the ^{31}P spectrum at 20.2 and 49.4 ppm; this big difference in chemical shift on changing from THF to EtCN is clearly consistent with solvent co-ordination to the metal.

Table 5.2

*NMR data for [Pd(d^{t}bpx)(COEt)(solv)]$^+$ (solv = THF, **5**; EtCN, **10**) at 193 K*

	EtCN	THF
δP_A	20.2	36.4
δP_B	49.4	83.4
$\delta C(O)$	233.2	232.0
$^2J(P_A\text{-}P_B)$	40	40
$^2J(P_A\text{-}C)$	92	83.9
$^2J(P_B\text{-}C)$	13	17.0

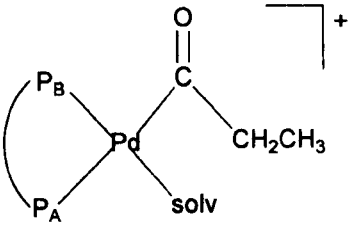

5.2.1 The dynamic behaviour of [Pd(d^{t}bpx)(COEt)(THF)]$^+$, 5

The VT $^{13}C\{^1H\}$ NMR spectra in the acyl region of the mono-enriched complex **5a** in THF are reported in Figure 5.3. The system is completely static at 173 K, where a doublet of doublets is present at *ca.* 232 ppm. With increasing the temperature, the two outer resonances of the multiplet do not change at all, whereas the two inner resonances start to broaden until at 213 K there is complete coalescence. At higher temperature, a new resonance at the centre of the two outer resonances starts to appear and, finally, at 243 K a triplet is clearly present with $^2J(P\text{-}C) = 50$ Hz. The observed coupling constant at high temperature is the average of the

cis and *trans* constants observed at low temperature; thus, the two P-atoms become equivalent in these conditions.

Figure 5.3

*VT $^{13}C\{^{1}H\}$ NMR spectra of [Pd(dbpx)(^{13}COEt)(THF)]$^{+}$, **5a**, in THF*

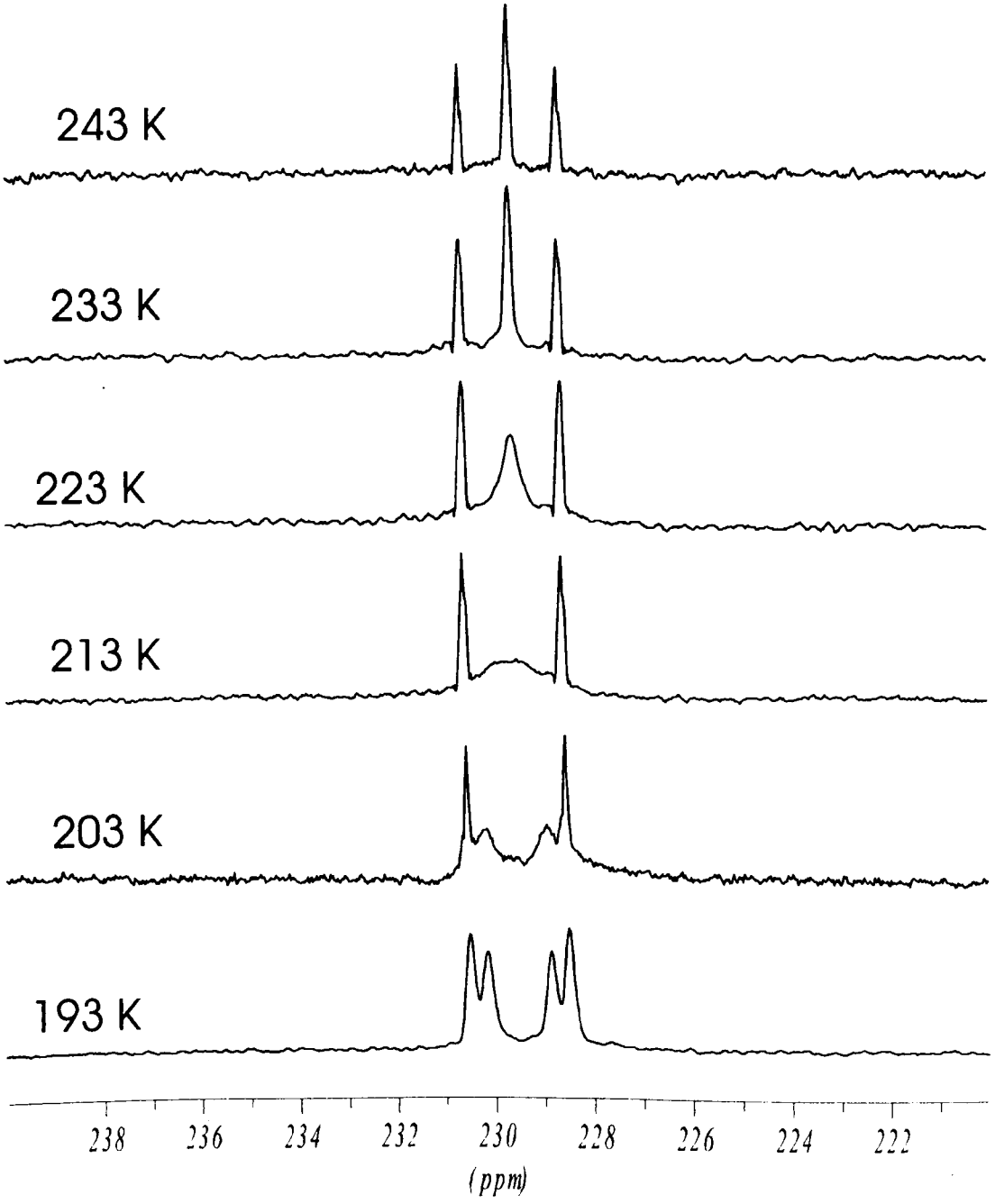

Using the doubly enriched sample (*i.e.* a mixture 1:1 of **5b** and **5c**), it has been possible to follow the exchange process looking at different atoms. Two sharp resonances are present at 176 K in the $^{31}P\{^{1}H\}$ NMR spectrum (see Figure 5.4), which start to broaden with increasing the temperature.

Figure 5.4

*VT $^{31}P\{^{1}H\}$ NMR spectra of a 1:1 mixture of **5b** and **5c** in THF/CH_2Cl_2*

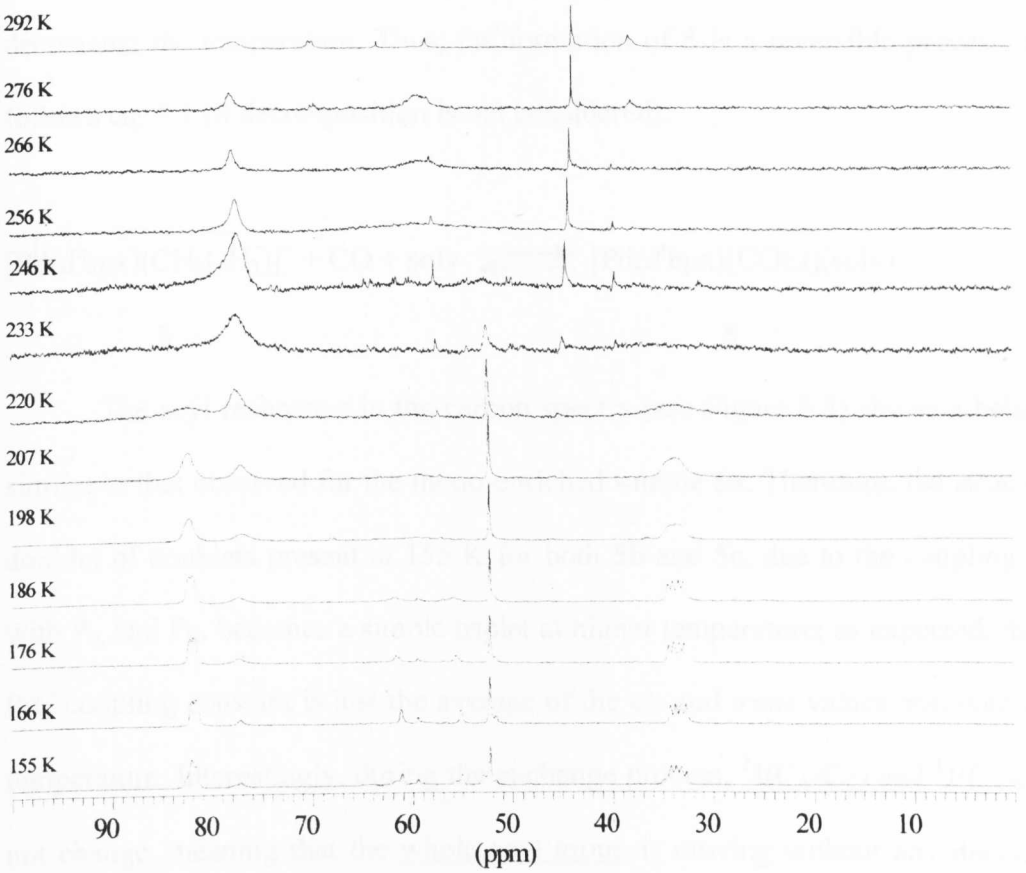

Above 220 K they are so broad that it is very difficult to distinguish them from the baseline. Finally, at 256 K a broad hump is clearly present at *ca.* 59 ppm, indicating the equivalence of the two P-atoms. The ethyl complex begins to appear, too, with increasing the temperature, as clearly indicated by the presence of two new

resonances at *ca.* 40 and 70 ppm. Whereas, the broad resonance at 78 ppm is due to $[Pd(d^tbpx)(\eta^2\text{-}TfO)]^+$, **11**, which is the thermodynamic product in non-alcoholic solvents (see Chapter 2). The sharp resonance at 52 ppm present at low temperature is probably a bis-solvento species present in equilibrium with **11**; a similar equilibrium has been discussed in Chapter 2 in the case of MeP as solvent. The other resonances which start to appear at high temperature are unknown decomposition products. In fact, their formation, as well as the formation of **11**, is not reversed on cooling the solution to 173 K; whereas, the ethyl complex **3** disappears with decreasing the temperature. Thus, the formation of **5** is a reversible process, which follows eq. 5.1 (if decomposition is not considered).

$$\underset{\mathbf{3}}{[Pd(d^tbpx)(CH_2CH_3)]^+} + CO + solv \rightleftharpoons \underset{\mathbf{5}}{[Pd(d^tbpx)(COEt)(solv)]^+} \qquad (5,1)$$

The acyl resonance in the carbon spectra (see Figure 5.5) shows a behaviour similar to that observed for the mono-enriched sample **5a**. Therefore, the structure of doublet of doublets present at 155 K for both **5b** and **5c**, due to the coupling of C_A with P_A and P_B, becomes a simple triplet at higher temperature; as expected, the new P-C coupling constant is just the average of the *cis* and *trans* values observed at low temperature. Interestingly, during the exchange process, $^2J(C_A\text{-}C_C)$ and $^1J(C_A\text{-}C_B)$ do not change, meaning that the whole acyl group is moving without any dissociation process. As a consequence, the resonances due to the CH_3 and CH_2 groups do not change at all in the temperature range examined (see Figure 5.6). In the case of the CH_2 group, this behaviour is also a consequence of the fact that $^2J(P_A\text{-}C_B)$ and $^2J(P_B\text{-}C_B)$ have the same value.

Figure 5.5

VT $^{13}C\{^1H\}$ NMR spectra of a 1:1 mixture of **5b** *and* **5c** *in THF/CH_2Cl_2*

(acyl region)

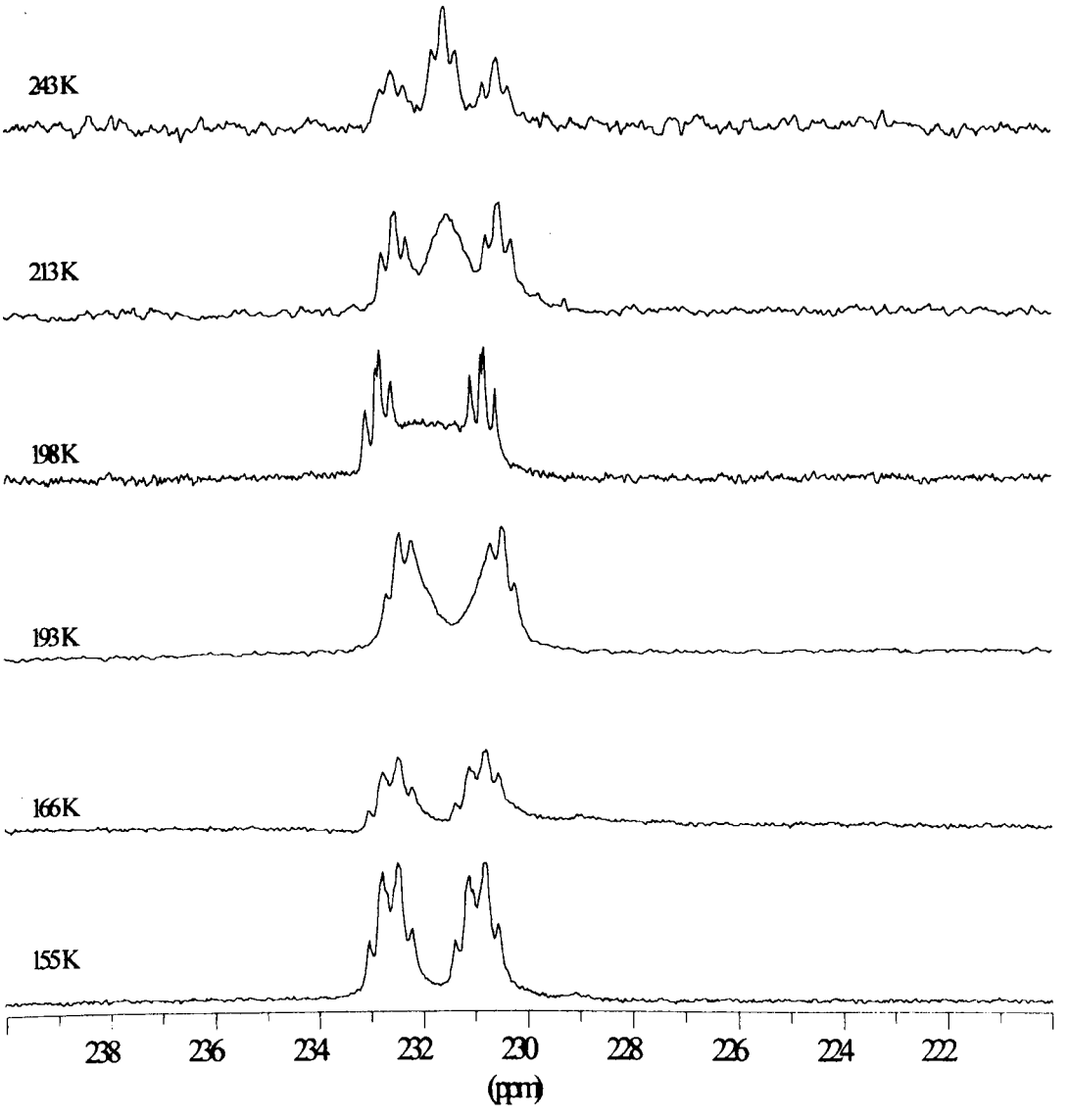

Figure 5.6

*VT $^{13}C\{^1H\}$ NMR spectra of a 1:1 mixture of **5b** and **5c** in THF/CH_2Cl_2*

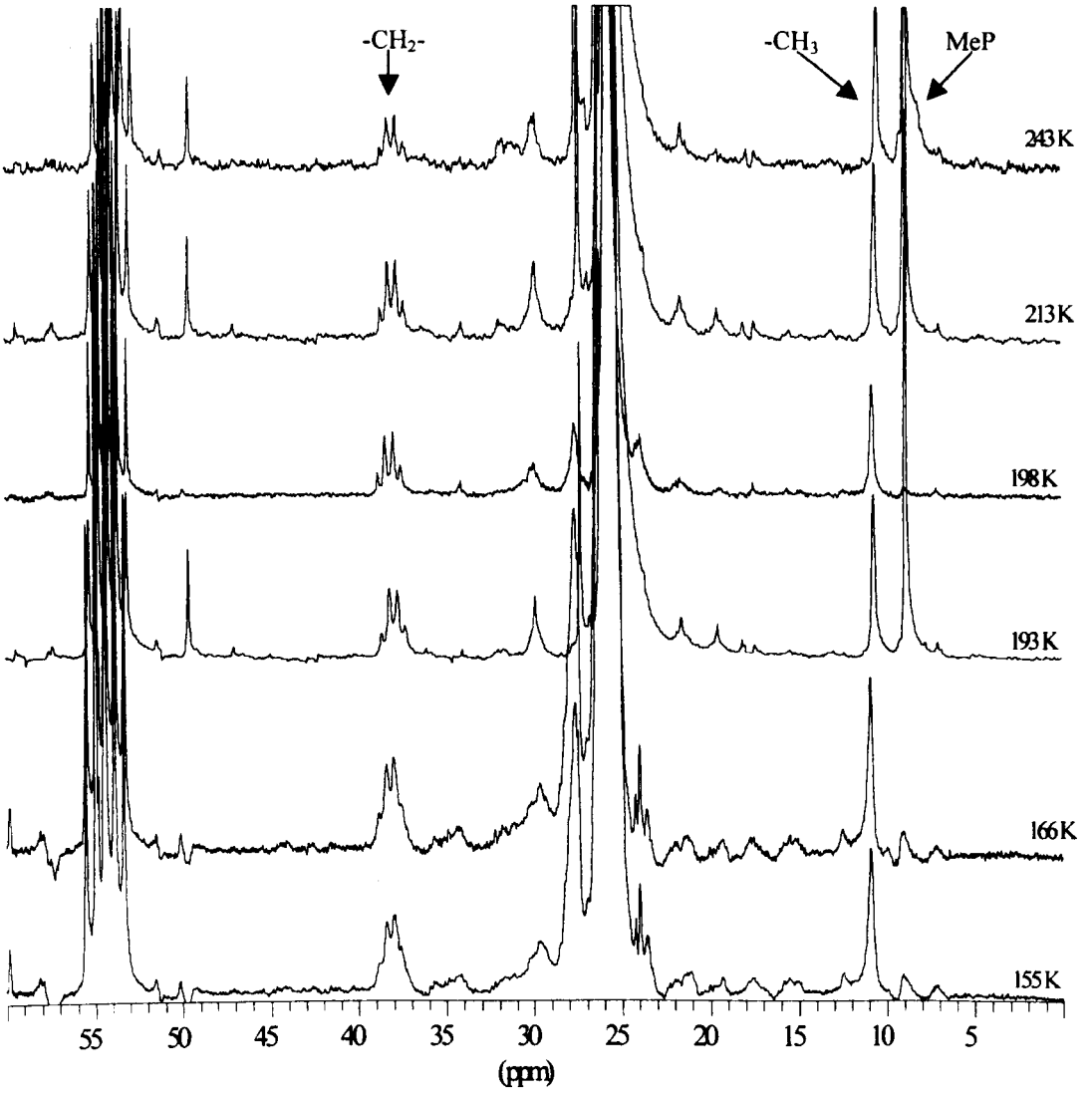

Two different mechanisms could be in agreement with all these data (see Scheme 5.7). The first one involves dissociation of the solvent, formation of a Y-shaped molecule followed by solvent association. The other one does not involve any dissociation process, but only an internal exchange *via* a tetrahedral intermediate.

Scheme 5.7

a) Dissociative mechanism

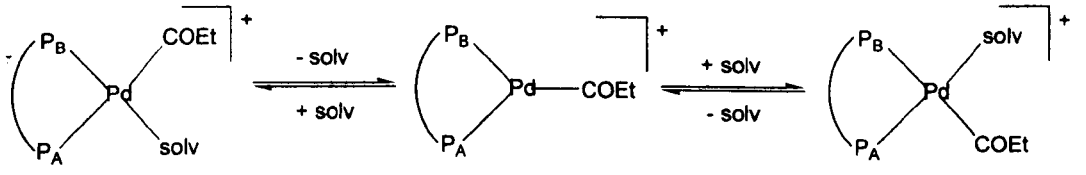

b) Intra-molecular mechanism

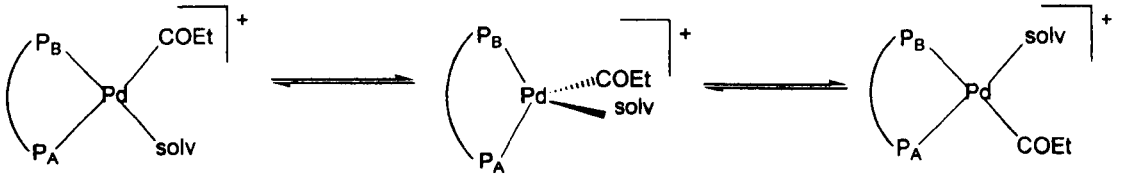

Two similar mechanisms have been proposed for the process which makes the P-atoms equivalent in **3** (see Chapter 4). Pd(d^{t}bpx)(COMe)Cl, **12**, can be obtained from Pd(COD)(Me)Cl, d^{t}bpx and CO (see Scheme 5.8). The $^{31}P\{^1H\}$ NMR spectrum of **12** at 196 K shows two sharp doublets, whereas at room temperature they are broader but still separated. This suggests that the exchange process is slower in the case of **12** than in the case of **5**, and supports the dissociative mechanism. In fact, dissociation of Cl^- is more difficult than dissociation of the solvent.

Scheme 5.8

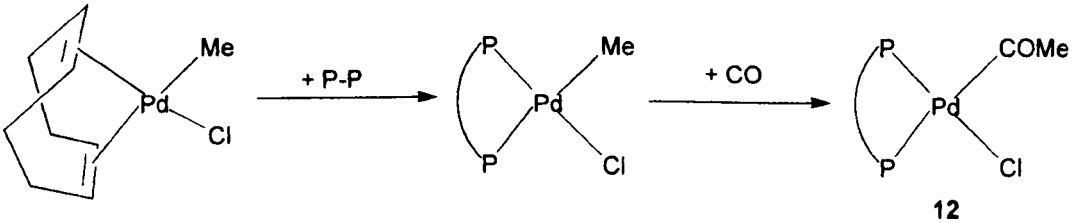

12

5.2.2 Reactivity of $[Pd(d^tbpx)(COEt)(THF)]^+$, 5

The acyl complex, **5**, is very unstable. At room temperature, it decomposes in a few minutes, whereas at low temperature it can be kept for *ca.* 10 hours. Decomposition of **5** in THF results mainly in the formation of **11**, Pd-metal and $[d^tbpxH_2]^{2+}$. Decomposition is accelerated by addition of excess CO; under 1 bar of CO, **5** decomposes in *ca.* 1 hour also at 193 K. Since the decomposition is very fast, it makes it very difficult to carry out mechanistic studies. Addition of 3 equivalents of CO to **5** in THF at 193 K results in the partial formation of a new species, although **5** is still the main species in these conditions. In the $^{13}C\{^1H\}$ spectrum (see Figure 5.7, ^{13}CO has been used in this experiment) there is still, in fact, the doublet of doublets due to **5**, but there is also a second acyl resonance, partially hidden by the first one.

Figure 5.7

*$^{13}C\{^1H\}$ NMR of $[Pd(d^tbpx)(^{13}COEt)(THF)]^+$, **5a**, + 3 ^{13}CO in THF at 173 K*

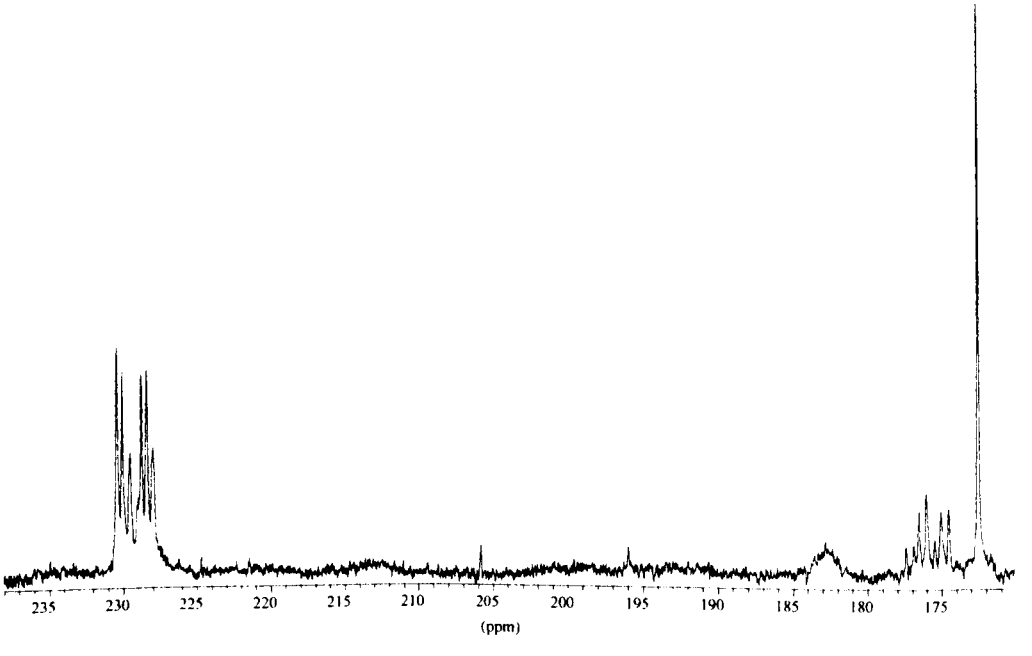

Because of this, it is impossible to deduce the fine structure of the second resonance. Moreover, at least one carbonyl resonance is present at *ca.* 176 ppm. One explanation could be that the excess CO partially displaces the solvent from **5** to give $[Pd(d^tbpx)(COEt)(CO)]^+$, **13**, as described by eq. 5.2.

$$[Pd(d^tbpx)(COEt)(THF)]^+ + CO \rightleftharpoons [Pd(d^tbpx)(COEt)(CO)]^+ + THF \qquad (5.2)$$

5 **13**

In the presence of up to 4 equivalents of CO, equilibrium 5.2 is shifted towards **5**; on adding more CO, complete decomposition is observed. This result is interesting, since it indicates that co-ordination of THF is preferred to CO co-ordination, and this is very unusual. For instance, Toth and Elsevier [14] have reported that carbonylation of $[Pd\{(S,S')\text{-BDPP}\}(Me)(solv)]^+$ results in the formation of $[Pd\{(S,S')\text{-BDPP}\}(COMe)(CO)]^+$; they do not observe the formation of $[Pd\{(S,S')\text{-BDPP}\}(COMe)(solv)]^+$ even on using a deficiency of CO. Moreover, they report that the reaction of $Pd\{(S,S')\text{-BDPP}\}(COMe)Cl$ with $AgBF_4$ under N_2 results in a 1:1 mixture of $[Pd\{(S,S')\text{-BDPP}\}(COMe)(CO)]^+$ and $[Pd\{(S,S')\text{-BDPP}\}(Me)(solv)]^+$. It is also interesting to note that carbonylation of $[Pd(d^ippe)(Me)(solv)]^+$ results in the analogous species $[Pd(d^ippe)(COMe)(CO)]^+$;[17] this species is stable only at low temperature for a short time. Hence, it further reacts resulting, finally, in the formation of $[Pd(d^ippe)(\mu\text{-CO})Pd(d^ippe)Me]^+$. Thus, small changes in the electronic and/or steric properties of the diphosphine ligand can significantly affect the chemistry of the carbonylation process.

5.3 Reactivity of $[Pd(d^tbpx)H(MeOH)]^+$, 2, with CO and mixtures CO/C_2H_4

The only process observed on reacting **2** with CO in MeOH at room temperature is decomposition of the complex to form Pd-metal and the protonated phosphine. Therefore, the reaction has been studied again at lower temperature, in order to see whether any intermediates could be detected in the decomposition process. The experiment has been carried out by adding a few equivalents of CO to a MeOH solution of **2** cooled in a dry ice/acetone bath and, then, the sample was transferred directly into the pre-cooled NMR probe, avoiding any warming of the sample. **2** is converted in these conditions into a new species and the complete conversion, in the presence of 2-3 equivalents of CO, takes place over *ca.* 20-30 minutes at 193 K; some other decomposition products are also formed. The $^{31}P\{^1H\}$ NMR spectrum at 193 K of the new compound shows two doublets at 61.0 and 31.4 ppm (see Figure 5.8), with $^2J(P_A\text{-}P_B)$ = 21.9 Hz. The resonance at higher field is further coupled in the ^{31}P NMR spectrum, $^2J(P_B\text{-}H)$ = 167.4 Hz, indicating that this new species is a hydride complex; consistent with this, a doublet of doublets is observed at –5.3 ppm in the ^1H NMR spectrum at 193 K [$^2J(P_B\text{-}H)$ = 15.8 Hz; $^2J(P_A\text{-}H)$ = 167.4 Hz]. In order to characterise the ligand present in the fourth co-ordination site of the complex, the experiment has been repeated using ^{13}CO. The resonance at lower field in the $^{31}P\{^1H\}$ NMR spectrum at 193 K is now a doublet of doublets (see Figure 5.9), due to additional coupling with a *trans* C-atom [$^2J(P_B\text{-}C)$ = 102 Hz], and a doublet of doublets at 183.3 ppm is observed in the $^{13}C\{^1H\}$ NMR spectrum.

Figure 5.8

*$^{31}P\{^{1}H\}$ NMR spectrum of $[Pd(d^{t}bpx)H(CO)]^{+}$, **14**, in MeOH at 193 K*

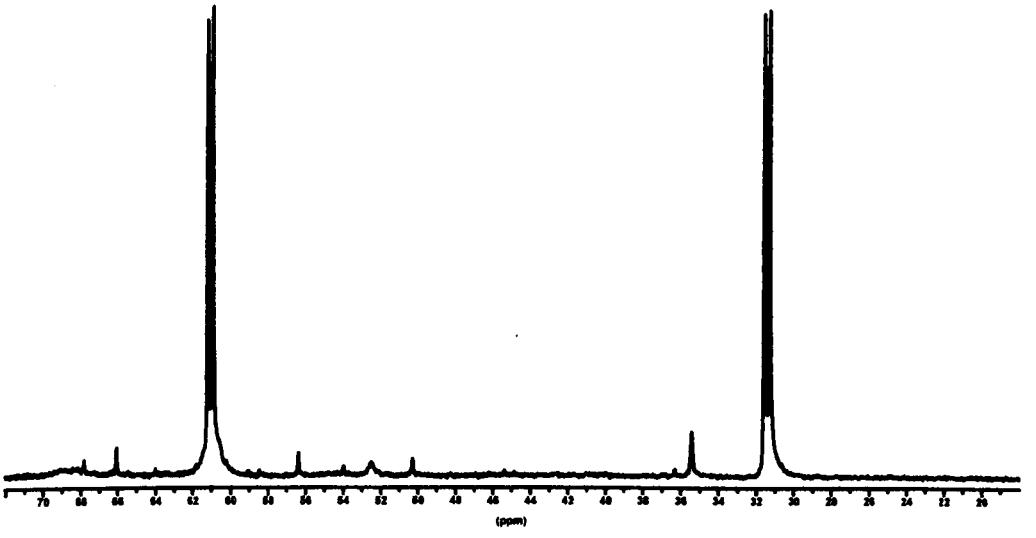

Figure 5.9

*$^{31}P\{^{1}H\}$ NMR spectrum of $[Pd(d^{t}bpx)H(^{13}CO)]^{+}$, **14**, in MeOH at 193 K*

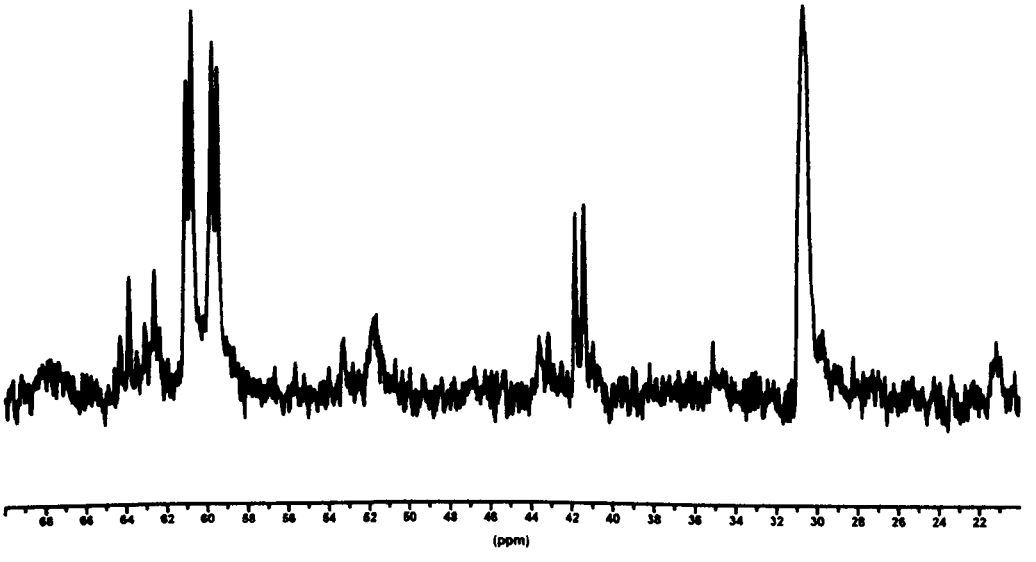

Therefore, it is possible to conclude that CO displaces solvent from **2** to give $[Pd(d^tbpx)H(CO)]^+$, **14** (see Scheme 5.9 for the atom labelling).

Scheme 5.9

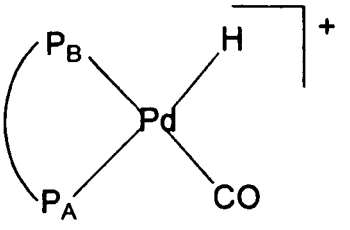

14

The hydride-carbonyl complex **14** is very unstable, and decomposes in a few minutes even at 223 K. This study suggests that the co-ordination of CO to the metal could play an important role in the decomposition of the catalyst. Hence, some further studies using ethene and mixtures ethene/CO have been done. Repeating the previous experiment using ethene instead of CO, **3** is formed quantitatively, suggesting that the insertion of the olefin into the Pd-H bond is also very fast at low temperature. Then, a mixture 1:1 of ethene/CO has been added to **2** using the same conditions. Running directly the phosphorus spectrum of this solution at 193 K without warming the sample, a *ca.* 1:1 mixture of **3** and **14** is present. By warming the solution up to 293 K, **14** completely disappears, and only **3** with some decomposition products are present. After 20 minutes at room temperature, complete decomposition has been observed. The same experiment was then repeated with a 9:1 mixture of ethene/CO and, in this case, a mixture *ca.* 20:1 of **3** and **14** is present at 193 K. Decomposition in this last experiment is not as fast as in the previous experiment, indicating that the rate of decomposition increases by increasing the concentration of CO. All these data clearly suggest that both CO and ethene

effectively compete in reacting with **2**. The reaction with ethene allows continuation of the catalytic cycle, whereas CO co-ordination induces fast decomposition (see Scheme 5.10).

Scheme 5.10

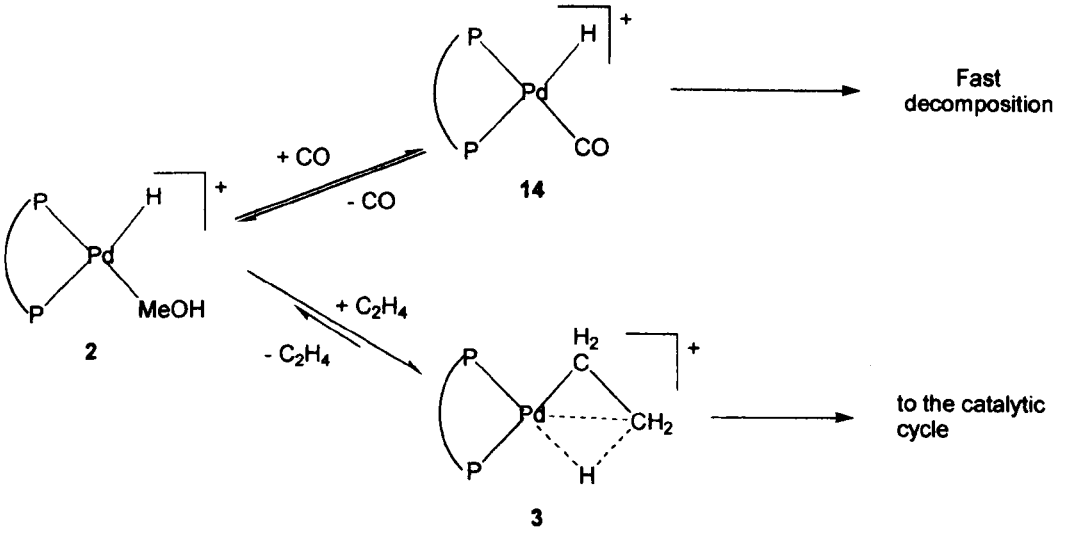

Finally, the reaction of $[Pd(d^tbpx)(\eta^2\text{-}MeSO_3)]^+$, **15**, with CO and mixtures CO/ethene has been studied. The only products observed by reacting **15** with CO are Pd-metal and $[d^tbpxH_2]^{2+}$; however, decomposition is slower than in the case of **2**. Decomposition has been observed also using a 1:1 mixture of CO/ethene; however, MeP is clearly formed in these conditions, too.

5.4 Synthesis and characterisation of new Pd(0)-carbonyl complexes

One of the major problems associated with all Pd-catalysed homogeneous catalytic processes is the formation of Pd-metal.[18-20] In particular, in the presence of CO it has been suggested that one possible step in the metal deposition is the reduction of a Pd(II)-complex to a Pd(0)-carbonyl complex, which then loses CO to give Pd-metal.[21,22] Hence, the attempted spectroscopic characterisation of Pd(0)-complexes containing CO and d^{t}bpx seemed to be a useful goal and ideally suited for an *in-situ* spectroscopic study of the Pd-catalysed reactions between CO and ethene. In order to do that, the reaction between **1** and CO has been studied. Two different compounds can be obtained. The first compound is obtained on bubbling CO for a few minutes through a THF solution of **1**; on addition of more CO, a second compound is gradually formed. The most relevant spectroscopic data for both these compounds are reported in Table 5.3. On the basis of the chemical and spectroscopic data, these two complexes can be formulated ad Pd(d^{t}bpx)(CO), **16** (trigonal planar, as for similar tri co-ordinated Pd(0) and Pt(0) complexes reported in literature [23]), and Pd(d^{t}bpx)(CO)$_2$, **17** (tetrahedral, as in the case of similar Ni(0), Pd(0) and Pt(0) complexes [23]). Their formation is well explained in eqs. 5.3 and 5.4:

$$\underset{\mathbf{1}}{Pd(d^tbpx)(dba)} + CO \rightleftharpoons \underset{\mathbf{16}}{Pd(d^tbpx)(CO)} + dba \qquad (5.3)$$

$$\underset{\mathbf{16}}{Pd(d^tbpx)(CO)} + CO \rightleftharpoons \underset{\mathbf{17}}{Pd(d^tbpx)(CO)_2} \qquad (5.4)$$

Table 5.3

*Spectroscopic data for Pd(d^{t}bpx)(CO)$_x$ (x = 1, **16**; 2, **17**) in THF*

	Pd(d^{t}bpx)(CO) 16	**Pd(d^{t}bpx)(CO)$_2$ 17**
ν(CO) (cm^{-1}) [a]	1948s	2019ms, 1998s
δP (ppm) [b]	45.5 (s)	51.1 (s)
δP (ppm) [c]	45.5 (d, $^2J_{PC}$ = 24.5 Hz)	51.1 (s)
δC (ppm) [c]	211 (t, $^2J_{PC}$ = 24.5 Hz)	197.9 (s) 198.8 (s)

[a] at 298 K. [b] at 173 K. [c] at 173 K using ^{13}CO

In agreement with this formulation, the IR and ^{13}C NMR spectra show the presence of the free dba ligand. Moreover, the first species should have one IR band, the second two bands (the symmetric and the asymmetric stretching vibrations) in the carbonyl region, as found in the observed spectra. Also, the observed frequencies of the bands agree with this formulation. In fact, **17** would be expected to have a higher value of ν(CO) than **16** because of the presence of two π-acid CO ligands.

The NMR data of **16** are in perfect agreement with its formulation as a trigonal planar complex. In the carbon spectrum, the CO-resonance is a triplet because of the equivalence of the two P-atoms, which is also consistent with the ^{31}P spectrum.

However, the NMR data of **17** are not so straightforward. All the spectra are well resolved only at 173 K. In these conditions, no P-C coupling has been observed in the ^{13}C and ^{31}P NMR spectra, even on using ^{13}C-enriched CO. This same behaviour had been observed in the past for analogous Ni(PR$_3$)$_2$(CO)$_2$ complexes,[24]

and it is assumed that the P-C coupling constants for a tetrahedral complex are very small. The other interesting point is that the two CO ligands in **17** appear to be inequivalent in the ^{13}C spectrum at 173 K. This depends on the fact that the two faces of the PdP_2 plane are inequivalent because of the conformation of the phosphine backbone (see Scheme 5.11).

Scheme 5.11

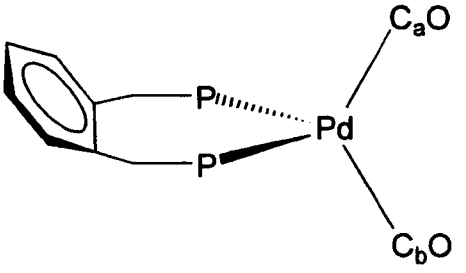

17

On increasing the temperature to 193 K, the two singlets in the ^{13}C spectrum become a broad signal at 198.5 ppm, showing that at this temperature the rate at which the two CO ligands exchange is similar to the NMR time-scale. The compounds $Pd(d^ippe)(CO)_2$ and $Pd(d^tbpe)(CO)_2$ have been reported in literature;[25] their IR and NMR data are reported in Table 5.4. Both these compounds show just one resonance in the ^{13}C spectrum; this is due to the fact that the phosphine backbone is symmetric respect to the PdP_2 plane and, therefore, the two CO ligands are equivalent. Moreover, the carbonyl resonance in both cases is a triplet with $^2J(P\text{-}C) \approx$ 4 Hz.

Finally, at room temperature intermolecular CO exchange between **16** and **17** occurs since there is only one resonance in the ^{31}P spectrum and the carbonyl region of the ^{13}C spectrum consists of a broad band at *ca.* 200 ppm.

Table 5.4

Spectroscopic data for $Pd(d^{i}ppe)(CO)_2$ and $Pd(d^{t}bpe)(CO)_2$[25]

	$Pd(d^{i}ppe)(CO)_2$	$Pd(d^{t}bpe)(CO)_2$
ν(CO) (cm^{-1})	2016, 1978	2012, 1969
δP (ppm)	59.5 (s)	81.2 (s)
δC (ppm)	199.0 (t, $^2J_{PC}$ = 4 Hz)	198.7 (t, $^2J_{PC}$ = 4.4 Hz)

5.5 Conclusions

It has been shown in this Chapter that $[Pd(d^{t}bpx)(CH_2CH_3)]^+$, **3**, reacts in MeOH with CO to give $[Pd(d^{t}bpx)H(MeOH)]^+$, **2**, and MeP. Moreover, when the same reaction is carried out in THF, it has been possible to isolate the acyl complex $[Pd(d^{t}bpx)(COEt)(THF)]^+$, **5**; addition of MeOH results again in the formation of **2** and MeP. In this way, all the complexes involved in the hydride catalytic cycle (see Chapter 1) have been identified and characterised as well as their chemical links. Moreover, it has been shown that $[Pd(d^{t}bpx)(\eta^2\text{-}MeSO_3)]^+$, **15**, is able to convert in MeOH a mixture of CO/ethene into MeP. Thus, even though **15** is not the catalytic active species, it can convert (at least partially) into it, allowing catalysis to take place. At the same time, **15** is more stable in the presence of CO than all the other complexes studied. Thus, it could act as a catalyst reservoir, and this would explain

why the catalytic system based on $MeSO_3H$ is more active than the one based on TfOH.

Decomposition remains one of the main problems with this catalytic process. The results described in this Chapter clearly indicate that decomposition is accelerated on increasing the concentration of CO. In these conditions, decomposition probably commences by CO co-ordination to the metal, either onto **2** or **5**. Both these two reactions are in competition with reactions which allow the continuation of the catalytic cycle.

5 has been fully characterised in solution. As far as we know, this is the first case in which a Pd-acyl complex containing a diphosphine and a labile solvent-molecule has been unambiguously identified. Other authors have reported similar complexes but with a strongly bound CO molecule instead of the solvent.[14,17] Whereas, **5** seems to prefer solvent co-ordination rather than CO co-ordination even in the presence of free CO; however, when CO co-ordination occurs, this results in a rapid decomposition of the complex.

It is reported in literature that the use of electron-rich diphosphine ligands results in the easy formation of Pd-dimers.[17] Examples include d^{i}ppe, d^{i}ppp, d^{i}ppb and d^{t}bpe,[17,25,26] which are closely related to d^{t}bpx and d^{t}bpp. However, dimer formation has never been observed with d^{t}bpx, even in conditions similar to the ones reported in literature for the dimerisation of the other phosphine complexes. Hence, steric factors should be very important in rationalising the chemistry of these ligands and their complexes. This point will be further discussed in the next Chapter.

References for Chapter Five

1. C. Elschenbroich and A. Salzer, *Organometallics- A Concise Introduction*, second edition, VCH, Weinheim, 1992
2. P. M. Maitlis, *The Organic Chemistry of Palladium*, Academic Press, New York, 1971
3. S. Kacker, J. S. Kim and A. Sen, *Angew. Chem. Int. Ed.*, **1988**, *37*, 1251
4. J. S. Brumbaugh, R. R. Whittle, M. A. Parvez and A. Sen, *Organometallics*, **1990**, **9**, 1735; S. Kacker and A. Sen, *J. Am. Chem. Soc.*, **1995**, *117*, 10591
5. R. Bardi, A. M. Piazzesi, A. del Pra, G. Cavinato and L. Toniolo, *Inorg. Chimica Acta*, **1985**, *102*, 99
6. R. Bardi, A. del Pra, A. M. Piazzesi and L. Toniolo, *Inorg. Chimica Acta*, **1979**, *35*, L345
7. K. Noack and F. Calderazzo, *J. Organomet. Chem.*, **1967**, *10*, 101
8. F. Ozawa and A. Yamamoto, *Chem. Lett.*, **1981**, 289
9. G. K. Anderson and R. J. Cross, *Acc. Chem. Res.*, **1984**, *17*, 67
10. J. P. Collman, L. S. Hegedus, J. R. Norton and R. G. Finke, *Principles and Applications of Organotransitions Metal Chemistry*, University Science Books, Mill Valley, CA, 1987, pp. 356-376
11. H. Berke and R. Hoffmann, *J. Am. Chem. Soc.*, **1978**, *100*, 7224
12. N. Koga and K. Morokuma, *Chem. Rev.*, **1991**, *91*, 823
13. P. E. Garrou and R. F. Heck, *J. Am. Chem. Soc.*, **1976**, *98*, 4115
14. I. Toth and C. J. Elsevier, *J. Am. Chem. Soc.*, **1993**, *115*, 10388
15. G. P. C. M. Dekker, C. J. Elsevier, K. Vrieze and P. W. N. M. van Leeuwen, *Organometallics*, **1992**, *11*, 1598

16. G. R. Eastham, Ph.D. Thesis, University of Durham, 1998

17. M. D. Fryzuk, G. K. B. Clentsmith and S. J. Rettig, *J. Chem. Soc., Dalton Trans.*, **1998**, 2007

18. A. Schoenberg and R. F. Heck, *J. Am. Chem. Soc.*, **1974**, *96*, 7761

19. F. Rivetti and U. Romano, *J. Organomet. Chem.*, **1978**, *154*, 323

20. F. Rivetti and U. Romano, *J. Organomet. Chem.*, **1979**, *174*, 221

21. A. Vavasori and L. Toniolo, *J. Mol. Cat. A*, **1996**, *110*, 13

22. E. Drent and P. H. M. Budzelaar, *Chem. Rev.*, **1996**, *96*, 663

23. P. M. Maitlis, P. E. Espinet and M. J. H. Russell, *Comprehensive Organometallic Chemistry*, ed. G. Wilkinson, Pergamon Press, 1982, vol.6

24. G. M. Badner, *Inorg. Chem.*, **1975**, *14*, 1932

25. R. Trebbe, R. Goddard, A. Rufinska, K. Seevogel and K. R. Porschke, *Organometallics*, **1999**, *18*, 2466

26. M. Portnoy and D. Milstein, *Organometallics*, **1993**, *12*, 1655

Chapter Six

Numbering scheme for Chapter 6

Pd(d^{t}bpx)(dba)	**1**
Pd(d^{t}ppx)(dba)	**1a**
Pd(^{t}b^{t}ppx)(dba)	**1b**
Pd(d^{t}bpp)(dba)	**1c**
Pd(dapx)(dba)	**1d**
Pd(dapp)(dba)	**1e**
Pd(dcpx)(dba)	**1f**
Pd(P-P)(dba)	P-P = dppp, **1g**; d^{i}ppx, **1h**
Pd(P-P)(dba)	P-P = dppx, **1i**; ^{t}bcpx, **1j**
[Pd(d^{t}bpx)H(MeOH)]$^+$	**2**
[Pd(d^{t}ppx)H(MeOH)]$^+$	**2a**
[Pd(^{t}b^{t}ppx)H(MeOH)]$^+$	**2b**
[Pd(d^{t}bpp)H(MeOH)]$^+$	**2c**
[Pd(dapx)H(MeOH)]$^+$	**2d**
[Pd(dapp)H(MeOH)]$^+$	**2e**
[Pd(d^{t}bpx)(CH_2CH_3)]$^+$	**3**
[Pd(d^{t}ppx)(CH_2CH_3)]$^+$	**3a**
[Pd(^{t}b^{t}ppx)(CH_2CH_3)]$^+$	**3b**
[Pd(d^{t}bpp)(CH_2CH_3)]$^+$	**3c**
[Pd(dapx)(CH_2CH_3)]$^+$	**3d**
[Pd(dapp)(CH_2CH_3)]$^+$	**3e**
[Pd(d^{t}bpx)(COEt)(solv)]$^+$	**4**
[Pd(d^{t}bpx)(η^2-$MeSO_3$)]$^+$	**5**
[Pd(P-P)$(CH_3CN)_2$]$^{2+}$	P-P = d^{t}bpx, **6**; dppx, **6a**
[Pd(dcpx)$(H_2O)_2$][$MeSO_3$]$_2$[$MeSO_3H$]	**7**
[Pd(dcpx)$(H_2O)_2$]$^{2+}$	**8**
Pd(d^{i}ppx)(η^1-$MeSO_3$)$_2$	**9**
[Pd(P-P)(dbaH)]$^+$	P-P = d^{t}bpx, **10**; dcpx, **10a**; dppx, **10b**
[Pd(dcpx)(dbaH)][$MeSO_3$][$MeSO_3H$][THF]$_2$	**11**
[Pd(^{t}bcpx)$(H_2O)_2$][TfO]$_2$	**12**
[Pd(^{t}bcpx)$(H_2O)_2$]$^{2+}$	**13**

The effect of the P-P ligand

6.1 Introduction

It has been shown in the previous Chapters that the methoxycarbonylation of ethene promoted by the catalyst based on Pd(d^{t}bpx)(dba), **1**, proceeds through a hydride cycle. All the most relevant intermediates (*i.e.* [Pd(d^{t}bpx)H(MeOH)]$^+$, **2**, [Pd(d^{t}bpx)(CH_2CH_3)]$^+$, **3**, and [Pd(d^{t}bpx)(COEt)(solv)]$^+$, **4**) have been synthesised and characterised in solution *via* variable temperature multinuclear NMR spectroscopy. In this way, the mechanism of the process seems to be understood, at least in its fundamental aspects. This Chapter deals with another basic problem of the process, *i.e.* the reasons for the very particular selectivity. As reported in Chapter 1, diphosphines usually result in the formation of polyketones and not MeP. There are only a few other complexes containing diphosphines which are good catalysts for the synthesis of MeP (see Section 1.5), and the catalyst based on d^{t}bpx is the best in terms of both selectivity and activity.

It has been pointed out several times in the last Chapters that d^{t}bpx is able to stabilise different palladium-species which are usually reported to be unstable. This particular behaviour had been previously outlined also by other authors. For instance, Moulton and Shaw [1] using this phosphine have been able to synthesise and characterise the first example of a *cis*-dihydride Pt(II)-complex, *i.e.* *cis*-Pt(d^{t}bpx)$(H)_2$. More recently, Spencer [2-6] has investigated the possibility of using d^{t}bpx and related ligands (*i.e.* dcpe, d^{t}bpe, dcpp, d^{t}bpp) in order to stabilise alkyl

compounds of metals of the platinum group containing an agostic interaction. All the ligands reported by Spencer result in the formation of these particular complexes. However, their stability and behaviour in solution is further affected by the nature of the ligand used. For instance, $Pt(COD)Et_2$ reacts with dcpe, d^{t}bpe, dcpp and d^{t}bpp resulting in the formation of $Pt(P\text{-}P)Et_2$, whereas the reaction with d^{t}bpx results in the formation of $Pt(d^tbpx)(C_2H_4)$.[6] These results have been rationalised by Spencer on the basis of the fact that d^{t}bpx is the bulkiest ligand and also the one with the most rigid backbone.

In order to shed further light on the reasons for the selectivity of this catalytic process, other diphosphine ligands will be considered in this Chapter (see Scheme 6.1 for the full list). All these ligands have been evaluated as their Pd(P-P)(dba) (P-P = d^{t}bpx, **1**; d^{t}ppx, **1a**; ^{t}b^{t}ppx, **1b**; d^{t}bpp, **1c**; dapx, **1d**; dapp, **1e**; dcpx, **1f**; dppp, **1g**; d^{i}ppx, **1h**; dppx, **1i**; ^{t}bcpx, **1j**) complexes in the reaction with BQ and TfOH. In some cases, this reaction results, as in the case of d^{t}bpx, in the formation of a hydride complex (see Section 6.2), in other cases they do not; only the case of ^{t}bcpx is not very clear (see Section 6.4.2). In the cases in which the hydride is formed, also the reactivity under ethene has been considered. Finally, these results will be compared with the performances in the catalysis of these complexes in Section 6.5

Scheme 6.1

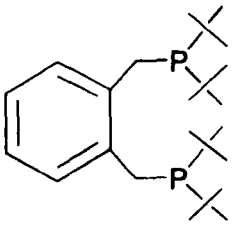

d^{t}bpx

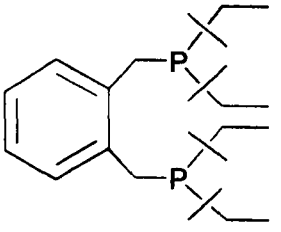

d^{t}ppx

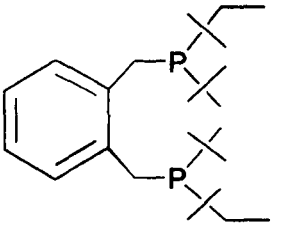

^{t}b^{t}ppx

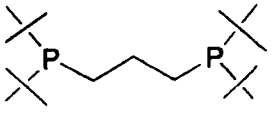

d^{t}bpp

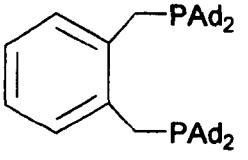

dapx

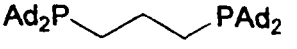

dapp

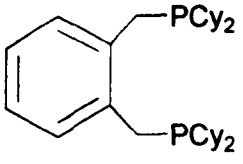

dcpx

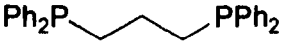

dppp

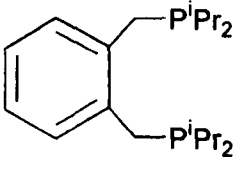

d^{i}ppx

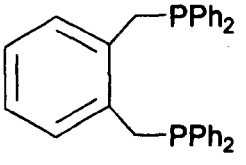

dppx

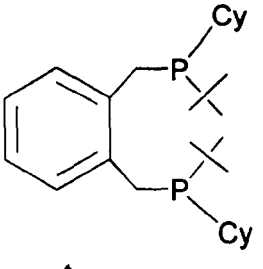

^{t}bcpx

6.2 The effect of the P-P ligand on the formation and stability of [Pd(P-P)H(solv)]$^+$

The reaction of Pd(P-P)(dba) (P-P = d^{t}ppx, **1a**; ^{t}b^{t}ppx, **1b**; d^{t}bpp, **1c**; dapp, **1d**; dapx, **1e**) with BQ and TfOH in MeOH results in the formation of the hydride [Pd(P-P)H(MeOH)]$^+$ (P-P = d^{t}ppx, **2a**; ^{t}b^{t}ppx, **2b**; d^{t}bpp, **2c**; dapx, **2d**; dapp, **2e**), as in the case of the analogous reaction of Pd(d^{t}bpx)(dba), **1**, which results in the formation of [Pd(d^{t}bpx)H(MeOH)]$^+$, **2**. Whereas, in the case of all the other ligands considered (*i.e.* dppp, dppx, dcpx, d^{i}ppx) no hydride has been observed; the case of ^{t}bcpx is not very clear, and it will be discussed in Section 6.4.2. The NMR data for all the hydride complexes are reported in Table 6.1.

Table 6.1

NMR data for [Pd(P-P)H(MeOH)]$^+$ in MeOH at 293 K

	δP_A (ppm)	δP_B (ppm)	δH (ppm)	$^2J(P_A\text{-}P_B)$ (Hz)	$^2J(P_A\text{-}H)$ (Hz)	$^2J(P_B\text{-}H)$ (Hz)
d^{t}bpx 2	23.9	75.7	-10.0	16.0	181	22.0
d^{t}ppx 2a	29.9	82.4	-10.3	16.0	179	23.0
^{t}b^{t}ppx 2b	26.9	78.8	-10 [a]	16.3	183	- [a]
d^{t}bpp 2c	22.8	74.5	-8.9	22.9	193	21.8
dapx 2d	15.8	72.5	-10.0	16.8	178	23.0
dapp 2e	17.1	74.1	-9.6	23.4	189	22.6

[a] ^{1}H data not very good, because this species is not very stable

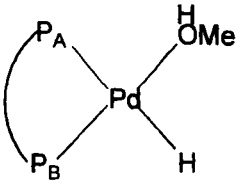

The $^{31}P\{^{1}H\}$ NMR spectrum always shows two doublets due to the presence of two *cis*-inequivalent P-atoms; moreover, the resonance at higher field is always strongly coupled to the *trans*-hydride ligand in the ^{31}P spectrum. The hydride in the proton spectra resonates in all cases at *ca.* –10 ppm, apart from the case of **2c**, which gives a doublet of doublets at –8.9 ppm. Moreover, all the spectra are always very well resolved at room temperature. In the case of **2b**, because of its instability, it has not been possible to obtain a good quality ^{1}H spectrum.

The formation rates of the hydrides **2a-e** are quite different. In the case of d^{t}bpx, d^{t}ppx, ^{t}b^{t}ppx and dapx, the hydride complexes **2**, **2a**, **2b** and **2d** are formed in a few minutes after mixing all the reagents, whereas, the complete formation of **2c** requires *ca.* 1 hour, and the formation of **2e** is complete only after a few days.

Also, the stability of $[Pd(P\text{-}P)H(MeOH)]^{+}$ depends strongly on P-P. The stability of these hydride complexes must be considered from two different points of view, *i.e.* (i) stability towards metallation and (ii) stability towards formation of Pd-metal and $[HP\text{-}PH]^{2+}$. It has been shown in Section 2.4.1 that complete metallation of **2** occurs only after addition of 50 equivalents of BQ; moreover, no metallation has been observed using O_2 as oxidant. No metallation has been observed in the case of **2c**, and only traces of a possible metallation product have been detected in the case of **2e**. Metallation, in the case of **2**, occurs on the benzene ring of d^{t}bpx, as shown in Chapter 2. Thus, the lack of metallation in the case of **2c** and **2e** can be due to the fact that the xylyl backbone has been replaced with a propane backbone. The metallation process is, instead, quite easy in the case of **2a**, and even easier in the case of **2b**. In both cases, it is enough to have a slight excess of BQ in order to have complete metallation and, for **2b**, metallation also occurs using O_2 instead of BQ. Also in the case of **2d**, metallation can occur using O_2 instead of BQ, but the process

is more difficult than in the previous cases. The NMR data for all the metallated phosphines are reported in Table 6.2. It is interesting to note that in the case of **2d** two different metallated products are formed, even though in different amounts. This can be explained by assuming that, in this case, metallation can occur either in the benzene ring (main product) or on one of the adamantyl substituents (minor product); this hypothesis agrees also with the fact that partial metallation has been observed in the case of **2e** but not with **2c**.

Table 6.2

MNR data for the metallated phosphine complexes in MeOH at 293 K

	δP (ppm)	δP' (ppm)	^{1}J(P-H)
d^{t}bpx	42.4	105.6	460
d^{t}ppx	38.0	110.0	488
^{t}b^{t}ppx	29.8	108.3	432
dapp	35.3	92.9	480
dapx	35.5	100.4 (Mayor) 98.7 (minor)	454

Decomposition of **2** to give Pd-metal occurs, at room temperature, in a few days. A similar behaviour has been observed for **2c** and **2e**. Whereas decomposition of **2d** is a little bit faster, **2d** is still stable in solution for more than one day at room temperature. Complete decomposition occurs in a few hours in the case of **2a** and **2b**. The high instability of **2a-b** makes it very difficult to reproduce their syntheses. The relative stability of all these hydrides is summarised in Scheme 6.2.

Scheme 6.2

a) Relative stability of the complexes [Pd(P-P)H(MeOH)]$^+$ towards formation of Pd-metal

$d^tbpx \approx d^tbpp \approx dapp > dapx >>> d^tppx >> {}^tb^tppx$

2 2c 2e 2d 2a 2b

b) Relative stability of the complexes [Pd(P-P)H(MeOH)]$^+$ towards metallation of the phosphine

$d^tbpp > dapp > d^tbpx >>> dapx >> d^tppx >> {}^tb^tppx$

2c 2e 2 2d 2a 2b

c) Relative rate of formation of [Pd(P-P)H(MeOH)]$^+$

$d^tbpx \approx dapx \approx d^tppx \approx {}^tb^tppx >> d^tbpp >>> dapp$

2 2d 2a 2b 2c 2e

6.3 The effect of the P-P ligand on the formation and stability of [Pd(P-P)(CH_2CH_3)]$^+$

In Chapter 4, it was shown that **2** reacts with ethene to give **3**. The complete conversion of the hydride into the ethyl complex needs only one mole of ethene per mole of hydride. Hence, the same reaction has been repeated with all the phosphine

ligands reported in Scheme 6.1, and the results obtained follow closely those outlined in Section 6.2. In fact, the formation of the ethyl complex has been observed only with the phosphines which give under nitrogen the hydride, *i.e.* d^{t}bpx, d^{t}ppx, ^{t}b^{t}ppx, d^{t}bpp, dapp and dapx. No trace of the ethyl complex has been observed with all the other ligands (*i.e.* dppp, dppx, dcpx, d^{i}ppx and ^{t}bcpx), even after bubbling ethene through the solution for 40-50 minutes.

The NMR data for all the $[Pd(P\text{-}P)(CH_2CH_3)]^+$ complexes (P-P = d^{t}bpx, **3**; d^{t}ppx, **3a**; ^{t}b^{t}ppx, **3b**; d^{t}bpp, **3c**; dapx, **3d**; dapp, **3e**) are summarised in Table 6.3. All these data have been obtained in MeOH at room temperature.

Table 6.3

NMR data for $[Pd(P\text{-}P)(CH_2CH_3)]^+$ in MeOH at 293 K

	δP_A (ppm)	δP_B (ppm)	$^2J(P_A\text{-}P_B)$ (Hz)
d^{t}bpx 3	36.3	67.7	31.0
d^{t}ppx 3a	46	78	br
^{t}b^{t}ppx 3b	43	75	br
d^{t}bpp 3c	39.3	65.3	37.0
dapx 3d	31.7	66.9	br
dapp 3e	33.8	62.7	36.4

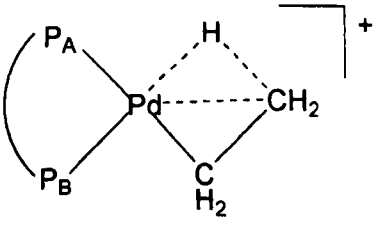

All these compounds show two well-separated resonances in the $^{31}P\{^{1}H\}$ spectrum at room temperature. The spectra of **3c** and **3e** are very well resolved in these conditions and, therefore, it is possible to resolve clearly the coupling constants. Using the same conditions, it is not possible for **3** to resolve the couplings without acquiring a lot of scans. In the case of **3a**, **3b** and **3d**, the resonances are very broad, even at low temperature, and, hence, no coupling constants have been measured. These three last compounds are also not very stable and, hence, it is very difficult to obtain better data.

3c, as found for **3**, is quite stable in THF at low temperature and, thus, it has been possible to characterise it too in THF. The spectra in MeOH and THF (see Table 6.4) look more or less the same, confirming also in this case the presence of an agostic interaction.

Table 6.4

*NMR data for $[Pd(d^tbpp)(CH_2CH_3)]^+$, **3c**, in MeOH and THF at 223 K*

	MeOH	**THF**
δP_A	37.4	37.1
δP_B	62.8	62.1
$^2J(P_A\text{-}P_B)$	35.2	36.0

The relative stability of the ethyl complexes **3a-e** closely follows the stability of the analogous hydrides **2a-e** (see Scheme 6.3). It is only interesting to note that **2d** is quite stable, whereas **3d** is not.

Scheme 6.3

Relative stability of the complexes $[Pd(P\text{-}P)(CH_2CH_3)]^+$

$d^tbpx \approx d^tbpp > dapp >> dapx >>> d^tppx >> {}^tb^tppx$

3 3c 3e 3d 3a 3b

6.4 Further information about the effect of the P-P ligands

The reaction of Pd(P-P)(dba) (P-P = dcpx, **1f**; dppp, **1g**; d^ippx, **1h**; dppx, **1i**) with BQ and TfOH in MeOH does not result in the formation of any hydride compound; moreover, no ethyl complex is formed after addition of ethene. All the species formed in these conditions show only one singlet in the $^{31}P\{^1H\}$ NMR spectrum at room temperature in MeOH, apart from the case of dcpx where two singlets at 45.6 (major) and 42.1 (minor) ppm are present (see Table 6.5). At 193 K, two singlets with different integrals are present in the case of dcpx and dppx, whereas three singlets (two major and one minor) are present in the case of d^ippx. The reaction of **1f** has also been studied using $MeSO_3H$ instead of TfOH in MeOH and THF (see Table 6.6). In this case, two resonances are present at 193 K in THF and four in MeOH. It is also interesting to note that in the case of the two isomers of $[Pd(d^tbpx)(\eta^2\text{-}MeSO_3)]^+$, **5**, $\Delta\delta$ was always less than 1.4 ppm. Whereas, in the case of the products of the reactions of **1f-i** with RSO_3H and BQ, $\Delta\delta$ is always bigger than 2 ppm. These data seem to rule out the possibility of formulating these products as

$[Pd(P\text{-}P)(\eta^2\text{-}MeSO_3)]^+$ (P-P = dcpx, **5f**; dppp, **5g**; d^ippx, **5h**; dppx, **5i**). Moreover, it has been shown in Chapter 3 that **5** dissolves in CH_3CN resulting in the formation of $[Pd(d^tbpx)(CH_3CN)_2]^{2+}$, **6**, and in that case $\Delta(\delta_{MeOH} - \delta_{MeCN}) = 18$ ppm. Whereas, on reacting **1i** with TfOH and BQ in CH_3CN a product showing a resonance at 22 ppm is formed; thus, $\Delta(\delta_{MeOH} - \delta_{MeCN}) = 8$ ppm in this case. If the species formed in these conditions is $[Pd(dppx)(CH_3CN)_2]^{2+}$, **6a**, it is then difficult to formulate the species present in MeOH as **5i**.

Table 6.5

^{31}P NMR data for the products of the reaction of Pd(P-P)(dba) with TfOH and BQ in MeOH

	δP (ppm) at 293 K *	**δP (ppm) at 193 K ***
dcpx	45.6 (1) 42.1 (0.1)	46.0 (1) 41.6 (0.25)
dppp	16.8	-
d^ippx	52.6	52.4 (1), 51.4 (0.2) 47.9 (1)
dppx	28.7	30.0 (20) 28.6 (1)

* Relative intensity reported in brackets when more than one resonance is present

Table 6.6

*^{31}P NMR data for the products of the reaction of Pd(dcpx)(dba), **1f**, with RSO_3H and BQ in MeOH and THF*

	δP (ppm) at 293 K *	δP (ppm) at 193 K *
TfOH in MeOH	45.6 (1) 42.1 (0.1)	46.0 (1) 41.6 (0.25)
$MeSO_3H$ in MeOH	44.2	45.7 (0.9), 44.9 (8.3) 42.0 (0.2), 41.1 (7.4)
$MeSO_3H$ in THF	41.3	42.6 (0.9) 40.6 (1.1)

* Relative intensity reported in brackets when more than one resonance is present

These systems have not been studied extensively, and it is therefore difficult to understand the nature of the species formed. Diffusion of n-hexane into a THF solution containing **1f**, $MeSO_3H$ and BQ resulted in the isolation of yellow crystals of a new species which was found to be $[Pd(dcpx)(H_2O)_2][MeSO_3]_2[MeSO_3H]$, **7**, after X-ray analysis (see Figure 6.1 for the structure and Table 6.7 for the main bond distances and angles). An extended network of hydrogen bonds between the two anions, the free acid molecule and the two molecules of water co-ordinated to the metal is present in the solid state. One of the cyclohexyl substituents of the dcpx ligand is partially disordered, but the structure refinement is quite good (R_1 = 0.0777). This salt contains the cation $[Pd(dcpx)(H_2O)_2]^{2+}$, **8**.

Figure 6.1

*Crystal structure of $[Pd(dcpx)(H_2O)_2]^{2+}$, **8**. Different views*

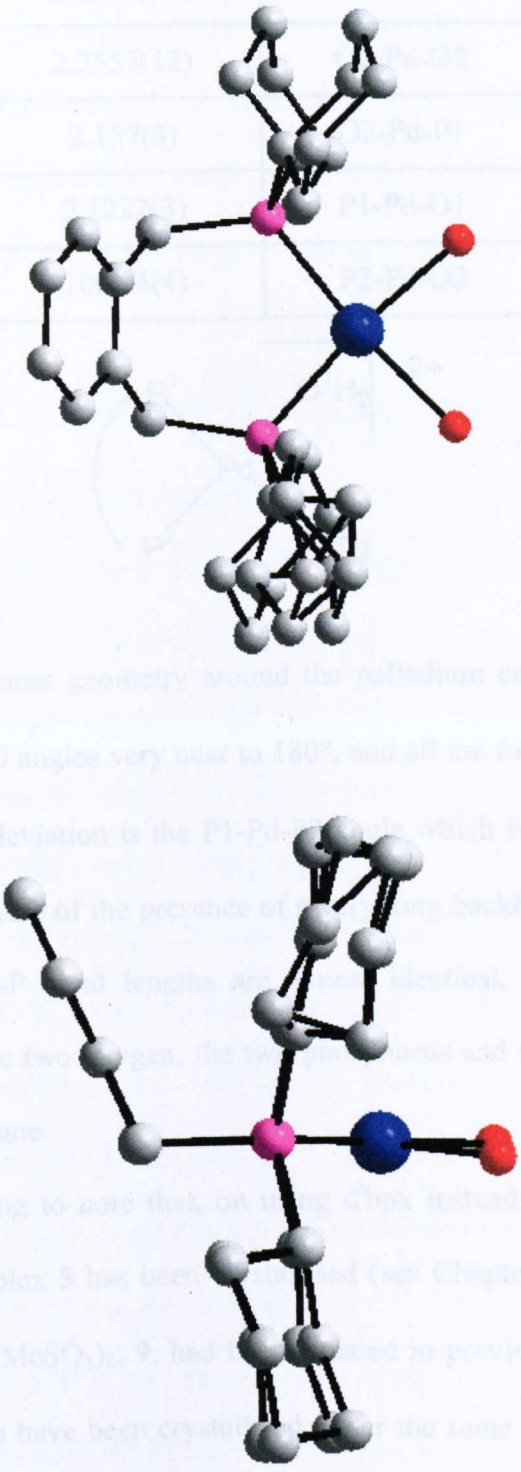

Table 6.7

Main bond distances (Å) and angles (deg) for $[Pd(dcpx)(H_2O)_2]^{2+}$, **8**

Pd-P1	2.2556(11)	P2-Pd-O1	172.42(11)
Pd-P2	2.2557(12)	O1-Pd-O2	87.31(4)
Pd-O1	2.137(3)	O2-Pd-P1	173.66(11)
Pd-O2	2.1222(3)	P1-Pd-O1	86.46(10)
P1-Pd-P2	100.24(4)	P2-Pd-O2	86.05(11)

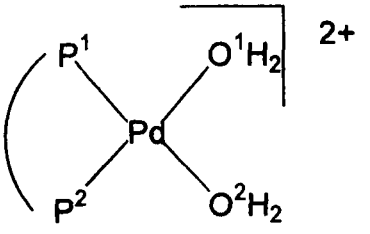

The square-planar geometry around the palladium centre is almost perfect, with the *trans* P-Pd-O angles very near to 180°, and all the four *cis* angles quite near to 90°. The biggest deviation is the P1-Pd-P2 angle which is *ca.* 100°, but this can easily explained because of the presence of a very long backbone in the diphosphine ligand. The two Pd-P bond lengths are almost identical, as also the two Pd-O distances. Finally, the two oxygen, the two phosphorus and the palladium atoms lie nearly in the same plane.

It is interesting to note that, on using d^{t}bpx instead of dcpx, under similar conditions, the complex **5** has been crystallised (see Chapter 3), whereas, on using d^{i}ppx, Pd(d^{i}ppx)(η^1-$MeSO_3$)$_2$, **9**, had been isolated in previous work.[7] The fact that the three compounds have been crystallised under the same conditions and found to result in the formation of different complexes, suggests that the nature of the diphosphine ligand plays a very important role in the chemistry of this class of

palladium complexes. Moreover, the differences do not seem to arise (in these cases) from the bite angle of the diphosphine ligand; in fact, in all three the cases, the P1-Pd-P2 angles are nearly the same [*i.e.* 100.24(4) for **8**; 100.58(7) for **7**; 99,17(3) for **9**]. Hence, the different behaviour of the three o-xylyl based ligands is probably due to the different steric properties of the tert-butyl groups compared to cyclohexyl and *iso*propyl. So, it seems that a very small change in the nature of the ligand is enough to change the behaviour of the resulting compounds.

*6.4.1 The crystal structure of [Pd(dcpx)(dbaH)]$^+$, **10a***

Reaction of **1f** and **1i** in MeOH with $MeSO_3H$ or TfOH in the absence of oxidants results in the formation of $[Pd(P\text{-}P)(dbaH)]^+$ (P-P = dcpx, **10a**; dppx, **10b**) as in the case of **1** which gives $[Pd(d^tbpx)(dbaH)]^+$, **10**. Also in this case, the NMR spectra do not depend on the acid used (see Table 6.8). In the case of **10b**, two conformers are present in solution, as in the case of **10**. However, the exchange process for **10b** is already slow at room temperature; thus, four sharp resonances are present. Whereas, in the case of **10a** the $^{31}P\{^1H\}$ spectrum at room temperature is broad, and only at 193 K does it become well resolved. Moreover, in this case three main species are present in solution. This is probably due to the fact that the substitution of the tert-butyl and phenyl groups of **10** and **10b**, with cyclohexyl groups in **10a** introduces more conformational possibilities into the complex.

Crystals of **10a** as the salt $[Pd(dcpx)(dbaH)][MeSO_3][MeSO_3H][THF]_2$, **11**, have been grown in THF/n-hexane and then analysed by X-ray diffraction (see Figure 6.7 for the structure of the cation and Table 6.9 for the main bond distances and angles). The palladium, the two phosphorus and the two co-ordinated carbon atoms are more or less in the same plane. The phosphine bite angle is 101.04°, *i.e.*

very close to the values found during this work for other diphosphine ligands with a o-xylyl backbone . It has been also possible to locate a proton on the oxygen atom of the dba ligand. As a consequence of the protonation, the C-O bond in **10a** is longer than in **1f** [7] (1.344 Å *vs.* 1.244 Å).

Table 6.8

^{31}P NMR data for [Pd(P-P)(dbaH)][X] (X = TfO, $MeSO_3$) in MeOH [a]

X =	dppx	dcpx
TfO (293 K)	21.1 + 15.2 (J = 67.8) [b] 26.8 + 14.7 (J = 82.9) [c]	-
TfO (193 K)	21.3 + 16.8 (J = 63.7) [b] 28.8 + 13.6 (J = 80.2) [c]	21.9 + 11.7 (J = 70) [a] 28.9 + 10.7 (J = 79.1) [d] 23.4 + 7.7 (J = 71.4) [c]
$MeSO_3$ (293 K)	-	12.3 (br) 24.6 (J = 67.9) 31.0 (J = 80.0)
$MeSO_3$ (193 K)	-	21.9 + 11.7 (J = 69.4) [b] 29.0 + 10.4 (J = 79.2) [d] 23.4 + 7.7 (J = 71.4) [c]

[a] Chemical shift in ppm, J in Hz. [b] Mayor species. [c] Minor species. [d] Intermediate species

Figure 6.2

*Crystal structure of [Pd(dcpx)(dbaH)]$^+$, **10a**. Different views*

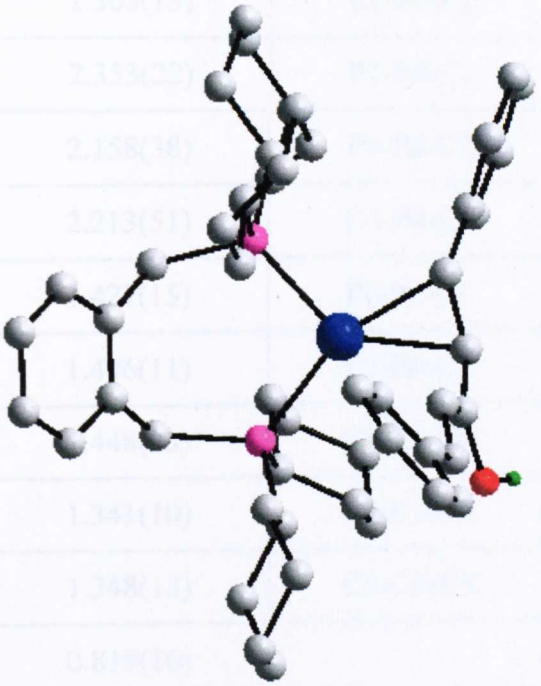

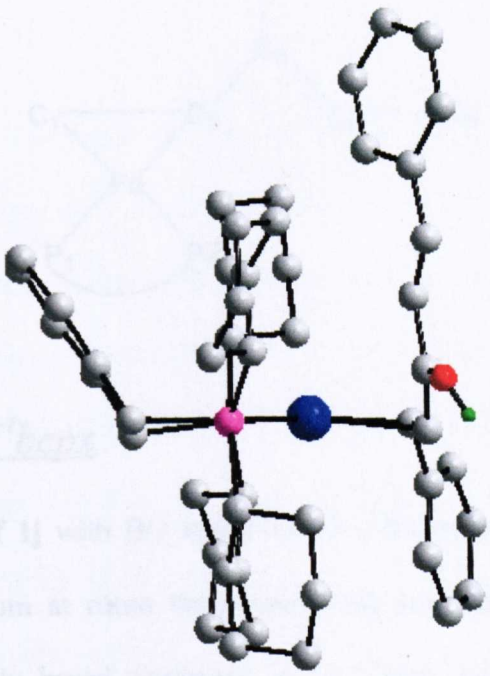

Table 6.9

*Main bond distances (Å) and angles (deg) for [Pd(dcpx)(dbaH)]$^+$, **10a***

Pd-P1	2.305(15)	P1-Pd-P2	101.04(4)
Pd-P2	2.353(22)	P1-Pd-C1	100.57(15)
Pd-C1	2.158(38)	P1-Pd-C2	138.18(15)
Pd-C2	2.213(51)	C1-Pd-C2	38.07(17)
C1-C2	1.427(15)	P2-Pd-C1	157.94(13)
C2-C3	1.406(11)	P2-Pd-C2	119.91(12)
C3-C4	1.448(23)	C1-C2-C3	123.42(55)
C4-C5	1.341(10)	C2-C3-C4	123.69)56)
C3-O	1.348(13)	C3-C4-C5	124.92(57)
O-H	0.819(16)		

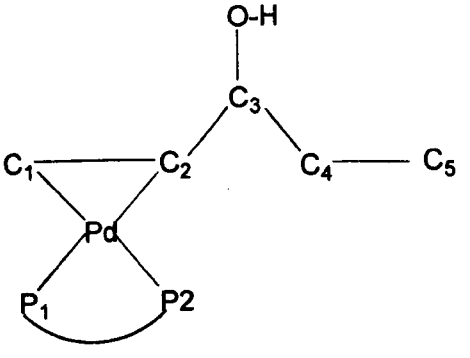

6.4.2 The case of ^{t}bcpx

The reaction of **1j** with BQ and TfOH in MeOH is quite complicated. The $^{31}P\{^1H\}$ NMR spectrum at room temperature run just after mixing the reagents shows only a relatively broad resonance at 54.7 ppm, whereas at 193 K a very complicated spectrum appears (see Figure 6.3), which is very difficult to understand.

Figure 6.3

*$^{31}P\{^{1}H\}$ NMR spectrum at 193 K in MeOH of the product of the reaction between Pd(^{t}bcpx)(dba), **1j**, TfOH and BQ*

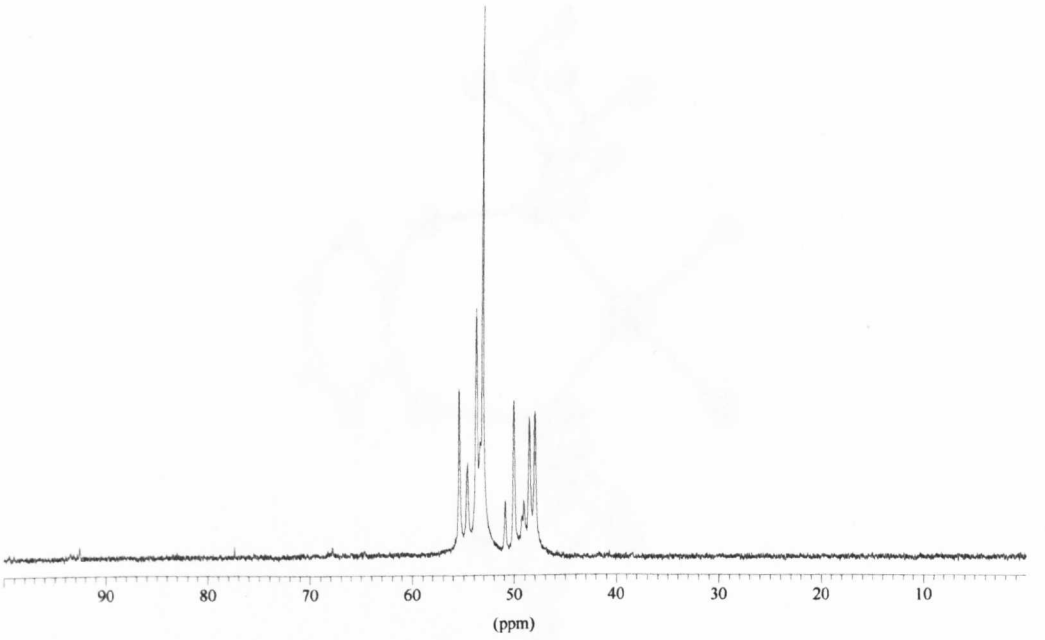

A similar behaviour has been observed also in THF. Diffusion of n-hexane in this second solvent causes the formation of yellow crystals, which were found to be $[Pd(^{t}bcpx)(H_2O)_2][TfO]_2$, **12**. One of the two anions is disordered because of the free rotation of the CF_3 group. However, this does not affect very much the refinement of the structure (R_1 = 0.0668). The cation $[Pd(^{t}bcpx)(H_2O)_2]^{2+}$, **13** (see Figure 6.4 and Table 6.10), is very similar to **8**. In fact, the palladium, the two oxygen and the two phosphorus atoms are nearly in the same plane. The fact that the bond angles around the palladium centre deviate from 90° is due to the bite angle of ^{t}bcpx (100.42°), as in the case of **8**. The two cyclohexyl groups are on the same side of the plane

determined by the palladium and the two P-atoms, as well as the benzene ring of the phosphine backbone.

Figure 6.4

*Crystal structure of $[Pd(^{t}bcpx)(H_2O)_2]^{2+}$, **13**. Different views.*

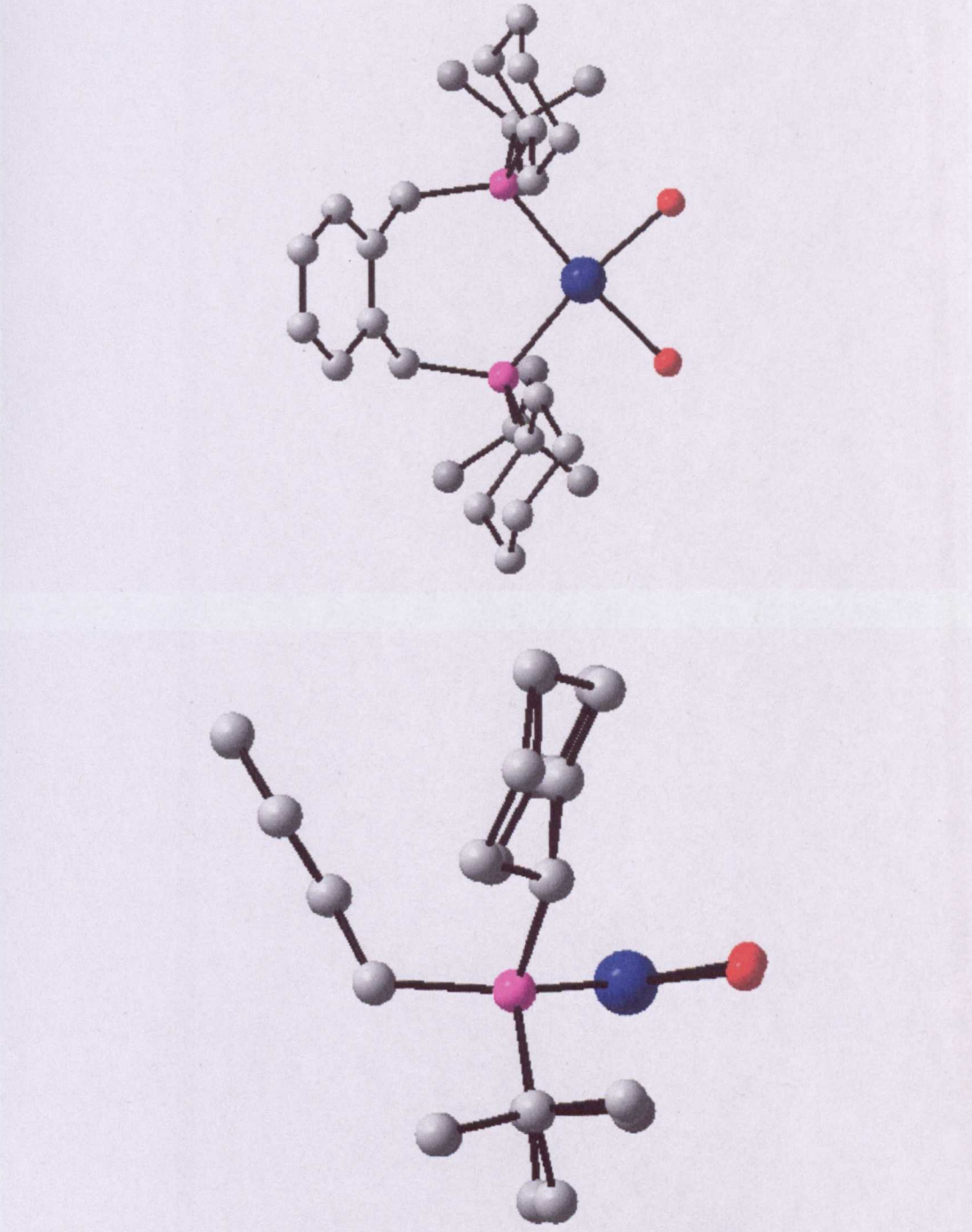

Table 6.10

Main bond distances (Å) and angles (deg) for $[Pd(^tbcpx)(H_2O)_2]^{2+}$, 13

Pd-P1	2.262(15)	P2-Pd-O1	173.24(1)
Pd-P2	2.264(1)	O1-Pd-O2	85.37(1)
Pd-O1	2.130(1)	O2-Pd-P1	170.88(1)
Pd-O2	2.140(15)	P1-Pd-O1	86.3()
P1-Pd-P2	100.42(1)	P2-Pd-O2	87.88(0)

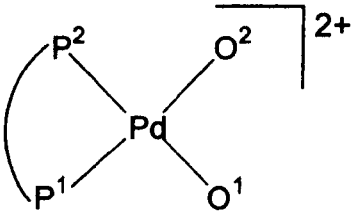

Dissolution of **12** in MeOH results in the same spectrum obtained by reacting **1j** with BQ and TfOH. The presence of the cation **13** cannot, of course, account for the spectrum at low temperature. It is probable that in solution more species are present, in part due to the stereochemistry of the diphosphine ligand, but maybe also due to the substitution of water by the solvent and/or the anion.

In all cases, this situation is not stable in MeOH; after a few days, the phosphorus spectrum changes (see Figure 6.5). Some resonances are now present at higher field, and part of them are split into doublets in the ^{31}P spectrum, with $^{2}J(P\text{-}H) \approx 180$ Hz, suggesting the formation of hydride species. However, the spectra are so complicated that it has not been possible to fully characterise the new products.

Figure 6.5

*NMR spectra at 193 K in MeOH of the product of the reaction between Pd(ᵗbcpx)(dba), **1j**, TfOH and BQ after 4 days*

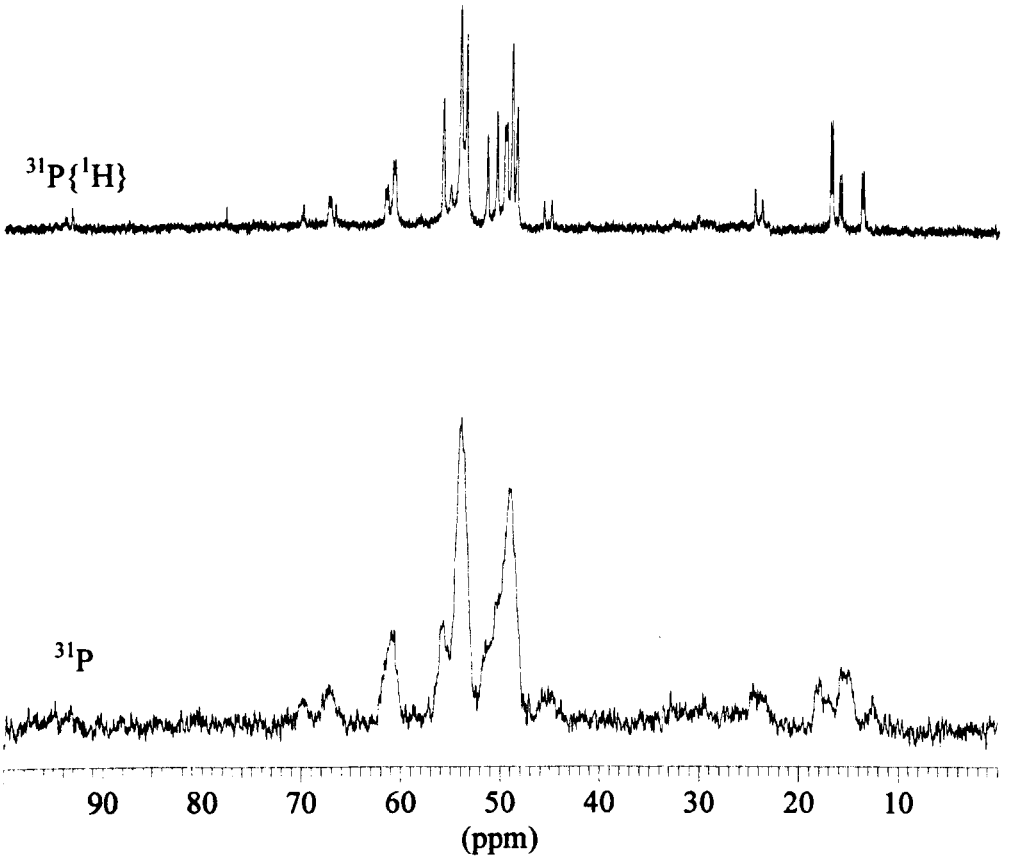

6.5 Conclusions

It has been shown in this Chapter that it is possible to divide all the phosphine complexes studied into two groups, on the basis of whether or not they form a hydride complex on reaction of the Pd(P-P)(dba) complex with BQ and TfOH in

MeOH. The first group (A) consists of all the ligands where it has been possible to characterise a hydride complex, *i.e.* d^{t}bpx, d^{t}ppx, ^{t}b^{t}ppx, d^{t}bpp, dapx and dapp; in group (B) are the ligands for which no hydride complex has been observed, *i.e.* dcpx, dppp, dppx and d^{i}ppx. The case of ^{t}bcpx remains uncertain. What is very interesting is the fact that complexes containing class A ligands always give catalysts which are selective for the synthesis of MeP, whereas using catalysts based on class B ligands, no activity or formation of polyketones has been observed.[7] Hence, it seems that the factors which control the formation of the hydride, control also the selectivity of the catalyst. The bite angle for the diphosphines considered (apart from dppp) is close to 100° (see Table 6.11) and, hence, this parameter does not appear to be the most important.

Table 6.11

Measured Bite Angles (deg) for different P-P ligands [a]

d^{t}bpx [b]	100.6	dppp [c]	94.9
d^{i}ppx [c]	104.3	^{t}bcpx [b]	100.4
dcpx [b]	100.2	d^{t}bpp [c]	98.09
dppx [c]	104.6	d^{t}ppx [c]	102.8

[a] Measured experimentally via X-ray analysis. [b] This work. [c] Ref. 7

It has been suggested in Chapter 1 that it is possible to correlate the selectivity with the parallel pocket angle.[8] This suggests that what is more important is the environment created by the groups present on the two P-atoms and, in particular, the size of the pocket in which the "reactive" ligands are situated. The

hydride and MeP are obtained only on using tert-butyl, tert-pentyl or adamantyl groups. The last two are just modifications of the first; moreover, the tert-pentyl group is more flexible than the tert-butyl, whereas the adamantyl substituent is more rigid. In all cases, the best results are obtained in the case of tert-butyl substituted ligands, which probably have the best compromise of all the required properties.

References for Chapter Six

1. J. Moulton and B. L. Shaw, *J. Chem. Soc. Chem. Commun.*, **1976**, 365
2. L. E. Crascall and J. L. Spencer, *J. Chem. Soc. Dalton Trans.*, **1992**, 3445
3. F. M. Conroy-Lewis, L. Mole, A. D. Redhouse, S. A. Lister and J. L. Spencer, *J. Chem. Soc. Chem. Commun.*, **1991**, 1601
4. N. Carr, B. Dunne, L. Mole, A. G. Orpen and J. L. Spencer, *J. Chem. Soc. Dalton Trans.*, **1991**, 863
5. L. Mole, J. L. Spencer, N. Carr and A. G. Orpen, *Organometallics*, **1991**, *10*, 49
6. N. Carr, L. Mole, A. G. Orpen and J. L. Spencer, *J. Chem. Soc. Dalton Trans.*, **1992**, 2653
7. G. R. Eastham, Ph.D. Thesis, University of Durham, 1998
8. W. Clegg, G. R. Eastham, M. R. J. Elsegood, R. P. Tooze, X. L. Wang and K. Whiston, *J. Chem. Soc. Chem. Commun.*, **1999**, 1877

Chapter Seven

Numbering scheme for Chapter 7

Pd(d^{t}bpx)(dba)	**1**
Pd(P-P)(dba)	P-P = d^{t}ppx, **1a**; ^{t}b^{t}ppx, **1b**; d^{t}bpp, **1c**; dapp, **1d**; dapx, **1e**; dcpx, **1f**; dppp, **1g**; dppx, **1h**; d^{i}ppx, **1i**; ^{t}bcpx, **1j**
[Pd(P-P)H(MeOH)]$^+$	P-P = d^{t}ppx, **2a**; ^{t}b^{t}ppx, **2b**; d^{t}bpp, **2c**; dapp, **2d**; dapx, **2e**
[Pd(d^{t}bpx)H(MeOH)]$^+$	**2**
[Pd(d^{t}bpx)(CH_2CH_3)]$^+$	**3**
[Pd(d^{t}bpx)(COEt)(solv)]$^+$	**4**
[Pd(d^{t}bpx)H(C_2H_4)]$^+$	**5**
[Pd(d^{t}bpx)H(MeOH)(C_2H_4)]$^+$	**6**
[Pd(d^{t}bpx)(CH_2CH_3)(CO)]$^+$	**7**
[Pd(d^{t}bpx)Et(CO)]$^+$	**8**
[Pt(d^{t}bpx)(CH_2CH_3)]$^+$	**9**
[Pt(d^{t}bpx)Et(CO)]$^+$	**10**
[Pt(d^{t}bpx)(COEt)(solv)]$^+$	**11**
[Pd(d^{t}bpx)(dbaH)]$^+$	**12**
[Pd(d^{t}bpx)(η^2-$MeSO_3$)]$^+$	**13a**
[Pd(d^{t}bpx)(η^2-TfO)]$^+$	**13b**
[Pd(d^{t}bpx)(η^2-TsO)]$^+$	**13c**
[Pd(d^{t}bpx)(solv)$_2$]$^{2+}$	**14**
[Pd(d^{t}bpx)(η^2-RSO_3)(solv)]$^+$	**15**
[Pd(d^{t}bpx)(η^1-$MeSO_3$)(solv)]$^+$	**16**
[Pd(d^{t}bpx)H(CO)]$^+$	**17**
[Pd(d^{t}bpx)(COEt)(CO)]$^+$	**18**

General Conclusions

7.1 The catalytic cycle

All the data presented in this Thesis support the fact that the methoxycarbonylation of ethene promoted by the catalyst based on Pd(d^{t}bpx)(dba), **1**, proceeds through a hydride cycle (see Scheme 7.1).

Scheme 7.1

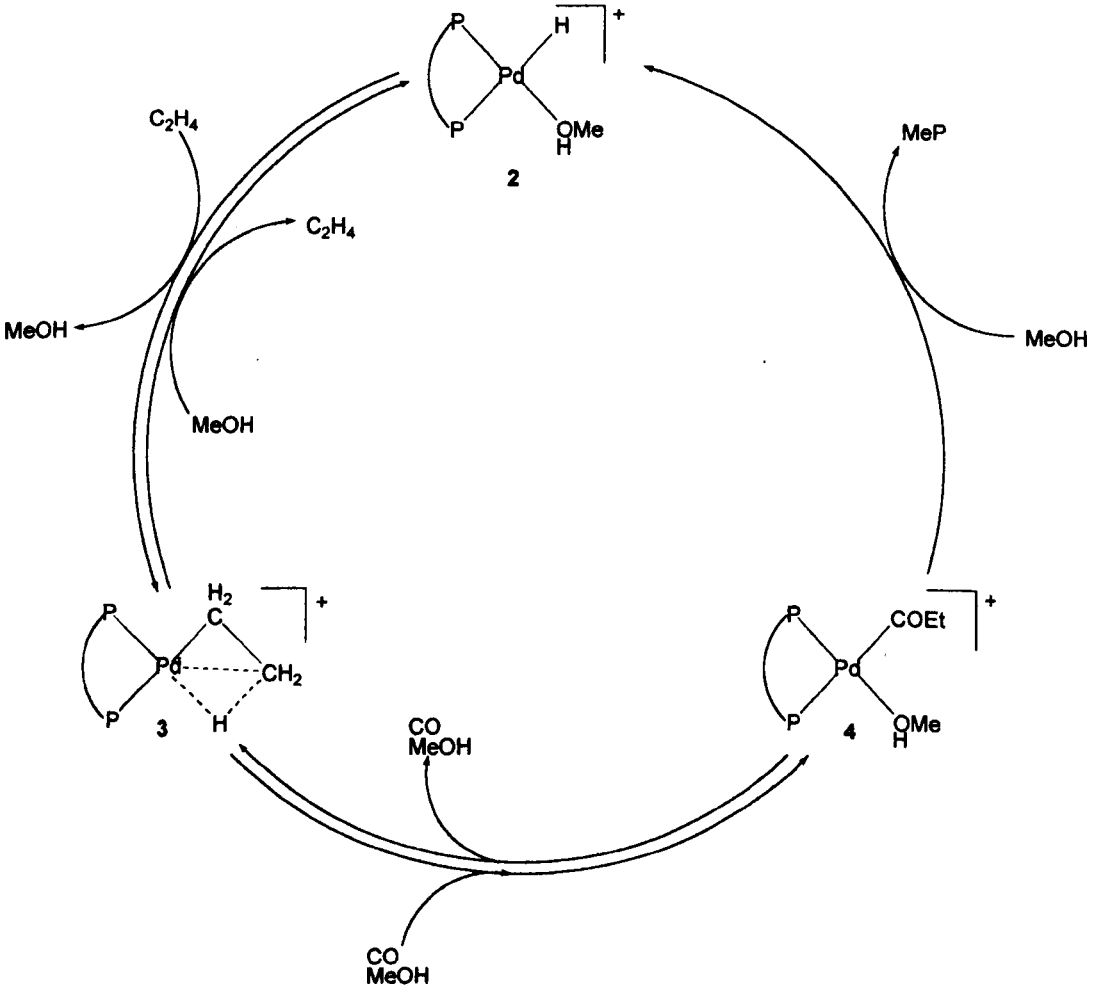

The three principle intermediates involved in this cycle, *i.e.* $[Pd(d^tbpx)H(MeOH)]^+$, **2**, $[Pd(d^tbpx)(CH_2CH_3)]^+$, **3**, and $[Pd(d^tbpx)(COEt)(solv)]^+$, **4**, have been synthesised and fully characterised in solution. Moreover, it has been shown that **2** can be formed from **1** and $MeSO_3H$ in MeOH at the same temperature at which the industrial process is operated (*i.e.* 80°C). Also, the presence in solution of **3** has been demonstrated at high temperature although, it is only possible to detect **4** at low temperature and in non-alcoholic media.

2 reacts with ethene resulting in the formation of **3** and the reaction is reversible at high temperature; CO-insertion into **3** to give **4** is a reversible reaction, too.

$$\underset{\mathbf{2}}{[Pd(d^tbpx)H(MeOH)]^+} + C_2H_4 \rightleftharpoons \underset{\mathbf{3}}{[Pd(d^tbpx)(CH_2CH_3)]^+} + MeOH \qquad (7.1)$$

$$\underset{\mathbf{3}}{[Pd(d^tbpx)(CH_2CH_3)]^+} + CO + MeOH \rightleftharpoons \underset{\mathbf{4}}{[Pd(d^tbpx)(COEt)(MeOH)]^+} \qquad (7.2)$$

Equilibrium 7.1 is always shifted towards the formation of **3**, and only at high temperature is an appreciable amount of **2** detected. Equilibrium 7.2 is also shifted towards the formation of **3** above room temperature. Thus, the concentration of **4** in the operating conditions of the process is very low. Both these insertion reactions, as well as their inverse reactions, are very fast, even at low temperature. Methanolysis of **4** is an irreversible process, and it is believed to be the rate determining step of the catalytic cycle. This hypothesis is supported by other authors who have studied the methoxycarbonylation of higher α-olefins.[1,2]

$$[Pd(d^tbpx)(COEt)(MeOH)]^+ + MeOH \longrightarrow [Pd(d^tbpx)H(MeOH)]^+ + EtCOOMe \quad (7.3)$$

4 **2**

Apart from the two equilibria 7.1 and 7.2 which involve the complexes **2**, **3** and **4**, other intra-molecular exchange processes involving **3** and **4**, but not **2**, have been detected (see Scheme 7.2). In the case of **3**, three exchange processes occur in solution, with different activation energies. The lowest energy process is the scrambling of the protons of the methyl group of the ethyl-agostic ligand, which occurs *via* the in-place mechanism described previously by Green and Wong.[3] This process results in the equivalence of all the β-protons at all the temperature studied (155-353 K). The next higher energy process is the exchange of the position of the two carbon atoms of the ethyl-agostic ligand, and involves an equilibrium between the ethyl-agostic complex and a ethene-hydride complex, $[Pd(d^tbpx)H(C_2H_4)]^+$, **5**; the coalescence temperature for this process is *ca.* 248 K, as evaluated in the $^{31}P\{^1H\}$ NMR spectrum. The last process is the inversion of the relative position of the two P-atoms, which probably occurs *via* dissociation of the agostic interaction and internal rearrangement of the complex *via* a Y-shaped tri-co-ordinate species. A similar process has been detected in the case of **4**. It is noteworthy the fact that the equivalence of the P-atoms in **3** occurs only at 353 K, whereas they are already equivalent below room temperature in the case of **4**.

On the basis of the data collected during this work, it is also possible to discuss in more detail the mechanism of the reactions 7.1-3.

Scheme 7.2

A) In-place rotation of the methyl group in **3**

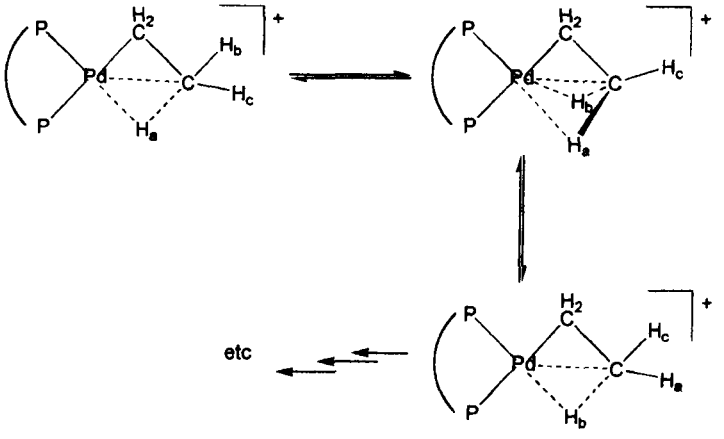

B) $^{13}C/^{12}C$ scrambling in **3**

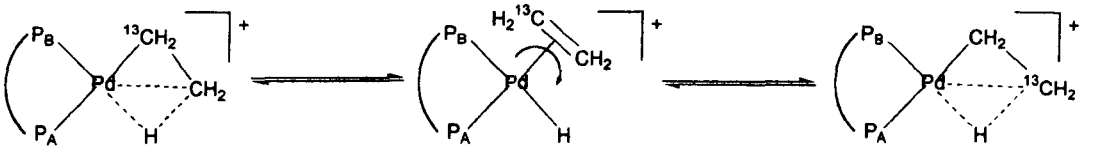

C) Exchange of the relative position of P-atoms in **3**

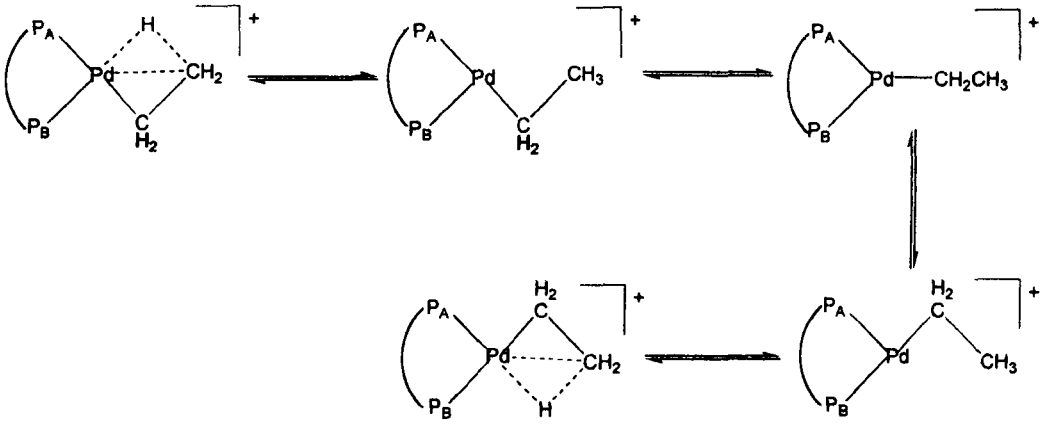

D) Solvent-exchange in **4**

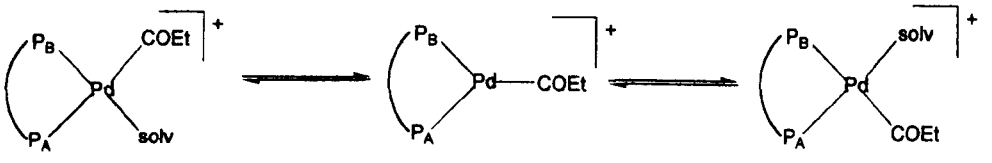

Insertion reactions in palladium square-planar complexes are usually believed to involve, first, co-ordination of CO or ethene and formation of a penta-co-ordinate species.[4] This species can have either a square-planar pyramidal structure or a trigonal bipyramidal geometry; in all cases, there is ready inter-conversion *via* pseudo-rotation. The insertion process can, then, occur directly on the five-co-ordinate species, or in a square-planar species obtained by elimination of one of the ligands (see Section 5.1).

In the case of the formation of **3**, ethene co-ordination to **2** would result in the formation of $[Pd(d^tbpx)H(MeOH)(C_2H_4)]^+$, **6**, which is probably the precursor for the substitution of MeOH with ethene, resulting in the formation of **5** (see scheme 7.3). Finally, ethene insertion into the Pd-H bond in **5** results in the formation of **3.** Neither **5** nor **6** have been directly detected; however, the study of the dynamic behaviour of **3** at different temperature has clearly indicated the presence of an equilibrium between **3** and **5**.

Scheme 7.3

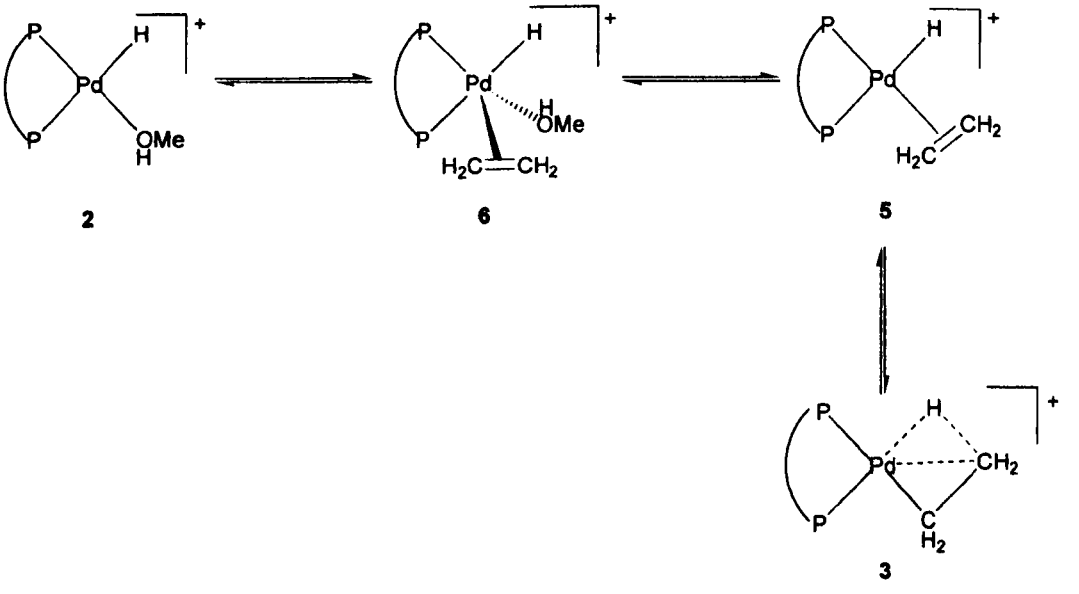

Formation of **4** probably proceeds *via* a similar mechanism (see Scheme 7.4). First, CO co-ordination to **3** results in the formation of $[Pd(d^tbpx)(CH_2CH_3)(CO)]^+$, **7**, which still contains an agostic interaction. Then, CO displaces the agostic interaction resulting in the formation of the square-planar complex $[Pd(d^tbpx)Et(CO)]^+$, **8**. Also in this case, neither **7** nor **8** have been directly detected, probably because both reactions are very fast. However, it has recently been shown [5] that CO addition to $[Pt(d^tbpx)(CH_2CH_3)]^+$, **9**, at low temperature results in the formation of $[Pt(d^tbpx)Et(CO)]^+$, **10**, the analogue of **8**; with increasing the temperature, **10** rearranges to give $[Pt(d^tbpx)(COEt)(solv)]^+$, **11**.

Scheme 7.4

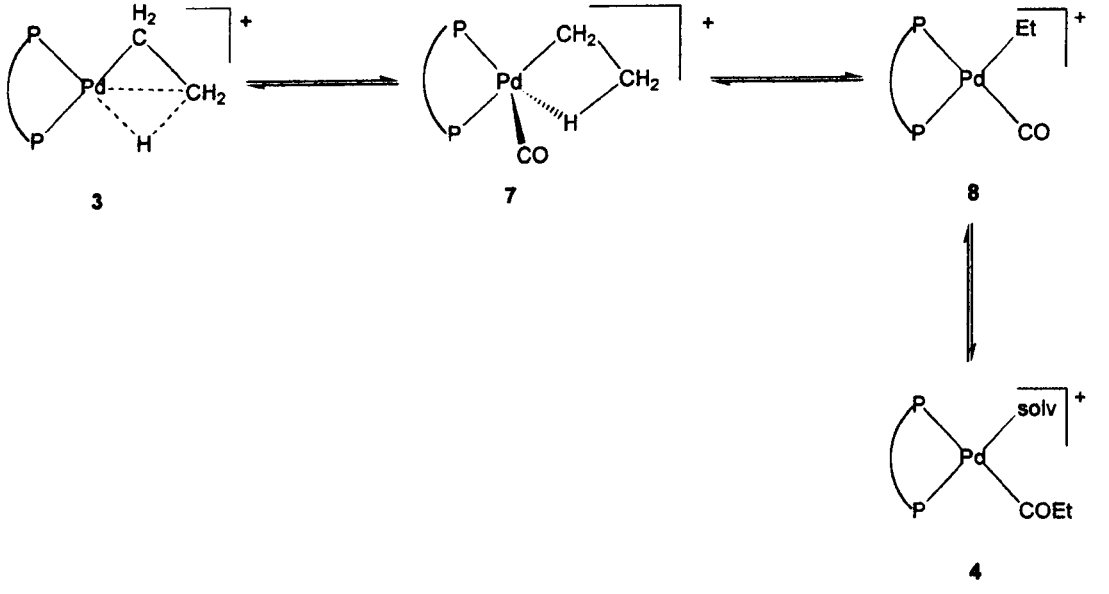

7.2 The activation process

Formation of the hydride **2** from **1** is not a direct process, but it takes place in at least four different steps (see Scheme 7.5). The first reaction is protonation of **1** to

give $[Pd(d^tbpx)(dbaH)]^+$, **12**. This reaction is irreversible and it is quite important since it transforms the insoluble compound **1** into the soluble species **12**. Moreover, it activates the starting Pd(0) species towards oxidation.

Scheme 7.5

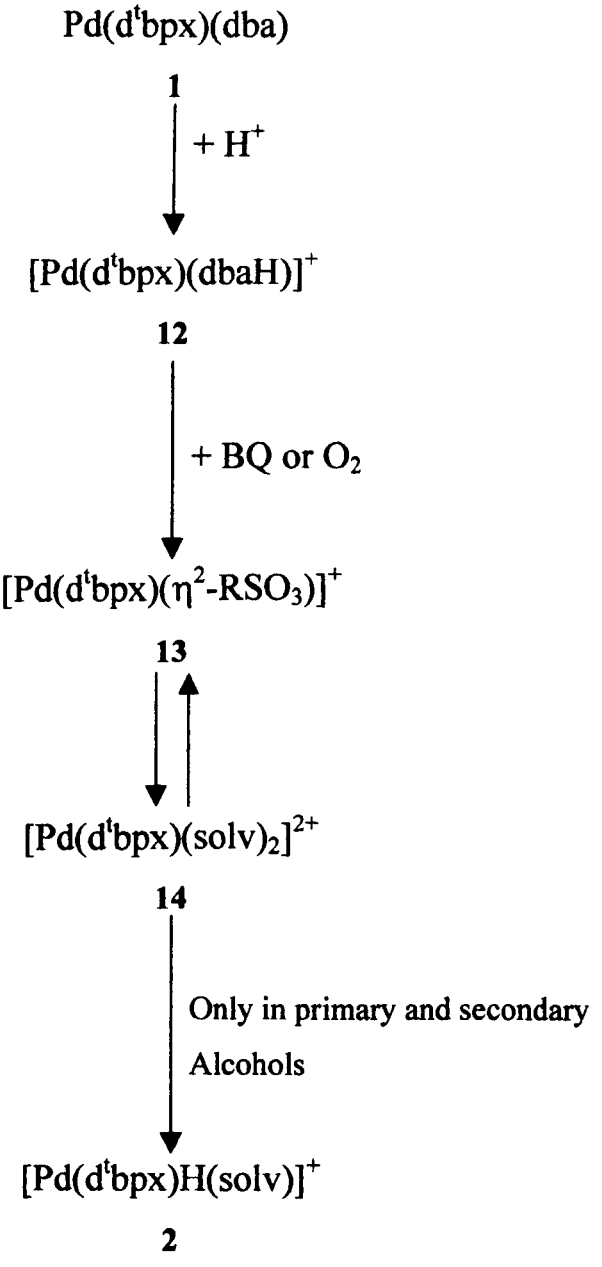

12 is readily oxidised by O_2 or BQ resulting in the formation of $[Pd(d^tbpx)(\eta^2\text{-}RSO_3)]^+$ (R = Me, **13a**; CF_3, **13b**; p-MeC_6H_4, **13c**); the oxidation is very fast at high temperature. Moreover, in the operating conditions of the industrial process, a very low concentration of catalyst is used and, thus, the presence of traces of O_2 are sufficient to obtain full conversion of **12** into **13**.

The third step is the displacement of the co-ordinated RSO_3^- anion and formation of $[Pd(d^tbpx)(solv)_2]^{2+}$, **14**. This reaction is an equilibrium (see eq. 7.4), and its position depends on the nature of the R-group present on the anion and the solvent used. Polar solvents favour formation of **14**, whereas basic R-groups shift the equilibrium 7.4 towards the formation of **13**.

$$[Pd(d^tbpx)(\eta^2\text{-}RSO_3)]^+ + 2solv \rightleftharpoons [Pd(d^tbpx)(solv)_2]^{2+} + RSO_3^- \qquad (7.4)$$

13 **14**

The replacement of RSO_3^- probably proceeds through three further steps (see Scheme 7.6). First, one molecule of solvent co-ordinates to the metal resulting on the formation of the penta-co-ordinate species $[Pd(d^tbpx)(\eta^2\text{-}RSO_3)(solv)]^+$, **15**; then, RSO_3^- changes its co-ordination mode from η^2 to η^1, resulting in $[Pd(d^tbpx)(\eta^1\text{-}RSO_3)(solv)]^+$, **16**. Thus, the co-ordinated anion, RSO_3^-, loses the extra-stabilisation due to the chelate effect and, therefore, it is readily displaced by a second molecule of solvent. In agreement with this mechanism, formation of the hydride **2** (which is the final result of all this process) is facilitated by addition of basic ligands (*e.g.* pyridine). However, the presence of basic ligands could be a problem in the catalytic process since such ligands bind strongly to the metal, preventing co-ordination of the monomers. In fact, it has been shown in this work that addition of pyridine prevents

DAMAGED TEXT IN ORIGINAL

the formation of **3**. Moreover, it has also been shown that excess pyridine results in removal of the hydride ligand from the metal.

Scheme 7.6

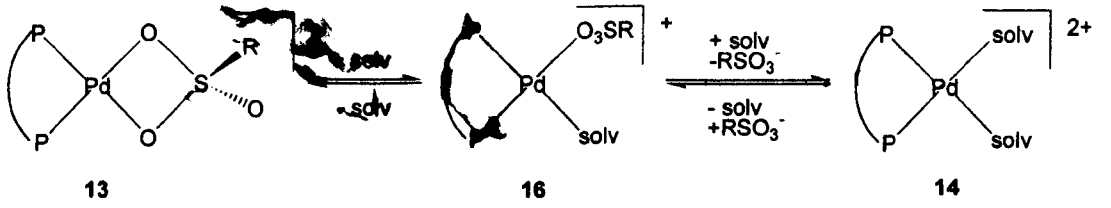

13 **16** **14**

The last step in the hydride formation is a redox process involving the solvent (see Scheme 7.7). This reaction is irreversible and involves β-hydride elimination from a primary or secondary alcohols which is co-ordinated to the metal; only in such a solvents is the hydride formed.

Scheme 7.7

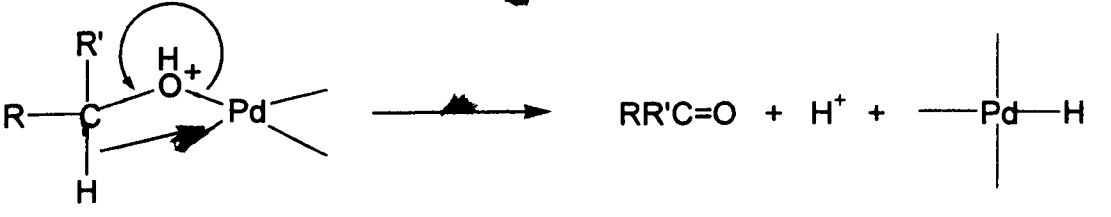

Thus, MeOH has at least three different roles in the catalytic process:

1) it is a reagent in the formation of MeP;
2) it is a reagent in the hydride formation;
3) it stabilises the hydride, probably *via* solvation of the ionic species present in solution and, in particular, H^+. For instance, **2** reacts in THF with H^+ to give **13** and H_2.

As a result of all these reactions, **2** is easily formed on using TfOH but more forcing conditions are required when $MeSO_3H$ is used. However, the best catalytic results are obtained with $MeSO_3H$ and not with TfOH. As it will be discussed in the next Section, this is mainly due to the different stabilities of the two systems.

It is interesting to note that when **1** is activated with $MeSO_3H$, the two main species present in solution are **3** and **13a**. These conclusions are based on analysis of all the data for all the equilibria described in this Thesis. Moreover, *in-situ* NMR experiments performed during this work support this hypothesis experimentally.

7.3 The deactivation process

A rapid decomposition of the catalyst to form Pd-metal and $[d^tbpxH_2]^{2+}$ is observed during the process. However, it is very noteworthy that, despite the easy decomposition, the catalyst is still very active. Nevertheless, decomposition remains one of the main problems of this process.

All the compounds studied in this Thesis spontaneously decompose in solution to form Pd-metal and $[d^tbpxH_2]^{2+}$; decomposition rates are always enhanced with increasing the temperature. Therefore, it is possible to refer to this process as "thermal decomposition", to distinguish it from the "CO-induced decomposition" which will be described later in this Section. Thermal stability strongly changes when different complexes are considered. Thus, **4** is quite unstable and, in fact it has been observed only below room temperature. However, its concentration during catalysis is very low and methanolysis is very fast. Thus, the possibility of getting out of the catalytic cycle by direct decomposition of **4** is noticeably reduced, and this

is probably one of the reasons why the catalyst is so active. **2** is also relatively unstable, even though it is far more stable than **4**. Whereas, **3** and especially **13a** are quite stable even at high temperature.

The stability of all these complexes dramatically depends on the concentration of CO. It is widely documented in the literature that Pd-complexes are not very stable in the presence of CO, especially in alcoholic solvents.[6-8] In all the cases reported, decomposition is so fast that a detailed mechanism is not available. During this Thesis, two different points for CO-induced decomposition of the Ineos Acrylics catalyst have been found. First, CO can co-ordinate to **2** resulting in the formation of $[Pd(d^tbpx)H(CO)]^+$, **17**, which is very unstable even below room temperature. Decomposition of **17** results, as usual, in the formation of Pd-metal and $[d^tbpxH_2]^{2+}$; the process is very fast and, hence, no intermediate has been detected. However, formation of **17** from **2** is a reversible process, and it competes with the reaction of **2** with ethene to give **3** (see Scheme 7.8).

Scheme 7.8

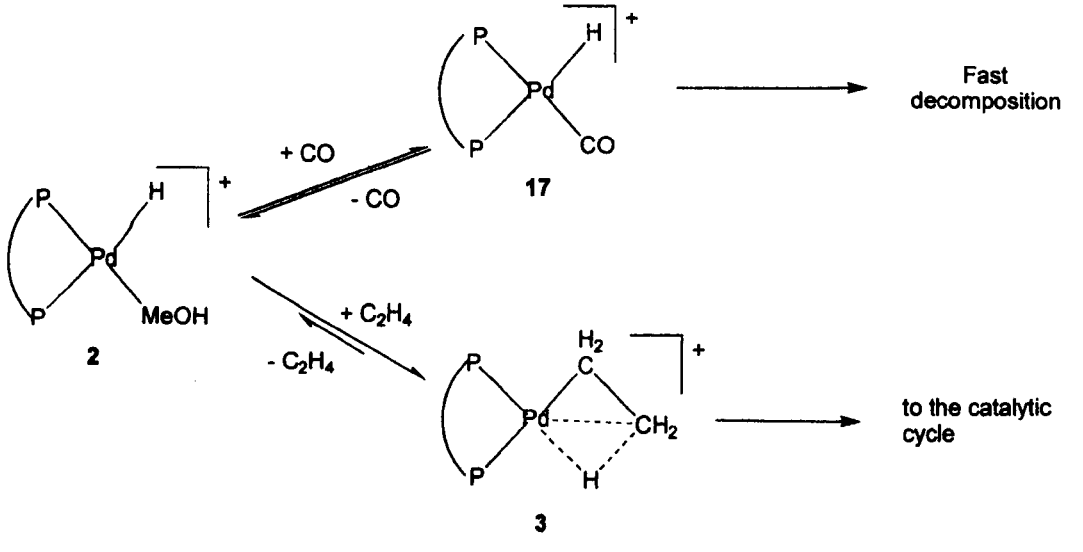

Therefore, competition between CO and ethene for reaction with **2** is fundamental in order to decide whether catalysis or decomposition takes place. Formation of **17** can be disfavoured by using a high C_2H_4/CO ratio. Nevertheless, even using these conditions, decomposition of the catalyst *via* **17** could remain quite important, since **17** decomposes very fast.

CO reacts also with **4** to give $[Pd(d^tbpx)(COEt)(CO)]^+$, **18**, and this compound is also highly unstable. Formation of **18** is a reversible process, and it competes with methanolysis (see Scheme 7.9). The same considerations made for **17** apply for the decomposition of the catalyst *via* **18**.

Scheme 7.9

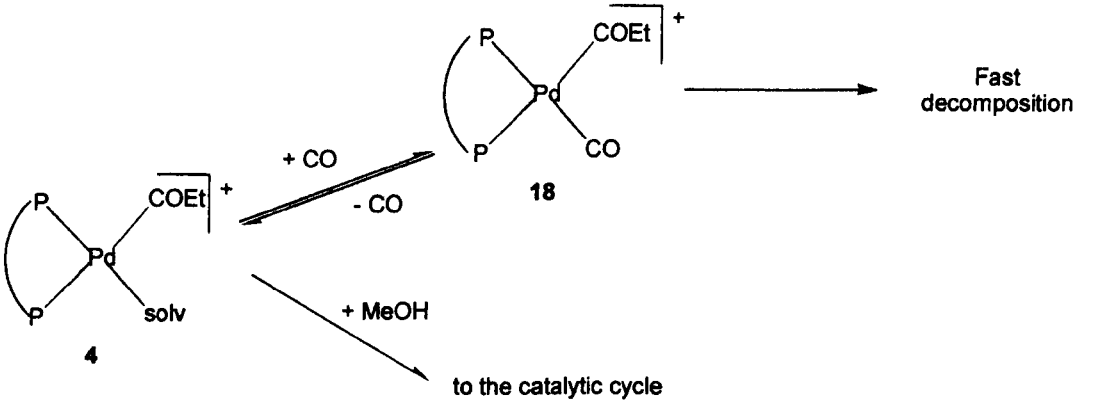

Decomposition of the catalyst can, therefore, start from many different points and, probably, thermal and CO-induced decomposition are both important. It is clear that decomposition remains the key point in determining the catalyst activity. Moreover, it has been shown that stability of the system increases on using $MeSO_3H$ instead of TfOH, probably because **13a**, in these conditions acts as a catalyst

reservoir. Thus, this is the reason why the best catalytic performances are obtained when **1** is activated with $MeSO_3H$.

7.4 Selectivity

One of the most surprising features of the catalytic system based on **1** is its very particular selectivity; most of the Pd-catalysts based on bidentate ligands result in the formation of polyketones. Only a few other diphosphines form Pd-complexes which promote the selective formation of MeP (see Chapters 1 and 6 of this Thesis). However, the catalytic system based on **1** is still the best one in terms of activity and selectivity.

Different complexes of the type Pd(P-P)(dba) (P-P = d^{t}bpx, **1**; d^{t}ppx, **1a**; ^{t}b^{t}ppx, **1b**; d^{t}bpp, **1c**; dapp, **1d**; dapx, **1e**; dcpx, **1f**; dppp, **1g**; dppx, **1h**; d^{i}ppx, **1i**; ^{t}bcpx, **1j**) have been studied during this work with regard to their reactivity in MeOH with oxidants (*i.e.* O_2 and BQ) and TfOH. Complexes **1** and **1a-e** result in the formation of $[Pd(P\text{-}P)H(MeOH)]^+$ (P-P = d^{t}bpx, **2**; d^{t}ppx, **2a**; ^{t}b^{t}ppx, **2b**; d^{t}bpp, **2c**; dapp, **2d**; dapx, **2e**), whereas in the other cases no hydride is formed. It is noteworthy the fact that all the complexes which can be transformed under these conditions into a hydride are also selective catalysts for the synthesis of MeP. Thus, a correlation between hydride formation and selectivity must exist. Very interestingly, the best catalytic system for MeP formation is the one based on d^{t}bpx, and this ligand is also the best one for the synthesis of the hydride, in term of stability and rate of formation of the complex.

All the ligands which allow formation of hydride complexes (and production of MeP) are very basic and very bulky. Moreover, all apart d^{t}bpp and dapp have an o-xylyl backbone. The bite angle of the diphosphine does not seem to be very important (see Chapter 1 and 6). Whereas, the selectivity of the catalyst and the possibility of forming hydride complexes correlate quite well with the parallel pocket angle ($\theta_\parallel$)of the ligand. Thus, the hydride (and MeP) is formed when $\theta_\parallel$ is smaller than 130° (see Chapter 1). The parallel pocket angle gives, basically, a measure of the space available on the plane for the growing chain and the monomer co-ordinated to the metal. A small pocket angle disfavours propagation and favours termination for steric reasons; moreover, the presence of a basic diphosphine, because of a strong *trans* effect, labilises the *trans* group favouring termination, too. Thus, steric and electronic effects co-operate in order to enhance the rate of the termination process, resulting in high selectivity towards MeP formation. The importance of steric effects is further substantiated by the analysis of $[Pd(d^tbpx)(CH_2CH_2(CH_2)_nH]^+$ (n = 0-12) complexes. As shown in Chapter 4, their stabilities dramatically decrease with increasing the length of the alkyl chain. The ethyl complex is very stable, whereas the propyl complex starts to eliminate propene already at room temperature. Thus, it seems that there is no physical space for a long chain to co-ordinate to the metal.

However, both steric and electronic parameters are important; it is, in fact, enough to slightly change the nature of the R-groups on the phosphorus or the backbone of the ligand in order to completely change the selectivity of the catalyst (and prevent hydride formation). Thus, the particular results obtained with these ligands are due to a delicate balance of different parameters.

As shown on many occasions in this Thesis, the particular behaviour of these ligands extend to different areas of their chemistry. On using d^{t}bpx (or analogous

ligands) is, in fact, possible to stabilise Pd-complexes which are otherwise very unstable and, in some cases, have never been observed before. The most important examples are listed below:

a) $[Pd(P\text{-}P)H(solv)]^+$. Pd-hydrides are usually unstable and, as far as we know, this is the first example of a fully characterised Pd-hydride containing a diphosphine ligand and a labile solvent molecule *cis* to the hydride ligand. Moreover, this complex is surprisingly very stable, even towards oxidation.

b) $[Pd(P\text{-}P)(CH_2CH_3)]^+$. These bulky ligands are able to stabilise ethyl-agostic complexes and, moreover, the agostic interaction is maintained even in strongly co-ordinating solvents.

c) $[Pd(d^tbpx)(COEt)(solv)]^+$. To the best of our knowledge, this is the first example of a fully characterised Pd-acyl complex containing a diphosphine ligand and a molecule of solvent. Usually CO co-ordination is more preferable than solvent co-ordination (see Chapter 5).

d) $[Pd(d^tbpx)(\eta^2\text{-}RSO_3)]^+$. RSO_3^- very rarely co-ordinates as a bidentate ligand (see Chapters 2 and 3) and, usually, the anion is readily lost in co-ordinating solvents. However, for **13a**, even the strongly co-ordinating solvent, CH_3CN, is not able to completely displace $\eta^2\text{-}RSO_3^-$.

References for Chapter Seven

1. A. Seayad, S. Jayasree, K. Damodaran, L. Toniolo and R. V. Chaudhari, *J. Organomet. Chem.*, **2000**, *601*, 100
2. G. Cavinato and L. Toniolo, *J. Mol. Cat.*, **1981**, *10*, 161
3. M. L. H. Green and L. L. Wong, *J. Chem. Soc. Chem. Commun.*, **1988**, 677
4. P. M. Maitlis, *The Organic Chemistry of Palladium*, Academic Press, New York, 1971
5. J. Wolowska, Ph.D. Thesis, University of Liverpool, *in progress*
6. A. Scoenberg and R. F. Heck, *J. Am. Chem. Soc.*, **1974**, *96*, 7761
7. A. Vavasori and L. Toniolo, *J. Mol. Cat. A.*, **1996**, *110*, 13
8. E. Drent and P. H. M. Budzelaar, *Chem. Rev.*, **1996**, *96*, 663

Chapter Eight

Experimental Section

8.1 General methods and procedures

This Chapter summarises all the experimental procedures and syntheses of complexes described in this Thesis. All the manipulations involving solutions or solids were performed under an atmosphere of nitrogen (or carbon monoxide or ethene where appropriate) using standard Schlenk line techniques. Most of the solvent were dried and distilled under nitrogen following standard literature methods; *i.e.* MeOH over $Mg(OMe)_2$, EtOH over Mg, THF over Na/benzophenone, CH_2Cl_2 over CaH_2, CH_3CN over CaH_2, n-hexane over Na and acetone over B_2O_3. All the other solvents were degassed under *vacuum* and stored under nitrogen. Deuterated solvents were degassed under *vacuum* in a liquid nitrogen bath and stored over activated 4 Å molecular sieves under nitrogen for at least 24 hours prior to use. All the reactions were carried out in a 10 mm NMR tube, unless stated otherwise. Most of the compounds have been characterised only in solution; thus, no yield nor elemental analysis is reported for them. The ^{13}CO and $^{13}CH_2{=}CH_2$ containing samples were prepared on using a high vacuum line with a mercury vapour pump.

All the reactions involving CO have been carried out in a well ventilated fume-hood. During the preparation of the samples for experiments under gas pressure, the NMR tubes have been always kept inside an appropriate metal or plastic protection. All the other experiments have been carried out following standard safety procedures.

All $^{31}P\{^{1}H\}$, ^{31}P, $^{13}C\{^{1}H\}$, ^{13}C and ^{1}H NMR measurements were performed on Bruker AMX200, AMX400, WM200 or WM250 instruments using commercial probes. The chemical shifts were referenced to external H_3PO_4 (85% in D_2O) for phosphorus, and to internal TMS for proton and carbon. Spectra of samples dissolved in non-deuterated solvents were referenced using an external deuterated solvent lock (*i.e.* CD_2Cl_2 for measurements at room and low temperature, D_2O for measurements at high temperature). ^{1}H NMR spectra of metal hydrides dissolved in non-deuterated solvents were recorded using the $^{1}H/^{31}P$ correlations measured *via* zero and double quantum coherences,[1] calibrated on *trans*-$^{2}J(P\text{-}H)$ measured in the ^{31}P NMR spectra. High pressure NMR measurements were recorded using a home-built special 10 mm thick glass wall tube or a 10 mm sapphire tube.

IR spectra were obtained in solution using cells with CaF_2 windows and in the solid state using KBr disks on a Perkin Elmer 1720-X Fourier transform spectrometer or on a Perkin Elmer 883 CW IR spectrometer.

X-ray structures were determined on a STOE-IPDS image plate diffractometer using graphite monochromated MoK_α radiation ($\lambda = 0.71073$ Å), apart from the case of $[Pd(d^tbpx)(\eta^2\text{-}MeSO_3)][MeSO_3][MeSO_3H]$ which was determined on a Rigaku AF65 diffractometer using graphite monochromated MoK_α radiation ($\lambda = 0.7169$ Å). Crystals were mounted in a glass fibre. Structures were solved by Direct Methods and structure refinements by full-matrix least-squares were based on all data using F^2.[2] All non-hydrogen atoms were refined anisotropically unless otherwise stated. Hydrogen positions were placed geometrically.

All the chemical products were purchased from Aldrich Chemical Co., except Pd_2dba_3,[3] $Pd(COD)(Me)Cl$,[4] $Pd(C_5H_5)(C_3H_5)$,[5] $Pd(d^tbpx)(C_2H_4)$,[6] and d^tbpx [7] which

were prepared by published methods. ^{13}CO (99.8 %) was purchased from Isotec Inc., and $^{13}CH_2=CH_2$ from Aldrich Chemical Co.

8.2 Preparation of the starting materials

8.2.1 Preparation of Pd(d^{t}bpx)(dba)

To a solution of Pd_2dba_3 (5.00 g, 5.47 mmol) dissolved in THF (200 ml) in a 500 ml two-necked round-bottomed flask equipped with a magnetic stirring bar and a gas inlet tube (N_2), d^{t}bpx (4.31 g, 10.9 mmol) was added as a solution in THF (100 ml). The deep purple colour of the starting solution of Pd_2dba_3 changed to bright orange after stirring for 1 hour. The reaction solution was stirred for a further 16 hours during which no further colour change occurred. The reaction solution was filtered through a glass sinter to remove any palladium metal, and the solvent removed under reduced pressure to yield an orange sticky gum. This was washed with cold n-hexane (243 K) followed by cold ether (243 K). The washings were discarded and the remaining solid dried under reduced pressure to yield the product as an orange powder.

Yield 2.56 g (32.1 %). Found: C, 67.14; H, 8.00 %. $C_{41}H_{58}OP_2Pd$ requires C, 67.03; H, 7.90 %.

$^{31}P\{^1H\}$ NMR at 293 K in THF: δ(ppm) = 49 (br), 51 (br)

$^{31}P\{^1H\}$ NMR at 193 K in THF: δ(ppm) = 43.1 (s), 46.2 (s), 47.3 (s), 49.7 (d, J = 8 Hz), 51.0 (s), 52.0 (d, J = 8.1 Hz)

$^{31}P\{^{1}H\}$ NMR at 293 K in MeOH: δ(ppm) =49 (br), 53 (br)

$^{31}P\{^{1}H\}$ NMR at 193 K in MeOH: δ(ppm) = 54.0 (d, J = 14 Hz), 49.3 (d, J = 14 Hz), 47.2 (d, J = 14 Hz), 42.9 (d, J = 14 Hz)

IR in THF at 293 K: ν(cm^{-1}) = 1646vs, 1623ms

Note: All the other Pd(P-P)(dba) (P-P = d^{t}ppx, ^{t}b^{t}ppx, d^{t}bpp, dapp, dapx, dcpx, d^{i}ppx, dppx, dppp, ^{t}bcpx) complexes were prepared in a similar way, using the appropriate diphosphine.

8.2.2 Preparation of Pd(d^{t}bpx)Cl$_2$

To a solution of Pd(d^{t}bpx)(dba) (2.00 g, 2.72 mmol) in Et_2O (100 ml) in a 250 ml two-necked round-bottomed flask, EtCOCl (2.60 g, 27.2 mmol) was added *via* a syringe. The solution turned from orange to yellow in colour immediately and a yellow precipitate began to form after 15 minutes. The reaction mixture was stirred for a further 2 hours before the precipitate was separated by filtration and dried *in vacuum*.

Yield 1.4 g (90 %). Found: C, 50.39; H, 7.65 %. $C_{24}H_{44}P_2Cl_2Pd$ requires: C, 50.43; H, 7.70 %.

$^{31}P\{^{1}H\}$ NMR at 293 K in CH_2Cl_2: δ(ppm) = 35.0 (s)

8.2.3 Preparation of Pd(d^{t}bpx)(η^{1}-TfO)$_2$

To a solution of Pd(d^{t}bpx)Cl_2 (1.50 g, 2.62 mmol) in CH_2Cl_2 (100 ml) in a 250 ml two-necked round-bottomed flask, AgOTf (1.35 g, 5.24 mmol) was added. A white precipitate of AgCl was immediately formed. The solution was further stirred

for 1 hour before removing the precipitate by filtration. The volume of the solution was, then, reduced *in vacuum* to *ca.* 40 ml and the product precipitated by addition of n-hexane (100 ml). The solid was separated by filtration and dried *in vacuum.*

Yield 1.8 g (86 %). Found: C, 38.66; H, 5.67 %. $C_{26}H_{44}P_2O_6S_2F_6Pd$ requires: C, 39.08; H, 5.55 %.

8.2.4 Preparation of Pd(d^{t}bpx)(Me)Cl

To a solution of Pd(COD)(Me)Cl (1.00 g, 3.77 mmol) in CH_2Cl_2 (50 ml) in a 200 ml Schlenk tube equipped with a magnetic stirring bar, d^{t}bpx (0.39 g, 3.8 mmol) was slowly added as a CH_2Cl_2 (50 ml) solution. The solution was stirred at room temperature for 4 hours and, then the volume reduced to *ca.* 30 ml. The product was precipitated by addition of n-hexane (100 ml), separated by filtration, washed with n-hexane (2x30 ml) and dried *in vacuum.*

Yield 1.8 g (88 %). Found: C, 54.39 %; H, 8.63 %. $PdC_{25}H_{47}P_2Cl$ requires: C, 54.45 %; H, 8.59 %.

$^{31}P\{^1H\}$ NMR at 293 K in CH_2Cl_2: δ(ppm) = 49.0 (d, J = 30.5 Hz), 18.4 (d, 30.5 Hz)

$^{31}P\{^1H\}$ NMR at 196 K in CH_2Cl_2: δ(ppm) = 47.8 (d, J = 29.5 Hz), 15.8 (d, J = 29.5Hz)

8.3 Experimental for Chapter Two

8.3.1 Synthesis of [Pd(d^{t}bpx)(dbaH)]X (X = $MeSO_3$, TfO, TsO, BF_4)

The reaction can be carried out in MeOH, THF or CH_2Cl_2 and, usually, one mole of acid per mole of Pd-complex is enough to have complete reaction. It is very important to avoid the presence of oxygen in order to prevent oxidation of $[Pd(d^tbpx)(dbaH)]^+$. Usually, to a solution of Pd(d^{t}bpx)(dba) (100 mg, 0.136 mmol) in the appropriate solvent (2 ml) the acid HX (X = TfO, TsO, $MeSO_3$, BF_4) was added with a micropipette (or in solid in the case of TsOH). The colour of the solution changes from yellow-orange to deep-red, with a concomitant change in NMR spectrum.

$^{31}P\{^1H\}$ NMR at 293 K in MeOH (using $MeSO_3H$): δ(ppm) = 43.9 (d, J = 48.7 Hz), 48.5 (d, J = 51.3 Hz), 63.3 (d, J = 48.7 Hz), 68.2 (d, J = 59 Hz)

$^{31}P\{^1H\}$ NMR at 193 K in MeOH (using $MeSO_3H$): δ(ppm) = 38.5 (d, J = 48.0 Hz), 43.6 (d, J = 48.0 Hz), 59.3 (d, J = 48.0 Hz), 65.3 (d, J = 48.0 Hz)

$^{31}P\{^1H\}$ NMR at 193 K in MeOH (using TfOH): δ(ppm) = 36.7 (d, J = 47.7 Hz), 41.8 (d, J = 47.8 Hz), 57.6 (d, J = 47.7 Hz), 63.7 (d, J = 47.8 Hz)

8.3.2 Synthesis of [Pd(d^{t}bpx)H(MeOH)][TfO]

A) Oxidation of [Pd(d^{t}bpx)(dbaH)][TfO] with O_2. To a solution of Pd(d^{t}bpx)(dba) (100 mg, 0.136 mmol) in MeOH (2 ml), TfOH (60.5 μl, 0.680 mmol) was added with a micropipette. Oxygen was, then, bubbled through the solution for *ca.* 20

minutes. The colour of the solution changed from deep-red to orange-yellow, and completion of the reaction was monitored *via* NMR spectroscopy.

B) Oxidation of [Pd(d^{t}bpx)(dbaH)][TfO] with BQ. Pd(d^{t}bpx)(dba) (100 mg, 0.136 mmol) and BQ (29.4 mg, 0.272 mmol) were mixed in solid and degassed under vacuum. The solids were partially dissolved under nitrogen in MeOH (2 ml) and then TfOH (60.5 μl, 0.680 mmol) was added *via* a micropipette. The product was formed in a few minutes, as revealed by NMR spectroscopy.

C) From Pd(d^{t}bpx)(η^1-TfO)$_2$. Pd(d^{t}bpx)(η^1-TfO)$_2$ (100 mg, 0.125 mmol) was dissolved in MeOH (2 ml) under nitrogen. The hydride was formed immediately.

$^{31}P\{^1H\}$ NMR at 293 K in MeOH: δ(ppm) = 25.8 (d, J = 17 Hz), 77.5 (d, J = 17 Hz)

^{31}P NMR at 293 K in MeOH: δ(ppm) = 25.8 (d, J = 179.4 Hz), 77.5 (br)

^1H NMR at 293 K in MeOH: δ(ppm) = -10.0 (dd, J = 179.7 and 14.3 Hz)

Note: The same three syntheses can be used for the preparation of analogous hydrides using other primary and secondary alcohols

8.3.3 Synthesis of [Pd(d^{t}bpx)H(solv)][TfO] (solv = THF, EtCN, CH_3CN, MeP)

A solution of [Pd(d^{t}bpx)H(MeOH)][TfO] (0.136 mmol) in MeOH (2 ml) was prepared as described in Section 8.3.2. The solution was, then, dried *in vacuum* and the residue dissolved in the appropriate solvent (2 ml). The product was then analysed *via* NMR spectroscopy. The best results were obtained preparing [Pd(d^{t}bpx)H(MeOH)][TfO] from Pd(d^{t}bpx)(η^1-TfO)$_2$. The NMR data are reported in Table 2.1.

8.3.4 Synthesis of [Pd(d^{t}bpx)(η^2-TfO)][TfO]

A) General synthesis. To a solution in an appropriate solvent (2 ml of THF, CF_3CH_2OH, CH_2Cl_2, MeP or acetone) containing Pd(d^{t}bpx)(dba) (65.0 mg, 0.088 mmol) and BQ (65.0 mg, 0.583 mmol), TfOH (39.0 µl, 0.440 mmol) was added through a micropipette. An orange solution was obtained and analysed by NMR. The same product can be obtained directly by dissolving Pd(d^{t}bpx)(η^1-TfO)$_2$ (100 mg, 0.125 mmol) in the same solvents.

$^{31}P\{^1H\}$ NMR at 293 K in THF: δ(ppm) = 80.0 (s); $^{31}P\{^1H\}$ NMR at 193 K in THF: δ(ppm) = 78.7 (s); $^{31}P\{^1H\}$ NMR at 293 K in CH_2Cl_2: δ(ppm) = 77.0 (s); $^{31}P\{^1H\}$ NMR at 293 K in acetone: δ(ppm) = 74.0 (s);

B) Synthesis in ^{t}BuOH. Pd(d^{t}bpx)(dba) (94.5 mg, 0.128 mmol) and BQ (82.0 mg, 0.759 mmol) were mixed as solids in an NMR tube, degassed *in vacuum* and put under nitrogen. Solid ^{t}BuOH (2.56 mg) was added and the tube warmed up to 303 K in order to melt the alcohol. At this point, the solution was red and TfOH (57.2 µl, 0.64 mmol) was added. An orange solution was obtained and the NMR spectrum recorded at 303 K

$^{31}P\{^1H\}$ NMR at 303 K in ^{t}BuOH: δ(ppm) = 70.8 (s);

C) Crystallisation of [Pd(d^{t}bpx)(η^2-TfO)][TfO]. To a solution of Pd(d^{t}bpx)(dba) (200 mg, 0.272 mmol) in THF (4 ml), BQ (29.4 mg, 0.272 mmol) and TfOH (200 µl, 1.36 mmol) were added in a Schlenk tube, resulting in the formation of a

homogeneous pale-yellow solution. Crystallisation was then induced by slow diffusion of n-hexane (5 ml). Yellow crystals of [Pd(d^{t}bpx)(η^2-TfO)][TfO] suitable for X-ray analysis were obtained. Crystal data and data collection parameters are reported in Table 8.1. The positions of the fluorine atoms of the non-co-ordinated anion are disordered.

Table 8.1

Crystal data and data collection parameters for [Pd(d^{t}bpx)(η^2-TfO)][TfO]

Chemical Formula	$C_{26}H_{42}F_6O_6P_2S_2Pd$	Z	4
FW	797.14	ρ_{calc}/g cm^{-1}	1.530
Crystal system	Orthorhombic	T/K	213(2)
Space group	P nma	λ(MoK_α)/Å	0.71073
a/Å	32.718(3)	μ(MoK_α)/mm^{-1}	0.730
b/Å	11.4933(15)	Data/parameters	2899/207
c/Å	9.2030(8)	R_1 (I>2σ(I))	0.1118
V/Å^3	3460.7(6)	wR_2 (all data)	0.2440

8.3.5 Synthesis of [Pd(d^{t}bpx)(CH$_3$CN)$_2$][TfO]$_2$

Pd(d^{t}bpx)(dba) (100 mg, 0.136 mmol) and BQ (82.0 mg, 0.759 mmol) were mixed as solids under nitrogen. Then, CH_3CN (2 ml) and TfOH (60.5 µl, 0.680 mmol) were added, resulting in the formation of an orange solution of [Pd(d^{t}bpx)(CH_3CN)$_2$][TfO]$_2$.

$^{31}P\{^{1}H\}$ NMR at 293 K in CH_3CN: δ(ppm) = 57.3 (s); $^{31}P\{^{1}H\}$ NMR at 246 K in CH_3CN: δ(ppm) = 55.5 (s); $^{31}P\{^{1}H\}$ NMR at 328 K in CH_3CN: δ(ppm) = 58.8 (s);

8.3.6 Synthesis of [Pd(d^{t}bpx)D(CD$_3$OD)][TfO]

Pd(d^{t}bpx)(η^1-TfO)$_2$ (100 mg, 0.125 mmol) was introduced into a 10 mm NMR tube under nitrogen. Addition of CD_3OD (2 ml) to the solid resulted in the immediate formation of the deuteride, which was the only product detected by NMR.

$^{31}P\{^{1}H\}$ NMR at 293 K in CD_3OD: δ(ppm) = 23.4 (sextet composed of six equal intense resonances, J = 17 and 23 Hz), 75.4 (sextet composed of six equal intense resonances, J = 17 and 3 Hz)

8.3.7 Synthesis of [Pd{η^2-P^{t}Bu$_2$CH$_2$C$_6$H$_3$CH$_2$PH^{t}Bu$_2$}{η^2-TfO}][TfO]

Pd(d^{t}bpx)(dba) (62.0 mg, 0.084 mmol) and BQ (406.5 mg, 3.76 mmol) were mixed as solids and then MeOH (2 ml) was added through a syringe. TfOH (37.6 μl, 0.420 mmol) was added to this red solution and the resulting orange solution analysed by NMR spectroscopy. [Pd{η^2-P^{t}Bu$_2$CH$_2$C$_6$H$_3$CH$_2$PH^{t}Bu$_2$}{η^2-TfO}][TfO] is the only product detected in these conditions.

$^{31}P\{^{1}H\}$ NMR at 293 K in MeOH: δ(ppm) = 42.4 (s), 105.6 (s)

^{31}P NMR at 293 K in MeOH: δ(ppm) = 42.4 (d, J = 460 Hz), 105.6 (s)

8.3.8 Synthesis [Pd(d^{t}bpx)H(H$_2$O)][TfO]

A) Synthesis in MeOH. BQ (14.7 mg, 0.136 mmol) and TfOH (100 µl, 0.680 mmol) were added to a solution of Pd(d^{t}bpx)(dba) (100 mg, 0.136 mmol) in MeOH (2 ml). Then, H_2O was added slowly and the reaction monitored *via* NMR spectroscopy. After the addition of 2 ml of H_2O, the starting complex, $[Pd(d^tbpx)H(MeOH)]^+$, was completely converted into the final product.

$^{31}P\{^1H\}$ NMR at 293 K in MeOH: δ(ppm) = 22.4 (br), 72.9 (br)

^{31}P NMR at 293 K in MeOH: δ(ppm) = 22.4 (d, J = 190 Hz), 72.9 (br)

B) Synthesis in THF. A solution of $[Pd(d^tbpx)H(THF)]^+$ (0.136 mmol) in THF (2 ml) was prepared as described in Section 8.3.3. Then, H_2O (5.00 µl, 0.278 mmol) was added with a micropipette and the reaction followed *via* NMR. Further addition of water results in the formation of $[Pd(d^tbpx)(H_2O)_2]^{2+}$.

$^{31}P\{^1H\}$ NMR at 293 K in THF: δ(ppm) = 23.1 (d, J = 18.3 Hz), 71.7 (d, J = 18.3 Hz)

^{31}P NMR at 293 K in MeOH: δ(ppm) = 23.1 (d, J = 186 Hz), 71.7 (br)

8.3.9 Synthesis of [Pd(d^{t}bpx)H(Py)][TfO]

BQ (14.7 mg, 0.136 mmol) and TfOH (100 µl, 0.680 mmol) were added to a solution of Pd(d^{t}bpx)(dba) (100 mg, 0.136 mmol) in MeOH (2 ml). Then, pyridine (52.4 µl, 0.653 mmol) was added with a micropipette and the solution analysed *via* NMR. It is better to add the pyridine slowly and to monitor the progress of the reaction *via* NMR, in order to avoid formation of $[Pd(d^tbpx)(Py)_2]^{2+}$.

$^{31}P\{^{1}H\}$ NMR at 293 K in MeOH: δ(ppm) = 23.3 (d, J = 18.4 Hz), 66.6 (d, J = 18.4 Hz)

^{31}P NMR at 293 K in MeOH: δ(ppm) = 23.3 (d, J = 182 Hz), 66.6 (br)

^{1}H NMR at 293 K in MeOH: δ(ppm) =-9.4 (dd, J = 17.1 and 182 Hz)

8.3.10 Synthesis of [Pd(d^{t}bpx)H(PPh$_3$)][TfO]

Solid PPh_3 (28.5 mg, 0.102 mmol) was added to a solution of [Pd(d^{t}bpx)H(MeOH)][TfO] (0.102 mmol) in MeOH (2 ml), prepared as described in Section 8.3.2. All the solid dissolved and the solution slightly changed colour from brown-orange to orange-red. The formation of the new complex was then detected through multinuclear NMR measurements.

$^{31}P\{^{1}H\}$ NMR at 293 K in MeOH: δ(ppm) = 11 (dd, J = 330 and 26 Hz), 35 (t, J = 27 Hz), 60 (dd, J = 330 and 26 Hz)

^{31}P NMR at 293 K in MeOH: δ(ppm) = 11 (d, J = 330 Hz), 35 (d, J = 160 Hz), 60 (d, J = 330 Hz)

^{1}H NMR at 293 K in MeOH: δ(ppm) = -8.1 (ddd, J = 160, 23 and 11 Hz)

8.3.11 Synthesis of Pd(d^{t}bpx)HX (X = Cl, Br, I)

$[NMe_4]X$ (X = Cl, Br, I) was slowly added as a solid to a solution of [Pd(d^{t}bpx)H(MeOH)][TfO] (0.136 mmol) in MeOH (2 ml), until all the starting material had completely reacted as indicated by NMR spectroscopy. The final products were not very soluble in MeOH. Hence, part of the data have been collected

in THF, after evaporation of the solvent *in vacuum* and dissolution of the residue in THF. The ^1H NMR spectrum of Pd(d^{t}bpx)HI has been recorded only at 193 K, because the compound is not very stable at room temperature. In all the reactions, Pd(d^{t}bpx)X_2 was formed as a by-product.

$^{31}P\{^1H\}$ NMR at 293 K in MeOH: δ(ppm) = 20.0 (d, J = 21.6 Hz), 67.2 (d, J = 21.6 Hz) (X = Cl); 21.6 (d, J = 21.4 Hz), 67.6 (d, J = 21.4 Hz) (X = Br); 21.0 (d, J = 21.2 Hz), 63.5 (d, J = 21.2 Hz)

^{31}P NMR at 293 K in MeOH: δ(ppm) = 20.0 (d, J = 180.7 Hz), 67.2 (br) (X = Cl); 21.6 (d, J = 203 Hz), 67.6 (br) (X = Br); 21.0 (d, J = 182 Hz), 63.5 (br) (X = I)

^1H NMR at 293 K in MeOH: δ(ppm) = -10.4 (dd, J = 18.4 and 180.7 Hz) (X = Cl); -9.7 (dd, J = 26.2 and 203 Hz) (X = Br); -9.3 (dd, J = 38.0 and 182 Hz) (X = I, in MeOH at 193 K)

8.4 Experimental for Chapter Three

8.4.1 Synthesis of [Pd(d^{t}bpx)(η^2-$MeSO_3$)][$MeSO_3$]

$MeSO_3H$ (45.7 μl, 0.680 mmol) was added with a micropipette to a solution of Pd(d^{t}bpx)(dba) (100 mg, 0.136 mmol) in MeOH (2 ml). Oxygen was then bubbled through the solution for *ca.* 30 minutes, until the colour of the solution turned from deep-red to pale-yellow. [Pd(d^{t}bpx)(η^2-$MeSO_3$)]$^+$ was the only species detected in solution *via* NMR at this point. Alternatively, the same product can be obtained by addition of BQ to the same deep-red solution. Crystals suitable for X-ray analysis

were obtained on layering n-hexane (3 ml) on this solution. The compound crystallises as $[Pd(d^tbpx)(\eta^2\text{-}MeSO_3)][MeSO_3][MeSO_3H]$; crystal data and data collection parameters are reported in Table 8.2.

$^{31}P\{^1H\}$ NMR at 193 K: 67.1 (s), 66.0 (s) in MeOH; 66.1 (s), 65.4 (s) in THF; 66.9 (s), 65.6 (s) in acetone; 66.2 (s) in CH_2Cl_2; 70.0 (s) in MeOH at 293 K.

Table 8.2

Crystal data and data collection parameters for $[Pd(d^tbpx)(\eta^2\text{-}MeSO_3)][MeSO_3][MeSO_3H]$

Chemical Formula	$C_{27}H_{54}O_9P_2S_3Pd$	V/Å^3	1784(3)
FW	787.27	Z	2
Crystal system	Triclinic	ρ_{calc}/g cm^{-1}	1.465
Space group	P -1	T/K	153(2)
a/Å	11.87(2)	$\lambda(MoK_\alpha)$/Å	0.71069
b/Å	15.410(7)	$\mu(MoK_\alpha)$/mm^{-1}	0.762
c/Å	11.168(6)	Data/parameters	3721/379
α/°	109.17(4)	R_1 (I>2σ(I))	0.0397
β/°	108.21(7)	wR_2 (all data)	0.0488
γ/°	72.06(6)		

8.4.2 Synthesis of $[Pd(d^tbpx)(\eta^2\text{-}TsO)][TsO]$

BQ (29.4 mg, 0.272 mmol) and $TsOH.H_2O$ (258.4 mg, 1.360 mmol) were added to a solution of Pd(d^{t}bpx)(dba) (200 mg, 0.272 mmol) in THF (4 ml), in a

Schlenk tube, resulting in a homogeneous pale-yellow solution. Crystals suitable for X-ray analysis were then obtained on layering n-hexane (6 ml) on this solution. The elemental cell contains two independent cations, two TsO^- anions, four molecules of free TsOH acid and six molecules of water. In the structure there were disordered groups that were split in two positions in the refinement, using distance and anisotropic displacement parameter restraints: the phenyl ring atoms and the methyl group in two of the four TsOH molecules of the asymmetric unit and the oxygen atoms belonging to a third acidic group. In the structure there are high residue electron densities that could not be attributed. This is due to the fact that the crystals were very small and of poor quality, leading to a rather high R factor. While the overall connectivity is not in doubt, the quality of the refinement does not allow a detailed discussion of the structural parameters. Crystal data and data collection parameters are reported in Table 8.3.

$^{31}P\{^1H\}$ NMR at 193 K: 68.3 (s) in MeOH; 68.4 (s), 68.2 (s) in THF; 67.8 (s), 66.9 (s) in CH_2Cl_2; 69.7 (s) in MeOH at 293 K.

Table 8.3

Crystal data and data collection parameters for [Pd(d^{t}bpx)(η^2-TsO)][TsO][TsOH]$_2$[H$_2$O]$_3$

Chemical Formula	$C_{52}H_{72}O_{21}P_2PdS_4$	V/Å^3	5871.2(14)
FW	1329.82	Z	4
Crystal system	Triclinic	ρ_{calc}/g cm^{-1}	1.504
Space group	P -1	T/K	213(2)

a/Å	14.919(2)	$\lambda(MoK_\alpha)$/Å	0.71073
b/Å	16.936(2)	$\mu(MoK_\alpha)/mm^{-1}$	0.516
c/Å	24.621(3)	Data/parameters	14595/1226
α/°	76.092(15)	R_1 ($I>2\sigma(I)$)	0.1447
β/°	76.814(16)	wR_2 (all data)	0.3715
γ/°	89.694(17)		

8.4.3 Study of the reactivity of Pd(d^{t}bpx)(dba) with $MeSO_3H$ in boiling MeOH

Pd(d^{t}bpx)(dba) (120 mg, 0.163 mmol) was suspended in MeOH (5 ml) in a 50 ml two-necked round bottomed flask. $MeSO_3H$ (52.8 µl, 0.815 mmol) was added and the resulting deep-red solution refluxed at 80°C under nitrogen (1 atm) for 1 hour. The final yellow solution was then cooled down to room temperature and analysed by NMR spectroscopy. See Figure 3.4.

8.5 Experimental for Chapter Four

8.5.1 Synthesis of [Pd(d^{t}bpx)(CH_2CH_3)][TfO]

Different syntheses are possible.

A) Ethene was bubbled for a few seconds through a solution of [Pd(d^{t}bpx)H(MeOH)][TfO] (0.136 mmol) in MeOH (2 ml), prepared as

described in Section 8.3.2. Immediately the solution turned from brown-orange to brown-yellow and the product was detected *via* NMR spectroscopy.

B) In a 10 mm NMR tube, Pd(d^{t}bpx)(dba) (100 mg, 0.136 mmol) and BQ (14.7 mg, 0.136 mmol) were mixed as solids under a C_2H_4 atmosphere (1 bar). Then, MeOH (2 ml) and TfOH (60.5 µl, 0.680 mmol) were added and the new complex detected in the NMR spectra.

C) To a suspension of Pd(d^{t}bpx)(C_2H_4) (100 mg, 0.189 mmol) in MeOH (2 ml), TfOH (84.3 µl, 0.945 mmol) was added *via* a micropipette. The resulting yellow solution was then analysed using NMR spectroscopy.

$^{31}P\{^1H\}$ NMR at 193 K in MeOH: δ(ppm) = 36.3 (d, J = 31 Hz), 67.7 (d, J = 31 Hz)

8.5.2 Characterisation of [Pd(d^{t}bpx)(CH_2CH_3)][TfO] via $^{13}CH_2$=CH_2

TfOH (100 µl, 0.680 mmol) was added with a micropipette to a MeOH solution (2.5 ml, 25% CD_3OD) of Pd(d^{t}bpx)(dba) (100 mg, 0.136 mmol) and BQ (14.7 mg, 0.136 mmol), in a Schlenk tube under N_2 (1 bar). A brown-orange solution containing [Pd(d^{t}bpx)H(MeOH)]$^+$ was formed immediately. After having controlled the purity of the sample *via* NMR spectroscopy, the solution was transferred to a 10 mm NMR tube equipped with a connection for the high vacuum line. The tube was then frozen in liquid nitrogen and evacuated on a high vacuum line equipped with a mercury diffusion pump. The liquid nitrogen bath was, then, removed and the tube put immediately in a dry ice/acetone bath, in order to avoid the condensation of ethene. To this solution, one equivalent of $^{13}CH_2$=CH_2 was added through the high

vacuum line, then the tube was put again in the liquid nitrogen bath and sealed. This sample was used for all ^{31}P and ^{13}C measurements at low temperature.

$^{31}P\{^{1}H\}$ NMR at 193 K in MeOH: δ(ppm) = 36.3 (d + dd, J = 31 and 38 Hz), 67.5 (d, J = 31 Hz)

$^{31}P\{^{1}H\}$ NMR at 293 K in MeOH: δ(ppm) = 38.3 (br), 70.2 (br)

$^{13}C\{^{1}H\}$ NMR at 193 K in MeOH: δ(ppm) = 8 (s), 32 (dd, J = 38 and 5 Hz)

8.5.3 Characterisation of [Pd(d^{t}bpx)(CH_2CH_3)][TfO] at high temperature

A MeOH solution (2 ml, 25% CD_3OD) of [Pd(d^{t}bpx)(CH_2CH_3)][TfO] (0.136 mmol) was prepared as described in Section 8.5.1 in a Schlenk tube under ethene (1 atm), and then transferred *via* a syringe to a 10 mm NMR sapphire tube. The tube was pressurised with 4 atm of ethene, and the phosphorus spectra of this solution were recorded in the temperature range 293-353 K.

$^{31}P\{^{1}H\}$ NMR at 293 K in MeOH: δ(ppm) = 37 (br), 70 (br)

$^{31}P\{^{1}H\}$ NMR at 353 K in MeOH: δ(ppm) = 54 (br)

8.5.4 Synthesis of [Pd(d^{t}bpx)($CH_2CH_2CH_3$)][TfO]

A solution of [Pd(d^{t}bpx)H(MeOH)][TfO] (0.136 mmol) in MeOH (2.5 ml, 25% CD_3OD) was prepared as described in Section 8.3.2. After having controlled the purity of the sample *via* NMR spectroscopy, the solution was transferred in a 10 mm NMR tube equipped with a connection for the high vacuum line. The tube was then

frozen in liquid nitrogen and evacuated on a high vacuum line equipped with a mercury diffusion pump. Then, the liquid nitrogen bath was removed and replaced with a dry ice/acetone bath. To this solution, two equivalents of propene were added through the high vacuum line, followed by cooling in liquid nitrogen and sealing. This sample was used for all the ^{31}P NMR measurements at low temperature.

$^{31}P\{^{1}H\}$ NMR at 193 K in MeOH: δ(ppm) = 37.8 (d, J=30.5 Hz), 67.6 (d, J=30.5 Hz)

8.5.5 Synthesis of [Pd(d^{t}bpx)(CH$_2$CH$_2$(CH$_2$)$_3$CH$_3$)][TfO]

A solution of [Pd(d^{t}bpx)H(MeOH)][TfO] (0.136 mmol) in MeOH (2 ml) was prepared as described in Section 8.3.2. Then, 1-hexene (42.0 μl, 0.400 mmol) was added and the ^{31}P NMR spectra were recorded in the temperature range 193-293 K.

$^{31}P\{^{1}H\}$ NMR at 196 K in MeOH: δ(ppm) = 38.6 (d, J=30.2 Hz), 67.7 (d, J=30.2 Hz)

8.5.6 Thermodynamic calculations for the equilibrium involving [Pd(d^{t}bpx)(CH$_2$CH$_2$(CH$_2$)$_3$CH$_3$)]$^+$ and [Pd(d^{t}bpx)H(MeOH)]$^+$

Let consider the following equilibrium:

$$[Pd(d^tbpx)H(MeOH)]^+ + C_6H_{12} \rightleftharpoons [Pd(d^tbpx)(CH_2CH_2(CH_2)_3CH_3)]^+ + MeOH$$

Pd_{hyd} Pd_{alk}

Its equilibrium constant is:

$K_{eq} = [Pd_{alk}] / [Pd_{hyd}][C_6H_{12}]$

Let define:

R = integral of the resonance due to Pd_{alk} / integral of the resonance due to Pd_{hyd}

C = total concentration of palladium in solution

A = total concentration of C_6H_{12} in solution

Hypotheses:

1. The concentration of phosphorus-containing species is directly proportional to the integral of their resonances in the NMR spectra, and the constant of proportion is the same for all the species. Hence: $R = [Pd_{alk}] / [Pd_{hyd}]$;
2. There are no side products. Hence: $C = [Pd_{alk}] + [Pd_{hyd}]$ and $A = [Pd_{alk}] + [C_6H_{12}]$.

Then:

$K_{eq} = R(1 + R)/(A + AR - CR)$

Using this last equation is possible to calculate from the experimental spectra K_{eq} at different temperatures. Then, applying the fundamental thermodynamic equations:

$\Delta G° = -RT\ln K_{eq}$

$\Delta G° = \Delta H° - T\Delta S°$

it is possible to calculate also $\Delta H°$ and $\Delta S°$.

8.6 Experimental for Chapter 5

8.6.1 Synthesis of [Pd(d^{t}bpx)(COEt)(THF)][TfO]

A solution in MeOH (2 ml) of [Pd(d^{t}bpx)(CH_2CH_3)][TfO] (0.136 mmol) was prepared as described in Section 8.5.1. The solution was, then, dried *in vacuum* and the residue dissolved in THF (2 ml, 25% d^8-THF) under N_2. The resulting solution was stored in a dry ice/acetone bath, and its purity checked *via* NMR spectroscopy. The solution was then transferred to a special 10 mm NMR tube equipped with a connection for the high vacuum line. The tube was frozen in liquid nitrogen and evacuated on a high vacuum line equipped with a mercury diffusion pump. To this solution, one equivalent of CO was added through the high vacuum line and, then, the tube was sealed. The experiment has been performed with either ^{12}CO and ^{13}CO.

$^{31}P\{^1H\}$ NMR at 173 K in THF (with ^{12}CO): δ(ppm) = 32.5 (d, J= 40 Hz), 79.9 (d, J= 40 Hz)

$^{31}P\{^1H\}$ NMR at 173 K in THF (with ^{13}CO): δ(ppm) = 32.5 (dd, J= 40 and 82.9 Hz), 79.9 (dd, J= 40 and 18.2 Hz)

$^{13}C\{^1H\}$ NMR at 173 K in THF (with ^{13}CO): δ(ppm) = 232 (dd, J= 82.9 and 18.2 Hz)

Note: It is possible to obtain a ^{13}C-double enriched acyl complex operating as follow. A solution of [Pd(d^{t}bpx)H(THF)][TfO] (0.136 mmol) in THF (2 ml, 25% d^8-THF) was prepared as described in Section 8.3.3. To this solution, one equivalent of $^{13}CH_2{=}CH_2$ was added through the high vacuum line following the procedure reported in Section 8.5.2 and, then ^{13}CO was added to the resulting ethyl complex as in the experiment described above.

8.6.2 Synthesis of Pd(d^{t}bpx)(COMe)Cl

Pd(d^{t}bpx)(Me)Cl (100 mg, 0.181 mmol) was dissolved in CH_2Cl_2 (2 ml) under CO (1 atm). In these conditions, the starting material is partially converted into Pd(d^{t}bpx)(COMe)Cl.

$^{31}P\{^1H\}$ NMR at 196 K in CH_2Cl_2: δ(ppm)= 15.4 (d, J=52.4 Hz), 43.8 (d, J=52.4 Hz)

$^{31}P\{^1H\}$ NMR at 293 K in CH_2Cl_2: δ(ppm)= 17.6 (br), 45.6 (br)

8.6.3 Synthesis of [Pd(d^{t}bpx)H(CO)][TfO]

A solution of [Pd(d^{t}bpx)H(MeOH)][TfO] (0.136 mmol) in MeOH (2 ml) was prepared as described in Section 8.3.2 and cooled in a dry ice/acetone bath. Then, *ca.* one equivalent of CO was added through a syringe. After 30 minutes, the NMR tube was directly transferred from the low temperature bath to the pre-cooled N MR probe and analysed *via* multinuclear NMR spectroscopy. A similar experiment using ^{13}CO was repeated on the high vacuum line.

$^{31}P\{^1H\}$ NMR at 193 K in MeOH: δ(ppm)= 31.4 (d, J=21.9 Hz), 61.0 (d, J=21.9 Hz)

^{31}P NMR at 193 K in MeOH: δ(ppm)= 31.4 (d, J=167.4 Hz), 61.0 (br)

^1H NMR at 193 K in MeOH: δ(ppm)= -5.3 (dd, J= 167.4 and 15.8 Hz)

8.6.4 Synthesis of Pd(d^{t}bpx)(CO)

Pd(d^{t}bpx)(dba) (100 mg, 0.136 mmol) was dissolved in THF (2 ml) and CO was, then, bubbled through the solution for 2 minutes. The resulting yellow-orange solution was analysed by NMR and IR spectroscopy. Storage of this sample in a

special 10 mm HP-NMR tube (thick glass tube) under 1 atm of ^{13}CO at 193 K resulted in the formation of Pd(d^{t}bpx)(^{13}CO).

$^{31}P\{^1H\}$ NMR at 173 K in THF: δ(ppm)= 45.2 (s)

$^{13}C\{^1H\}$ NMR at 173 K in THF: δ(ppm)= 211 (t, J = 24.5 Hz)

IR in THF at 293 K: ν(cm^{-1}) = 1948s

8.6.5 Synthesis of Pd(d^{t}bpx)(CO)$_2$

Pd(d^{t}bpx)(dba) (100 mg, 0.136 mg) was dissolved in THF (2 ml) and CO was, then, bubbled for 40 minutes, adding periodically new THF in order to replace the evaporated solvent. The resulting yellow-orange solution was analysed by NMR and IR spectroscopy under CO. Storage of the solution in a special 10 mm HP-NMR tube (thick glass tube) under ^{13}CO (3 atm) resulted in the formation of Pd(d^{t}bpx)(^{13}CO)$_2$.

$^{31}P\{^1H\}$ NMR at 173 K in THF: δ(ppm)= 51.1 (s)

$^{13}C\{^1H\}$ NMR at 173 K in THF: δ(ppm)= 197.9 (s), 198.8 (s)

IR in THF at 293 K: ν(cm^{-1}) = 2019ms, 1998s

8.7 Experimental for Chapter 6

8.7.1 Synthesis of [Pd(P-P)H(MeOH)][TfO] (P-P = d^tbpp, d^tppx, $^tb^t$ppx, dapx and dapp)

In all five cases, BQ (14.7 mg, 0.136 mmol) and TfOH (100 μl, 0.680 mmol) were added to a solution of the appropriate Pd(P-P)(dba) complex (0.136 mmol) in MeOH (2 ml). The products were then analysed *via* NMR spectroscopy. The formation of the hydride takes place in a few minutes in the cases of d^tppx, $^tb^t$ppx and dapx. Whereas, its complete formation occurs in *ca.* 1 hour in the case of d^tbpp and in 2-3 days in the case of dapp. The NMR data are reported in Table 6.1, Chapter 6.

8.7.2 Synthesis of [Pd(P-P)(CH_2CH_3)][TfO] (P-P = d^tbpp, d^tppx, $^tb^t$ppx, dapx and dapp)

A solution of the appropriate hydride complex (0.136 mmol) in MeOH (2 ml) was prepared as described in Section 8.7.1 and, then, ethene (1 atm) was added. The NMR data are reported in Table 6.3, Chapter 6.

8.7.3 Synthesis of [Pd(dcpx)(dbaH)][$MeSO_3$]

Pd(dcpx)(dba) (200 mg, 0.238 mmol) was dissolved in THF (5 ml) in a Schlenk tube, and $MeSO_3H$ (77.2 μl, 1.19 mmol) was added *via* a micropipette, resulting in the formation of a deep-red solution of $[Pd(dcpx)(dbaH)]^+$. Then, n-hexane (5 ml) was layered over the solution; after a week, some red crystals, which

X-ray analysis showed to be $[Pd(dcpx)(dbaH)][MeSO_3][MeSO_3H][THF]_2$, were formed. Crystal data and data collection parameters are reported in Table 8.4.

$^{31}P\{^1H\}$ NMR at 193 K in MeOH: δ(ppm)= 7.5 (d, J = 71.7 Hz), 11.0 (d, J = 78.6 Hz), 11.8 (d, J = 70.2 Hz), 21.7 (d, J = 69.4 Hz), 23.2 (d, J = 72.5 Hz), 28.9 (d, J = 79.4 Hz)

Table 8.4

Crystal data and data collection parameters for

$[Pd(dcpx)(dbaH)][MeSO_3][MeSO_3H][THF]_2$

Chemical Formula	$C_{59}H_{90}O_9P_2PdS_2$	V/Å^3	2995.6(11)
FW	1175.95	Z	2
Crystal system	Triclinic	ρ_{calc}/g cm^{-1}	1.304
Space group	P -1	T/K	293(2)
a/Å	14.422(3)	λ(MoK$_\alpha$)/Å	0.71073
b/Å	15.236(3)	μ(MoK$_\alpha$)/mm^{-1}	0.423
c/Å	15.695(3)	Data/parameters	7168/672
α/°	72.45(3)	R_1 (I>2σ(I))	0.0538
β/°	85.34(3)	wR_2 (all data)	0.1403
γ/°	65.79(2)		

8.7.4 Synthesis of [Pd(dcpx)(H_2O)$_2$][$MeSO_3$]$_2$

This compound has been originally obtained as a side product during the crystallisation of [Pd(dcpx)(dbaH)][$MeSO_3$][$MeSO_3H$][THF]$_2$ (see Section 8.7.3); X-ray analysis of the yellow crystals of the side product showed them to be [Pd(dcpx)(H_2O)$_2$][$MeSO_3$]$_2$[$MeSO_3H$]. Crystal data and data collection parameters are reported in Table 8.5. The same compound can be obtained easily by reaction of [Pd(dcpx)(dbaH)]$^+$ (0.136 mmol) in MeOH or THF (2 ml) with O_2 (bubbled for 1 hour) or BQ (14.7 mg, 0.136 mmol).

$^{31}P\{^1H\}$ NMR at 293 K in MeOH: δ(ppm)= 44.2 (s)

Table 8.5

Crystal data and data collection parameters for

[Pd(dcpx)(H_2O)$_2$][$MeSO_3$]$_2$[$MeSO_3H$]

Chemical Formula	$C_{35}H_{65}O_{11}P_2PdS_3$	Z	4
FW	926.52	ρ_{calc}/g cm^{-1}	1.441
Crystal system	Monoclinic	T/K	213(2)
Space group	P 21/c	λ(MoK$_\alpha$)/Å	0.71073
a/Å	12.0457(14)	μ(MoK$_\alpha$)/mm^{-1}	0.631
b/Å	18.5776(14)	Data/parameters	5566/486
c/Å	19.825(2)	R_1 (I>2σ(I))	0.0342
β/°	105.762(13)	wR_2 (all data)	0.0777
V/Å^3	4269.7(8)		

8.7.5 Synthesis of [Pd(tbcpx)(H2O)2][TfO]2

TfOH (60.5 μl, 0.680 mmol) was added with a micropipette to a solution containing Pd(tbcpx)(dba) (115.5 g, 0.136 mmol) and BQ (14.7 mg, 0.136 mmol) in MeOH (2 ml), resulting in a orange-yellow solution. Crystals suitable for X-ray analysis were obtained on layering n-hexane (4 ml) over this solution. Crystal data and data collection parameters are reported in Table 8.6.

Table 8.6

Crystal data and data collection parameters for

[Pd(tbcpx)(H2O)2][TfO]2

Chemical Formula	$C_{30}H_{52}F_6O_8P_2PdS_2$	Z	4
FW	887.28	ρ_{calc}/g cm^{-1}	1.441
Crystal system	Monoclinic	T/K	293(2)
Space group	P 21/n	$\lambda(MoK_\alpha)$/Å	0.71073
a/Å	12.4596(14)	$\mu(MoK_\alpha)$/mm^{-1}	0.544
b/Å	19.034(3)	Data/parameters	6523/443
c/Å	19.877(3)	R_1 ($I>2\sigma(I)$)	0.0668
β/°	94.923(14)	wR_2 (all data)	0.2216
V/Å^3	4696.5(11)		

References for Chapter Eight

1. A. Bax, R. H. Griffey and B. L. Hawkins, *J. Magn. Reson.*, **1983**, *55*, 301
2. G. M. Scheldrick, SHELX-97, *Programs for Crystal Structure Solution and Refinement*, University of Gottingen, Germany, 1997
3. M. F. Retting and P. M. Maitlis, *Inorganic Syntheses*, **1977**, *17*, 134
4. E. R. Rulke, J. M. Ernsting, A. L. Spek, C. J. Elsevier, P. W. N. M. van Leeuwen and K. Vrieze, *Inorg. Chem.*, **1993**, *32*, 5769
5. Y. Tatsuno, T. Yoshida and S. Otsuka, *Inorganic Syntheses*, **1979**, *19*, 221
6. F. M. Conroy-Lewis, L. Mole, A. D. Redhouse, S. A. Lister and J. L. Spencer, *J. Chem. Soc. Chem. Commun.*, **1991**, 1601
7. J. Moulton and B. L. Shaw, *J. Chem. Soc. Chem. Commun.*, **1976**, 365